



Through the lens of a Video Plankton Recorder:  
Optical imaging and insights into zooplankton ecology

Anouk Ollevier

2024



# Through the lens of a Video Plankton Recorder

Optical imaging and insights into zooplankton ecology

Anouk Ollevier







# **Through the lens of a Video Plankton Recorder:**

Optical imaging and insights into zooplankton ecology

Anouk Ollevier

**Flanders Marine Institute**

Jacobsenstraat 1  
8400 Oostende  
Belgium

**Ghent University**

Faculty of Sciences  
Biology Department  
Marine Biology Research Group  
Campus Sterre S8  
Krijgslaan 281  
9000 Gent  
Belgium

**Printed by**

Silhouet bvba

**Cover and layout**

Anouk Ollevier

**Co-authored one or more chapters:**

Wieter Boone, Klaas Deneudt, Marleen De Troch, Roeland Develter, Cedric Goossens, Pascal I. Hablützel, Rune Lagaisse, Lorenz Meire, Klas O. Möller, Jonas Mortelmans, Koen Planken, Leandro Ponsoni & Michiel B. Vandegehuchte

For citation to the published work reprinted in this thesis, please refer to the original publications (as mentioned at the beginning of each chapter).

Please cite this thesis as:

Ollevier, A. (2024) Through the lens of a Video Plankton Recorder: Optical imaging and insights into zooplankton ecology. PhD Thesis, Ghent University, Belgium



**Through the lens of a Video Plankton Recorder:  
Optical imaging and insights into zooplankton ecology**

Door de lens van een Video Plankton Recorder:  
Optische beeldvorming en inzichten in zoöplankton  
ecologie

**Anouk Ollevier**

**Promotors**

Prof. Dr. Marleen De Troch (UGent)

Prof. Dr. Pascal Hablützel (VLIZ)

Academic year 2023-2024

Thesis submitted in partial fulfillment of the requirements for the degree of Doctor in Sciences:  
Marine Sciences





## **Promotors**

Prof. Dr. Marleen De Troch *Ghent University (UGent), Belgium*

Prof. Dr. Pascal Hablützel *Flanders Marine Institute (VLIZ), Belgium*

*Vrije Universiteit Brussel (VUB), Belgium*

## **Supervisors**

Jonas Mortelmans *Flanders Marine Institute (VLIZ), Belgium*

Klaas Deneudt *Flanders Marine Institute (VLIZ), Belgium*

## **Members of the examination committee**

Prof. Dr. ir. Jana Asselman *Ghent University (UGent), Belgium*

Prof. Dr. Jan Mees *Flanders Marine Institute (VLIZ), Belgium*

*Ghent University (UGent), Belgium*

Prof. Dr. Tom Moens (chair) *Ghent University (UGent), Belgium*

Dr. Klas Ove Möller *Helmholtz-Zentrum Hereon (Hereon),  
Germany*

Prof. Dr. Koen Sabbe *Ghent University (UGent), Belgium*

Dr. Lodewijk van Walraven *Wageningen Marine Research (WUR), Den  
Helder, The Netherlands*



# Table of contents

Dankwoord.....	i
Summary.....	iii
Samenvatting.....	vii
<b>Chapter 1 General introduction.....</b>	<b>1</b>
1.1 Plankton in the world's ocean.....	2
1.2 Innovations and hurdles in plankton sampling techniques.....	8
1.3 Research questions and thesis outline.....	12
<b>Chapter 2 A Video Plankton Recorder user guide: Lessons learned from in situ plankton imaging in shallow and turbid coastal waters in the Belgian part of the North Sea.....</b>	<b>17</b>
2.1 Introduction.....	19
2.2 Methodology.....	20
2.3 Results.....	26
2.4 Discussion.....	32
2.5 Conclusion.....	39
<b>Chapter 3 Picturing plankton: How optical imaging methods can improve assessing plankton community dynamics.....</b>	<b>41</b>
3.1 Introduction.....	43
3.2 Methodology.....	44
3.3 Results.....	50
3.4 Discussion.....	59

## TABLE OF CONTENTS

3.5 Conclusion.....	64
<b>Chapter 4 Diel vertical migration and tidal influences on plankton densities in dynamic coastal systems.....</b>	<b>67</b>
4.1 Introduction.....	69
4.2 Methodology.....	71
4.3 Results.....	74
4.4 Discussion .....	80
4.5 Conclusion.....	84
<b>Chapter 5 Plankton fatty acid profiles in West Greenland: Implications for trophic relationships in a changing climate .....</b>	<b>87</b>
5.1 Introduction.....	89
5.2 Methodology.....	90
5.3 Results.....	96
5.4 Discussion .....	104
5.5 Conclusion.....	109
<b>Chapter 6 General discussion.....</b>	<b>113</b>
6.1 Plankton diversity and community composition .....	114
6.2 Spatiotemporal patterns and environmental conditions .....	120
6.3 Trophic interactions and food webs.....	127
6.4 General conclusion.....	128
Cited literature .....	133
Supplementary material .....	157
Publication list.....	181

# Dankwoord

Vier en een half jaar zijn naar mijn gevoel voorbijgevlogen. Toch is het moment nu aangebroken waarop ik in dit proefschrift kan tonen waar ik al die tijd mee bezig was. Het is ook het moment waarop ik mijn oprechte dank kan uitspreken aan degenen die in grote of kleine mate hebben bijgedragen, want zonder hen zou dit doctoraat zijn huidige vorm niet hebben aangenomen.

Eerst en vooral wil ik mijn begeleider Jonas bedanken, wiens kennis over zoöplankton en de Noordzee mijn onderzoek heeft gevormd. Je passie, verbazing en enthousiasme van resultaten, hoe klein of hoe groot, werkten aanstekelijk en inspirerend. Je hebt mij begeleid gedurende het hele traject, maakte me wegwijs in de wondere wereld van het plankton en bood hulp om de juiste koers te varen. Ik ben blij dat ik al die jaren aan je zij mocht helpen met de LifeWatch campagnes, momenten die me nog lang zullen bijblijven. Ook Klaas wil ik graag bedanken voor de kans die ik heb gekregen om bij het MOC-team te starten, voor je vele werk achter de schermen, en voor het mede mogelijk maken van de campagne naar Groenland.

Marleen, onze paden hebben elkaar al eerder gekruist, maar ik ben blij dat ik uiteindelijk de kans kreeg om een doctoraat te starten in samenwerking met de onderzoeksgroep Mariene Biologie van de UGent, onder jouw begeleiding als promotor. Bedankt om mede te waken over de biologische insteek van de thesis en voor je bemoedigende en motiverende woorden wanneer ik het overzicht even verloor.

Pascal, door omstandigheden nam je pas laat het roer over als mijn VLIZ promotor, maar ik mag me gelukkig prijzen met zo'n betrokken promotor als jij. Ik heb veel geleerd van je kritische blik, je statistische hulp en je streven naar excellentie. Dit alles heeft mijn PhD zonder twijfel naar een hoger niveau getild.

Roeland, we beleefden onze eerste dag op het VLIZ samen, maar wisten toen nog niet dat we zo nauw zouden samenwerken. Ik durf te zeggen dat er zonder jou geen VPR, of toch zeker geen

## DANKWOORD

functionerende VPR, geweest zou zijn. Bedankt voor alle technische hulp en je gezelschap tijdens de vele campagnes.

Wieter, jouw aanmoediging om te dromen en groots te denken, maakte onderzoek op één van de mooiste plekken op aarde mogelijk. De onderzoekscruise naar Groenland was dan ook het hoogtepunt van mijn doctoraatstraject. Het was een genoegen om deze met jou en de rest van het fantastisch team mee te maken. Mijn tijd aan boord was werkelijk onvergetelijk.

Daarnaast zijn er ook heel wat anderen die een bijdrage hebben geleverd; gaande van samenwerkingen, technische of IT-hulp, het verzorgen van een vlotte dataflow, logistieke diensten, hulp aan boord van onderzoeksschepen, het valideren van VPR-beelden en het analyseren van data. Daarom ook een dikke merci aan Nick, Rune, Wout, Roeland, Bruno, Leandro, Nore, Thomas, Lorenz, Dick, Klas, het IT en infrastructuur departement van VLIZ, de bemanning van de Simon Steven, en de stagairs en thesisstudenten die ik mocht begeleiden.

I'd also like to thank my fellow PhD students and colleagues at VLIZ for creating such a pleasant atmosphere and making VLIZ a great place to work. Many of you are more than just colleagues and the many moments and laughs we shared will be an everlasting memory. During my last PhD year, I received an equally warm welcome by the marbiol and copepod group at UGhent for which I am very grateful.

Verder wil ik mijn familie en vrienden bedanken voor hun onvoorwaardelijke steun, aanmoedigingen en de nodige afleiding. Een bijzondere vermelding gaat hierbij uit naar mijn verloofde Floris. Dankjewel om er altijd te zijn voor mij, voor je wijze raad en voor het nalezen van mijn teksten. Jouw steun en hulp waren van onschatbare waarde, en jij was misschien wel mijn grootste motivator om de titel van Dr. in de wacht te slepen.

# Summary

Plankton play a crucial role in the marine ecosystem and provide various ecosystem functions. They dominate marine life in terms of abundance and biomass and are essential contributors to the food web and biological carbon pump. In addition, plankton can act as sentinels in a changing world. Due to their fundamental ecosystem functions, sheer abundance, and role as bioindicators it is important to study, understand and monitor plankton. For a long time, plankton nets captured our knowledge of plankton. However, to overcome the limitations inherent to net samples and to enhance spatiotemporal resolution, *in situ* optical methods that photograph plankton inside the water column such as a Video Plankton Recorder (VPR) have been developed. As the VPR takes photographs inside the water column while being towed by a vessel, it allows to observe organisms without damaging them and to collect simultaneous depth and environmental data. The aim of this PhD thesis is to assess the applicability of the VPR for plankton research (chapters 2 - 3) and to use this device to gain insights into plankton ecology (chapters 4 - 5).

In **chapter 2** of this PhD thesis, the VPR was examined as a sampling technique for zooplankton observations. To determine how and where the VPR can be best used, three continuous towing procedures and four magnification settings of the VPR were compared to find the most suitable sampling methodology for plankton studies and to allow future VPR users to make a well-considered choice on VPR deployment method for their research purpose. When the VPR is towed behind a research vessel, the vessel can sail in different directions and make different patterns. For three different towing procedures the practical feasibility, characteristics and output were assessed and the assets and liabilities for each of the tow types were discussed. A Z-shaped and a clover-shaped tow type were the best fit for detailed characterization of the plankton community in a limited geographical area. A straight tow type was more suitable for plankton studies over a larger area, with the potential to capture local plankton abundance peaks and to determine its relation with the spatial variation of the environmental conditions. The capacity of the various VPR magnification settings to capture specific plankton taxa or size groups, was tested during four straight line transects with different magnifications. The VPR offered a range of four

## SUMMARY

magnification settings, which had a direct impact on the size range of the captured particles. A higher magnification was effective for smaller organisms (0.3 – 0.7 mm), while a lower magnification was better for larger organisms (1.0 – 3.8 mm). The size of the plankton specimen or plankton community under study should determine the used magnification setting. In addition, also the turbidity limit of the VPR was investigated by sailing through various turbidity levels. Elevated turbidity levels resulted in blurry images and reduced contrast between plankton particles and the background. Turbidity values higher than 6.2 NTU inhibited the collection of usable data for plankton research, making the VPR not usable in turbid coastal waters. The study underscored the significant influence of water turbidity on the VPR's applicability, and the general limitations of turbidity for optical imaging devices. The VPR's efficacy was contingent upon the choice of towing procedures, magnification settings, and the level of water turbidity. Researchers must consider these factors when designing studies in coastal and transitional waters.

**Chapter 3** focused on assessing the accuracy of the VPR in evaluating zooplankton communities compared to conventional net-based sampling methods. This evaluation took into account different oceanic and coastal conditions. It compared spatial and temporal patterns in plankton densities and communities using VPR, WP2 and MultiNet samples from two distinct environments: one with clear waters and low plankton densities (Greenland) and the other with more turbid waters and higher plankton densities (southern North Sea). The comparison between VPR and net-based approaches revealed varying estimations of plankton density, influenced by the environmental characteristics of the study area and the specific plankton community. In the southern North Sea, the VPR consistently underestimated zooplankton densities as compared to the WP2 net. However, in Greenland, density estimates were more aligned with those from the MultiNet. Factors such as water column turbidity, plankton size, community density, and net mesh size were identified as likely contributors to these discrepancies between sampling sites. This indicated that the VPR tends to be more effective in clear waters with lower plankton densities. Both net and optical methods observed 24-hour fluctuations in plankton densities, suggesting that both methodologies capture changes in plankton populations. However, the complexity of using calibration factors became apparent, revealing the need for area and taxa-specific adjustments, which might also vary seasonally. In addition, the non-invasive nature of the VPR allowed for better quantitative estimations of fragile and gelatinous organisms, presenting an advantage in its ability to observe these organisms without causing damage. In summary, despite variations in density estimates between net and optical methods in specific environments, optical methods demonstrated an ability to capture similar short-term patterns. Consequently, optical methods could complement traditional net



sampling by quantitatively estimating fragile and gelatinous taxa and they possess the potential to offer valuable and deeper insights into zooplankton ecology and distribution that traditional nets cannot provide. This enhancement allows for a deeper understanding of the role of zooplankton in marine ecosystems.

In **chapter 4**, the VPR was used in a small-scale study in the Belgian part of the North Sea (BPNS) to research how plankton is distributed over fine spatial and temporal scales in dynamic coastal systems under strong tidal forces. Data was collected at a fixed station over a 24-hour period, encompassing both tidal and diel cycles. We detected vertical migration patterns in both pelagic and benthic taxa. Although much is known about these migration patterns in pelagic environments, this information is lacking from shallow coastal systems. Notably, this study is the first to describe the vertical migration of the hyperbenthic taxa Amphipoda and Cumacea from the sea bottom to high up into the water column at night in the BPNS, shedding new light on the dynamics of invertebrate communities in shallow coastal waters. Moreover, our observations showed significant fluctuations in plankton and detritus densities over the 24-hour span, with density peaks aligning with the patterns of a tidal cycle, albeit with some time lags relative to high or low tide. We infer that a plankton patch with higher densities was oscillating back and forth with the tidal currents, rather than the tides themselves had a direct effect on the plankton community. The tidal cycle emerged as a pivotal factor in elucidating a significant portion of the variability in plankton densities, being different from the more commonly recognized factors such as phenological or seasonal fluctuations. The considerable variation in plankton densities over a 24-hour period, highlighted the patchy distribution of plankton and emphasized the importance of considering tidal currents when analyzing data from stationary observations. This small-scale geographic variation in plankton densities has implications for ecosystem assessment, biodiversity prediction, and overall understanding of plankton ecology in coastal environments.

In **chapter 5**, a large-scale study is performed in the fjords and shelf area of West Greenland. This chapter focused on how the fatty acid (FA) composition of plankton varies across different zooplankton size classes within fjords, and how copepods are distributed along and within fjords. Climate change-induced warming, particularly pronounced in high-latitude regions such as the Arctic, is causing rapid changes in marine ecosystems. To study the potential effects on the food quality of zooplankton for higher trophic levels, this study analyzed the FA profiles of micro and mesozooplankton using gas chromatography and mass spectrometry, and linked with the distribution of copepods by deploying a VPR. Significant differences in FA composition between micro and mesozooplankton indicated potential consequences for the nutritional quality of prey for higher trophic levels, with lower content of polyunsaturated FAs such as stearidonic acid (18:4(n-3)) in microzooplankton. These variations in FA profiles of zooplankton were partly

## SUMMARY

attributed to taxonomy or phylogenetic constraints, in addition to dietary influences. Plankton distribution along a gradient from the offshore shelf area towards the inner fjord showed large variation. Large copepods dominated the offshore areas whereas small copepods were more abundant in the inner fjord. Small copepods showed a preference for deeper waters compared to large copepods and had in-fjord peak abundances around 20 - 30 m depth compared to the in-fjord peaks of large copepods at 5 - 20 m. In addition, small copepods were distributed in low abundances throughout the deeper water. Anticipating climate-driven shifts in plankton communities, we hint at a future scenario with a change in quality and distribution of FAs. Alterations in food quality may exert a negative influence on fish and higher trophic levels, yielding repercussions for the overall functioning of the ecosystem.

# Samenvatting

Planktonische organismen spelen een cruciale rol in het mariene ecosysteem en voorzien verschillende ecosysteemfuncties. Ze domineren het mariene leven in termen van densiteiten en biomassa en leveren een essentiële bijdrage aan het voedselweb en de biologische koolstofpomp. Daarnaast kan het plankton fungeren als vroege indicator van een snel veranderende mariene wereld. Vanwege hun fundamentele functies in ecosystemen, hun enorme densiteiten en hun rol als bio-indicatoren is het belangrijk om plankton te bestuderen, te begrijpen en te monitoren. Lange tijd werd onze kennis van het plankton verworven met behulp van planktonnetten. Om de tekortkomingen van net stalen te overwinnen en de spatiotemporele resolutie te verbeteren zijn er echter *in situ* optische instrumenten ontwikkeld die plankton in de waterkolom fotograferen, zoals de Video Plankton Recorder (VPR). Aangezien de VPR foto's maakt in de waterkolom terwijl het wordt voortgetrokken door een schip, kunnen organismen in hun natuurlijke oriëntatie worden geobserveerd zonder ze te beschadigen en kan tegelijkertijd data over diepte en omgeving worden verzameld. Het doel van deze thesis is enerzijds om een beoordeling te maken van de toepasbaarheid van de VPR bij planktononderzoek (hoofdstuk 2 - 3), anderzijds om door middel van deze methode inzichten te verwerven in de ecologie van het plankton (hoofdstuk 4 - 5).

In **hoofdstuk 2** van dit doctoraat werd de VPR onderzocht als methode voor het observeren van zoöplankton. Om te bepalen hoe en waar de VPR het best gebruikt kan worden, werden drie continue sleepprocedures en vier vergrotingsinstellingen van de VPR vergeleken. Zo slaagden we erin om de meest geschikte staalnamemethode voor planktonstudies te vinden en toekomstige VPR-gebruikers een leidraad te bieden bij het inzetten van de VPR voor hun specifieke onderzoeksdoel. Wanneer de VPR achter een onderzoeksschip wordt gesleept, kan het schip in verschillende richtingen varen en verschillende patronen maken. Voor drie verschillende sleepprocedures werden de praktische haalbaarheid, kenmerken en uitkomst beoordeeld en werden de voor- en nadelen van elke procedure besproken. Een Z-vormige en een klavervormige sleepprocedure bleken het meest geschikt voor een gedetailleerde karakterisering van de

## SAMENVATTING

planktongemeenschap in een beperkt geografisch gebied. Een rechte sleepprocedure was dan weer geschikt voor planktonstudies over een groter gebied. Deze laatste sleepprocedure bood de mogelijkheid om lokale pieken in planktondensiteiten vast te leggen en de relatie met de omgevingsgebonden variabelen beter te bepalen. De capaciteit van de verschillende vergrotingsinstellingen van de VPR om specifieke planktontaxa of -groottegroepen vast te leggen, werd getest tijdens vier rechte lijntranssecten met verschillende vergrotingen. De VPR heeft vier vergrotingsinstellingen, die een directe invloed hadden op de grootte van de geobserveerde partikels. Een hogere vergroting was effectief voor kleinere organismen (0,3 - 0,7 mm), terwijl een lagere vergroting beter was voor grotere organismen (1,0 - 3,8 mm). De grootte van het bestudeerde planktonorganisme of -gemeenschap moet de gebruikte vergrotingsinstelling bepalen. Tenslotte werd ook de troebelheidsgrens van de VPR onderzocht door langsheen verschillende troebelheidsniveaus te varen. Hogere troebelheidsniveaus resulteerden in wazige beelden en een verminderd contrast tussen planktondeeltjes en de achtergrond. Troebelheidswaarden hoger dan 6,2 NTU verhinderden het verzamelen van bruikbare plankton data, waardoor de VPR niet bruikbaar was in kustwateren. Het onderzoek onderstreepte de significante invloed van de troebelheid van het water op de toepasbaarheid van de VPR en de algemene beperkingen van troebelheid voor optische beeldvormingsapparaten. Samengevat blijkt de doeltreffendheid van de VPR afhankelijk te zijn van de keuze van de sleepprocedures, de vergrotingsinstellingen en de troebelheid van het water. Onderzoekers moeten met deze factoren dan ook rekening houden bij het ontwerpen van studies in kustwateren en overgangswateren, maar kunnen zich op deze studie beroepen als leidraad.

**Hoofdstuk 3** richtte zich op het beoordelen van de nauwkeurigheid van de VPR bij het evalueren van zoöplanktongemeenschappen in vergelijking met conventionele staalnamemethoden met netten. Bij deze evaluatie werd rekening gehouden met verschillende ocean- en kustomstandigheden. De ruimtelijke en temporele patronen in planktondensiteiten en -gemeenschappen werden vergeleken aan de hand van VPR, WP2 en MultiNet stalen uit twee verschillende omgevingen: één met helder water en lage planktonconcentraties (Groenland) en één met meer troebel water en hogere planktonconcentraties (zuidelijke Noordzee). De vergelijking tussen de VPR en de netten toonden zeer verschillende schattingen van planktondensiteiten, die beïnvloed werden door de milieukeurmerken van het studiegebied en de specifieke planktongemeenschap. In de zuidelijke Noordzee onderschatte de VPR consequent de zoöplanktondensiteit in tegenstelling tot het WP2-net. In Groenland kwamen de densiteitsschattingen echter meer overeen met die van het MultiNet. Factoren zoals de troebelheid van de waterkolom, de grootte van het plankton, de densiteit van de planktongemeenschap en de maaswijdte van het net waren factoren die waarschijnlijk

bijdroegen aan de verschillen tussen de staalnamelocaties. Dit suggereert dat de VPR effectiever is in helder water met lagere planktondensiteiten. Zowel bij de netten als bij de optische methoden werden 24-uursfluctuaties in de planktondensiteit waargenomen, wat toont dat beide methoden veranderingen in planktonpopulaties registreren. Bovendien maakte de niet-invasieve aard van de VPR betere kwantitatieve schattingen van fragiele en geleiachtige organismen mogelijk, wat een voordeel is omdat deze organismen geobserveerd kunnen worden zonder schade aan te richten. Samenvattend, ondanks variaties in densiteitsschattingen tussen netten en optische methoden in specifieke omgevingen, lieten optische methoden zien dat ze in staat waren om vergelijkbare kortetermijnpatronen vast te leggen. Bijgevolg kunnen optische methoden een aanvulling vormen op de traditionele staalnames met netten door een kwantitatieve schatting te maken van fragiele en geleiachtige taxa en bezitten ze het potentieel om waardevolle en diepere inzichten te bieden in de ecologie en verspreiding van zoöplankton die traditionele netten niet kunnen bieden. Deze verbetering draagt bij aan het beter begrijpen van de rol van het zoöplankton in mariene ecosystemen.

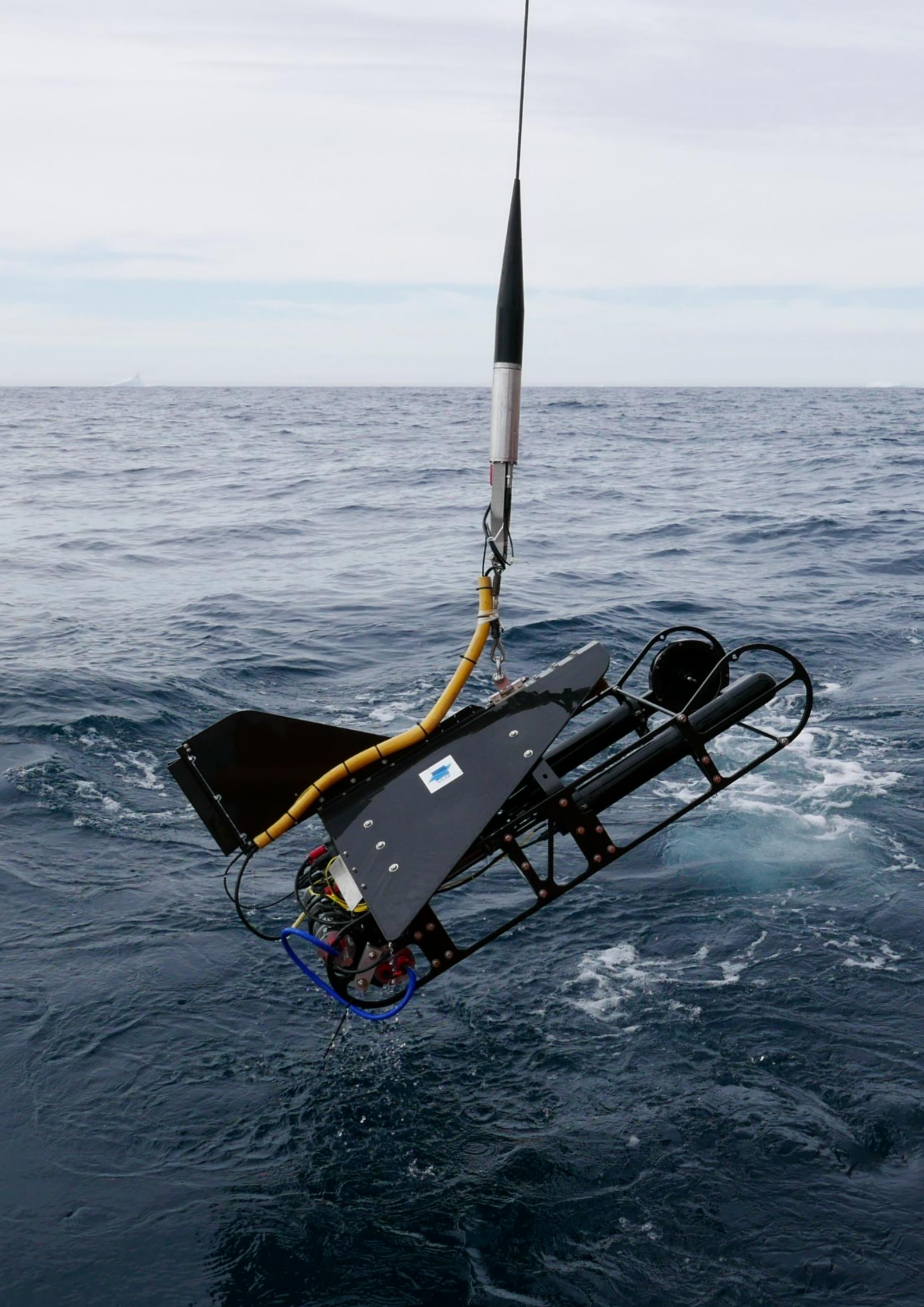
In **hoofdstuk 4** werd de VPR gebruikt in een fjnshalig onderzoek in de Belgisch deel van de Noordzee (BDNZ). We gingen na hoe het plankton zich verdeelt over fijne ruimtelijke en temporele schalen in dynamische kustsystemen met sterke getijden. De gegevens werden verzameld op een vast station gedurende een periode van 24 uur, wat zowel getijden als diurnale cycli omvatte. We ontdekten verticale migratiepatronen in zowel pelagische als bentische taxa. Hoewel er veel bekend is over deze migratiepatronen in pelagische milieus, is dat niet het geval in ondiepe kustsystemen. Deze studie is de eerste die de verticale migratie beschrijft van de hyperbentische taxa Amphipoda en Cumacea van de zeebodem naar hoog in de waterkolom gedurende de nacht in het BDNZ en werpt daarmee een nieuw licht op de dynamieken van ongewervelde gemeenschappen in ondiepe kustwateren. Bovendien toonden onze waarnemingen significante fluctuaties in de densiteiten van het plankton en detritus over een periode van 24 uur, waarbij de densiteitspieken overeenkwamen met de patronen van een getijdencyclus, zij het met enige vertraging ten opzichte van hoog- of laagwater. We leiden hieruit af dat een planktonwolk met hogere dichtheden heen en weer beweegt met de getijdenstromingen, en dat de getijden zelf geen direct effect lijken te hebben op de samenstelling van de planktongemeenschap. De getijdencyclus bleek een cruciale factor te zijn die een aanzienlijk deel van de variabiliteit in planktondensiteiten verklaarde, naast de meer algemeen erkende factoren zoals fenologische of seizoensfluctuaties. De aanzienlijke variatie in planktondensiteiten over een periode van 24 uur, benadrukte de fragmentarische verspreiding van het plankton en wees op het belang om rekening te houden met getijdenstromingen bij het analyseren van gegevens van stationaire waarnemingen. Deze kleinschalige geografische variatie

## SAMENVATTING

in planktondensiteiten heeft implicaties voor de beoordeling van ecosystemen, de voorspelling van biodiversiteit en de algemene inzichten in de planktonecologie in kustomgevingen.

In **hoofdstuk 5** is een grootschalig onderzoek uitgevoerd in de fjorden en het continentaal plat van West-Groenland. Dit hoofdstuk richtte zich op hoe de vetzuursamenstelling van het plankton varieert tussen verschillende zoöplanktongrootteklassen binnen fjorden, en hoe eenoogkreeftjes zich verspreiden langs en binnen fjorden. Klimaatopwarming veroorzaakt snelle veranderingen in mariene ecosystemen, vooral in gebieden op hoge breedtegraden zoals het noordpoolgebied. Om de mogelijke effecten op de voedselkwaliteit van zoöplankton te bestuderen, analyseerde deze studie de vetzuurprofielen van het micro- en mesozoöplankton met behulp van gaschromatografie en massaspectrometrie, en richtte zich op de distributie van eenoogkreeftjes door het gebruik van een VPR. Significante verschillen in vetzuursamenstelling tussen het micro- en mesozoöplankton wezen op mogelijke gevolgen voor de voedingskwaliteit van het plankton voor hogere trofische niveaus, met een lager gehalte aan meervoudig onverzadigde vetzuren zoals stearidonzuur (18:4(n-3)) in het microzoöplankton. Deze variaties in vetzuurprofielen van het zoöplankton werden deels toegeschreven aan taxonomie of fylogenetische beperkingen, naast invloeden door dieet. De verspreiding van het plankton langs een gradiënt van het continentaal plat naar het centrale deel van de fjord vertoonde een grote variatie. Grote eenoogkreeftjes domineerden de offshore gebieden, terwijl kleine eenoogkreeftjes talrijker waren in de fjorden. Kleine eenoogkreeftjes hadden een voorkeur voor diepere wateren in vergelijking met grote eenoogkreeftjes en hadden een piekdichtheid in de fjorden rond de 20 - 30 m diepte in vergelijking met de pieken van grote eenoogkreeftjes in de fjorden op 5 - 20 m diepte. In anticipatie op verschuivingen in planktongemeenschappen als gevolg van klimaatverandering, schetsen wij een toekomstscenario waarin er een verandering optreedt in zowel de kwaliteit als de verdeling van vetzuren. Veranderingen in de voedselkwaliteit kunnen een negatieve invloed hebben op vissen en hogere trofische niveaus, met gevolgen voor het algehele functioneren van het ecosysteem.







# 1

General introduction

## 1.1 Plankton in the world's ocean

### 1.1.1 What are plankton?

The marine environment covers 71 % of Earth's surface and is inhabited by a myriad of life forms (Appeltans *et al.*, 2012). Among these inhabitants, planktonic organisms emerge as key players, ubiquitous and dominating life in the ocean in terms of abundance and biomass (Bar-On and Milo, 2019), with concentrations reaching up to millions of cells per cubic meter of water (Sidabutar *et al.*, 2020). Plankton, named after the Greek "planktos" meaning "drifter", are a taxonomically diverse group of organisms composed of plants, animals and bacteria that are adrift on the currents. They are defined by their incapability to swim against the prevailing currents and instead are carried by the water's movements (Hedgpeth and Ladd, 1957). Within this community, there are two primary categories of functional groups: phytoplankton, which bear resemblance to plant-like organisms, and zooplankton, which refer to the animal constituents. Additionally, there are bacterioplankton, comprising the bacterial elements, and virioplankton, which encompass the viral components within this ecosystem. Planktonic organisms span a broad size range and can also be categorized according to size. They can be categorized as femtoplankton ( $< 0.2 \mu\text{m}$ , e.g., marine viruses), picoplankton ( $0.2 - 2 \mu\text{m}$ ), nanoplankton ( $2 - 20 \mu\text{m}$ ), microplankton ( $20 - 200 \mu\text{m}$ ), mesoplankton ( $0.2 - 20 \text{mm}$ , e.g., many zooplankton species), macroplankton ( $2 - 20 \text{cm}$ ), and megaplankton ( $> 20 \text{cm}$ , e.g., the lion's mane jellyfish reaching a hood diameter of 2.3 m) (Omori and Ikeda, 1992). Despite being often almost invisible to the naked eye, plankton play a pivotal role in marine ecosystems.

### 1.1.2 Global importance of plankton

At the base of the marine food web (Figure 1.1), phytoplankton takes a prominent position. These microalgae utilize sunlight and nutrients to perform photosynthesis and produce organic matter, which serves as the primary energy source for marine life. During this process they convert carbon dioxide into oxygen, producing about half of the Earth's oxygen which makes them one of the planet's most important producers of oxygen (Field *et al.*, 1998). Whereas phytoplankton are the main primary producers in marine ecosystems, zooplankton are the main primary consumers. They mainly feed themselves by grazing on phytoplankton, but bacteria, detritus, or other zooplankton also belong to the diet of certain species. They consist of species such as krill, copepods, and jellyfish, but also many fish and bottom-dwelling organisms start their life as plankton. Zooplankton, in turn, are consumed by a variety of larger organisms, including economically important fish species, seabirds and marine mammals. It is interesting to note that the ocean's most colossal inhabitants, like baleen whales, feed solely on zooplankton (Murison

and Gaskin, 1989). Zooplankton thus form the crucial link between the primary producers and higher trophic levels and ensure the flow of energy and nutrients from the bottom to the top of the marine food web, supporting a diverse array of marine life. In the marine food web, bacterioplankton are responsible for decomposing particulate organic matter, which includes detritus from phytoplankton. Through this process, they regenerate essential nutrients and recycle dissolved components, which in turn can be reused by phytoplankton (Bowman and Ducklow, 2019).

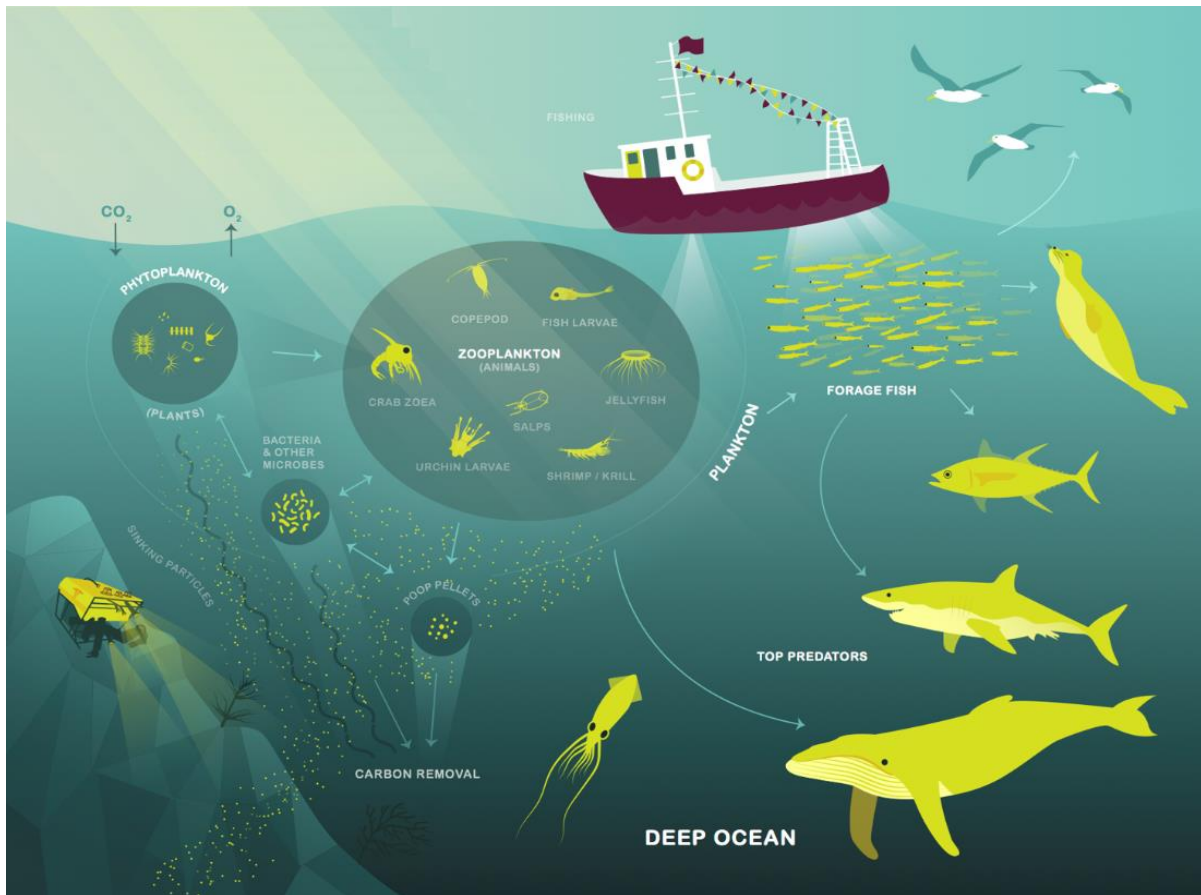


Figure 1.1. Schematic illustration of the marine food web, the interaction between zooplankton and other trophic levels, and the ecosystem services the marine food web provides. Illustration adjusted from Aurelia *et al.* (2014).

Plankton also contribute to the ocean's capacity to absorb and store carbon dioxide, thereby playing a vital role in mitigating the effects of climate change (Reid *et al.*, 2009, Richardson, 2008). About 30 % of current anthropogenic emissions of CO<sub>2</sub> has been taken up by oceans, reducing its contribution as a greenhouse gas in the atmosphere (IPCC, 2021). The ocean's capability to function as a sink for carbon partly relies on a process known as the biological carbon pump (Figure 1.2), where plankton aids in the transport of organic carbon created by phytoplankton to deeper waters. Zooplankton, through their consumption of phytoplankton and other organic

particles, accumulate carbon within their bodies. This carbon biomass can be quite substantial. For instance, the Antarctic krill species *Euphausia superba* contributes approximately 0.05 gigatons of carbon to the global biomass, placing them on par with other prominent species like humans (Bar-On *et al.*, 2018). When phyto- and zooplankton die or excrete waste, they release this carbon in the form of sinking particles ('gravitational pump'). Much of the organic carbon in these particles are recycled via heterotrophic microbes back into the water as dissolved inorganic carbon (DIC). A small fraction of the organic matter is exported from the surface layers of the ocean to the deeper, colder layers, effectively sequestering carbon as DIC in the deep ocean and sediments for extended periods up to hundreds or thousands of years. Zooplankton further enhance the efficiency of carbon transport to the deep ocean depths through their daily migration or seasonal diapausing behavior ('migrant pump'). The latter functions as an impactful seasonal lipid pump, effectively sequestering carbon into the deep ocean and is estimated to contribute to approximately 10 % of the overall biological carbon pump (Boyd *et al.*, 2019; Jónasdóttir *et al.*, 2015).

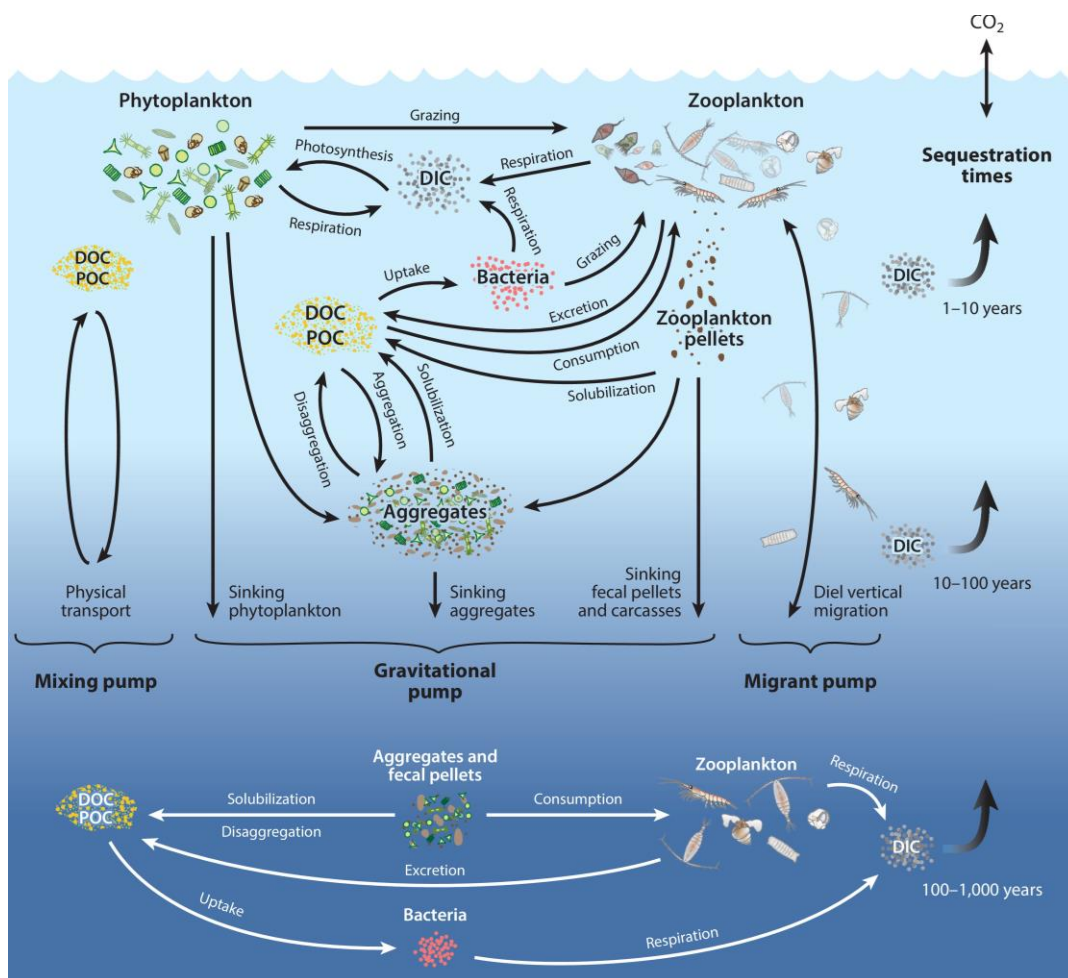


Figure 1.2 Diagram illustrating the three export pathways of the biological pump, their regulating processes, and the timescales for carbon sequestration. (a) The euphotic-zone food web and the

many ecological and biogeochemical processes regulating its relationship with the gravitational, migrant, and mixing pumps that transport organic carbon to depth. (b) Beneath the euphotic zone, organic carbon is remineralized back to DIC via food-web processes in the mesopelagic zone. The depths to which that organic carbon is transported set the timescale of its sequestration. Abbreviations: DIC, dissolved inorganic carbon; DOC, dissolved organic carbon; POC, particulate organic carbon. (Illustration and caption from Siegel *et al.*, 2023)

### 1.1.3 Indicators of ecosystem change

Zooplankton communities serve as useful bioindicators of ecosystem health due to their sensitivity to alterations in environmental conditions, whether these are arising from natural or anthropogenic sources. In our ever-changing world characterized by climate change, rising sea surface temperatures, and ocean acidification, this makes zooplankton valuable organisms for assessing the impact of human activities on marine ecosystems. Several characteristics make zooplankton well-suited as bioindicators. Firstly, the majority of zooplankton species are poikilothermic, meaning their physiological functions are directly influenced by fluctuations in environmental factors such as ambient temperatures (references in Huntley *et al.*, 1992). Secondly, zooplankton possess fast generation times and often exhibit short life spans (Hays *et al.*, 2005). These traits enable a quick detection of potential impacts, as alterations in the environment are readily observable in subsequent generations of these organisms. Furthermore, most plankton species are not subject to harvesting efforts, with the exception of certain instances such as jellyfish fisheries in southeast Asia primarily for food consumption, or the harvesting of krill and *Calanus* fisheries for dietary supplements (see Box 1) and/or aquaculture and animal feed (Prado-Cabrero and Nolan, 2021; Nicol and Foster, 2002; Omori and Nakano, 2001; Omori, 1978). Consequently, trends observed in zooplankton populations predominantly reflect environmental or biological influences rather than the consequences of their exploitation, unlike studies on other marine groups such as fish (Richardson, 2008). This attribute enhances their reliability as indicators of ecosystem health and changes therein. Furthermore, plankton may serve as more responsive indicators of environmental changes compared to the environmental variables themselves, owing to the potential of plankton communities to amplify subtle signals in the environment (Taylor *et al.*, 2002). Resulting from these features, plankton data for example finds application in the Marine Strategy Framework Directive, where plankton abundance, biomass, and life form pairs are instrumental for the status assessment of pelagic habitats, and for descriptors related to biodiversity, food webs, and eutrophication (Bedford *et al.*, 2018). This EU directive establishes a framework to safeguard the marine environment in European waters, using 'state indicators' to gauge the 'Good Environmental Status' of ecosystem components.

## CHAPTER 1

In the context of climate change, the establishment of long-term time-series, described as studies where ecological data is systematically collected from one or multiple sites over a period of more than 10 years (Giron-Nava *et al.*, 2017; Lindenmayer *et al.*, 2012), is increasingly important to detect zooplankton responses to climate-induced stressors (Semmour *et al.*, 2023). As previously noted, temperature plays a crucial role in zooplankton physiology and growth, but it also serves as a fundamental determinant of their habitat. As a result, the ongoing ocean warming is causing significant shifts in the distribution range, phenology timing, and body size of zooplankton (Ratnarajah *et al.*, 2023). Typically, these shifts encompass a poleward geographical migration, an earlier seasonal timing of spring or summer species and later occurrence of autumn species, and shift toward smaller sizes in warmer conditions (references in Richardson, 2008). For example, the Continuous Plankton Recorder survey that has been running since the 1940s revealed a climate-related northward shift of temperate zooplankton by more than 10 degrees latitude between 1960 and 1999 (Beaugrand *et al.*, 2002). In the Subarctic North Pacific Ocean the timing of the annual maximum of the dominant copepod species (*Neocalanus plumchrus*) has shifted dramatically over the past 50 years, with biomass peaking 60 days earlier in warm than in cold years (Mackas *et al.*, 1998). A global study by Campbell *et al.* (2021) reported that temperature better predicted copepod size than did latitude or oxygen, with body size decreasing by 43.9 % across the temperature range (-1.7 to 30 °C). Other time-series initiatives in the North Sea include the LifeWatch project in Belgium (Mortelmans *et al.*, 2019) or the Helgoland Road data-series in Germany (Wiltshire *et al.*, 2009) and the need for such monitoring programs has been pointed out numerous times (Ratnarajah *et al.*, 2023; Boon and Kromkamp, 2022; Hays *et al.*, 2005). In addition, data-series also enable the assessment of species introductions (e.g., *Mnemiopsis leidyi*) or potential harmful species (e.g., *Noctiluca scintillans*), and monitor their effects on the local community (Ollevier *et al.*, 2021; Boersma *et al.*, 2007).

### **Box 1. Harvesting of Antarctic krill and the copepod *Calanus finmarchicus* for dietary supplements**

Several companies across the globe are engaged in harvesting zooplankton for the production of dietary supplements. It is known that fish oils are rich in the omega-3 fatty acids (FAs) EPA (eicosapentaenoic acid) and DHA (docosahexaenoic acid). These omega-3's are essential in our diet and have a multitude of health benefits, including enhanced cardiovascular health, vision, cognition, and anti-inflammatory properties (Prado-Cabrero and Nolan, 2021).

In the search for alternative sources of EPA and DHA to reduce the reliance on traditional fish sources, companies have turned their attention to zooplankton species. The growing interest

in harvesting Antarctic krill (*Euphausia superba*) in the Southern Ocean and *Calanus finmarchicus* in Norwegian waters as a source of omega-3 FAs has arisen from the idea that instead of harvesting these FAs from fish, these can be extracted directly from their food source at a lower trophic level. This practice is called ‘fishing down the food web’ (Pauly *et al.*, 1998) and is motivated by the substantial biomasses of these species in our oceans.

However, the harvesting of these species for dietary supplements has raised concerns. Despite the set quota, harvesting zooplankton puts pressure on the local ecosystem. Climate change already affects the exploited Arctic and Antarctic ecosystems and the fisheries may aggravate this impact. Harvesting significant quantities of these species could disrupt these ecosystems due to their pivotal role in marine food webs, affecting higher trophic levels and potentially triggering ecological imbalances (Prado-Cabrero and Nolan, 2021).



Figure 1.3. *Calanus finmarchicus* with its lipid sac indicated in orange. Lipids are mainly stored in a lipid sac which can fill more than 80 % of the body cavity (Lee *et al.*, 2006; Miller *et al.*, 2000). Image from Woods Hole Oceanographic Institution, (n.d.).

### 1.1.4 Plankton distribution disparities

Spatial variability of plankton abundance is a prevalent feature within marine environments. Across diverse scales, spanning from the microscale (ranging from 0.01 to 1 m) to the mesoscale (extending from tens to hundreds of kilometers; Haury *et al.*, 1978), plankton aggregate in both vertical and horizontal dimensions. The formation of these high-density plankton patches is a result of a dynamic interplay between physical processes, such as ocean currents, waves, thermal stratification and the influence of biological mechanisms (Robinson *et al.*, 2021). Although plankton are not able to swim in the opposite direction of the currents, they often are able to determine their vertical position in the water column. The behavior of zooplankton, specifically diel vertical migration (DVM), plays a pivotal role in driving this vertical distribution. During DVM, zooplankton synchronize their vertical movements with the day-night cycle. In the most common form called nocturnal vertical migration, they ascend to the productive surface waters

at night to feed and then descend to deeper waters during daytime to avoid predators that rely on visual hunting (Bandara *et al.*, 2021). Other types are reverse and twilight DVM, where they ascend throughout the day or during the transitional periods of dusk and dawn, respectively (Hutchinson, 1957). Additionally, plankton can also be found at different depths depending on the season, influenced by seasonal changes in the environment. For instance, in Arctic environments copepods engage in seasonal migration (Jónasdóttir *et al.*, 2015). In late summer and autumn, copepods accumulate lipids as crucial reserves. As winter approaches, they move to deeper waters due to the reduced primary production and the harsh conditions in the surface layers. These lipid reserves serve as vital energy stores, sustaining them through the winter or helping with egg production (Madsen *et al.*, 2001; Pasternak *et al.*, 2001). When spring arrives, copepods ascend to the surface, typically at the onset of a spring bloom (Jónasdóttir *et al.*, 2015). The vertical migrations can be strikingly extensive and rapid, with zooplankton traveling hundreds of meters in just a few hours (Behrenfeld *et al.*, 2019). The spatial variability of plankton has ecological consequences for the local grazing rate on phytoplankton (Rothschild and Osborn, 1988), the survival of larval fish (Letcher and Rice, 1997) and thus in general the trophic energy transfer efficiencies through the food web (Robinson *et al.*, 2014). The position and the size of aggregates shape the foraging behavior of predators (Bernard *et al.*, 2017). For example, shallower or larger krill aggregates or prey fields lead to higher encounter rates for visual predators (Grünbaum and Veit, 2003) and reduce the surface recovery time for diving penguins, allowing them to spend more time submerged during foraging (Chappell *et al.*, 1993). Additionally, the spatial variability poses technical challenges, making the collection of representative samples for the system more complicated. Despite the importance of plankton patchiness across diverse spatial scales, our understanding of both the distribution of plankton across these scales and the mechanisms responsible for sustaining these patches remains limited.

## 1.2 Innovations and hurdles in plankton sampling techniques

Given the crucial role plankton play in marine ecosystems and the functions they provide, thorough research on these organisms is valuable. However, studying plankton can be a challenging and complex endeavor. These organisms come in various sizes and exhibit a vast diversity of forms and structures (see Box 2). Their sheer abundance, combined with their broad size spectrum and diversity, makes sampling plankton a challenging task.



Traditional plankton research starts from physically collected samples from nets, water bottle samplers or pumping systems. Plankton nets are considered one of the oldest, simplest and least expensive methods of sampling plankton (Gutkowska *et al.*, 2012). Various nets are being used including an Apstein net, WP2 net, Bongo net, MIKnet, MultiNet, and MOCNESS, designed to target different size classes. They differ in net opening diameter, mesh size, the number of nets, the towing direction (horizontal or vertical tows) or the part of the water column they target (specific depth range or whole water column). Yet, all collect a physical plankton sample in the cod end of the net for further identification.

These samples are typically processed via microscopy in order to identify plankton samples down to the species level and different lifestages. This microscopic analysis provides data regarding species abundance, community composition, and spatial distribution. However, microscopy analysis is a time-consuming and labor-intensive task that requires the expertise of a taxonomic specialist. Even when samples are diluted (e.g., Motoda splitter (Motoda, 1959)), the high densities of plankton can significantly extend the duration of analysis. One way to optimize the processing time of net samples in the lab is by using bench top optical devices like the ZooScan (Grosjean *et al.*, 2004) that facilitate the digitalization of zooplankton samples. The ZooScan employs a scanning bed to systematically image and digitize these samples, creating a comprehensive digital record of the plankton community within the sample. Specialized software and trained classifiers are then used to semi-automate the assignment of names to the organisms in the images to allow automated identification at the lowest taxonomic level possible. However, it is important to note that the image quality is insufficient for classification to species level. A final verification of these identifications by a trained scientist is still necessary, in order to conduct a detailed review to ensure the accuracy and reliability of the data. This technological advancement expedites the initial identification process compared to microscopy. Nonetheless, net sampling methods exhibit additional inherent limitations. These drawbacks encompass their depth integrative nature, resulting in lower fine-scale resolution, and their destructive collection mode, which may lead to inadequate sampling of fragile or gelatinous organisms (Raskoff *et al.*, 2003) that can be damaged or destroyed during net hauls.

### Box 2. Diversity of the drifting world

Ernst Haeckel was a German biologist, naturalist, and artist who lived from 1834 to 1919. One of Haeckel's notable achievements was his extensive research on and illustrations of marine organisms, particularly plankton. His drawings of plankton are remarkable for their aesthetic beauty and his detailed illustrations captured the intricate structures and diversity of these organisms. His work helped to make plankton more accessible and understandable to both the general public and fellow scientists. Therefore, it contributed significantly to our understanding of marine biology and ecology. Through his illustrations and research, numerous species of plankton were classified and described (Dolan, 2019, 2023).

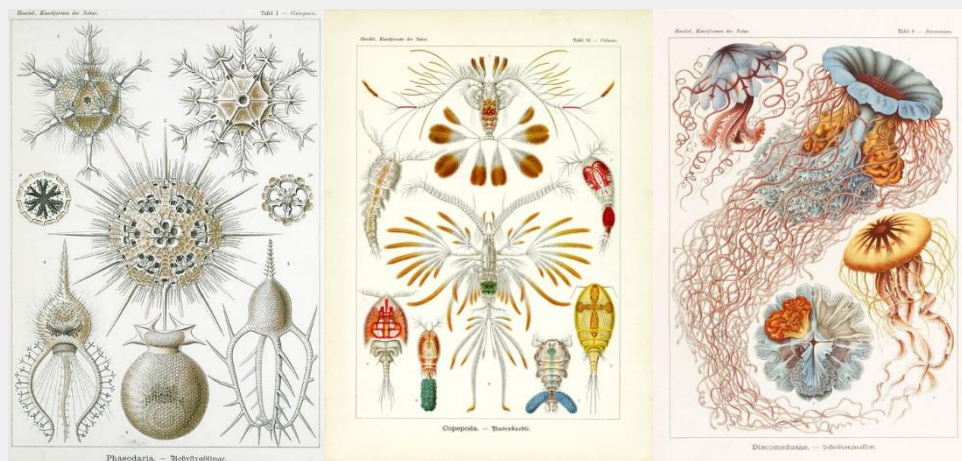


Figure 1.4. Illustrations of phaeodarians, copepods and jellyfishes from Ernst Haeckel's book *Kunstformen der Natur* (Haeckel, 1900).

The drive to enhance zooplankton data collection, particularly in the face of budget constraints and increased demand, along with the prospect of gaining new insights into various facets of zooplankton dynamics and capturing temporal and spatial variance, has spurred the advancement of innovative technologies for collecting zooplankton data. Molecular techniques, such as DNA metabarcoding, have emerged as pivotal tools for plankton identification at species level. These methods delve into the genetic material of plankton, offering an understanding of species composition, genetic diversity, and even functional traits (Hablützel *et al.*, 2021). Concurrently, technical progress has also resulted in optical imaging as a powerful tool for *in situ* observations of plankton. Various instruments, including the Video Plankton Recorder (VPR), Underwater Video Profiler (UVP), Continuous Particle Imaging and Classification System (CPICS), Shadow Image Particle Profiling Recorder (SIPPER), *In Situ* Ichthyoplankton Imaging System (ISIIS), and HOLOMAR underwater holographic camera system, have been developed to facilitate

the continuous sampling of plankton images in the ocean. These devices effectively overcome some of the limitations associated with traditional plankton net sampling methods.

The Real Time VPR (Seascan, Inc; Seascan, 2014), the device that is the common thread throughout this PhD (Box 3), is essentially an underwater microscope that takes photos of plankton and marine particles from 100  $\mu\text{m}$  up to a few centimeters (mainly targeting the mesoplankton). The initial VPR design dates back to the 90s (Davis *et al.*, 1992), and since then, it has undergone substantial refinement over the years through various technical adaptations. This continuous evolution has given rise to alternative versions, like the Digital Autonomous Video Plankton Recorder (Seascan, Inc; e.g., used in Jacobsen and Norrbin (2009)), broadening the spectrum of available technologies in this field. Sampling with a VPR or *in situ* imaging devices offers various advantages. First, as *in situ* imaging devices take photos inside the water column, they can observe fragile organisms such as gelatinous, e.g., jellyfishes, or colonial forming, e.g., chain forming diatoms, species in their natural orientation and environment without damaging them (Remsen *et al.*, 2004). Secondly, traditional physical net samples are typically collected from a single geographic point, limiting their spatial and temporal resolution. In contrast, the VPR can be towed continuously over vast distances and extended time periods, allowing for the collection of samples on a broad spatial scale (Ashjian *et al.*, 2001). Thirdly, the flexibility of mounting additional sensors on the VPR frame enables the simultaneous collection of abiotic, spatial and geographic measurements. This capability empowers researchers to study marine communities in 3D and explore their relationships with water quality parameters at a fine-grained spatial resolution (e.g., Pan *et al.*, 2018; Jacobsen and Norrbin, 2009). Lastly, having the samples in a digital format can allow for a faster validation with artificial intelligence classifiers and opens up opportunities for more advanced analytical techniques (e.g., automated length measurements).

### **Box 3. The Real Time Video Plankton Recorder**

A Real Time VPR is an instrument designed for the real-time and *in situ* sampling of plankton and marine particles (Figure 1.5 A). It operates while being towed underwater behind a research vessel, capturing images and sensor data. The VPR is connected to its dedicated winch that is positioned on the vessel's afterdeck. Through the winch cable, it transmits data in real-time to the VPR computer on deck, providing researchers with a live feed of incoming data and images. Based on user-defined parameters in the computer software (AutoDeck software (Seascan, Inc.)), the incoming full frame images are thresholded and checked for relevant information. Plankton and other particle images are extracted from each full frame image as regions of interest (ROIs) and saved to the computer's hard drive. Each ROI is tagged using a

timestamp to allow synchronization with the hydrographic parameters that were stored in a separate file.

The VPR employs dark-field illumination (Figure 1.5), a technique developed for microscopic imaging of translucent samples. A circular strobe, shielded in the center, generates a hollow light cone. As organisms and particles pass through the converging point of the light cone, they diffract light into the camera lens, which is positioned on the other side and in the dark zone of the strobe. The only light entering the camera sensor is light diffracted by specimen in the focal point. The 1380 by 1034 pixel-sized images of the Real Time VPR are captured by the 1.4 MegaPixel color camera at 25 frames per second.

Complementing the strobe and camera, a lens completes the optical setup. Three motors intricately control the lens's aperture, focus, and the distance between the camera and lens, effectively managing zoom and magnification. The system offers four motor position presets, providing researchers with the flexibility to choose their preferred image size or field of view: 8.8 x 6.6 mm, 20.8 x 15.2 mm, 33.8 x 25.5 mm, and 46.5 x 34.5 mm (Seascan, 2014).

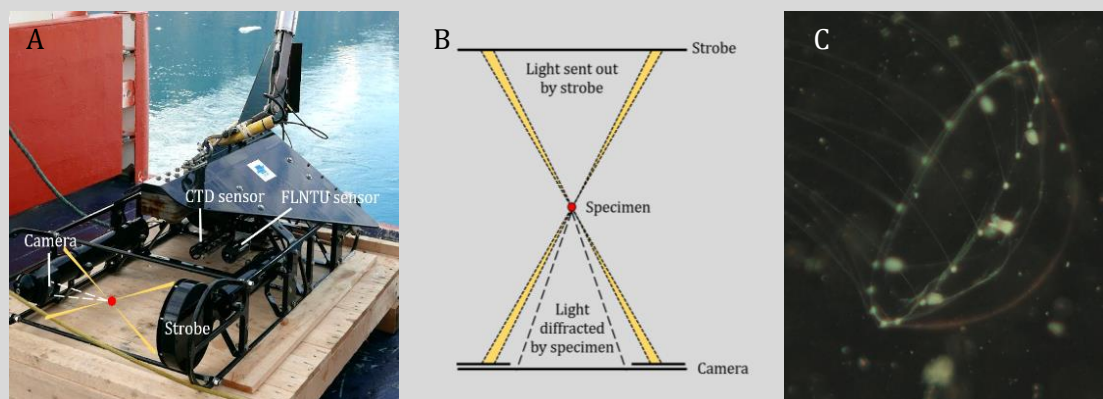


Figure 1.5. (A) The Real Time VPR before deployment on the afterdeck of a vessel, with indications of its components and sensors, (B) Schematic overview of dark-field imaging (adjusted from *MicrobiologyUSP* (n.d.)), and (C) Example of a dark-field ROI, with a jellyfish on it, as captured by the Real Time VPR.

### 1.3 Research questions and thesis outline

This PhD is infrastructure driven, with the Real Time VPR as the main point of focus. However, it is crucial to acknowledge that the VPR serves as just one example of *in situ* imaging methods. Many of the methodologies and findings presented are not confined solely to the VPR; rather, they hold broader applicability to a range of *in situ* imaging systems. The outline of this thesis can be

divided into two large parts, first a technical part (chapters 2 - 3), where it was studied how and where the VPR can be used in turbid coastal areas, and how the VPR results compare to net sampling data. Secondly, in the ecological part (chapters 4 - 5), the VPR is used in two case studies, on a small and large spatial scale (Figure 1.6). In the first case study the spatial distribution of plankton is studied in coastal environments over a 24-hour time period. In the second case study the food quality of plankton and distribution of copepods is analyzed in fjords in Greenland.

The four research chapters (2-5) aim to answer the following questions:

- Chapter 2: Which towing procedures and instrument settings are best suited for VPR users, in particular in the southern North Sea? What is the turbidity limit of the VPR?
- Chapter 3: What are similarities and discrepancies in the plankton abundance and community composition obtained from VPR and net sampling methods?
- Chapter 4: How is plankton distributed over fine spatial and temporal scales within the water column in dynamic coastal systems under strong tidal forces?
- Chapter 5: What is the spatial and size class distribution of copepods in fjord systems and how does the fatty acid composition of plankton vary accordingly?

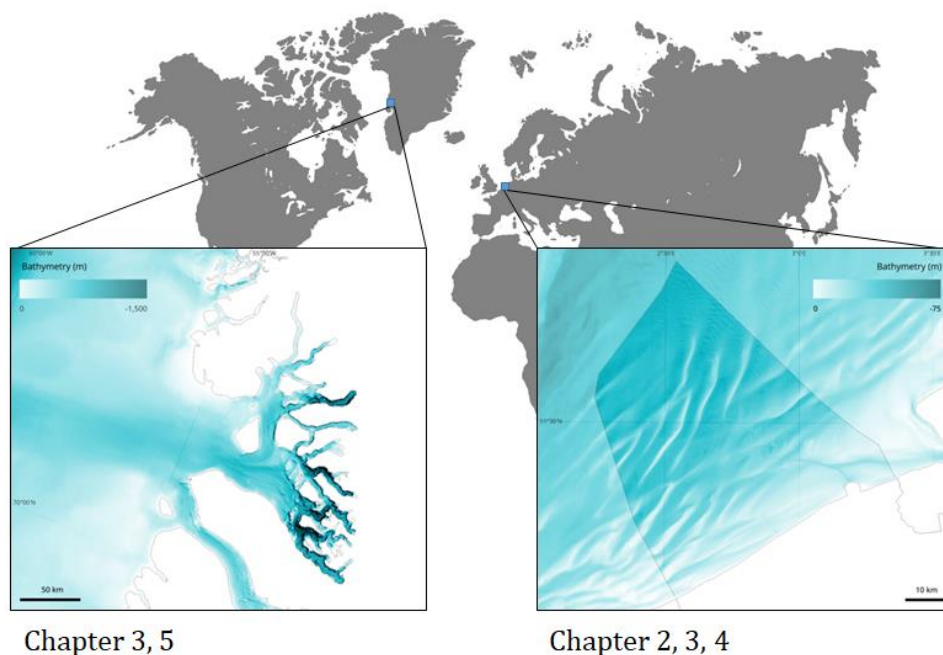


Figure 1.6. Map of sampling areas throughout this PhD thesis with indications of the chapters where the corresponding data was used. Left: Uummannaq area in Greenland; right: Belgian part of the North Sea situated in the southern North Sea.

Applying a VPR in turbid coastal waters, such as the southern North Sea, comes with a number of challenges. During VPR deployment various methodological choices need to be made (e.g., towing

## CHAPTER 1

procedure, magnification, and instrument settings), but in addition also limitations can be expected related to the physical characteristics of the water column, more specifically regarding the suspended matter concentration and turbidity. In **chapter 2**, we therefore aim to analyze how we can use the VPR by evaluating three towing procedures and four magnification settings. Secondly, we aim to find out where the VPR can be used by analyzing the technical limitations of the VPR related to turbidity. This will allow the identification of water conditions suitable for VPR deployment and the establishment of a turbidity limit for accurate plankton analysis.

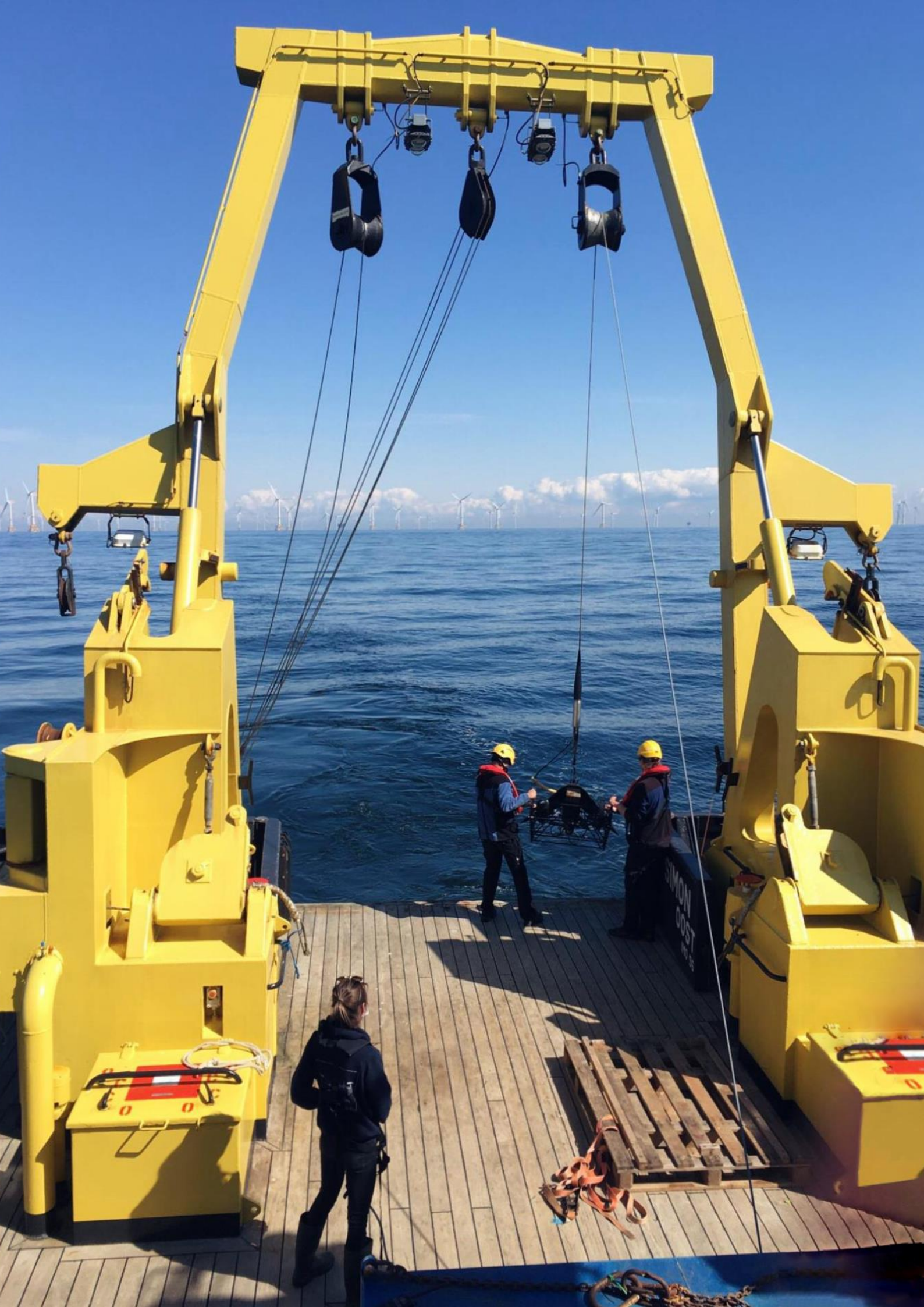
In **chapter 3**, a comparative analysis between the VPR and net sampling methods was conducted. The study encompasses the collection of samples from contrasting environments, including clear, low-plankton-density waters in West Greenland and more turbid waters with high plankton densities in the southern North Sea. This approach allows for the evaluation of spatial and temporal trends in plankton densities and community composition. Such a comparison is essential to assess the efficiency and applicability of the VPR in relation to established net sampling methods and how these methods relate to each other. This helps to reveal the additional value that a VPR can contribute in terms of both sampling efficiency and accuracy to the field of marine biology and in particular plankton research.

In **chapter 4**, we use a VPR to study the distribution patterns of plankton over 24-hour periods, timescales encompassing two tidal cycles and one diel cycle, in a dynamic coastal area. By collecting extensive data, including both biotic and abiotic factors, we aim to understand how plankton are vertically distributed across fine spatial and temporal scales within the water column. By conducting this research, we aim to gain valuable insights into the dynamics of planktonic communities in well-mixed water columns, enhancing our understanding of phenomena such as diel vertical migration and other distribution patterns in marine ecosystems.

In **chapter 5**, the food quality of zooplankton is studied in various fjords and the connecting shelf area in Greenland. The FA profiles of the micro and mesozooplankton size fraction were analyzed using gas chromatography and mass spectrometry, and the distribution of copepods along and within fjords was studied by deploying a VPR. In the context of our rapidly changing world characterized by climate warming, a deeper understanding of zooplankton size classes, their food quality, and distribution becomes imperative.

To conclude, **chapter 6** discusses the results of the research chapters within the broader framework of plankton ecology, tackles future perspectives and research ideas, and gives a comprehensive overview on the key findings of this thesis.







# 2

## A Video Plankton Recorder user guide: Lessons learned from *in situ* plankton imaging in shallow and turbid coastal waters in the Belgian part of the North Sea

Adjusted from:

Ollevier, A., Mortelmans, J., Vandegehuchte, M. B., Develter, R., De Troch, M., & Deneudt, K. (2022). A Video Plankton Recorder user guide: Lessons learned from *in situ* plankton imaging in shallow and turbid coastal waters in the Belgian part of the North Sea. *Journal of Sea Research*, 188, 102257. <https://doi.org/10.1016/j.seares.2022.102257>

## Abstract

Optical imaging devices such as the Video Plankton Recorder (VPR) harness unique capabilities to perform in-situ observations and observe planktonic organisms in their natural environmental context. However, applying this technology in shallow and turbid coastal waters comes with a number of challenges. Depending on the research goal, methodological choices need to be made regarding the appropriate towing procedure and instrument settings, like magnification or field of view. In addition, limitations can be expected related to the physical characteristics of the water column, more specifically regarding suspended matter concentration and turbidity. To inform VPR users on the possibilities and limitations of the device in shallow and turbid coastal waters, this paper evaluates a number of specific deployment procedures in the Belgian part of the North Sea. For three different towing procedures the practical feasibility, characteristics and output are assessed and the assets and liabilities for each of the tow types are discussed. A Z-shaped and a clover tow type are seen as best fit for detailed characterization of the plankton community of a limited geographical area. A straight tow type is more suitable for plankton studies over a larger area, with the potential to determine the relation with the spatial variation of the environmental conditions and to capture local plankton abundance peaks. The capacity of the various VPR magnification settings to capture specific plankton taxa or size groups, was tested during four straight line transects each with a different magnification. The highest magnification can be used for organisms from 0.3 to 0.7 mm while the low magnification allows to observe larger organisms in the size range of 1.0 to 3.8 mm. Finally, also the boundary conditions for turbidity of the water column were defined and the implications for successful deployment within the study area were investigated. This study shows that high turbidity values over 6.2 NTU inhibit the collection of useable data, complicating its application in many coastal and transitional waters.

## 2.1 Introduction

Zooplankton is a significant component of the marine ecosystem (Castellani and Edwards, 2017), as they play a pivotal role in biogeochemical cycles (Steinberg and Landry, 2017), and form a crucial link between phytoplankton and higher trophic levels, to which e.g., economically important fish species belong (Nielsen *et al.*, 1993). Most zooplankton species are short-living, have a fast generation time and are sensitive to temperature fluctuations (Chivers *et al.*, 2017; Mackas *et al.*, 2012). With climate change, rising sea temperatures and ocean acidification, this makes them highly suitable organisms to evaluate the effects of anthropogenic influences on ecosystem functioning.

Typically, plankton research starts from physical samples collected by means of vertical hauls (e.g., Castellani and Edwards, 2017) followed by time-consuming species identification and estimation of zooplankton abundances at the species level under a light microscope. As a result of this labor-intensive work, this methodology is restricted to a limited spatiotemporal coverage. It is not able to grasp large-scale distribution patterns of the plankton community, such as the vertical distribution (Jacobsen and Norrbin, 2009) or small-scale patchiness of species and communities (Ashjian *et al.*, 2001; Gallienne *et al.*, 2001). Additionally, it misses information on fragile particles such as detritus and gelatinous plankton (Remsen *et al.*, 2004), as these can be damaged or destroyed during the sampling process.

To counter the problems of physical sampling, *in situ* imaging tools have been developed and are nowadays frequently used for plankton research. An example of such a device is the VPR. It is essentially an underwater microscope that captures *in situ* photographs of plankton and marine particles in the size range of 100  $\mu\text{m}$  up to a few centimeters. It has the advantage to observe marine diversity without damaging it, and the simultaneous abiotic, spatial and geographic measurements allow to visualize marine communities in 3D and to research their affinities with water quality parameters (Gallienne *et al.*, 2001), vertical stratification (Pan *et al.*, 2018; Jacobsen and Norrbin, 2009) or interactions with detritus and marine snow (Möller *et al.*, 2012). It has proven to be a successful device for research strategies that aim to document the vertical distribution of organisms through the water column or where high spatial and temporal resolution is necessary, which cannot be achieved with traditional sampling methods.

Literature review showed that various sampling methods with the VPR have been used. During deployment of the VPR, a dedicated winch is used to tow the device behind the research vessel. Depth of the VPR (by reeling the winch cable in or out), the speed of winching (by reeling the winch faster or slower), the magnification of the camera, the user-defined parameters in the

AutoDeck software and the sail trajectory are chosen by the scientist. These decisions result in different sampling methods and for each research question a specific strategy and customized towing procedures can be used. Few VPR studies substantiated their choices for the used tow types and up to our knowledge, no comparative studies on the deployment ways of the VPR have been published so far.

This paper aims to allow future VPR users to make a well-taught choice on VPR deployment method and application, based on the research purpose. We evaluate three types of towing the VPR in a continuous way, to exploit the full potential of the VPR, and four magnification settings. Secondly, the technical limitations of the VPR related to turbidity are investigated, to inform users in which water conditions the VPR can be deployed and what the turbidity threshold for good images is to allow plankton analysis.

## 2.2 Methodology

### 2.2.1 Video Plankton Recorder

The Real Time VPR (Seascan, Inc.) is an optical underwater instrument for real-time and *in situ* observation of plankton specimens and marine particles in the size range from 100  $\mu\text{m}$  up to a few centimetres. The VPR makes use of dark field illumination, whereby the light sent out by the stroboscope is diffracted by particles of interest into the camera lens. The 1380 by 1034 pixel-sized images are captured by the 1.4 MegaPixel color camera at 25 frames per second. The arms on which the stroboscope and camera are mounted are located 590.8 mm away from each other. The VPR is equipped with a SBE 49 CTD (Sea-Bird Electronics, Inc.) and ECO Puck FLNTU fluorometer and turbidity sensor (WETLabs) to simultaneously collect position and hydrographic/environmental data. Image and sensor data is transferred in real-time over a single mode fiber optic cable and captured by the AutoDeck software (Seascan, Inc.). Based on selected parameters (e.g., segmentation threshold, focus) plankton and other particle images are extracted from each image frame as regions of interest (ROIs) and saved to the computer hard drive as TIFF files. Each ROI is tagged using a timestamp to allow synchronization with the hydrographic parameters that were stored in a separate logfile. The image data were manually classified by sorting the zooplankton into the following categories/taxa: Amphipoda, Annelida, Appendicularia, Brachyura zoea, Calanoida, Caridea, Cnidaria, Ctenophora, Cumacea, Echinodermata, fish larvae, and Harpacticoida. Other particles were classified as Appendicularia house, *Noctiluca*, *Phaeocystis*, detritus, bubbles, fibres, or unknown. All image and corresponding sensor data were subsequently stored in a MongoDB database, that was consulted using the Studio 3T graphical user interface.

During deployment of the VPR, the scientist has to select the VPR's magnification setting and the parameters in the AutoDeck software. The VPR has four preset motor positions that determine the field of view: 8.8 x 6.6 mm, 20.8 x 15.2 mm, 33.8 x 25.5 mm, 46.5 x 34.5 mm (Seascan, Inc., 2014). These correspond to magnification settings S0 till S3 which are the most zoomed in and zoomed out settings, respectively. The user-defined parameters in AutoDeck are segmentation threshold – low, segmentation threshold – high, focus – sobel, focus – std dev, growth scale (%), minimum blob size (area) and minimum join distance and determine whether or not an image is saved as a ROI. The incoming images are thresholded, with pixels categorized as white or black based on a specified threshold value. The white regions of the image (i.e. the regions with information) are then boxed in rectangles and identified as ROIs. These ROIs are further checked for information. The light gradient of each ROI, assessed through the sobel parameter, acts as the initial checkpoint. Subsequently, texture analysis based on standard deviation becomes the next determinant. Only when all three criteria – thresholding, gradient check, and texture analysis – are met, the ROI is saved. Minimum blob size depicts the minimum size of a thresholded area before being accepted and minimum join distance can allow small ROIs to be joined into one image. The growth scale factor enlarges accepted ROIs, especially useful for preserving details like antennas. The segmentation threshold and focus parameters in AutoDeck in combination with the magnification setting determine the imaged volume per frame and are calculated by the CalDeck software.

With the imaged volume, one can calculate how much water was sampled by the VPR during a transect as is represented in formula 1. To know the sampled volume one has to multiply the imaged volume with the number of frames per second (for the Real Time VPR this is 25 fps) and the duration that the VPR collects data. In this study, densities are based on the entire trajectory but densities can also be calculated for a specific part of a trajectory. A shorter deployment time with the respective number of plankton observed within that part of the trajectory should then be used in formula 1 and 2.

$$\text{Sampled volume [mL]} = \text{Imaged volume [mL frame}^{-1}] * 25 [\text{frames s}^{-1}] * \text{Duration [s]} \quad (1)$$

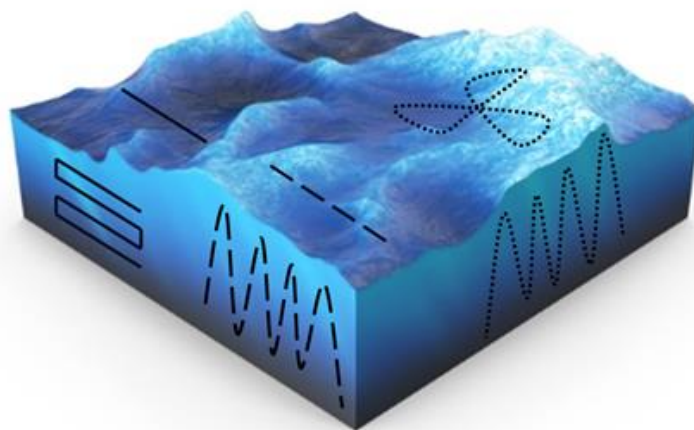
After validation of the ROIs, the plankton density [ind m<sup>-3</sup>] per taxa of a VPR transect can be determined as:

$$\text{Density [ind m}^{-3}] = (\text{Number of individuals [ind]} / (\text{Sampled volume [mL]} * 1,000,000) \quad (2)$$

In formula 2 there is a multiplication with 1,000,000 to convert the unit ind mL<sup>-1</sup> to ind m<sup>-3</sup>.

## 2.2.2 Tow types

Three tow types were tested (Figure 2.1) and although the VPR can be used when remaining stationary, it was decided to compare continuous transects, to explore the large-scale potential of the VPR. The tow types were performed immediately after each other and have a starting point in the same area. The first tow type is a Z-shape, whereby the research vessel sails back and forth on a straight line. Each time the vessel turns, the VPR is deployed at a different depth, eventually resulting in a zigzag or Z-shaped pattern as viewed from the side of the water column. The trajectory is divided into three parts where the VPR was deployed at 24, 12 and 5 meters depth, respectively. The VPR was used for approximately 30 minutes at each depth. The second tow type is undulating the VPR while sailing a clover-shaped pattern. Here the winch cable is reeled in and out at a speed of  $0.05 \text{ m s}^{-1}$ , in order to allow the VPR to move up and down through the water column. Seen from above, the vessel sails in the shape of a three-leafed clover, whereby each loop takes around 30 minutes. The third type is obtained by sailing a straight line whereby the VPR is undulating with a winch speed of  $0.05 \text{ m s}^{-1}$ . Hereafter, these tow types will be referred to as a 'Z-shaped', 'clover-shaped' and 'straight' pattern. The duration of each tow type was 1 h 43 min, 1 h 27 min and 1 h 38 min for the Z-shaped, clover-shaped and straight pattern, respectively. During all transects, the vessel and VPR maintained a constant speed of 3 - 4 knots relative to the water column, independent of the current speed and direction.



*Figure 2.1. Schematic representation of the three different tow types. Solid line: a Z-shape while sailing a straight line ('Z-shaped pattern'). Dashed line: undulating the VPR while sailing a straight line ('straight pattern'). Dotted line: undulating the VPR while sailing a clover-shaped pattern ('clover-shaped pattern').*

For each tow type, the imaged volume of a VPR frame was 17.821 mL. This was based on magnification setting S1, a segmentation threshold – low of 0, a segmentation threshold – high of 135, a focus – sobel of 34 and a focus – std dev 1 in AutoDeck (see formula 1). For the different tow types the AutoDeck parameters were kept the same to not introduce additional variance. The three tow patterns were compared to each other based on feasibility, biological data and abiotic data. In RStudio (version 1.4.1106; RStudio Team, 2020), biological and abiotic patterns were visually explored with 3D graphs (R package ‘plot3D’ and ‘plot3Drgl’) and evaluated by grouping data according to depth or location.

### 2.2.3 Magnification settings

In June 2020, four VPR transects with different magnification settings were performed (Figure 2.2). The imaged volume for the magnification setting S0, S1, S2 and S3 were 2.021 mL, 23.391 mL, 192.657 mL and 285.758 mL, respectively (formula 1). This was based on a segmentation threshold – low, segmentation threshold – high, focus – sobel and focus – std dev of 0, 130, 15, 1 for S0; 0, 135, 25, 3 for S1 and S2; and 0, 155, 40, 5 for S3 in AutoDeck. Settings S1 till S3 were deployed for about one hour, S0 for approximately half an hour (S0: 23 min, S1: 64 min, S2: 71 min, S3: 59 min). The transect was performed as a straight line while undulating the VPR. Maximum 10 images of each taxon at each magnification setting were manually measured in ImageJ. After setting the scale, measurements were made based on a straight line that spanned the extreme ends of an organism. The measurements thus are not the head-tail length, but are the longest or widest part of an organism to estimate the order of magnitude a given magnification setting can detect a particle. For species such as Annelida or Appendicularia that are sometimes curved or contorted on the image, the measurement is an underestimation of the actual head-to-tail length of the organism. The results were compared with ZooScan length measurements of a WP2 sample taken close to the transect to estimate the general size of the plankton community during that month. For this, zooplankton was sampled with a 200 µm WP2 net which was deployed vertically and equipped with a flowmeter, following the protocol of Mortelmans *et al.* (2019). Zooplankton collected in the cod-end was sedated by soda water and fixated in a 4 % formaldehyde solution. In the lab, the fixative was replaced by 70 % ethanol. The sample was digitized by the ZooScan plankton imaging device and processed by ZooProcess and Plankton Identifier (PkID) in order to detect, measure and classify the digitized objects (Gorsky *et al.*, 2010; Grosjean *et al.*, 2004). Size estimations of the body length by the ZooScan were based on the major axis of the best fitting ellipse (Gorsky *et al.*, 2010). It should be noted that fixation in formaldehyde causes shrinkage of specimens, in particular of soft-bodied organisms such as Appendicularia, Chaetognatha, Ctenophores and Cnidaria (Thibault-Botha and Bowen, 2004; Nishikawa and

Terazaki, 1996; De Lafontaine and Leggett, 1989), causing length measurements from the ZooScan to be smaller compared to the ImageJ measurements from living organisms.

### 2.2.4 Turbidity

To assess the turbidity limitations of the VPR, a transect parallel to a known turbidity gradient (SPM concentrations from Flanders Marine Institute, 2019) was followed (Figure 2.2). By towing the VPR through different turbidity zones, the impact of turbidity on the operation of the VPR and the capturing of images was investigated. Turbidity measurements by the turbidity sensor on the VPR are expressed in mV and can be converted to NTU values with formula 3, where 0.069 is a value based on the calibration of the sensor.

$$\text{Turbidity [NTU]} = 200 * (\text{voltage of turbidity sensor [V]} - 0.069) \quad (3)$$

To assess turbidity for the whole BPNS, 17 stations were sampled for Suspended Particulate Matter (SPM) and Secchi depth, following the protocol of Mortelmans *et al.* (2019). To determine the SPM concentrations, one liter of unfiltered seawater from the Niskin bottles, closed at 3 m depth, was taken and poured in a labelled recipient and stored at 4 °C. After the cruise the samples were processed by the Flanders Environment Agency. For the Secchi disk measurements, a 30 cm Secchi disk was lowered into the water column from the side of the vessel until it was no longer visible. It was subsequently hauled up and the depth at which it became visible was noted. Based on these data, interpolated maps ('sp' package) for the entire BPNS were made in RStudio. The VPR trajectory, of which it was known when the VPR images became blurry or unusable, was subsequently plotted on these maps to determine at which SPM and Secchi values the VPR no longer functioned optimally.

### 2.2.5 Study area

The Belgian part of the North Sea (BPNS) is a relatively shallow area (up to 40 m) with several subtidal sandbanks (Vanaverbeke *et al.*, 2000). The water column is well-mixed and characterized by a high nutrient concentration (De Galan *et al.*, 2004) due to the outflow from the rivers IJzer, Scheldt and Maas (Nihoul *et al.*, 1978). Especially the Scheldt has a dominant influence in terms of SPM, forming a high turbidity zone near the coast (Fettweis *et al.*, 2007).

Three cruises (Figure 2.2) with the RV Simon Stevin were performed to study the tow types, magnification settings and turbidity limit of the VPR. For the tow type cruise (May 2020) and magnification setting cruise (June 2020) a region with a low SPM concentration was selected where turbidity was not expected to pose a problem for the effective use of the VPR. To find the



turbidity limit of the VPR (June 2020), a location near the mouth of the Scheldt was chosen. This region is, based on previous experience in the study area, known to hamper the collection of images with the VPR due to relatively high concentrations of SPM and low visibility of the water column. The turbidity gradient with lower turbidity values in the areas away from the Scheldt allows to determine the turbidity limit of the VPR. Depending on the functioning of the VPR at this start point, the vessel would sail away from or towards the coast, heading towards clearer or more turbid conditions, respectively.

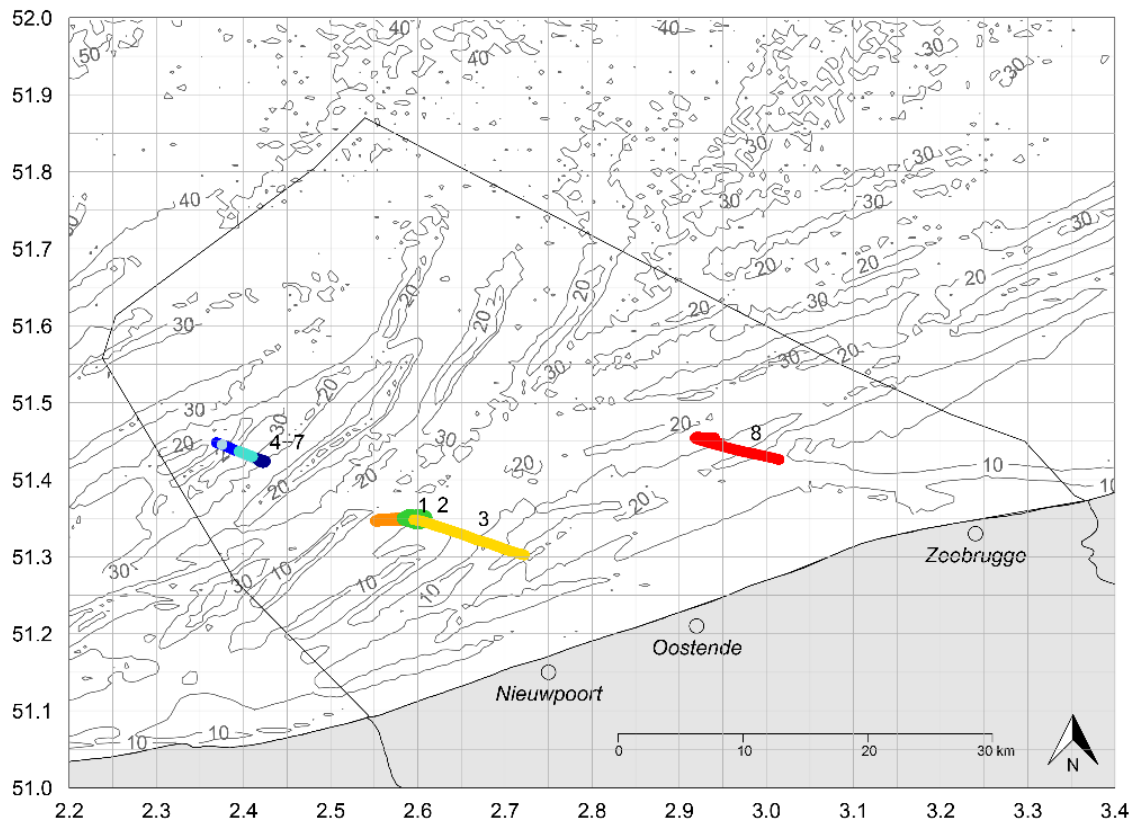


Figure 2.2. Map of the Belgian part of the North Sea, with indication of the trajectories. The tow type cruise with (1) the Z-shaped pattern, (2) the clover pattern and (3) the straight pattern. The magnification setting cruise with (4-7) magnification setting S0, S1, S2 and S3. The turbidity cruise (8). In addition to the numbers, each trajectory was also represented with a different color for clarity because some trajectories are positioned close to each other.

## 2.3 Results

### 2.3.1 Tow types

#### *2.3.1.1 Travelled distance*

For each tow type, the vessel sailed approximately 1.5 h at 3-4 knots and travelled a distance of 10.2, 10.2 and 8.3 km for the Z-shaped, clover and straight pattern, respectively. For the Z-pattern, the vessel sailed back and forth on the same transect so only for a 3.4 km transect there is information for the three depths of the water column.

#### *2.3.1.2 Biotic measurements*

The densities of most plankton taxa were of the same order of magnitude compared over the tow types (Table 2.1). Calanoida and Cnidaria were more abundant in the Z-pattern. In the clover pattern, higher *Phaeocystis* abundances and lower Echinodermata and *Noctiluca* abundances were observed compared to the other tow types. For the less abundant taxa it was noted that two taxa were not encountered in the clover pattern and that four taxa were absent in the Z-pattern. Despite the absence of certain taxa in the Z-pattern, it had the highest total summed abundance of species, i.e. 17576.32 ind m<sup>-3</sup>. For the clover and straight pattern, this was 16952.09 and 16100.34 ind m<sup>-3</sup>, respectively.

Community composition was calculated for each tow type as taxa proportional distributions (Table 2.1). In all tow types *Noctiluca* and *Phaeocystis* were the most abundant taxa, together contributing for 73.62, 79.50 and 74.49 % of the encountered organisms, in the Z, clover and straight pattern, respectively. These were followed by Calanoida, Echinodermata and Cnidaria, together contributing 22.93, 17.29 and 20.84 % to the plankton community, respectively.

The three dimensional spatial distribution of the most abundant taxa was analyzed. The most striking differences in taxon abundance were present in the vertical distribution of the Z-pattern and in the horizontal distribution of the straight pattern. For the Z-pattern, a segment of 20 minutes of data for each depth was selected from a part of the transect that overlapped. Calanoida, Cnidaria, *Noctiluca* and *Phaeocystis* had a pronounced differences in densities between depths (Supplementary table 2.1). Calanoida were less abundant in the surface layer and most abundant in the middle layer. Cnidaria were absent in the top layer and most specimens were present in the middle layer. *Noctiluca* was more abundant closer to the surface whereas *Phaeocystis* reached higher abundances closer to the sea floor. The data of the straight pattern was divided in a part north and south of the Kwintebank, a sandbank in front of Nieuwpoort (Supplementary table 2.2). This separation showed that Calanoida, Cnidaria and *Phaeocystis* were more abundant north of

the sandbank, with densities being 8, 1.2 and 4 times higher, respectively. *Noctiluca* however, was less abundant in the area north of the Kwintebank.

Table 2.1. The absolute [ind m<sup>-3</sup>] and relative [%] plankton density per tow type

Taxon	Absolute density [ind m <sup>-3</sup> ]			Relative density [%]		
	Z-shaped	Clover-shaped	Straight	Z-shaped	Clover-shaped	Straight
Amphipoda	0.00	21.46	9.50	0.00	0.13	0.06
Annelida	63.52	128.75	171.08	0.36	0.76	1.06
Appendicularia	453.70	268.23	351.66	2.58	1.58	2.18
Brachyura zoea	18.15	42.92	47.52	0.10	0.25	0.30
Calanoida	2050.72	1555.73	1435.15	11.67	9.18	8.91
Caridea	54.44	53.65	76.03	0.31	0.32	0.47
Cnidaria	653.33	375.52	437.20	3.72	2.22	2.72
Ctenophora	0.00	0.00	19.01	0.00	0.00	0.12
Cumacea	0.00	21.46	47.52	0.00	0.13	0.30
Echinodermata	1324.80	997.81	1482.68	7.54	5.89	9.21
Fish larvae	18.15	0.00	9.50	0.10	0.00	0.06
Harpacticoida	0.00	10.73	19.01	0.00	0.06	0.12
<i>Noctiluca</i>	9518.62	7682.09	9086.14	54.16	45.31	56.43
<i>Phaeocystis</i>	3420.90	5793.75	2908.33	19.46	34.17	18.06
Σ	17576.32	16952.09	16100.34	100	100	100

### 2.3.1.3 Abiotic measurements

Temperature differences within a tow were observed (Figure 2.3). For the Z and clover-shaped patterns, the temperature differed with 0.2 and 0.3°C between the bottom and surface layer. In the clover-shaped pattern the vertical temperature gradient was visible in every undulation. For the straight pattern (Figure 2.3C) there were also vertical temperature differences, but the main temperature difference appeared horizontally between the beginning and end of the trajectory (difference of 0.7°C). In the straight pattern, the end point was located the furthest away from the start point (8.3 km) compared to the other tow patterns, so that the differences that existed over a larger area were observed.

## CHAPTER 2

For all tow types, a similar pattern was observed with higher turbidity values close to the sea bottom (Figure 2.4). The majority of the observed turbidity values in the water column ranged between 0 and 4 NTU, although maximum turbidity values could reach to 10.2, 15.2, 19.0 NTU for a short period of time in the three patterns.

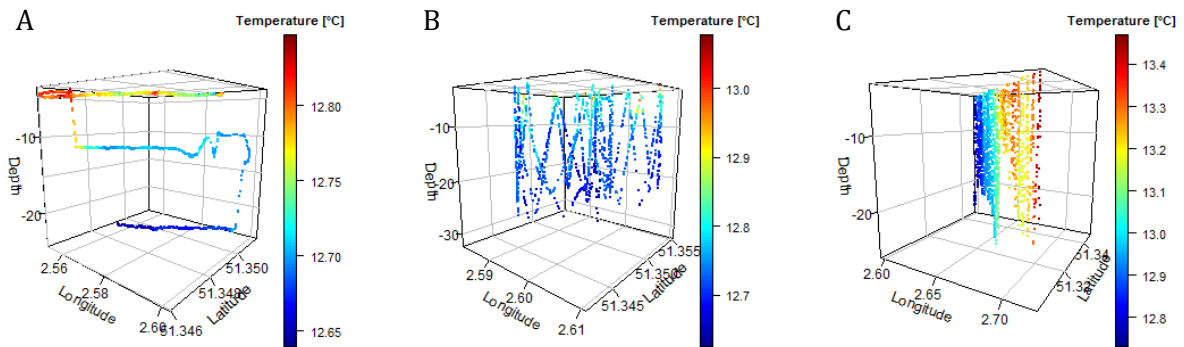


Figure 2.3. Plots of the temperature [°C] for each tow type: (A) Z-pattern, (B) clover pattern and (C) straight pattern. Note the different scales on the axes: the straight pattern spans a much wider latitudinal range.

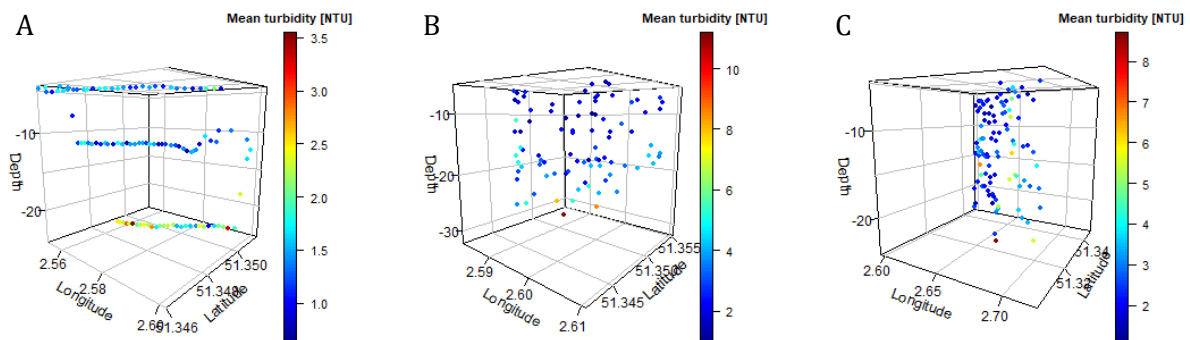


Figure 2.4. Turbidity measurements [NTU] grouped and averaged per minute for each tow type: (A) Z-pattern, (B) clover pattern and (C) straight pattern. Note the different scales on the axes: the straight pattern spans a much wider latitudinal range.

## 2.3.2 Magnification settings

### 2.3.2.1 Densities

The number of saved ROIs was higher for the low magnification settings (S3) compared to high magnification settings (S0). Even though setting S3 was deployed about half the time of S0, S1 and S2, it still captured more images (Supplementary table 2.3). Remarkable is the relatively high number of Appendicularia houses observed at magnification setting S3. With S3, also the higher number of plankton taxa was observed. S0 on the other hand observed only three plankton taxa.

The density data shows significant differences in abundance of certain plankton taxa (e.g., Calanoida) between the magnification settings. The densities of the high magnification settings are often calculated based on just a few ROIs.

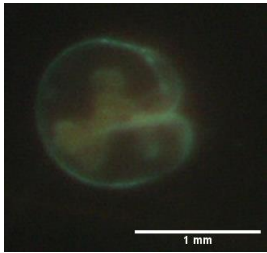
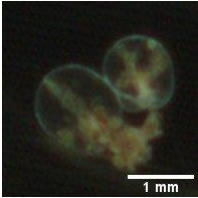

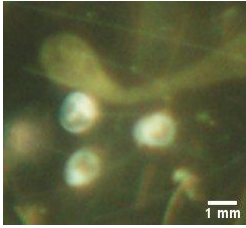
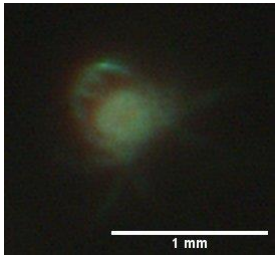
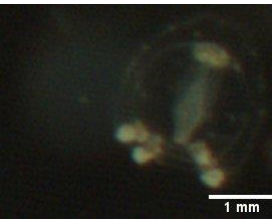
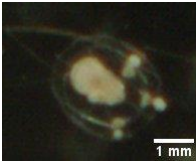

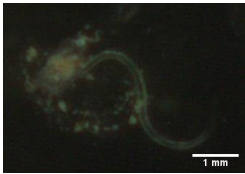
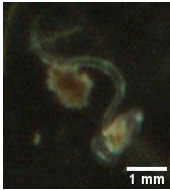
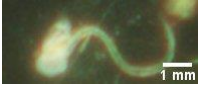
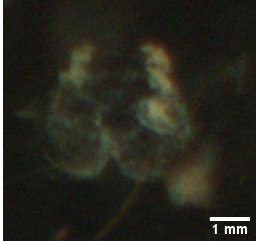
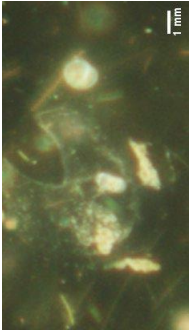

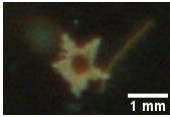
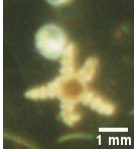
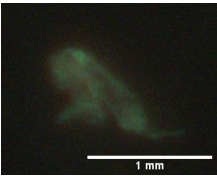
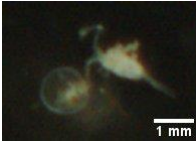
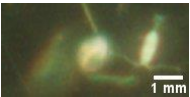
### 2.3.2.2 Information contained in image data

The magnification and hence information contained in the images differs per magnification setting. More details were distinguishable with the high magnification setting as the images are more zoomed in (Table 2.2). Stomach content of *Noctiluca* cells was visible with S0, in contrast to S3 where a *Noctiluca* cell merely looks like a small sphere. In the latter, organisms appeared smaller with a less pronounced shape and thus are harder to identify. However, despite the higher resolution of S0, it is still not high enough to classify organisms to species level. Furthermore, the majority of the S0 ROIs contained one particle, without overlap with any other plankton or detritus particle. For S1, S2 and S3, multiple particles were sometimes present on one image, which can give insight into how plankton interacts with the environment. It for example allows us to observe plankton feeding on detritus.

Cnidaria were observed at all magnification settings: at S0, S1 and S2 we mainly observed relative small Cnidaria, whereas in S3, another type of Cnidaria with a larger bell was observed which constituted a large part of the observed Cnidaria. Due to the large field of view, S3 is also suitable for observing larger species of jellyfish. The same principle probably holds for Appendicularia and its gelatinous houses. They were not observed at the S0 magnification. However, Appendicularia and its houses were detected abundantly by the S3 setting, meaning that they were commonly present in the water column. The size of the particles is therefore probably the reason why they were not detected by S0.

During the campaign in June, *Phaeocystis* was only observed with the S3 magnification. During the tow type cruise in May, the species was however abundantly observed with the S1 magnification. Analyzing the images shows that in May the colonies were spherical, while in June the majority of the colonies had an elongated shape.

Table 2.2. Captured images of various plankton taxa observed with the four magnification settings.

	S0	S1	S2	S3
<b>Noctiluca</b>				
<b>Cnidaria</b>				
<b>Appendicularia</b>	/			
<b>Appendicularia house</b>	/	/		
<b>Echinodermata</b>	/			
<b>Calanoida</b>		/		

### 2.3.2.3 Length measurements

The mean size of the plankton taxa ranged between 0.350 mm and 0.859 mm in the WP2 net sample (Supplementary table 2.4) and between 0.379 and 3.766 mm on the VPR images (Supplementary table 2.3). The larger organisms captured by the VPR (> 2 mm) were fish larvae, *Phaeocystis* colonies, Caridea, Cnidaria, Appendicularia and its houses and Annelida. Of those taxa, Appendicularia and Cnidaria were present in the WP2 sample, but with smaller mean sizes (0.803 mm and 0.859 mm, respectively) compared to the sizes observed at the different magnifications of the VPR (2.064 - 2.563 mm and 0.379 - 2.205 mm, respectively). For the majority of the VPR taxa imaged by the VPR, the mean size was larger in the lower magnification settings corresponding to the fact that the lower magnification settings are capable to capture larger specimens. The mean size of taxa ranged between 0.379 and 0.715 mm for S0, 0.683 and 2.191 mm for S1, 0.694 and 3.069 mm for S2 and between 0.965 and 3.766 mm for S3.

## 2.3.3 Turbidity

### 2.3.3.1 Turbidity measurements

Turbidity data collected by the VPR shows a gradient with lower offshore turbidity values and high nearshore turbidity values with turbidity peaks up to 25.5 NTU. Simultaneous measurements on Secchi depth and SPM showed the same pattern with lower offshore turbidity values and high nearshore turbidity values (Figure 2.5). Especially near the Scheldt Estuary low Secchi disk depths and high concentrations of SPM were observed.

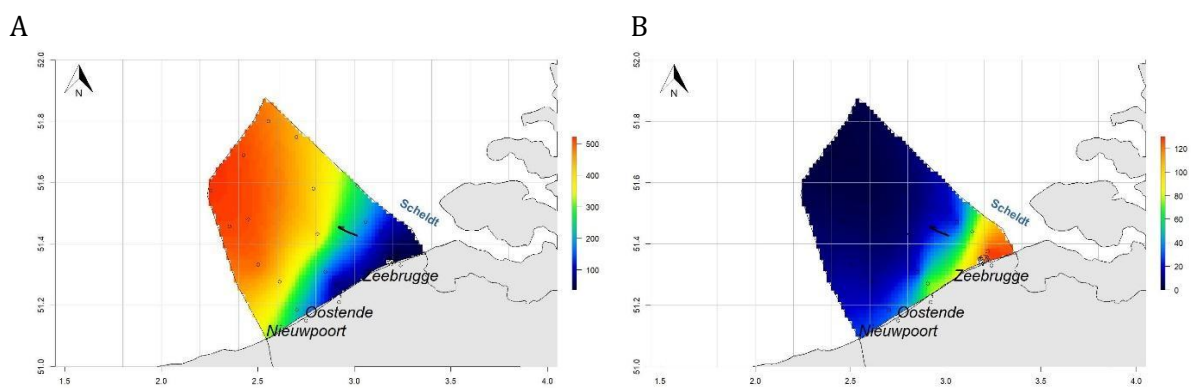


Figure 2.5. Interpolated map of (A) the Secchi depth [cm] and (B) SPM concentrations [ $\text{mg L}^{-1}$ ] in June 2020. The VPR trajectory is represented in black.

### 2.3.3.2 Image data

When sailing through the turbidity zones, a distinction could be made based on the images captured by the AutoDeck software. In the areas further from the coast with a turbidity around

3.2 NTU there were no problems and good images were taken (Supplementary table 2.5). The plankton particles were bright and contrasted with the dark background. In nearshore areas, a turbidity around 6.2 NTU yielded blurry images. The background on the images was much brighter, therefore making it harder to distinguish the particles of interest. When turbidity rose to 10.2 NTU, no images could be recorded (Supplementary table 2.5). The point when no more ROIs can be stored corresponded approximately to a Secchi depth of 200 cm and SPM concentrations of 30 mg L<sup>-1</sup>.

## 2.4 Discussion

### 2.4.1 Tow types

Each of the investigated tow types had their own advantages and limitations, resulting in different possibilities for analyses of the plankton community and abilities to distinguish patterns (Table 2.3). The Z-shaped pattern was an easy pattern to sail. Despite the fact that the VPR was deployed for 1.5 h, information was only collected on a relatively small surface. Moreover, the information was collected at three fixed depths, which could lead to the overlooking of important data in the intermittent layers (in case of e.g., stratification). Although the total plankton density was large, the results show that this tow type yielded the largest number of absent taxa. However, for the most abundant taxa there were clear vertical distribution patterns because extensive data had been collected at those specific depths. We could therefore say that in case there is sufficient prior knowledge of the marine system or species behavior, and the research question focuses on specific depths (e.g., differences above and below a thermo- or halocline, layer where certain abundant organisms occur), this tow type is adequate. It is also useful to perform quick technical tests because it does not require a dedicated person winching during data collection.

The clover pattern was the most difficult pattern to sail because the current speed, the maximum speed that can be used when deploying the VPR, and the time each loop must have, must be taken into account. Undulating the VPR requires a focused winch operator. This person has to control the VPR's depth continuously, to safeguard the VPR from hitting the seafloor or colliding with the afterdeck of the ship. At all times, the VPR has to stay far enough from the sea surface and the shallow seafloor which changes in depth during deployment. During the transect, various factors such as the sailing direction, sailing speed and current direction relative to the vessel continuously change, making it harder to translate and interpret abiotic parameters linked to currents and tides. The (a)biotic data covers the whole water column although no clear biological vertical patterns could be distinguished, compared to the Z pattern. The Z pattern had approximately 30 minutes of observations on a fixed depth, whereas the clover pattern samples



all depths, yet only for a short period. When the clover data is grouped per depth, only a few organisms are encountered at a specific depth, making differences less pronounced. For the reasons stated above, the use of the clover pattern is not recommended in general or as a tow type to investigate the influence of the environment on the plankton distribution.

The straight pattern collected data on the whole water column over a long distance. It is an easy pattern to sail and requires a focused winch operator. Compared to the other tow types, this type recorded the highest number of plankton taxa. As with the clover pattern, vertical distribution patterns in plankton abundance were hard to detect, yet a clear difference was observed horizontally on each side of the sandbank. Both horizontally and vertically valuable abiotic data were collected in which gradients and patterns were recognizable. Because the data were collected in one straight line, it is easier to grasp how e.g., currents influence the observations. This tow pattern is suitable for monitoring purposes, studies in a stratified environment or studies interested in plankton distributions.

When comparing these tow types with previous VPR studies, it is noted that most studies undulated the VPR vertically through the water column while remaining almost stationary with the research vessel (Sainmont *et al.*, 2014; Jacobsen and Norrbin, 2009; Ashjian *et al.*, 2005; Dennett *et al.*, 2002). This method yields detailed information on the vertical distribution of species and their interactions with the environment on certain stations, but only provides information very locally. An advantage of the VPR is that it can be operated while sailing, allowing it to collect data covering large areas with a high small-scale spatial resolution and allowing it to look into spatial (horizontal and vertical) distribution of plankton. Therefore some studies performed long straight transects (Gislason *et al.*, 2016; Takahashi *et al.*, 2015) or sailed a, as viewed from above, clover-shaped patterns (Möller *et al.*, 2012) or zigzag patterns (Davis *et al.*, 2004) to get more insight into the 3D distribution of plankton. In these previous studies it was often not argued why the choice was made for a particular towing technique. In certain cases where the VPR was used as a stationary sampling technique, a continuous technique could have given in-depth insight. For example when examining Cnidaria around a density discontinuity (Jacobsen and Norrbin, 2009), the VPR was lowered on 44 stations. A continuous technique could provide additional fine-scale information on the areas between the discrete sampling points; therefore connecting the dots into a bigger picture and gaining 3D insight on the density discontinuity in the whole area. However, in most research sampling campaigns different sampling activities are combined so that long VPR transects may not be possible and a middle ground must be found. When ship time is not an issue, long straight tows are preferred because they give the most complete overview of the water column. When a study wants to collect 3D data on a broad surface, the straight pattern could also be extended to make a zigzag pattern as seen

## CHAPTER 2

from above (as in Davis *et al.* 2004) instead of a straight line, collecting data on depth, length and width.

Things to keep in mind when deploying the VPR, especially during Z-profiles and clover-shaped patterns, are currents and tides. In coastal areas these play an important role and strongly determine the water displacement. With a semi-diurnal regime in our study area (Baeye *et al.*, 2011) the current direction and speed quickly changes. For the Z pattern and clover-shaped patterns, it is necessary to tow in the same area to have information on the same waterbody at different depths. When Z patterns are performed at many depths, it is possible that the currents have supplied a new water mass by the time the entire water column has been traversed. Changes between top and bottom layers may therefore be due to the new water mass brought in by currents or tides, rather than changes or gradients within the same water body. The same problem applies to the clover pattern as it assumes that the same area around a central point is sampled. If the loops are too large, the area will not be mapped more extensively, but different water masses will be mapped. The semidiurnal tidal cycling in the BPNS causes an anti-clockwise veering of the water during the ebb and flood currents (Otto *et al.*, 1990) with current velocities maxima up to  $1.66 \text{ m s}^{-1}$  (Verfaillie, 2008). It cannot be ruled out that the currents had an impact on the data collected within a particular tow type, although we expect that the impact was minimal because no significant abiotic changes could be observed between the loops of the clover pattern. The clear temperature changes observed in the Z-pattern are thus likely related to depth rather than the effect of the currents.

It should be noted that the comparison between the tow types in the field is hard to do in exactly the same water mass. The time between the start of the first and the end of the last tow type covers almost a half tidal cycle (i.e., the transition from ebb till flood), as a result of which the water mass at the start and end point possibly strongly differ. The tow types were performed immediately after each other, to restrict natural variation to a minimum, but this is an unavoidable parameter during field studies.

Table 2.3. Comparison of the three tow types: the Z-shaped, clover-shaped and straight pattern.

	Z-shaped	Clover-shaped	Straight
<b>Sailing the pattern</b>	Easy. However the vessel didn't sail back over the exact same coordinates.	Difficult maneuver to make for the captain.	Easy.
<b>Operating the VPR</b>	Easy.	Requires a focused person.	Requires a focused person.
<b>Distance covered</b>	Vessel sailed 10.2 km, but only a $\pm 3.4$ km trajectory was sampled at three depths.	10.2 km	8.3 km
<b>Total abundance of all plankton</b>	17,576 ind m <sup>-3</sup>	16,952 ind m <sup>-3</sup>	16,100 ind m <sup>-3</sup>
<b>Presence/absence of taxa (relative to the other tow types in this study)</b>	4 taxa absent	2 taxa absent	No taxa absent
<b>Biological patterns</b>	Clear differences in vertical distribution of abundant taxa.	Vertical differences less clear.	Vertical differences less clear. Large difference in horizontal distribution of abundant taxa between each side of the sandbank.
<b>Abiotic measurements: temperature and turbidity</b>	Vertical differences in water temperature and turbidity observed. Only information on 3 fixed depths.	Vertical differences in water temperature and turbidity observed. Information on the whole water column.	Vertical and horizontal differences in water temperature and turbidity observed. Information on the whole water column.
<b>Recommended application</b>	-Research interest in specific depths -Research in small area	-Research in small area	-In stratified environments -Research interest in horizontal or vertical (e.g., vertical migration) distribution of plankton -Monitoring purposes -General insight in plankton community -Research in large area, covering great distance

## 2.4.2 Magnification settings

The magnification of the VPR will impact which size range of particles are captured by the VPR. The field of view magnification setting S0 is 8.8 mm by 6.6 mm, which theoretically implies that particles up to 8.8 mm could be photographed. However, we see that this is not the case and that

## CHAPTER 2

the largest mean size of plankton taxa observed with S0 was 0.715 mm, while the ZooScan and ImageJ measurements indicated that plankton particles of 0.35 until 3.77 mm were present in the water column. The results also show that with a high magnification setting mainly smaller organisms (around 0.4 - 0.7 mm) are observed while a low magnification setting captures larger particles (around 1.0 - 3.8 mm), as is represented in Table 2.4.

Choosing the most suitable magnification setting is a trade-off between image detail, image size range and encounter chance of particles. When there is a research interest for a specific plankton taxon or size fraction of the plankton community, then this can be the main driver to decide on the used magnification setting. When there is an interest in larger organisms (> 2 - 3 mm) such as cnidarians the lowest magnification setting is the most suitable due to its large field of view. Pan *et al.* (2018) decided to use the lowest magnification setting due to the dominance of macrozooplankton with copepods and gelatinous species in their study area. Vice versa, Möller *et al.* (2012) used the largest magnification due to the small particle and plankton sizes in the sampling area, which was deemed suitable for imaging small sized adult calanoid copepod species (e.g., *Acartia* spp., *Temora longicornis* and *Pseudocalanus acuspes*), known to dominate the mesozooplankton community in their study area. Beside plankton taxa and abundance, there is also additional information to be obtained from the image such as stomach content, presence of an egg sac, length of appendages, colony formation, foraging on detritus, ... When a study wants to focus on a particular feature of an organism, a high magnification setting can give the most detailed image with the highest resolution possible where features are the clearest visible. If the researcher is however interested in larger aggregates of e.g., colony forming organisms or organisms feeding on detritus, then a lower magnification might be more suitable due to the larger field of view where large aggregates can be photographed. When research is dealing with a less common organism, a low magnification setting could enlarge the encounter chance with it because of the large field of view and larger sampled water volume. When there is a general interest in the whole plankton community, then the results indicate that S1 is a good middle ground to avoid that only too small or too large images are missed, without losing too much image detail and still being able to observe interactions with the environment (e.g., particles feeding on detritus). If, however, the VPR would be used additionally to traditional net sampling techniques, then it might be interesting to use setting S3. The VPR could then, in addition to the regular observations, detect organisms (like large gelatinous species) that are otherwise missed or destroyed with net sampling techniques (Remsen *et al.*, 2004; Dennett *et al.*, 2002). It also should be noted that despite the various magnifications, the VPR provides information about organisms only in a coarse taxonomic resolution and not down to species level, even with the highest magnification (Davis *et al.* 2004).

Table 2.4. Comparison of the four magnification settings.

	S0	S1	S2	S3
<b>Field of view</b>	8.8 x 6.6 mm	20.8 x 15.2 mm	33.8 x 25.5 mm	46.5 x 34.5 mm
<b>Imaged volume per image in the campaign in June 2020</b>	2.021 mL	23.391 mL	192.657 mL	285.758 mL
<b>Particles on photo</b>	-Single particle on ROI	-Multiple particles on ROI possible -Possibility to see the interaction with environment (e.g., organisms feeding on detritus)	-Multiple particles on ROI possible -Possibility to see the interaction with environment (e.g., organisms feeding on detritus)	-Multiple particles on ROI possible -Possibility to see the interaction with environment (e.g., organisms feeding on detritus)
<b>Image detail</b>	Most detailed (e.g., stomach content of <i>Noctiluca</i> visible)			Least detailed
<b>Plankton size of captured images</b>	Approximately 0.4 to 0.7 mm	Approximately 0.7 to 2.2 mm	Approximately 0.7 to 3.1 mm	Approximately 1.0 to 3.8 mm (e.g., larger gelatinous species or colony-forming species)

### 2.4.3 Turbidity

*In situ* optical sampling methods cannot be used in every water type. In general, the VPR is towed in clear, low turbidity waters such as Atlantic or Arctic environments (Sainmont *et al.*, 2014; Jacobsen and Norrbin 2009; Dennett *et al.*, 2002). These open water systems are much different from the turbid coastal area in this study. The results show that high turbidity values over 6.2 NTU hamper the efficient use of the VPR, illustrating the importance of turbidity on the use of the VPR. As turbidity rises, images become more blurry until no more images are captured at all. The VPR makes use of dark field imaging, whereby the light sent out by the stroboscope is diffracted by particles of interest into the camera lens. When turbidity is high, other particles in the background, whether these are detritus, phytoplankton blooms or other small particulate matter

suspended in the water column, can as well diffract light, thereby highlighting the background and making the particle of interest less visible and less contrasting with the background. This observation is also noted by Davis *et al.* (1992): VPR images from *in situ* field experiments had a slightly lower contrast compared to laboratory images due to the fairly turbid conditions in the field. When turbidity in the BPNS exceeds 10.2 NTU, no more images are captured: the AutoDeck software that automatically extracts and saves ROIs from the raw VPR images is no longer able to distinguish the particles from the background.

In the coastal area there is a clear gradient with high turbidity values close to the shore towards low turbidity values further away from the coast. During a transect towards the coast with the same AutoDeck settings, gradually less images would be taken when the coastline is approached. Fewer plankton will be captured at the end of the transect even if the plankton densities were the same in the whole study area, resulting in an underestimation of the plankton community at the end of the transect. When deploying the VPR, it is therefore important to sail in areas with sufficient clear water in terms of turbidity (< 6.2 NTU) and to avoid ending a transect in turbid zones.

Due to the turbidity restrictions on the use of the VPR, coastal areas or areas with a too high turbidity, will require other techniques to sample the plankton community. Plankton net samples can offer a solution and optical methods where the lens and light source are closer together (e.g., CPICS (Coastal Ocean Vision, Inc.; Gallager, 2016)) could enlarge the sampling range to a limited extent.

Despite the restrictions of a high turbidity on the capture of images, it does not affect the turbidity and CTD sensor. Additionally there is the possibility, based on own experience, to mount extra sensors such as a LISST-200X (Sequoia Scientific, Inc.) on the back of the VPR causing the VPR to also be a suitable device to get more information on the composition or grains size of the entirety of suspended particles that cause turbidity.

### 2.4.4 Case study of applicability in the BPNS

The conditions that impact VPR effectiveness are not just limited to turbidity or other water masses that are brought in by currents. These are of course important in dynamic and shallow coastal waters, but depth, tide, and wave height also influence the VPR deployment. A safety distance of e.g., 3 meter from the seabed and surface is advised to avoid a collision of the VPR with the seabed or rear deck. This leaves little room to undulate through the water column in shallow areas, with e.g., sand banks or during low tide. Significant wave height conditions above 1.5 m impede putting the VPR in the water and retrieving it on deck in a safe way for machine and crew.

The BPNS is an intensively used area and shipping routes, ship wrecks and windmill parks impose restrictions on where the VPR can be used (Supplementary figure 2.1). The North Sea area contains some of the busiest shipping routes in the world and due to the shallow depths, vessel traffic is confined within narrow navigation channels (Volckaert *et al.*, 2006). Within the route system, also anchorage zones are established, receiving vessels waiting to enter the final lap to their destination (De Meyer *et al.*, 2008). These areas can be transversed with the research vessel but sailing back and forth should be avoided to limit the possibilities of collision. Additionally, permissions are needed to enter the windmill parks and a safe distance to the windmill pillars has to be guaranteed. Also shipwrecks, of which there are more than 290 shipwrecks scattered throughout the BPNS (Van Besauw, 2018), must be treated with caution as it is not always possible to estimate how high some wrecks protrude above the seabed.

## 2.5 Conclusion

The VPR has proven to be a valuable instrument that is flexible to the local conditions and can be adapted to the research objective. It can be particularly useful in studies where it is essential to look at the vertical distribution of organisms through the water column or where high spatial and temporal resolution is necessary, which cannot be achieved with traditional net sampling methods (Remsen *et al.*, 2004; Dennett *et al.*, 2002). Our study shows that depending on the towing procedure, the information to be extracted from the collected data and the ability to distinguish (a)biotic patterns differs. Whereas a Z-shaped and a clover tow type are suitable for detailed characterization of the plankton community of a limited geographical area, a straight tow type is more suitable for plankton studies over a larger area, with the possibility to more easily interpret the influence of environmental factors on the plankton community, compared to the other tow types. The size of the plankton taxa under study should be the main determinant when choosing the magnification setting, with high magnifications being more suitable for smaller organisms (0.3 – 0.7 mm) and vice versa (1.0 – 3.8 mm). If there is no specific focus on a certain taxon, then an intermediate magnification setting S1 is suggested as it avoids that only too large or only too small particles are excluded, while still having sufficient image detail. This study also highlighted some restrictions considering the employability and working range of the VPR. It shows that in areas with a high turbidity, such as coastal systems, the VPR no longer functions optimally, inhibiting the collection of useable image data. The VPR, and with extension other optical methods, therefore needs to be deployed in sufficiently clear waters, with a turbidity threshold of 6.2 NTU for the type of VPR studied here.





# 3

## Picturing plankton: How optical imaging methods can improve assessing plankton community dynamics

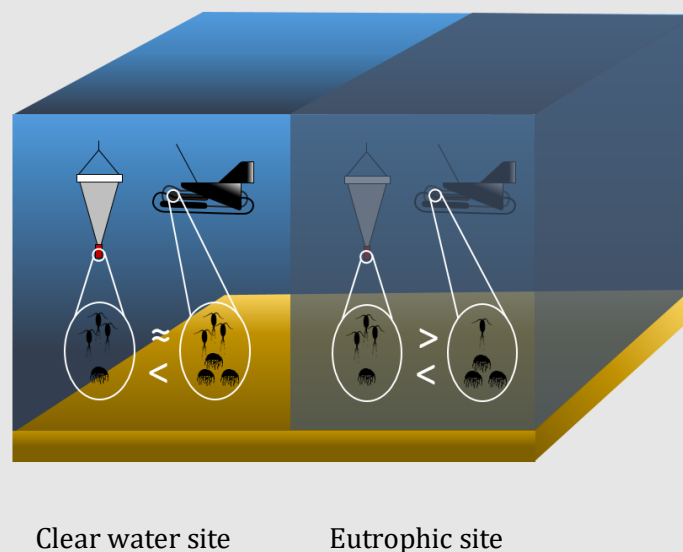
Redrafted after:

Ollevier, A., Mortelman, J., Boone, W., Deneudt, K., De Troch, M., Develter, R., Goossens, C., Meire, L., Möller, K. O., Ponsoni, L. & Hablützel, P. I. (in prep.). Picturing plankton: How optical imaging methods can improve assessing plankton community dynamics.

## Abstract

In the past years, optical imaging has emerged as a promising tool for *in situ* observations of plankton. In this study, we aimed to compare the plankton community estimates obtained from a Video Plankton Recorder (VPR) imaging device with net-based approaches. By collecting VPR and net samples in clear waters with large-sized plankton and eutrophic waters with small-sized plankton, spatial and temporal patterns in plankton densities and community composition were compared. Furthermore, it allowed the evaluation of the performance of imaging methods under diverse hydrographic conditions. We observed pronounced spatial differences in density estimates. In the eutrophic site, the WP2 net densities consistently surpassed those from a VPR, while in the clear water site the observed densities of the VPR and a MultiNet were more similar. Variations in water column turbidity, plankton body size, and plankton nets and their mesh size were found to likely play a role in the observed inconsistencies between the sampling sites. The results suggested that a VPR is particularly well suited for use in clear waters inhabited by large-sized plankton. The VPR was able to improve density estimates of fragile (*Phaeocystis*) and gelatinous taxa (Cnidaria and Ctenophora) in a quantitative manner due to being non-invasive, highlighting the larger contribution of gelatinous species to the zooplankton community. Overall, the VPR and optical imaging devices show valuable insights into zooplankton ecology and distribution, complementing density estimates of traditional net sampling methods, and enhancing our understanding of the role of zooplankton in marine ecosystems.

## Graphical abstract



## 3.1 Introduction

Zooplankton communities are crucial for the functioning of marine ecosystems. They form the link between phytoplankton and higher trophic levels, such as many economically important fish (Nielsen *et al.*, 1993), and play a pivotal role in biogeochemical cycles (Steinberg and Landry, 2017). Most zooplankton species are short-living, have a fast generation time and are sensitive to temperature fluctuations (Chivers *et al.*, 2017; Mackas *et al.*, 2012), making them suitable indicator organisms to evaluate the effects of environmental and anthropogenic pressures on ecosystem functioning. Gaining insight into zooplankton ecology and biology will therefore help to understand the functioning of marine ecosystems and predict their response to environmental changes.

Despite their importance, studying zooplankton can be an intricate task due to their small size, high diversity, and complex life cycles. They can vary in shape, size, and behavior, making it difficult to identify them accurately (Hablützel *et al.*, 2021). Moreover, their patchy distribution patterns and seasonal variations are also challenging to predict, further increasing the complexity. There are various methods to study the plankton community (Hablützel *et al.*, 2021). Typically, plankton research starts from physical samples collected by plankton nets followed by often time-consuming species identification and counts at the species level under a microscope. This technique has been used for over a century, and has provided valuable information about the abundance, diversity, and distribution of plankton. However, due to the labor-intensive nature of this methodology, it is often constrained to a limited spatiotemporal coverage. Moreover, net samples only represent a single point in time and space, failing to encompass the variability among biotic and abiotic components across a continuum of spatiotemporal scales.

Nowadays *in situ* imaging tools have been developed and are more frequently used for plankton research. Optical imaging devices such as the VPR harness unique capabilities to perform continuous *in situ* observations and observe planktonic organisms in their natural environmental context across various spatial scales. It has some specific characteristics that overcome the limits of traditional net sampling methods. It has the advantage of observing fragile marine diversity non-invasively without damaging it, and the simultaneous abiotic, spatial and geographic measurements allow for a tight coupling between plankton and the environment to research its vertical distribution and affinities with water quality parameters. Also having the sample in a digital format can allow for a faster processing time with automated classifiers.

The aim of this study is to evaluate the accuracy of *in situ* imaging estimates in assessing the plankton community compared to different net-based approaches. This study will involve a

comparison of plankton abundances and short-term patterns using an *in situ* Real Time VPR (Davis *et al.*, 2004), a WP2 net and a MultiNet mini under different hydrographic conditions.

## 3.2 Methodology

### 3.2.1 Study area

In this study, we focus on two distinct geographical regions (Figure 3.1), each presenting unique environmental characteristics. The first of these study areas is the Belgian part of the North Sea which covers approximately 3600 km<sup>2</sup>. Situated in the southern North Sea, it serves as a transitional zone between the Atlantic Ocean and the North Sea. This region is relatively shallow with maximum depths of 40 m and encompasses several sandbanks (Van Lancker *et al.*, 2012). The strong tidal currents result in a well-mixed water column with very weak salinity and temperature stratification (Fettweis and Nechad, 2011) which seasonally range between 28 - 35 NTU and 6 - 22 °C, respectively (Flanders Marine Institute, 2020). The eutrophic water column sustains a dense plankton community and is characterized by a high nutrient concentration (De Galan *et al.*, 2004) due to the outflow from the rivers Ijzer, Scheldt and Maas (Nihoul *et al.*, 1978). Especially the river Scheldt has a dominant influence in terms of suspended particulate matter (SPM), forming a high turbidity zone near the coast (Fettweis *et al.*, 2007).

The second study area is the Uummannaq fjord system in West Greenland (between ca. 70 – 72 °N; ca. 50 – 55 °W). Inshore, the fjord system is connected to the Greenland Ice Sheet via numerous streams and tidewater glaciers, and to Baffin Bay offshore. The complex interplay between these boundaries determines the local hydrography and water masses distribution. Depending on depth and water mass, the salinity and temperature of the water column exhibit a broad range, varying between 24 and 35 NTU and -2 to 9 °C (Carroll *et al.*, 2018), respectively. The fjord system depth varies from approximately 250 to 600 m. A key bathymetric feature is the 700-800-m deep trough that extends to the continental shelf break, through which oceanic water masses can flow into the fjords (Rignot *et al.*, 2016).

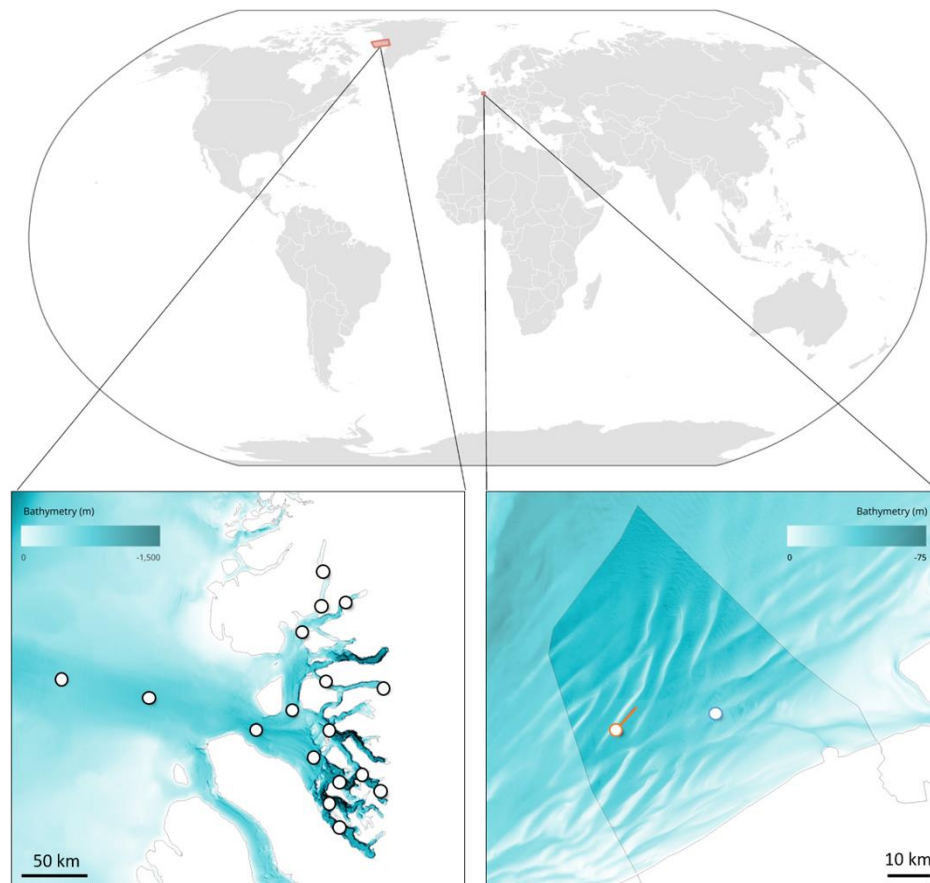


Figure 3.1. Map with sampling locations in Greenland and the Belgian part of the North Sea. Orange circle and transect = ‘methodological cruise’ in March 2021; blue circle = ‘24-hour cruise’ in May 2021; black circles = ‘Greenland cruise’ in June-July 2022.

### 3.2.2 Data collection

Data was collected during three cruises (Figure 3.1, Table 3.1). The first cruise (‘methodological cruise’) took place in March 2021 aboard the RV Simon Stevin in the southern North Sea when samples were specifically collected to compare a WP2 net and a Real Time VPR (Seascan Inc., USA) samples. Different towing procedures and magnification settings of the VPR were used, since these parameters are known to affect the measurements of the VPR and therefore the zooplankton density estimates (Ollevier *et al.*, 2022; chapter 2). A Real Time VPR comprises four preset magnification settings denoted as S0 till S3, each providing distinct fields of view and resulting in different imaged volumes. Three WP2 net samples were collected, followed by three downcasts with the VPR and a 1-hour transect (~7.77 km) undulating the VPR through the water column using a high magnification setting (S1; field of view: 20.8 × 15.2 mm). After returning to the location of the WP2 haul, three more VPR downcasts and a continuous 1-hour VPR transect were performed using a low magnification setting (S3; field of view: 46.5 × 34.5 mm). The

## CHAPTER 3

continuous VPR transects allow for the assessment of the zooplankton community in a larger area around the location of the WP2 haul. During data collection, the VPR was undulated between 3 and 34 m depth with a winch at a speed of  $0.15 \text{ m s}^{-1}$ , while the vessel sailed at 3-4 knots relative to the water column.

Zooplankton was sampled with a  $200 \mu\text{m}$  WP2 net (57 cm diameter opening), which was deployed vertically and equipped with a flowmeter, following the protocol of Mortelmans *et al.* (2019). The net was lowered to just above the sea bottom and hauled up with a maximum speed of  $1 \text{ m s}^{-1}$ . Upon retrieval, the outside of the WP2 net is rinsed with a hose to gather the remaining zooplankton into the cod-end. Zooplankton collected in the cod-end was sedated by carbonated water and fixated in 4 % formalin. In the lab, net samples were digitized by using the ZooScan (Hydroptic Inc., France), a benchtop plankton imaging device. To accomplish this, formalin was drained from the samples, which were then rinsed. Following this, the samples were fractionated using a Motoda splitter (Motoda, 1959), which served to dilute them and prevent organism overlap in the scanned images (Gorsky *et al.*, 2010; Grosjean *et al.*, 2004). After scanning, the fixative was changed to 70 % ethanol. The obtained scans were processed in ZooProcess and Plankton Identifier software (v. 1.3.4, Gasparini and Antajan, 2018) in order to detect and classify the digitized objects (Gorsky *et al.*, 2010; Grosjean *et al.*, 2004). Predictions were manually verified and finally assigned to one of the following taxa: Annelida, Anomura, Appendicularia, Brachyura, Branchiopoda, Calanoida, Chaetognatha, Cirripedia, Cnidaria, Ctenophora, Cumacea, Echinodermata, fish eggs, fish larvae, Harpacticoida, Mollusca, and *Noctiluca*. Non-planktonic categories included artifacts, detritus, and fibres.

Plankton was also sampled by means of a VPR. The collected image data, consisting of regions of interest (ROIs) that were automatically segmented from each image full frame by the AutoDeck software, was manually classified by sorting the zooplankton into the categories Amphipoda, Annelida, Appendicularia, Brachyura, Calanoida, Cnidaria, Ctenophora, Cumacea, Echinodermata, fish larvae, and Harpacticoida. Other particles were classified as *Noctiluca*, *Phaeocystis*, detritus, bubbles, fibres, or unknown. Plankton densities were calculated as the number of individuals per sampled volume and then linearly extrapolated to cubic meters of water [ $\text{ind m}^{-3}$ ], to allow a comparison between VPR and nets, in which sampled volume is determined by:

$$\text{Sampled volume [mL]} = \text{Imaged volume [mL frame}^{-1}] * 25 [\text{frames s}^{-1}] * \text{Duration [s]}$$

During the methodological cruise, the imaged volume of every VPR frame corresponded to 33.342 mL at the high magnification setting and 436.136 mL at the low magnification setting, which was computed as the field of view multiplied by focal depth. This latter was determined by the parameters used with the VPR AutoDeck software (Supplementary table 3.1). A high

magnification (S1) was chosen as it deemed to be a suitable setting for the general plankton community in the southern North Sea, but also a low magnification (S3), was included in the analysis because of its suitability for larger organisms (Ollevier *et al.*, 2022; chapter 2).

During the second cruise ('24-hour cruise'), data was collected during a 24-hour campaign in May 2021 whilst the RV Simon Stevin laid at anchor in the southern North Sea. Every hour, a WP2 sample was collected and the VPR was deployed for approximately 15 minutes, while it was vertically lowered and raised between 3 and 20 m depth at a speed of  $0.15 \text{ m s}^{-1}$ . During the first hours the imaged volume of every VPR frame was 29.564 mL. From 3:00 (UTC+2) onwards, these parameters were unintentionally changed, resulting in an imaged volume of 26.345 mL for the rest of the cruise. A high magnification setting (S1) was used for the whole duration of the cruise.

A third cruise ('Greenland cruise') took place in the Uummannaq fjord system in West Greenland aboard the RV Sanna in June-July 2022. On 17 locations inside the fjords and the connecting shelf area, samples were collected with a MultiNet mini (Hydrobios) and VPR. The MultiNet consists of five  $50 \mu\text{m}$  nets with openings of  $35.5 \times 35.5 \text{ cm}$  that open and close at predefined depth intervals. The topmost net sampled the upper 50 m, the second topmost net the upper 50 - 100 m, and the remaining net intervals varied according to the water column depth respectively. It was deployed vertically at a speed of  $0.4 \text{ m s}^{-1}$ . During retrieval, the outside of the net was rinsed to wash the organisms into the cod-end. The zooplankton collected in the cod-end was transferred to a recipient and was fixed with borax-buffered formaldehyde to a final concentration of 4 %. Using microscopy, the samples were subsequently counted, identified at species or genus level, and classified by stage by the Arctic Agency in Poland. To allow for density estimations between the MultiNet and VPR, species or genera were relabeled according to the VPR taxa, which have lower taxonomic levels. The VPR was deployed for approximately 1.5 h at each station, while it was vertically lowered and raised through the water column between 3 and 250 m (restricted by the length of the winch cable) at a winch speed of  $0.15 \text{ m s}^{-1}$ . The imaged volume of every VPR frame was 335.622 mL based on the low magnification setting (S3). A low magnification setting was chosen due to the large size of the plankton. During deployment, maximum depth of the VPR was limited by the length of the winch cable and resulted in maximum depths of 150 - 250 m for individual stations, depending on the current and vessel speed. To match sampled depths between the two sampling methods, only the top 150 m of each dataset was included in further analysis.

CHAPTER 3

Table 3.1. Overview of the VPR methodology and settings for the three cruises. Overview of the (mean) sampling time [min or h], field and depth of view [mm], imaged volume per frame [mL] and (mean) total sampled volume [m<sup>3</sup>] per WP2 or MultiNet haul and VPR cast or transect. Note: for the MultiNet the mean sampled volume of the top 150 m layer was given in order to compare it better with the mean sampled volume of the VPR in Greenland.

	Methodological cruise				24-hour cruise		Greenland cruise		
	March 2021				May 2021		June – July 2022		
Magnification and towing procedure	WP2 haul	High downcast	High transect	Low downcast	Low transect	WP2 haul	High downcast	MultiNet haul	Low transect
Sampling time	-	6.2 min	1 h	5.6 min	1 h	-	15 min	-	± 1.5 h
Field of view [mm]	-	20.8 x 15.2	20.8 x 15.2	46.5 x 34.5	46.5 x 34.5	-	93.5, after 3:00	-	46.5 x 34.5
Depth of view [mm]	-	105.5	105.5	271.9	271.9	-	29.564, after 3:00	-	209.2
Imaged volume per frame [mL]	-	33.342	33.342	436.162	436.162	-	29.564, after 3:00	-	335.622
Total sampled volume [m <sup>3</sup> ]	8.93	0.31	3.01	3.67	38.25	6.17	0.65	18.75 (top 150 m)	46.08



### 3.2.3 Data analysis

Data from the methodological cruise (including WP2 samples and four deployment methods of the VPR) and the Greenland cruise (involving MultiNet and VPR data) was evaluated by comparing plankton density estimates, zooplankton relative abundances and presence/absence of taxa. The taxa *Noctiluca* (dinoflagellates) and *Phaeocystis* (algae) were included in the analysis because their size range aligns with the mesoplankton fraction, allowing their observation through nets and/or the VPR. Taxon-specific Kruskal-Wallis tests and Dunn tests were performed on the density estimates to test if and what density estimates are significantly different between sampling methods. A Kruskal-Wallis test was performed to test if the Shannon diversity index significantly differed between sampling methods. A regression was plotted for each comparable taxon and a correlation analysis using Kendall's rank correlation coefficient ( $\tau$ ) was conducted to examine the relationship between density estimates of the WP2 and VPR for each taxon. Only taxa present in more than five of the VPR and net samples were included in the regression plot. For data from the methodological cruise, the Shannon diversity index was calculated for each sample as a proxy for the capability of a method to observe a portion of diversity of the plankton community.

To assess temporal patterns of density, the data from the 24-hour cruise was used. A comparison of temporal autocorrelation between WP2 and VPR data was made for each taxon to investigate how strongly counts are predicted by the preceding counts, using the *tscout* package (Liboschik *et al.*, 2017). Data exploration, representation, and analysis were done in R v4.0.3 (R Core Team, 2020). The *FSA* v. 0.9.4 package (Ogle *et al.*, 2023) was used to conduct multiple non-parametric pairwise comparisons (Dunn test) after Kruskal-Wallis rank sum tests were performed. Shannon diversity indexes were generated using the *vegan* v. 2.6-2 package (Oksanen *et al.*, 2022).

Length measurements of the observed organisms in the southern North Sea, based on data from the methodological cruise, were made to assess the size range of the sampling methods. Size estimations of the body length by the ZooScan were based on the major axis of the best fitting ellipse (Gorsky *et al.*, 2010). It should be noted that fixation in formaldehyde causes shrinkage of specimens, in particular of soft-bodied organisms such as Appendicularia, Chaetognatha, Ctenophores, and Cnidaria (Thibault-Botha and Bowen, 2004; Nishikawa and Terazaki, 1996; De Lafontaine and Leggett, 1989), causing length measurements from the ZooScan to be smaller compared to the ImageJ measurements from living organisms. To determine the size ranges of the VPR data, a total of maximum 10 images per taxon and per tow was selected and measured in ImageJ software. First, the scale was set depending on the magnification setting of the VPR. The

size for the VPR images was calculated by measuring the maximum distance of the specimen on the image without excluding appendages.

## 3.3 Results

### 3.3.1 Density estimates and community composition

Zooplankton densities obtained from the WP2 net and VPR during the methodological cruise varied substantially. Taxa observed by both methods had consistently higher density estimates for the WP2 net (Figure 3.2, Table 3.2), with the three most abundant taxa (Calanoida, Cirripedia, and Appendicularia) having densities exceeding 418 ind m<sup>-3</sup>. In contrast, the VPR data at a high magnification recorded densities ranging from 3.33 to 144 ind m<sup>-3</sup>, while the densities of these taxa were less than 12 ind m<sup>-3</sup> at a low magnification. There is however one taxon, *Phaeocystis*, that reaches high abundances in the VPR samples with densities up to 532 ind m<sup>-3</sup>, suggesting that there was a *Phaeocystis* bloom at the moment of sampling. VPR downcasts showed slightly higher densities than continuous transects, but observed less taxa. Only for the less abundant taxa Amphipoda, Cumacea, Harpacticoida, Anomura, Branchiopoda, Chaetognatha, Mollusca, and fish eggs statistically significant differences (Krukall-Wallis, chi-squared = 9.7059 – 10, df = 4, p < 0.05) between density estimates of sampling methods were found.

Certain taxa were only observed by one sampling method or magnification setting of the VPR. The VPR clearly observed *Phaeocystis*, whereas this taxon was not observed by the WP2 net. Furthermore, there are a few taxa such as Amphipoda and fish larvae which were recorded in low abundances by the VPR, but not by the WP2 net. On the contrary, the WP2 showed low densities of Anomura, Branchiopoda, Chaetognatha, Mollusca, and fish eggs which were not captured by the VPR. The VPR only observed Brachyura, Cirripedia, Cumacea, and Harpacticoida with the high magnification setting.

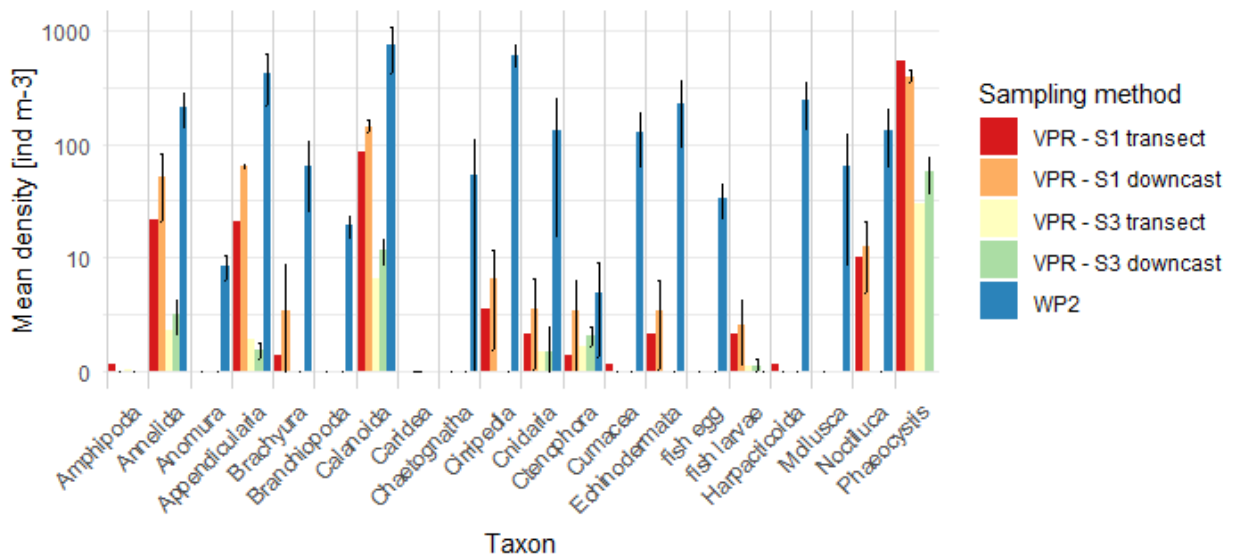


Figure 3.2. Plankton taxa densities estimated by the WP2 net and different settings of the VPR. The mean density of WP2, VPR - S1 (high magnification), and VPR - S3 (low magnification) were based on three net samples for the first, and three downcast profiles for the two latter. Mean density is presented with a log<sub>10</sub> scale.

Count data (Table 3.2) indicated that the number of organisms collected in a WP2 sample is much higher than the number of plankton ROIs collected by a cast or transect from the VPR, when considering the entire collected WP2 sample (images scanned by the ZooScan multiplied by its dilution factor of 5-6 times for the samples collected in March 2021). Comparing the VPR towing procedures shows that tows with a similar sampling time (VPR downcast high magnification vs downcast low magnification; VPR transect high magnification vs transect low magnification) yielded similar counts, but that Cnidaria and Ctenophora were observed more frequently with a low magnification compared to a high magnification and that *Noctiluca* was not observed with the low magnification. A longer sampling time (transect vs downcasts) resulted in a higher count of individuals. The total sampled volume in the methodological campaign was 8.93 m<sup>3</sup> for the WP2 hauls and 0.31, 3.01, 3.67, and 38.25 m<sup>3</sup> for the VPR high magnification downcast, high magnification transect, low magnification downcast, and low magnification transect, respectively (Table 3.1).

CHAPTER 3

Table 3.2. Average counts ( $\pm$  stdev) [ind], average density ( $\pm$  stdev) [ind m<sup>-3</sup>], and relative abundance [%] as estimated by the WP2 net and various deployment methods of the VPR. The counts for the WP2 net represent the counted individuals by the ZooScan of a fraction of the sample (fractionated 5 to 6 times). Counts and density are given for the mesoplankton community, relative abundances were based on the zooplankton community (i.e. excluding the taxa *Noctiluca* and *Phaeocystis*).

Taxon	Counts [ind]					Density [ind m <sup>-3</sup> ]					Relative abundance [%]				
	WP2	VPR low, downcast	VPR low, transect	VPR high, downcast	VPR high, transect	WP2	VPR low, downcast	VPR low, transect	VPR high, downcast	VPR high, transect	WP2	VPR low, downcast	VPR low, transect	VPR high, downcast	VPR high, transect
<b>Amphipoda</b>	0	0	1	0	4	-	-	0.33	-	0.1	0	0	0.24	0	0.83
<b>Annelida</b>	36 $\pm$ 5	16 $\pm$ 10	66	10 $\pm$ 4	74	211.54 $\pm$ 69.98	51.14 $\pm$ 30.13	21.96	2.86 $\pm$ 1.14	1.93	7.2	18.3	15.87	15.81	15.99
<b>Anomura</b>	2 $\pm$ 1	0	0	0	0	8.37 $\pm$ 2.07	-	-	-	-	0.28	0	0	0	0
<b>Appendicularia</b>	70 $\pm$ 21	20 $\pm$ 1	63	3 $\pm$ 1	56	418.3 $\pm$ 202.11	63.26 $\pm$ 2.66	20.96	0.92 $\pm$ 0.35	1.46	14.23	22.64	15.14	5.09	12.1
<b>Brachyura</b>	12 $\pm$ 9	1 $\pm$ 2	2	0	0	64.54 $\pm$ 39.93	3.17 $\pm$ 5.5	0.67	-	-	2.2	1.13	0.48	0	0
<b>Branchiopoda</b>	4 $\pm$ 2	0	0	0	0	19.12 $\pm$ 4.14	-	-	-	-	0.65	0	0	0	0
<b>Calanoida</b>	125 $\pm$ 35	45 $\pm$ 6	255	42 $\pm$ 10	245	733.82 $\pm$ 314.4	143.66 $\pm$ 18.02	84.84	11.62 $\pm$ 3.05	6.4	24.97	51.41	61.3	64.23	53.02
<b>Chaetognatha</b>	9 $\pm$ 7.55	0	0	0	0	52.58 $\pm$ 55.7	-	-	-	-	1.79	0	0	0	0
<b>Cirripedia</b>	106.33 $\pm$ 23.8	2 $\pm$ 1.73	10	0	0	604.74 $\pm$ 129.14	6.4 $\pm$ 5.46	3.33	-	-	20.58	2.29	2.41	0	0
<b>Cnidaria</b>	21.67 $\pm$ 14.57	1 $\pm$ 1	5	3 $\pm$ 4.36	32	131.47 $\pm$ 116.14	3.24 $\pm$ 3.18	1.66	0.86 $\pm$ 1.28	0.84	4.47	1.16	1.2	4.75	6.96

COMPARISON

<b>Ctenophora</b>	1 ± 1	1 ± 1	2	5.6 7 ± 1.5 3	41	4.78 ± 4.14	3.2 ± 3.12	0.67	1.56 ± 0.49	1.07	0.16	1.15	0.48	8.62	8.86
<b>Cumacea</b>	21 ± 6	0	1	0	0	125. 49 ± 63.4 3	-	0.33	-	-	4.27	0	0.24	0	0
<b>Echino- dermata</b>	38 ± 16	1 ± 1	5	0	0	227. 08 ± 132. 68	3.2 ± 3.12	1.66	-	-	7.73	1.15	1.2	0	0
<b>Fish eggs</b>	6 ± 4	0	0	0	0	33.4 6 ± 10.9 6	-	-	-	-	1.14	0	0	0	0
<b>Fish larvae</b>	0	1 ± 1	5	1 ± 1	9	-	2.16 ± 1.88	1.66	0.27 ± 0.27	0.24	0	0.77	1.2	1.49	1.99
<b>Harpacti- coida</b>	41 ± 11	0	1	0	0	239. 03 ± 105. 71	-	0.33	-	-	8.13	0	0.24	0	0
<b>Mollusca</b>	10 ± 7	0	0	0	0	64.5 4 ± 56.0 1	-	-	-	-	2.2	0	0	0	0
<b>Noctiluca</b>	23 ± 11	4 ± 3	30	0	0	131. 47 ± 67.7 8	12.6 9 ± 8.02	9.98	-	-	-	-	-	-	-
<b>Phaeocystis</b>	0	12 3 ± 21	159 8	20 9 ± 80	114 2	-	394. 25 ± 51.2 9	531. 64	56.5 9 ± 19.9 5	29.8 6	-	-	-	-	-

Relative abundances of zooplankton taxa differed between the WP2 and VPR sampling methods, and between the magnification settings of the VPR (Table 3.2). The most abundant zooplankton taxon, i.e. with the exclusion of the taxa *Noctiluca* and *Phaeocystis*, across all sampling methods was Calanoida, accounting for 24.97 % of the zooplankton community in WP2 nets and for 51.41 -64.23 % as observed by the VPR. Cirripedia and Appendicularia were the second and third most abundant in the WP2 data, with relative densities of 20.58 and 14.23 %, respectively, followed by Harpacticoida, Echinodermata, and Annelida contributing between 7.20 and 8.13 % to the zooplankton community. For the VPR, Appendicularia and Annelida were frequently observed and contributed to the zooplankton community with relative abundances of 5.09 - 22.64 % and 15.81 - 18.30 %, respectively. Cirripedia, Harpacticoida, and Echinodermata were, however, rarely or never observed by means of the VPR. Cnidaria and Ctenophora accounted for a higher percentage in the VPR data with magnification S3 compared to other samples. The remaining taxa had low relative densities across all sampling methods.

## CHAPTER 3

The highest Shannon diversity was found in WP2 samples (Figure 3.3), but the Shannon diversity index did not differ significantly between sampling methods and VPR settings (Kruskal-Wallis, chi-squared = 8.8485, df = 4, p-value > 0.05).

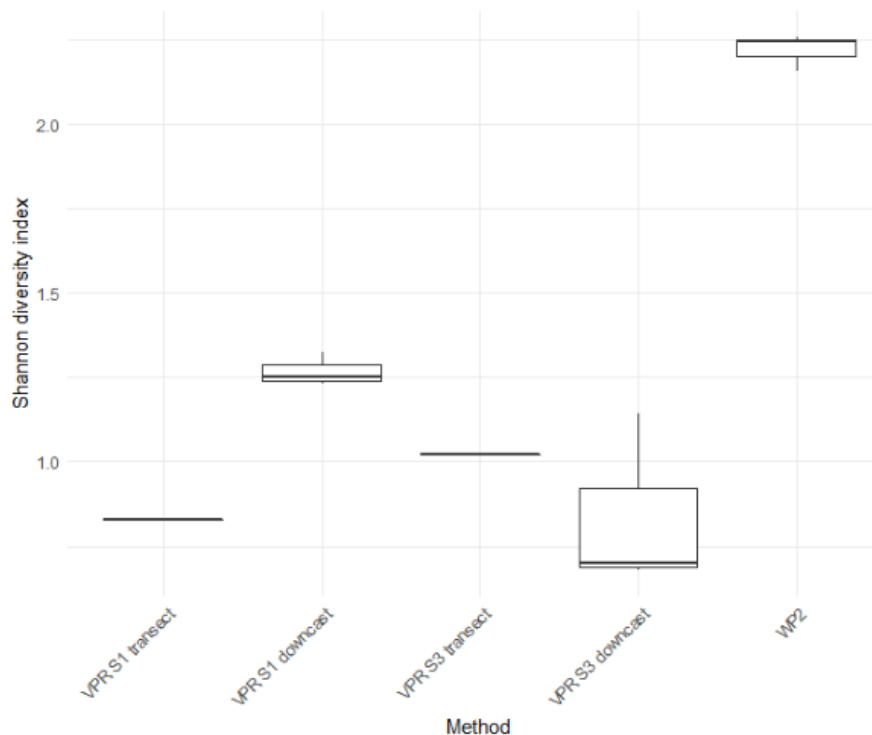


Figure 3.3. Shannon diversity index of mesoplankton community observed by the WP2 and VPR sampling methods.

Plankton density estimates of samples taken by the WP2 net and VPR were plotted against each other, based on the data from the May 2021 cruise (Figure 3.4A). Of the taxa in the regression plot, the correlation analysis revealed a significant positively related rank correlation between WP2 and VPR densities for the taxon *Noctiluca* ( $z = 2.5464$ ,  $p < 0.05$ ,  $\tau = 0.3639$ ). The tau correlation coefficient suggests a moderate positive relationship. This means that as the plankton density recorded by WP2 increases, there is a corresponding tendency for an increase in density as measured by VPR.

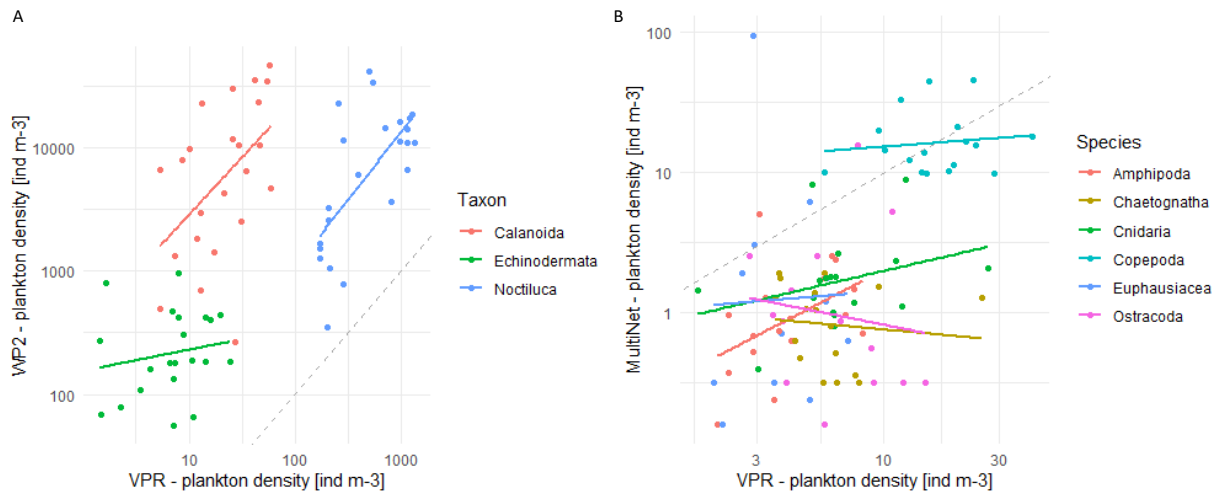


Figure 3.4. Regression plots to compare density estimates between (A) a WP2 net and VPR based on data from a 24-hour campaign in the southern North Sea and (B) a MultiNet mini and VPR based on data from Greenland. Points and lines are colored per taxon. Solid lines show the line of the best fit. The dashed line represents the 1:1 line.

Plankton densities of the top 150 m of the water column in Greenland estimated by the MultiNet and VPR are often in the same order of magnitude. The three most abundant groups in the MultiNet were Copepoda, other meroplankton, and Euphausiacea together contributing 71.33 % to the plankton community. Average densities of these groups ranged between 6 and 19 ind m<sup>-3</sup> (Table 3.3). Other meroplankton categories included Gastropoda, Bivalvia, Echinodermata, Bryozoa, and Pilidium, of which Bivalvia larvae had the most important contribution to this group. In the VPR samples none of the taxa grouped under other meroplankton were observed, nor were Cirripedia, other crustaceans, and Rotifera. In the collected VPR data, Copepoda, Cnidaria, and Chaetognatha were the most observed taxa, together contributing 78.91 % to the mesozooplankton community and having average densities between 6 and 17 ind m<sup>-3</sup>. These latter two taxa also had higher relative abundances in the VPR data (15.53 and 13.45 %, respectively), compared to the MultiNet data (3.72 and 1.63 %, respectively).

## CHAPTER 3

Table 3.3. Average density ( $\pm$  stdev) [ind m<sup>-3</sup>], relative abundance [%], and average counts ( $\pm$  stdev) [ind] per sampling station as estimated by the MultiNet net and the VPR in Greenland. The MultiNet counts represent the individuals counted through microscopy within a subsample that underwent fractionation (1 to 6 times). This representation serves to clarify the specific values used for calculating the actual densities.

Taxon	Density [ind m <sup>-3</sup> ]		Relative abundance [%]		Count [ind]	
	MultiNet	VPR	MultiNet	VPR	MultiNet	VPR
<b>Amphipoda</b>	1.28 $\pm$ 1.17	4.16 $\pm$ 2.18	2.12	8.72	7.33 $\pm$ 4.81	7.59 $\pm$ 6.65
<b>Annelida</b>	2.6 $\pm$ 4.24	0.42 $\pm$ 1.23	4.32	0.88	14 $\pm$ 16.81	1.5 $\pm$ 0.71
<b>Appendicularia</b>	3.28 $\pm$ 8.42	0.53 $\pm$ 1.23	5.44	1.11	11.08 $\pm$ 18.28	1.33 $\pm$ 0.58
<b>Chaetognatha</b>	0.98 $\pm$ 0.56	6.42 $\pm$ 5.18	1.63	13.45	8.72 $\pm$ 5.68	14.41 $\pm$ 9.82
<b>Cirripedia</b>	0.28 $\pm$ 0.66	0 $\pm$ 0	0.46	0	2.17 $\pm$ 1.94	0 $\pm$ 0
<b>Cnidaria</b>	2.24 $\pm$ 2.4	7.41 $\pm$ 5.83	3.72	15.53	22.83 $\pm$ 17.71	55.76 $\pm$ 29.71
<b>Copepoda</b>	18.74 $\pm$ 11.39	17.02 $\pm$ 9.19	31.11	35.67	1039.61 $\pm$ 143.47	599.29 $\pm$ 360.12
<b>Ctenophora</b>	0.06 $\pm$ 0.17	1.6 $\pm$ 2.94	0.1	3.35	1 $\pm$ 0	5 $\pm$ 5.39
<b>Euphausiacea</b>	6.49 $\pm$ 22.3	3.05 $\pm$ 2.43	10.77	6.39	25.36 $\pm$ 51.38	9.62 $\pm$ 10.52
<b>Fish larvae</b>	0 $\pm$ 0	0.73 $\pm$ 1.69	0	1.53	0 $\pm$ 0	1.25 $\pm$ 0.5
<b>Other meroplankton</b>	17.74 $\pm$ 40.67	0 $\pm$ 0	29.45	0	22.69 $\pm$ 28.31	0 $\pm$ 0
<b>Ostracoda</b>	2.67 $\pm$ 4.34	5.71 $\pm$ 4.22	4.43	11.97	11.22 $\pm$ 15.48	6.33 $\pm$ 5.55
<b>Other</b>	2.97 $\pm$ 7.2	0 $\pm$ 0	4.93	0	20.6 $\pm$ 21.45	0 $\pm$ 0
<b>Other crustaceans</b>	0.26 $\pm$ 0.29	0 $\pm$ 0	0.43	0	1.77 $\pm$ 1.09	0 $\pm$ 0
<b>Pteropoda</b>	0.51 $\pm$ 0.74	0.67 $\pm$ 1.67	0.85	1.4	2.4 $\pm$ 1.26	2 $\pm$ 1
<b>Rotifera</b>	0.14 $\pm$ 0.33	0 $\pm$ 0	0.23	0	1 $\pm$ 0	0 $\pm$ 0



A Kruskal-Wallis test per taxon showed significant differences (chi-squared = 4.358 - 27.462, df = 1,  $p < 0.05$ ) for less abundant taxa such as Amphipoda, Annelida, Appendicularia, Chaetognatha, Cirripedia, Cnidaria, other meroplankton, Ostracoda, other crustaceans, fish larvae.

Plankton density estimates of MultiNet and VPR samples were plotted against each other (Figure 3.4B). However, the correlation analysis yielded results indicating that there is no statistically significant rank correlation between MultiNet and VPR densities for the taxa depicted in Figure 3.4B. This implies that there is no consistent association between MultiNet and VPR densities for the taxa under consideration in Figure 3.4B and that these two methods may not provide synchronized estimates of plankton density for these taxa.

### 3.3.2 Size measurements

Length measurements (Table 3.4) of the WP2 sample and the VPR data at a high magnification generally yielded similar size measurements for the plankton, except for ctenophores that were larger in the VPR data. In the case of the low magnification of the VPR, larger specimens were consistently observed compared to the WP2 and VPR high magnification data, particularly among Ctenophora and Cnidaria. Notably, images captured by the low magnification of the VPR often included the tentacles of ctenophores, and cnidarians with larger hoods compared to the high magnification.

### 3.3.3 Comparison of plankton patterns over time

The densities of Calanoida, *Noctiluca*, Echinodermata, and Cumacea taxa abundantly present in both WP2 and VPR data from the 24-hour cruise, significantly differed between sampling methods (Figure 3.5). Densities differed some orders of magnitude. Changes in plankton density for these taxa over a 24-hour period, however, followed similar patterns, where peaks and valleys generally, except for a few high density outliers, coincide between methods. Calanoida displayed three peaks, *Noctiluca* and Echinodermata two peaks, whereas Cumacea were mostly observed during the night.

The autoregression coefficients (Supplementary table 3.2) were relatively high in both WP2 and VPR methods for Amphipoda, indicating strong positive temporal autocorrelation. Past counts of Amphipoda seem to be a good predictor of its later counts, gradual changes over time. Other taxa such as *Phaeocystis*, *Noctiluca*, and Annelida in the VPR dataset and Cirripedia and Harpacticoida in the WP2 dataset had moderate coefficients and signify some level of temporal autocorrelation. These values imply that there might be some relationship between previous counts and current

## CHAPTER 3

counts. The VPR tends to have higher autocorrelation coefficients for specific taxa compared to the WP2 net.

*Table 3.4. Mean size ( $\pm$  stdev) [mm] of plankton taxa in the WP2 and VPR samples. Note that size does not reflect the head-tail length of the organisms but are the longest or widest part of an organism including appendages and antennae.*

<b>Taxon</b>	<b>WP2</b>	<b>VPR high magnification downcast</b>	<b>VPR high magnification transect</b>	<b>VPR low magnification downcast</b>	<b>VPR low magnification transect</b>
<b>Amphipoda</b>	-	-	1.28	-	2.45 $\pm$ 1.21
<b>Annelida</b>	1.04 $\pm$ 0.26	1.33 $\pm$ 0.35	1.11 $\pm$ 0.34	1.32 $\pm$ 0.34	1.5 $\pm$ 0.39
<b>Anomura</b>	1.66 $\pm$ 0.33	-	-	-	-
<b>Appendicularia</b>	1.8 $\pm$ 0.75	2.39 $\pm$ 0.45	2.22 $\pm$ 0.71	2.7 $\pm$ 1.03	2.87 $\pm$ 0.51
<b>Brachyura</b>	1.11 $\pm$ 0.44	0.85 $\pm$ 0.19	1.98 $\pm$ 1.73	-	-
<b>Branchiopoda</b>	0.49 $\pm$ 0.09	-	-	-	-
<b>Calanoida</b>	0.89 $\pm$ 0.23	0.72 $\pm$ 0.19	0.83 $\pm$ 0.32	0.89 $\pm$ 0.24	0.94 $\pm$ 0.21
<b>Chaetognatha</b>	2.64 $\pm$ 0.72	-	-	-	-
<b>Cirripedia</b>	0.6 $\pm$ 0.14	0.47 $\pm$ 0.14	0.64 $\pm$ 0.26	-	-
<b>Cnidaria</b>	2.36 $\pm$ 1.59	1.41	2.71 $\pm$ 2.01	6.17	7.65 $\pm$ 8.23
<b>Ctenophora</b>	1.33 $\pm$ 0.54	2.35 $\pm$ 1.64	5.71 $\pm$ 4.19	4.62 $\pm$ 2.2	5.8 $\pm$ 3.58
<b>Cumacea</b>	1.36 $\pm$ 0.48	0.67	0.9	-	-
<b>Echinodermata</b>	0.63 $\pm$ 0.3	1.32 $\pm$ 0.42	1.67 $\pm$ 0.19	-	-
<b>Fish egg</b>	1.05 $\pm$ 0.58	-	-	-	-
<b>Fish larvae</b>	-	1.76	3.24 $\pm$ 1.07	3.85 $\pm$ 0.76	5.57 $\pm$ 2.23
<b>Harpacticoida</b>	0.57 $\pm$ 0.1	-	0.55	-	-
<b>Mollusca</b>	0.39 $\pm$ 0.15	-	-	-	-
<b>Noctiluca</b>	0.51 $\pm$ 0.14	0.64 $\pm$ 0.11	0.57 $\pm$ 0.06	-	-
<b>Phaeocystis</b>	-	2 $\pm$ 0.56	2.02 $\pm$ 0.87	3.41 $\pm$ 0.91	3.2 $\pm$ 1.32

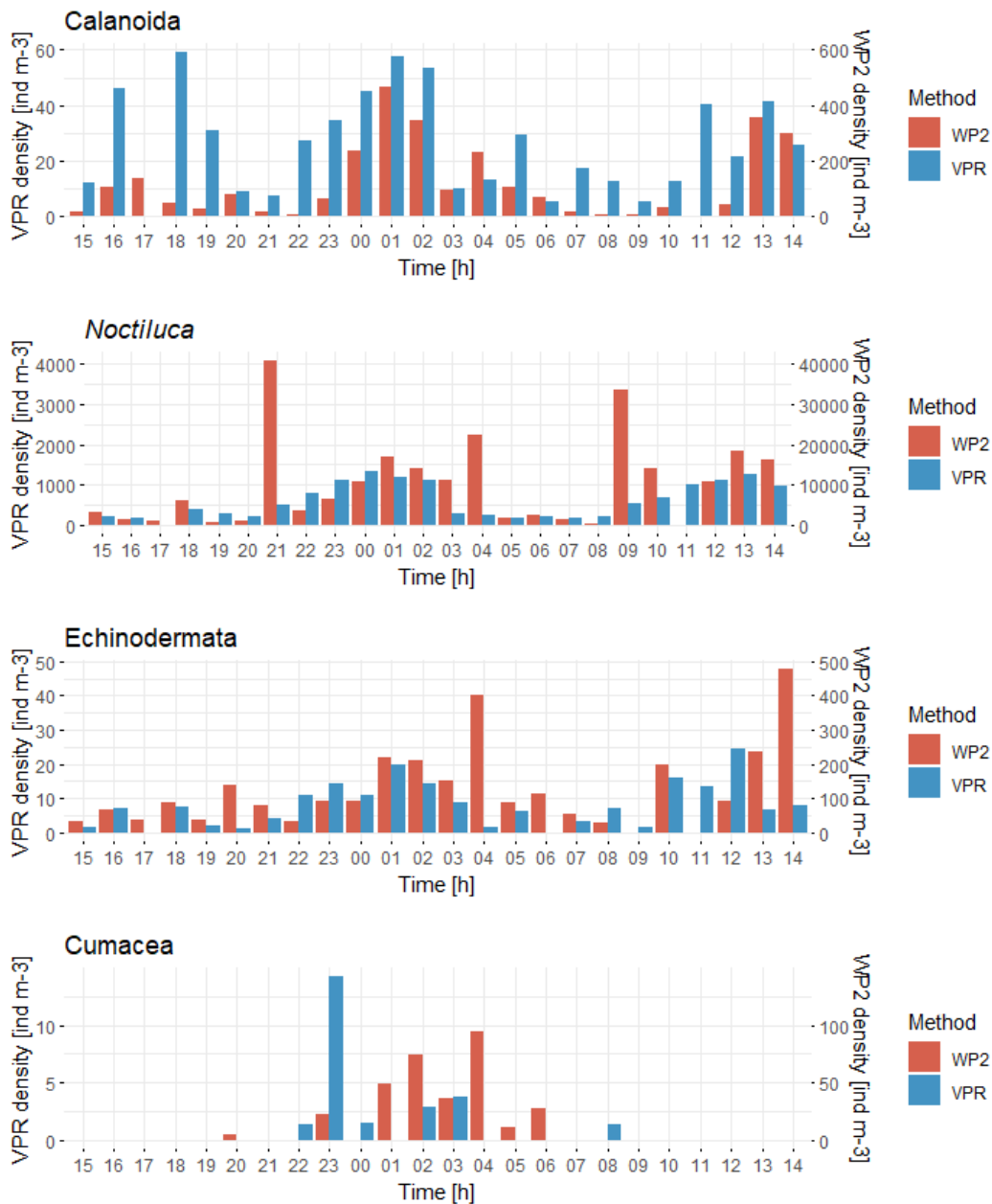


Figure 3.5. Density estimates [ind m<sup>-3</sup>] of Calanoida, Noctiluca, Echinodermata, and Cumacea over a 24-hour period as observed by the WP2 net and VPR with the high magnification setting. Note that two y-axes are used, one for each sampling method.

## 3.4 Discussion

### 3.4.1 Imaging and net sampling methods for plankton estimates

Density estimates varied across different study areas for the various sampling methods employed. Results from the two sampling campaigns in the southern North Sea showed that the VPR in general underestimates plankton densities compared to WP2 net hauls for the majority of

## CHAPTER 3

the taxa. The most abundant non-gelatinous taxa in the WP2 sample (Calanoida, Cirripedia, Harpacticoida, Echinodermata, and Annelida), together accounting for more than 65 % of the total zooplankton community, all had densities that were considerably higher, although not statistically significant, than those observed in the VPR sample and often differed one order in magnitude. This is in contrast to the density estimates of the VPR and MultiNet in Greenland, where density estimates were more similar and often lied within the same order of magnitude. The observations from the Greenland campaign are in line with previous studies with nets and optical imaging devices, which generally showed similar density estimates for abundant taxa in net and VPR samples (Beroujon *et al.*, 2022; Strand *et al.*, 2020; Broughton and Lough, 2006; Benfield *et al.*, 1996). The VPR and MultiNet data showed similar density estimates for the most abundant taxon, i.e., Copepoda. However, the VPR did not observe any of the taxa grouped under other meroplankton (Gastropoda, Bivalvia, Echinodermata, Bryozoa, and Pilidium) which were abundant and accounted for almost a third of the plankton community in the MultiNet samples. The predominant constituents of this group were identified as Bivalvia. It is likely that the VPR did not record any of the taxa under other meroplankton due to the small size of Bivalvia, outside the effective magnification range of the VPR, and infrequent occurrences of the other taxa, some observed only once.

The VPR is thought to be suitable for fragile and gelatinous taxa as *in situ* optical imaging devices can observe particles inside the water column without damaging or destroying them. Other studies with a high resolution sampler (SIPPER/OPC) indicated that nets underestimate Cnidaria and Ctenophora abundance by 1200 % (Remsen, 2004). In the samples from Greenland, the density and relative abundance estimates of the fragile and gelatinous taxa Cnidaria, Ctenophora, and Chaetognatha ranged from 3 to 33 times higher in the VPR samples in terms of density and relative abundance compared to the MultiNet samples. This corroborates observations of Beroujon *et al.* (2022) in East Greenland where gelatinous taxa were underestimated by a WP2 net compared to an autonomous VPR. In the samples from the southern North Sea, however, densities of gelatinous species were undersampled by the VPR, but regarding relative abundances, Cnidaria and Ctenophora made a slightly greater contribution to the plankton community in the VPR data, particularly in magnification setting S3 (4.75 - 8.86 %), compared to the WP2 data (0.16 - 4.47 %). This, however, may be because the WP2 net observed a higher number of taxa and thus a higher proportion of the biodiversity. The tendency to have higher (relative) abundances with the VPR compared to net sampling methods highlights the potential advantage of the VPR in observing delicate and gelatinous species. This is further supported by the observations of *Phaeocystis*, a fragile colonial forming phytoplankton species, that was very abundant in the VPR data, but absent in the WP2 net data in the southern North Sea despite being

in the size range of the WP2 net as the colonies are likely destroyed during net sampling (Bender *et al.*, 2018).

### 3.4.2 Discrepancies between sampling areas

The comparison of net hauls and the VPR yielded different results between sampling campaigns in the southern North Sea and Greenland. Because the findings from the Greenland campaign are in line with previous studies, it raises the question why the VPR underestimated most plankton densities in the southern North Sea compared to net-based approaches. First of all, different net sampling methods were used between the study areas, each having a different mesh size, net opening and towing speed. This factor itself already gives rise to variation in how the plankton community is sampled and estimated (Skjoldal *et al.*, 2013, 2019) and thus introduces variation in the community we compare to the VPR results. Nevertheless, considering that both WP2 and MultiNet nets are widely used in plankton research, this underscores the significance of comparing the outcomes of a VPR to these established methods. The intercomparison of net sampling methods by Skjoldal *et al.* (2013) indicated that the mesh size had a major influence on the biomass and species composition of the zooplankton community. Reducing the mesh size may increase the retention of small organisms, but may lower the filtration efficiency and increase the avoidance of large organisms. Conversely, increasing the towing speed and mesh size may improve the catch efficiency of larger zooplankton, but results in greater loss of small individuals by extrusion through the mesh of the net. Additionally, nets are susceptible to clogging, particularly during events like phytoplankton blooms (e.g., of *Phaeocystis*), which can prevent the passage of plankton and result in an undersampling of the community. During the May campaign *Phaeocystis* was blooming, but not to the extent that the nets were clogged.

Secondly, there exists a substantial contrast in the plankton communities between the two sampling locations. The VPR was originally designed for open ocean use with low densities of copepods (Tiselius, 1998). However, conditions in the southern North Sea are very different with high densities of smaller-sized plankton. Conversely, the plankton community in Greenland is typified by larger specimens, such as *Calanus hyperboreus*, capable of reaching a body length of 7 mm (Leinaas *et al.*, 2016), yet they exist in lower densities. The plankton size itself could affect the density estimations. Small plankton will appear smaller and less distinctive on the ROIs, causing them to be potentially overlooked and harder to identify during the manual validation process depending on the magnification used. Inherently connected to the magnification setting is the size range wherein particles are observed. The low magnification setting is mainly suitable for larger organisms as seen in the results, causing the lack of observing small taxa. In the studies

## CHAPTER 3

of Beroujon *et al.* (2022) and Strand *et al.* (2020), densities of smaller organisms were also generally underestimated.

Thirdly, the environmental conditions and physical characteristics of the two regions may also play a role in the discrepancy. In particular, turbidity of the water column strongly impacts the performance of the VPR (Ollevier *et al.*, 2022; chapter 2), resulting in less or no capturing of images when turbidity levels are too high (values exceeding 6.2 NTU). Turbidity of the water column inside the fjords in West Greenland is, except for areas with freshwater runoff or glacial influence (van Genuchten *et al.*, 2022; Holinde and Zielinski, 2016), generally low. In contrast, the southern North Sea receives a lot of SPM from rivers which raises the turbidity in the coastal areas. The sampling location within the southern North Sea was specifically chosen to be located in an area below the turbidity threshold value mentioned above to minimize the impact of turbidity on the capture of images, resulting in only small disparities in average water column turbidity compared to sampling locations in Greenland.

Next, another factor that could contribute to differences in plankton densities between nets and the VPR is the sampling depth. The top three meters of the water column were sampled during a net haul, but not during VPR deployment as a safety range is kept to avoid collision with the vessel and to avoid turbulence in the ship's wake. Organisms are not homogeneously vertically distributed in the water column (Jónasdóttir and Koski, 2011; Conway and Minton, 1976; Ollevier *et al.*, submitted; chapter 4) and in case they aggregate in high density patches in these zones, this can also contribute to the undersampling of the plankton community by the VPR. Furthermore, in terms of safety ranges, the VPR does not sample the bottom three meters of the water column. This precaution was applied in the southern North Sea, but for the Greenland campaign this was not applicable due to the considerable depth of the seabed beyond the VPR's sampling range. Consequently, this exclusion may result in the undersampling of hyperbenthic organisms such as Cumacea, which are closely associated with the seabed.

Finally, variations in the total sampled volume, coupled with potential errors in volume estimations, may contribute to the observed disparities. The imaged volume per frame of the VPR is low, particularly at higher magnification settings, resulting in a generally low total sampled volume compared to net sampling methods. This discrepancy becomes more pronounced in brief deployments, as evidenced during campaigns in the southern North Sea (Table 3.1). Contrastingly, in Greenland, the total sampled volume exceeded that of the surface 150 meters sampled by the MultiNet. This is due to the employment of lower magnification settings, leading to a larger imaged volume per frame, and a longer deployment of the VPR. The increased total sampled volume in Greenland might ensure a more comprehensive representation of the water

column and contribute to more comparable density estimates between methods. Further, Basedow *et al.* (2013) pointed out that small errors in the estimated sampling volume of the VPR can give rise to large errors in the estimated densities. The VPR's sampling volume relies on the user-defined AutoDeck setting which determines the depth of view, the magnification which determines the field of view and the duration of the VPR deployment. Alterations in these settings can substantially affect the sampling volume, yet the direct translation of these changes to corresponding alterations in densities remains unclear. One might consider that the sampled volume per frame leans towards a slight overestimation, possibly resulting in lower observed densities for the VPR per cubic meter of water. This could further emphasize the observed disparities, although this aspect remains challenging to test definitively. Broughton and Lough (2006) also highlighted the importance of accurate calibration of the VPRs field of view, as inaccurate calibration in their study was potentially the reason for errors in density estimates. Calibration in their paper had to be done manually by gluing a copepod to a hair and moving it back and forth and judging when the plankton imaged was too dark or out of focus to be readily identified, whereas now Seascan is using targets with drilled holes with a constant speed which is less subjective. The calibration of the VPR was not reevaluated after the sampling campaign in this study because the findings from the Greenland campaign aligned with outcomes from other studies, indicating that the system's calibration was not the reason for the undersampling observed in the southern North Sea.

### 3.4.3 Temporal patterns

Despite the VPR's tendency to underestimate density in the southern North Sea, consistent patterns were observed in density variations of abundant taxa over a 24-hour period, showing that both the VPR and WP2 net capture the underlying dynamics of zooplankton communities. To address density discrepancies between sampling methods, the implementation of a calibration factor has been suggested (Broughton and Lough, 2006). Previous studies used a correction factor for certain specific taxa (Ohman and Lavaniegos, 2002) or for the whole community (Remsen *et al.*, 2004). Based on our observations, determining a calibration factor for the whole community or even specific taxa might be difficult due to variations in the regression lines between taxa and study regions. It should also be determined whether a region specific correlation factor would remain valid during different seasons. Furthermore, the examination of the temporal autocorrelation of taxa-specific densities indicated that the VPR tends to have higher autoregression coefficients, suggesting that it has a higher measurement precision or that it is less vulnerable to density variations at small spatial scales compared to WP2 samples.

### 3.4.4 Added value of optical methods

Both optical imaging devices and net sampling methods possess unique advantages and drawbacks. Net methods present a straightforward and standardized approach for collecting discrete plankton samples and have become widely adopted. An advantage is that physical net samples, identifiable through microscopy and expert classification, can be identified to low taxonomic levels that *in situ* images, constrained by their low resolution, may not reach. On the other hand, optical imaging methods provide researchers a multitude of benefits, such as the ability to employ various magnifications and both discrete and continuous deployment methods. This flexibility allows researchers to tailor their investigations to meet specific needs. Additionally, the combination of optical imaging devices with CTD sensors facilitates *in situ* sensing and allows to investigate plankton distribution with a high spatial resolution in the order of centimeters and allows for a tight coupling with simultaneously collected abiotic, spatial, and geographic measurements. In previous studies, imaging devices such as a VPR have been deployed to study the interaction between marine snow and zooplankton (Möller *et al.*, 2012), the aggregation of hydromedusae around a density continuity (Jacobsen and Norrbin, 2009), the diurnal vertical migration of zooplankton (Pan *et al.*, 2018; Sainmont *et al.*, 2014), and the formation and life cycle of a bloom (Takahashi *et al.*, 2015). Optical imaging methods therefore are crucial for studies focussing on the vertical distribution of organisms through the water column and those requiring high spatial and temporal resolutions, which cannot be achieved with traditional net sampling methods. Additionally, ongoing advancements in automated classifiers will facilitate the more accurate, rapid, and cost-effective identification of images generated by optical methods. This progress will enable the (real-time) handling of extensive data volumes without a proportional increase in resources, meeting the rising demand for more data in plankton monitoring and research.

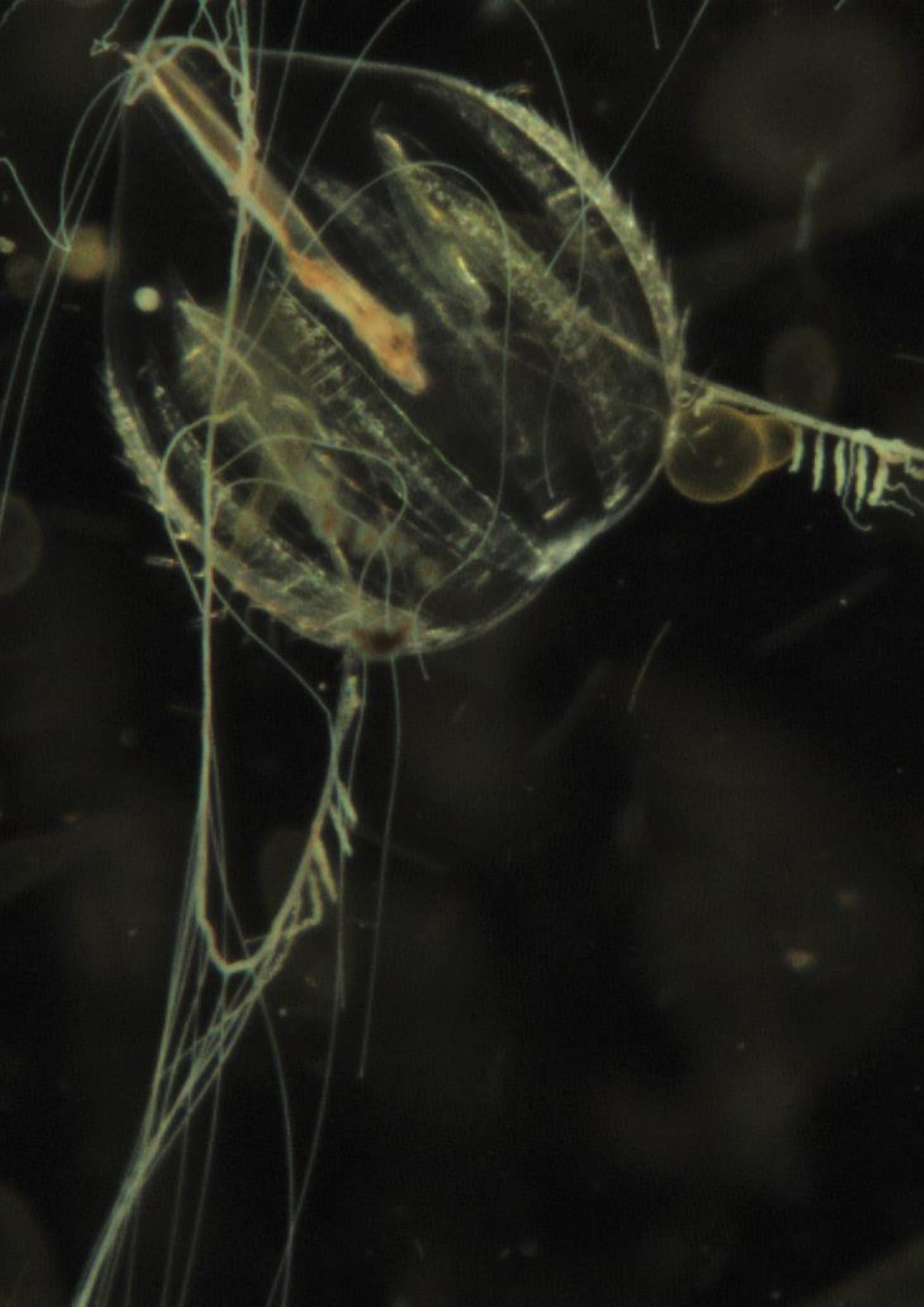
## 3.5 Conclusion

The aim of this study is to evaluate the accuracy of *in situ* imaging estimates in assessing the plankton community compared to different net-based approaches. The comparison between the VPR and net-based approaches resulted in different plankton density estimations depending on the environmental characteristics of the study area and the type of plankton community. Whereas the VPR consistently underestimated zooplankton densities compared to the WP2 net in the southern North Sea, density estimates in Greenland were similar to those from the MultiNet. A combination of factors linked to water column turbidity, plankton body size, and plankton nets



and its net mesh size probably contributed to the discrepancies between study areas. It suggests that a VPR is more suitable in clear waters with low plankton densities.

For a long time, our knowledge of plankton relied on plankton nets. However, our results show that the VPR quantitatively improves estimates of gelatinous and fragile taxa that are often damaged and therefore under sampled by net sampling methods. Furthermore, despite the differences in absolute density estimates between optical devices and nets, both methods observed similar patterns over a 24-hour period, indicating that the density fluctuations of zooplankton were consistent regardless of the sampling approach. This consistency underscores the ability of both methods to capture similar temporal variations in zooplankton populations. All these aspects, together with the higher spatiotemporal resolution, concurrent measurements with additional sensors, and the expedited identification process of extensive data volumes, signify the potential of optical methods to significantly contribute to plankton research. By leveraging both net-based and optical imaging approaches, future studies can improve spatial coverage and enhance the accuracy and comprehensiveness of zooplankton assessments, leading to a deeper understanding of their ecological significance in marine ecosystems.



# 4

## Diel vertical migration and tidal influences on plankton densities in dynamic coastal systems

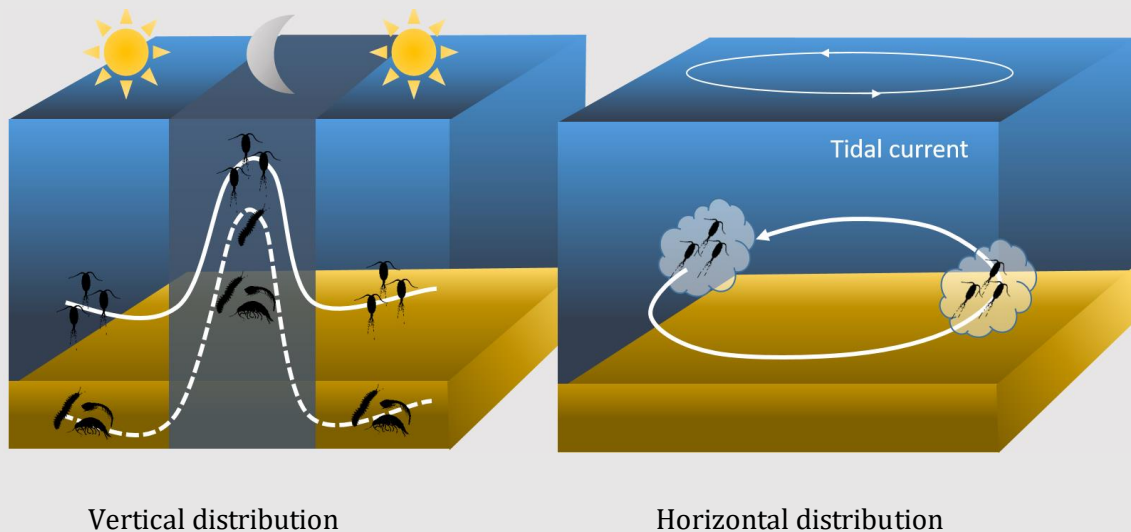
Adjusted from:

Ollevier, A., Mortelmans, J., Deneudt, K., Hablützel, P. I., & De Troch, M. Diel Vertical Migration and Tidal Influences on Plankton Densities in Dynamic Coastal Systems. Submitted to *Estuarine, Coastal and Shelf Science*.

## Abstract

Recent increased application of optical imaging devices have facilitated efficient capture of plankton abundance and community composition, enabling the study of plankton distribution *in situ* and at a high spatiotemporal resolution. In this study, we aim to investigate how the abundances and distribution patterns of plankton taxa relate over 24-hour periods, covering tidal and diel cycles, in the southern North Sea using data from a WP2 net and a Video Plankton Recorder (VPR). In the highly dynamic southern North Sea, we document diel vertical migration patterns in the pelagic zone of both pelagic and hyperbenthic taxa, including Calanoida (Copepoda), Amphipoda, Annelida, and Cumacea. In addition, the densities of plankton taxa showed significant small-scale geographical variation over a 24-hour period for which tidal currents played an important role, a source of considerable variation that is typically not accounted for. This study adds to the current understanding of plankton distribution and behavior, particularly in the context of coastal areas characterized by strong tidal cycles and currents, obtained by using state-of-the-art *in situ* imaging techniques.

## Graphical abstract



## 4.1 Introduction

Plankton are passive drifters in the water, subject to the effects of wind, waves, and currents. While they lack the ability to swim against these forces, some possess a degree of mobility that allows them to determine their vertical position in the water column. Plankton plays a crucial role in the marine food web by contributing to organic matter flux and nutrient recycling (Steinberg and Landry, 2017). Vertical migration can therefore lead to the mobilization of a considerable biomass through the water column and acts as a vehicle for carbon export in the marine carbon cycle (Steinberg and Landry, 2017). This flux of organic matter is estimated to account for 4 – 34 % of the total particulate organic carbon flux in various regions worldwide (reviewed in Ducklow *et al.*, 2001).

Both plankton and its predators respond to sunlight. While autotrophic phytoplankton (primary producers) try to maximize sunlight exposure for photosynthesis (Vernet, 2000), fish predators (secondary consumers) often require light to detect their zooplanktonic prey (Guthrie, 1986). Fish, and to some extent also phytoplankton, migrate vertically in response to light availability (de Graaf *et al.*, 2004; Gerbersdorf and Schubert, 2011; Wirtz and Smith, 2020). The movements of zooplankton (primary consumers) in the water column therefore often relate to the vertical distribution of phytoplankton (their prey) and fish (their predator; Haupt *et al.*, 2009; Reichwaldt and Stibor, 2005). Many zooplankton species perform diel vertical migration (DVM; Bandara *et al.*, 2021) which can be categorized in three general migration patterns (Hutchinson, 1967): nocturnal, twilight, and reversed vertical migration, with zooplankton rising from deeper waters towards the surface during night, at twilight, and during daytime, respectively. Nocturnal or twilight migration is the most common behavior observed among plankton. The underlying mechanisms driving DVM can be behavioral responses to exogenous factors such as light, gravity, temperature, salinity, oxygen, hydrostatic pressure, the availability of food, and potential mates, or endogenous changes in behavior and physiology (Cohen and Forward, 2016). Various hypotheses were proposed to explain why these organisms perform DVM, but it is commonly assumed to be primarily driven by a trade-off between predator avoidance and foraging opportunities (Loose and Dawidowicz, 1994). Gut fullness plays a significant role in this trade-off and studies observed that fatter or fuller individuals prioritize predator avoidance in deeper waters over risky feeding in upper waters (Hays, 2001) and that DVM behavior in organisms co-occurred with higher feeding rates at night (Daro, 1985). Furthermore, the size-dependent predation risk caused by visual predators led to a hypothesis suggesting that larger copepods predominantly engage in DVM due to their increased susceptibility to visual predation (Hays, 1995).

## CHAPTER 4

The vertical distribution of plankton is traditionally studied with nets. Often, systems consisting of multiple nets that can open and close during a vertical haul (e.g., MultiNet, MOCNESS) are deployed within different depth ranges of the water column (Keskinen *et al.*, 2004; Luo *et al.*, 2000). One limitation of this approach is that organisms are in many cases pooled within depth intervals, resulting in a loss of precision regarding their depth and diminishing statistical power when investigating differences in depth distributions between day and night (Pearre 2003; Pinel-Alloul 1995). Advancements in technology to collect *in situ* data led to the development of optical imaging devices such as the VPR (Davis *et al.*, 1992). These devices photograph plankton and other particles within the water column and simultaneously collect depth and environmental data, allowing a tight coupling between the environment and plankton community. As a result, a VPR can efficiently capture variation in zooplankton abundance and community composition in 3D and through time, allowing to study the plankton and hyperbenthic taxa distribution with a high vertical spatial resolution. Due to its capabilities, the VPR proved to be very useful to detect small-scale plankton aggregations (Möller *et al.*, 2014; Jacobsen and Norrbin, 2009).

In this study, we use the VPR technology to investigate the relationships between abundances and distribution patterns of several plankton taxa over 24-hour periods, a timescale covering two tidal and one diel cycle, during two seasons, in a shallow coastal region with a (nearly) permanently mixed water column (van Leeuwen *et al.*, 2015). These areas experience strong tidal cycles and currents, resulting in a water column with a very weak salinity and temperature stratification (Fettweis and Nechad, 2011). While in certain areas of the North Sea or neighboring areas some studies failed to detect diel vertical migration of zooplankton (e.g. in the English Channel by Daro, 1985), migratory patterns in copepods were observed in the Southern Bight of the North Sea (Daro, 1985) and in the retention basin of a disused scouring sluice in the harbor of Ostend, Belgium, which is only sporadically connected to the sea (Daro, 1974). This study utilizes a compelling combination of zooplankton abundance data collected throughout the entire water column using a WP2 net processed by the ZooScan, alongside zooplankton abundance data obtained by a VPR at different depths. These data, along with a comprehensive set of (a)biotic variables, allow us to analyze how plankton is distributed vertically over fine spatial and temporal scales within the water column. By conducting this research, we aim to gain valuable insights into the dynamics of planktonic communities in well-mixed water columns over 24-hour periods, thereby enhancing our understanding of diel vertical migration and other migratory patterns in the marine environment.

## 4.2 Methodology

### 4.2.1 Study area

The Belgian part of the North Sea (Figure 4.1) is located in the southern North Sea and is positioned in the transitional region between the Atlantic Ocean and the North Sea. It is a relatively shallow area with maximum depths of about 40 meters. The strong semi-diel tidal currents and the alongshore residual current, flowing towards the northeast, result in a well-mixed water column with very weak salinity and temperature stratification (Fettweis and Nechad, 2011). The tidal currents are dominated by tides ranging from 3 m (neap tide) to 4.5 m (spring tide) and can have high velocities with maxima up to  $1.66 \text{ m s}^{-1}$  (Verfaillie, 2008). They are mainly driven by tides and wind force, resulting in anti-clockwise gyres (Otto *et al.*, 1990).

### 4.2.2 Sample collection

Data were collected during two 24-hour sampling campaigns in May 2021 (19-05-2021 15:37 to 20-05-2021 14:19) and November 2022 (22-11-2022 14:42 to 23-11-2022 09:30) whilst the RV Simon Stevin laid on anchor at station 330 ( $2.8091^\circ \text{E}$ ;  $51.4341^\circ \text{N}$ ; red point in Figure 4.1). In May 19, 2021, the moon phase was first quarter, which produces moderate tides known as neap tides, while on November 22, 2022, the moon phase was a waning crescent, resulting in tidal bulges that are increasing in size until they reach their maximum during the spring tides at new moon phase. Every hour, data on mesoplankton and associated water parameters were collected. Mesoplankton were imaged *in situ* by means of a Real Time VPR (Seascan, Inc.). The VPR was deployed each hour for approximately 15 minutes, while it was lowered and raised vertically through the water column at a speed  $0.15 \text{ m s}^{-1}$ . It was deployed 3 m from the seafloor and 3 m beneath the surface to avoid hitting the seafloor or the ship.

The image data was manually classified by sorting the mesoplankton into the categories: Amphipoda, Annelida, Appendicularia, Appendicularia house, Brachyura zoea, Calanoida, Caridea, Chaetognatha, Cirripedia cypris, Cirripedia nauplius, Cnidaria, Ctenophora, Cumacea, Echinodermata, fish larvae, Harpacticoida, *Noctiluca*, and *Phaeocystis*. The prymnesiophyte *Phaeocystis* was counted in numbers of colonies, as the VPR has the capacity to detect and observe these collective formations but not individual cells. Other particles were classified as detritus, bubbles, fibres or unknown. Plankton densities were calculated as the number of individuals per sampled volume and then linearly extrapolated to cubic meters of water [ $\text{ind m}^{-3}$ ].

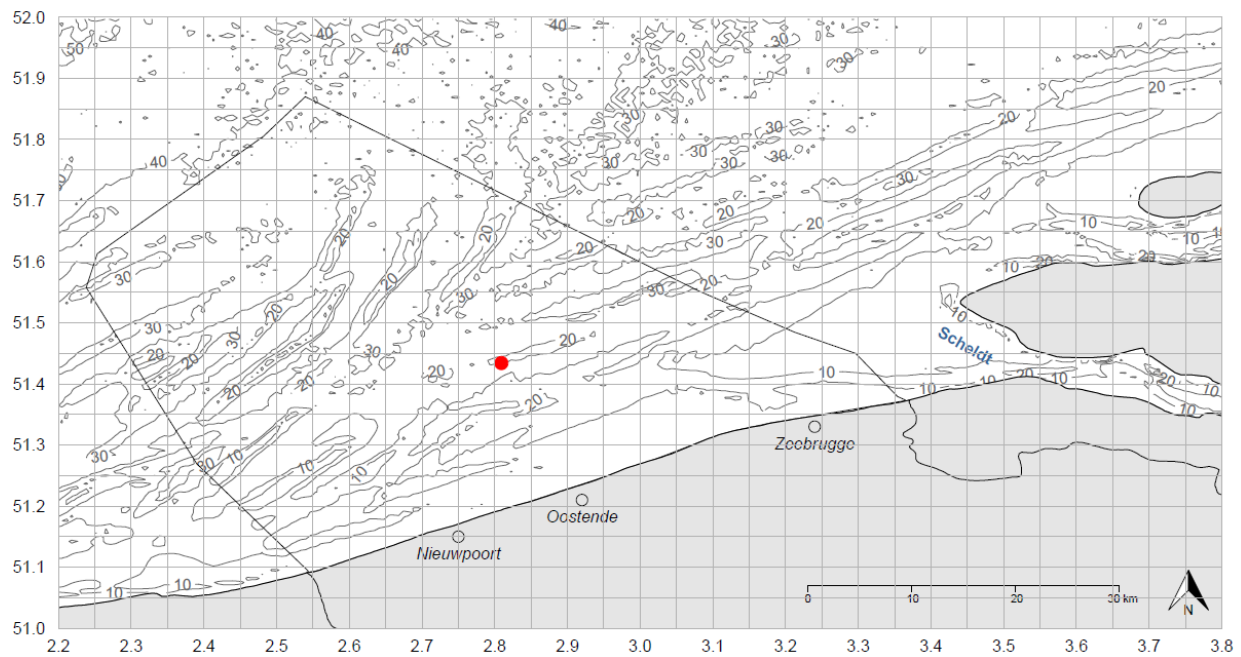


Figure 4.1. Sampling station 330 represented as a red point within the Belgian part of the North Sea (black outline). The depth of the water column [m] is represented by the grey lines and values. The X-axis represents longitude [°E] and the Y-axis latitude [°N].

During the first hours of the cruise in May, the imaged volume of every VPR frame was 29.564 mL which was calculated as the field of view (magnification setting S1: 20.8x15.2 mm) multiplied by focal depth. The latter was determined by the parameters used with the VPR AutoDeck software: a segmentation threshold – low of 0, a segmentation threshold – high of 131, a focus – sobel of 23, and a focus – std dev of 2. From 3:00 (UTC+2) onwards, these parameters were accidentally changed, resulting in an imaged volume of 26.345 mL for the remainder of the cruise (a segmentation threshold – low of 0, a segmentation threshold – high of 132, a focus – sobel of 25, and a focus – std dev of 2). As a result of the smaller sampling volume, approximately 10% less organisms were encountered. The mean total sampled volume was 0.65 m<sup>3</sup> per deployment. The second highest magnification, S1, was chosen as a trade-off between image detail and observation chance of particles (Ollevier *et al.*, 2022; chapter 2). In November, the imaged volume was 23.391 mL for the whole campaign, based on magnification setting S1, a segmentation threshold – low of 0, a segmentation threshold – high of 135, a focus – sobel of 25, and a focus – std dev of 1. Simultaneously, fluorescence, turbidity, salinity, temperature, and depth data were collected with the ECO Puck FLNTU fluorometer and turbidity sensor (WETLabs), and SBE 49 CTD sensor (Sea-Bird Electronics, Inc.) that was mounted on the VPR, allowing linking plankton images with *in situ* environmental and position data at the moment of collection. Salinity was measured using the Practical Salinity Scale. Data on average current speed and averaged current direction were derived from the ERDDAP data server of RBINS (Royal Belgian Institute of Natural Sciences, n.d.).



Mesoplankton were also hourly sampled with a 200  $\mu\text{m}$  WP2 net, which was deployed vertically and equipped with a flowmeter, following the protocol of Mortelmans *et al.* (2019). The mean total sampled volume per haul was 6.17  $\text{m}^3$  in May. Zooplankton collected in the cod-end were sedated by soda water and fixed in 4 % formalin. In the lab, the fixative was changed to 70 % ethanol. The samples were digitized by the ZooScan plankton imaging device and processed by ZooProcess and Plankton Identifier in order to detect and classify the digitized objects (Gorsky *et al.*, 2010; Grosjean *et al.*, 2004). Images were manually controlled and validated to the categories Amphipoda, Annelida, Anomura, Appendicularia, Branchiopoda, Brachyura megalopa, Brachyura zoea, Calanoida, Chaetognatha, Cirripedia cypris, Cirripedia nauplius, Cnidaria, Ctenophora, Cumacea, Echinodermata larvae, fish egg, fish larvae, Harpacticoida, Mollusca, Mysida, artefact, detritus, fibres, and *Noctiluca*.

### 4.2.3 Data analysis

Due to adverse weather conditions during the November campaign, VPR data could only be gathered from 14:00 until 9:00. The weather also hindered the collection of a continuous series of WP2 net samples. Net samples from November are therefore not considered in this study. Plankton densities and distributions through the water column were visually represented with the *ggplot2* package (Wickham, 2016) in R v4.0.3 (R Core Team, 2020). The depth under which 75 % of the community could be found at day and night was represented by the 25th percentile. Nighttime was defined as the period between sunset and sunrise, specifically, between 21:31 and 05:47 in May, and between 16:48 and 08:11 in November. Conversely, observations made outside of these periods were categorized as daytime. To assess the relative influence of environment, tides and diel cycle on plankton community composition and species abundances, variation partitioning analysis was used. This method allows us to dissect the variance in community data attributed to these factors. For this analysis, plankton community data, aggregated per VPR deployment, was Hellinger transformed (Borcard *et al.*, 2011). The Hellinger transformation is suitable for compositional data, preserving the Euclidian distance and aiding in the analysis of community structure. The model was then built as a function of environmental, tidal and diel cycle parameters using redundancy analysis (RDA). RDA was chosen for its ability to handle complex ecological datasets and is well-suited for modeling relationships between the entire plankton community and multivariate predictor variables. The environmental dataset contained temperature, salinity, turbidity and chlorophyll concentration. The tidal dataset consisted of data on maximum sampling depth (which serves as a proxy for tide, i.e. the alternate rising and falling of the sea), average current direction and average current speed. In the diel effect dataset solar altitude ('sunAngle' function from the *oce* v.1.7-2 package; Kelley and Richards, 2022) was

included. The number of environmental and tidal predictors was reduced using a forward selection procedure. These final set of predictor variables were used for variation partitioning analysis using the *vegan* v. 2.6-2 package (Oksanen *et al.*, 2022) in R. The role of tidal and diel patterns on the depth distribution of taxa was analysed using generalised additive models (GAMs) with a log-link function assuming a Poisson distribution of the response variables (counts of the individual plankton taxa). Unlike generalized linear models, which are constrained by the assumption that all explanatory variables are linked in a linear combination with the response variable, GAMs can model non-linear relationships between predictors and the response variable by applying smooth functions and uncover complex patterns and relationships in the data (Zuur *et al.*, 2009). However, it is essential to note that in the present study, GAMs were primarily employed for visualizing underlying patterns within the raw data. The emphasis was placed on exploring and understanding complex relationships, as opposed to interpreting the significance of the statistical test, given that certain assumptions required for conventional model interpretation were not met (Zuur *et al.*, 2009). These analyses were carried out with the *mgcv* package (Wood, 2013) in R. The models included 'depth', 'diel', 'tides', and 'detritus' as predictors and allowed for an interaction term for 'depth', and 'diel' (see formulas in Supplementary table 4.1). By incorporating 'detritus' in the GAMs of the various taxa, the influence of passive particle distribution driven by diel and tidal patterns is taken into account, which allows to distinguish and analyze the distribution patterns of the taxa itself.

## 4.3 Results

### 4.3.1 Abiotic environment over time

During the 24-hour cycle in May, it was high tide at 19:11 and 8:10 and low tide at 2:21 and current speed ranged between  $0.15 \text{ m s}^{-1}$  and  $0.64 \text{ m s}^{-1}$ . The CTD upcasts (Supplementary figure 4.1) measured temperatures ranging between  $11.2$  and  $11.7$  °C and observed no stratification layers in the water column but slight surface-bottom differences of  $0.1$  °C were found. In some cases, the temperature was homogeneously distributed along the entire water column, although in most cases there were slight surface-bottom differences where the surface part had a maximally  $0.1$ °C higher temperature than the seafloor. The strongest differences between top and bottom occurred between high and low tide at the turning of the tides, i.e. currents changing direction. Overall, salinity ranged between  $32.8$  and  $33.8$ , and was not stratified over the water column. Based on the FLNTU and turbidity sensor on the VPR, mean turbidity was  $1.19$  NTU (Q1:  $0.91$  - Q3:  $1.53$ ) and mean chlorophyll a concentration  $1.19 \mu\text{g L}^{-1}$  (Q1:  $0.60$  - Q3:  $1.72$ ). In November, it was low tide at 18:25 and 6:46, and high tide at 0:09, with current speeds ranging between  $0.20$  and  $1.00 \text{ m s}^{-1}$ . CTD upcasts revealed water temperatures between  $13.3$  and  $13.6$

°C and salinity values between 34.6 and 34.7. These measurements indicated a homogenous water column without stratification. Mean turbidity was 1.75 NTU (Q1: 0.8 - Q3: 2.4) and mean chlorophyll a concentration was 1.11  $\mu\text{g L}^{-1}$  (Q1: 0.90 - Q3: 1.30)

### 4.3.2 Species abundance over time

The densities of plankton taxa showed large variation over the 24-hour time period, both for the WP2 and VPR data. Although the order of magnitude of densities differed, similar abundance patterns were often observed by the two methods (Figure 4.2, Supplementary table 4.2, 4.3). The peaks did not coincide with high or low tide, but displayed some time lag. *Noctiluca*, Calanoida and Echinodermata were observed throughout the whole period by both methods and exhibited a pronounced pattern in density over time with two peaks for *Noctiluca* and a third peak for Calanoida and Echinodermata. *Phaeocystis*, only observed by the VPR, displayed a similar pattern with two distinct peaks. *Noctiluca* and *Phaeocystis* were most abundant in the VPR dataset with peak densities of 1,320  $\text{ind m}^{-3}$  and 1,818  $\text{ind m}^{-3}$ , respectively. Calanoida and Echinodermata had maximum densities of 59 and 24  $\text{ind m}^{-3}$ , respectively, with the VPR. Calanoida and *Noctiluca* showed the highest peak densities in the WP2 dataset with densities of 14,650  $\text{ind m}^{-3}$  and 12,623  $\text{ind m}^{-3}$ , respectively.

In both observation methods Amphipoda, Annelida, and Cumacea were mainly observed during nighttime. Other taxa such as Appendicularia, Caridea, Chaetognatha, Cirripedia cypris, Cirripedia nauplius, Cnidaria, fish eggs, and Harpacticoida were sporadically observed with the VPR during the day (Supplementary table 4.2). For most of these taxa this was also the case for the WP2 data, except for the taxa Cirripedia nauplius, Cirripedia cypris, and Harpacticoida, which were observed more frequently throughout the day and had two peaks with sometimes a third smaller peak. Other species that were additionally sporadically observed by the WP2 net were Anomura, Brachyura megalopae, Brachyura zoeae, Mollusca, and Porcellanidae (Supplementary table 4.3).

## CHAPTER 4

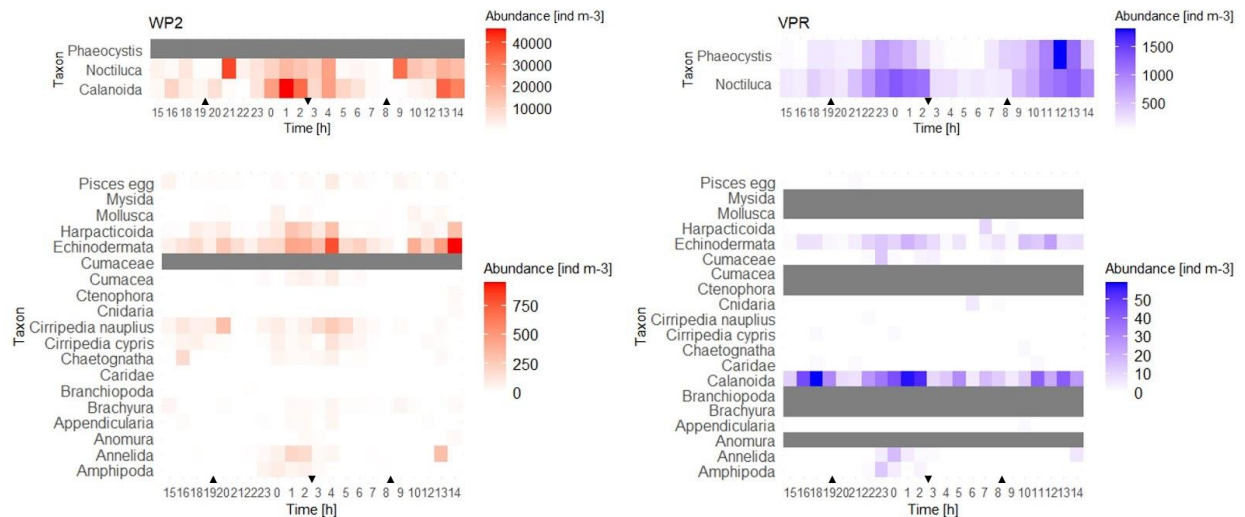
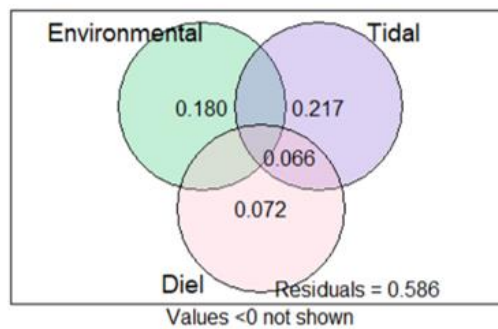


Figure 4.2. Plankton depth-integrated densities [ind m<sup>-3</sup>] over a 24-h time period [h] in May as observed by a WP2 net (red) and VPR (blue). Taxa that were not observed by a sampling method are represented in grey. High and low tide are symbolized by an ascending and descending triangle, respectively. Note that different scales are used for abundance [ind m<sup>-3</sup>] between the plots.

### 4.3.3 Effect of environmental conditions on species abundances and community composition

Variation partitioning indicated that environmental, tidal, and diel predictors together explained 41.4 % of the variation in taxa abundances of the plankton community (Figure 4.3 A). The selected predictors were chlorophyll concentration (environmental), maximum sampling depth (tidal), and altitude of the sun (diel). The environmental predictors explained 18.0 % ( $p < 0.001$ ). Tidal predictors explained the largest part of the variation and accounted for 28.3 % of which 21.7 % ( $p < 0.001$ ) could be attributed purely to the tidal effect. Diel predictors explained 13.8 %, of which nearly half was shared variation explained by both diel cycle and tides. Diel variation alone accounted for 7.2 % of the variation ( $p < 0.05$ ). The RDA biplot (Figure 4.3 B) shows that the first axis is positively correlated with all parameters, but has the strongest association with the tidal parameter. The second axis is positively associated with diel and tidal variables, but negatively with environmental ones. Distinct taxa are Calanoida, *Noctiluca*, and *Phaeocystis* and the cluster of Amphipoda, Annelida, and Cumacea.

A



B

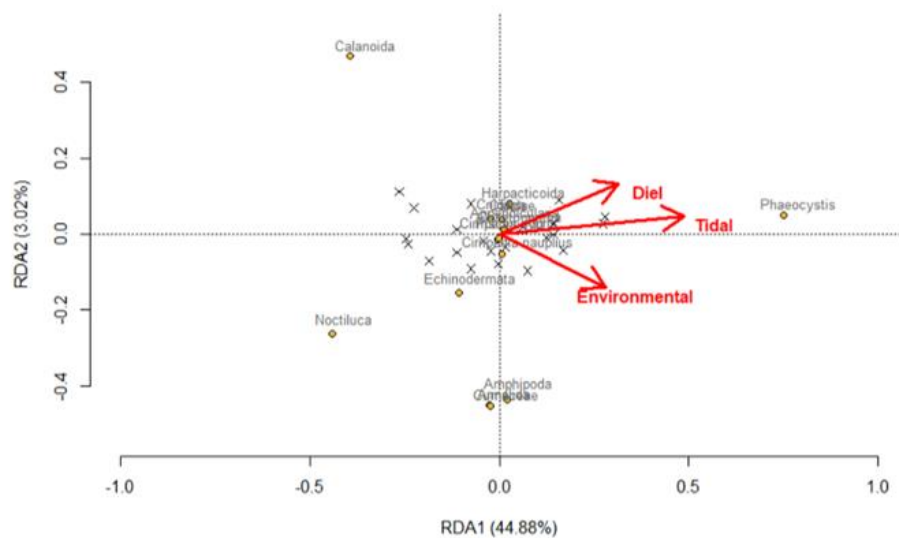


Figure 4.3. (A) Venn diagram showing the variation partitioning results for Hellinger-transformed plankton abundance data explained by unique and joint effects of environmental (green), tidal (purple), and diel (pink) factors. Only significant effects ( $p < 0.05$ ) are represented. (B) Biplot of RDA showing the effect of the environmental, tidal, and diel variables (red arrows). Species are represented as yellow dots, the sampling times as crosses.

#### 4.3.4 Diel vertical migration

Certain taxa in the dataset showed clear displacements through the water column over the observed 24-hour period in May. The taxa Amphipoda, Annelida, and Cumacea were not or hardly observed during the day, while being observed several times during the night (Figure 4.4 A, B, D). Calanoida, an abundant taxa in the zooplankton community, on the other hand, were observed during the entire 24-hour period, but the majority of calanoids was found in shallower water layers at night compared to their position at daytime (Figure 4.4 C). During the day 75 % of the

## CHAPTER 4

calanoid copepod community was present below 9.2 m whereas at night this was at 5.7 m (Supplementary table 4.4). In November only Cumacea (Figure 4.4 H) were sufficiently present for meaningful statistical analysis in the VPR data and therefore are the only taxa visualized in November. Cumacea were regularly observed at night, but because only a limited number of observations were made during daytime in the 17-hour period, it is not possible to know if the taxon was present or absent during the unsampled times of the day. Hence, drawing definitive conclusions about DVM patterns of Cumacea in November is challenging. Moreover, the distribution of detritus was visualized (Figure 4.4 E) as this provides insights into the dispersion of passive particles within the water column as they are primarily influenced by hydrodynamical forces. Elevated densities were found in the deeper layers and density peaks occur approximately 12 hours apart from each other over the course of the 24-hour period.

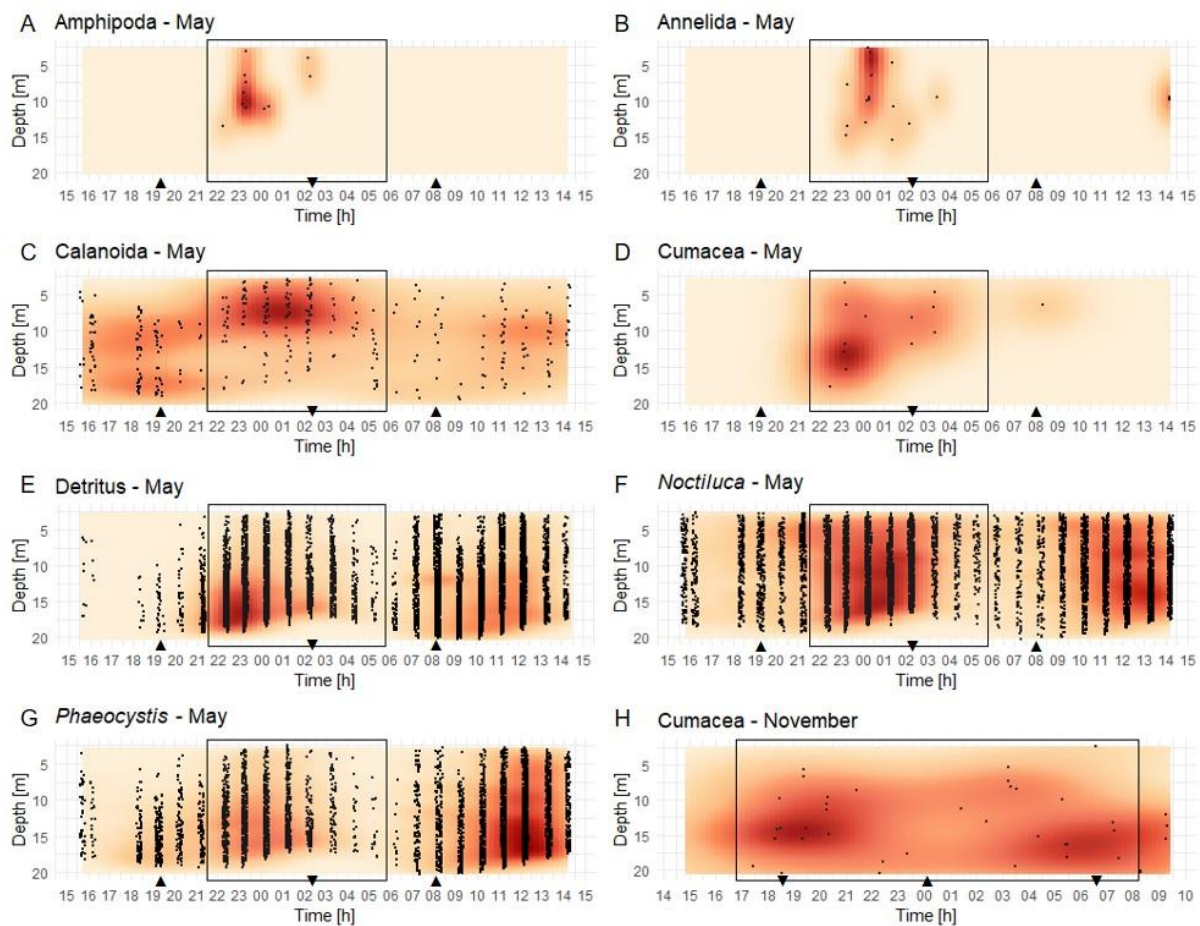


Figure 4.4. Kernel density plots for the depth distribution of individual observations (black dots) of (A) Amphipoda, (B) Annelida, (C) Calanoida, (D) Cumacea, (E) detritus, (F) Noctiluca, and (G) Phaeocystis in May and (H) Cumacea in November over time [h] based on VPR data. The red areas represent higher interpolated densities for the group under consideration and the rectangular box represents nighttime. Remark: from 3:00 onwards (in May) a smaller sampled volume was used

resulting in  $\pm 10\%$  less observed particles. In May there was no data collected at 17:00. Note that the depth range varies depending on the tides. High and low tide are symbolized by an ascending and descending triangle, respectively.

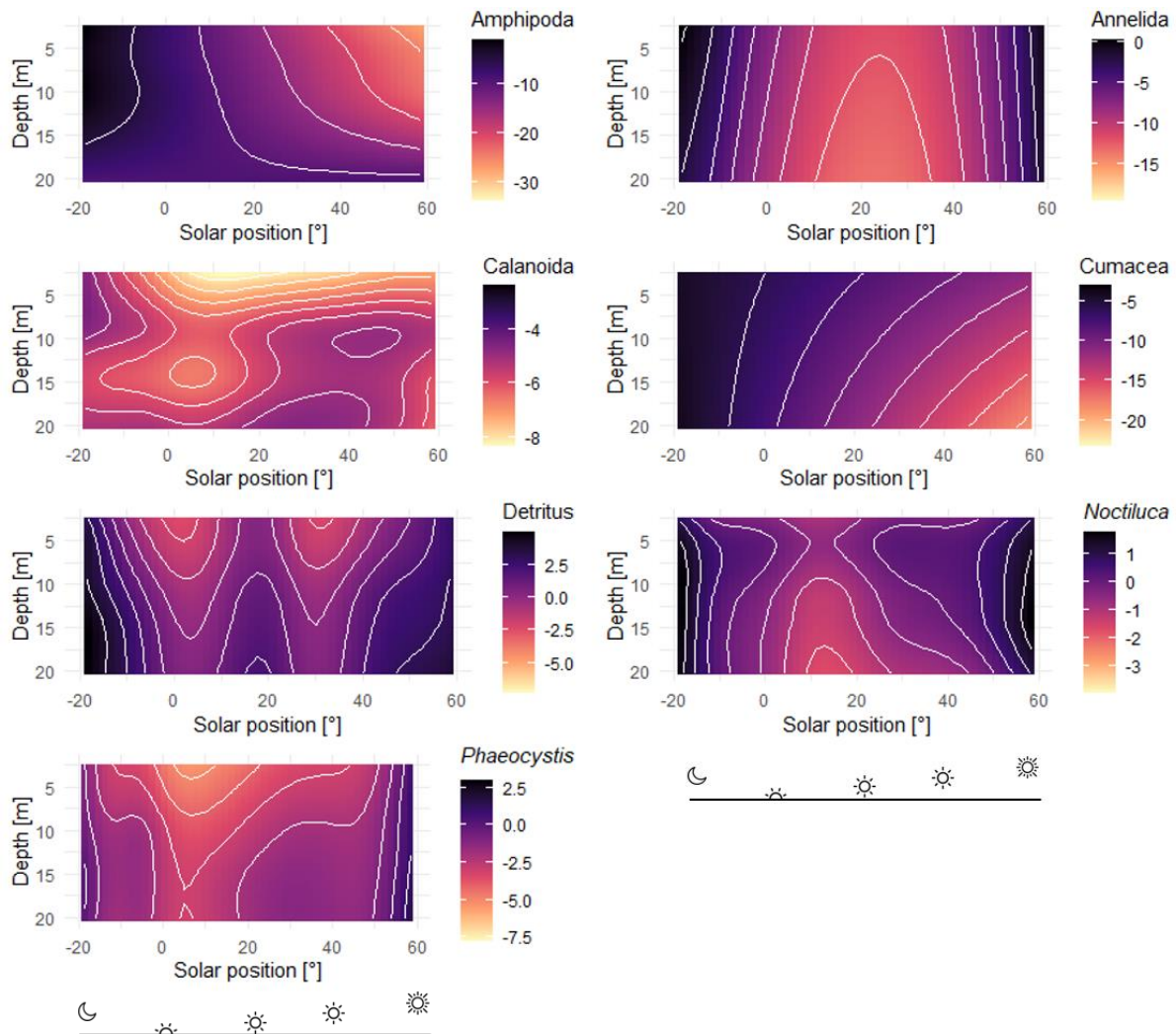


Figure 4.5. Visualization of the predicted distribution of Amphipoda, Annelida, Calanoida, Cumacea, detritus, Noctiluca, and Phaeocystis across different depths [m] and times of day based on the fitted GAM. Predicted abundances are shown using a color gradient (yellow: low abundance; purple: high abundance). The x-axis represents the angle of the sun [°] respective to the horizon as a proxy for a diel variable (Values from -20 until 0 represent night. Higher values correspond to a higher solar position and are closer to noon.).

The GAMs (see Supplementary table 4.1) explained 6.17, 17.2, 28.7, and 44.9 % of the variation in the distribution of Calanoida, Noctiluca, Phaeocystis, and detritus, respectively. For the hyperbenthic taxa Amphipoda, Annelida, and Cumacea these numbers were 26.4, 22.1, and 21.1% of the variance, respectively. The visualisations of the model for the taxa represented in Figure 4.5 show that Calanoida (Figure 4.5 C) will be present in the surface layers at night and in the

deeper layers during the day and that the hyperbenthic Amphipoda and Cumacea (Figure 4.5 A, D) will be more present in the water column during night-time. Annelida (Figure 4.5 B) probably follows the same pattern as the latter two taxa, but there is an outlier observation during the day (see Figure 4.4 B; between 14:00 and 15:00) that skews the pattern in the visualisation of the predicted distribution. The slightly symmetrical GAM prediction patterns of *Noctiluca*, *Phaeocystis*, and detritus (Figure 4.5 F, G, E) suggest semidiurnal changes in densities.

## 4.4 Discussion

Our study detected DVM patterns for Calanoida and observed an upward migration of them at night. This corroborates earlier observations by Daro (1974, 1985) in the southern North Sea that described DVM in the following copepod species: *Acartia bifilosa*, *Pseudocalanus elongatus*, and *Temora longicornis*. Although DVM rhythms are extensively studied for pelagic migrators in the open ocean, they remain relatively unexplored in shallow and well-mixed waters. In the open ocean, organisms are known to undertake migrations spanning distances of tens to hundreds of meters (Ringelberg, 2010). Yet, our study unveiled that DVM patterns also manifest on a smaller scale, with migrations exhibiting only a few meters in amplitude. The results demonstrate that individuals engage in DVM even over short distances, with migrations as narrow as approximately  $\pm 3.5$  meters, within shallow and well-mixed waters.

Our data shows that DVM rhythms also occur in hyperbenthic taxa. So far, DVM of hyperbenthic organisms in the southern North Sea were described for Annelida (*Polydora ciliata*), Gastropoda (*Crepidula fornicata*), and Bivalvia larvae (*Magallana gigas*; Daro 1974). Our study confirms DVM for Annelida and extends this list of taxa displaying DVM with Amphipoda and Cumacea for which this behavior was not yet reported in the southern North Sea. Due to the limitations in the taxonomic resolution of our data, species names cannot be provided for the organisms displaying DVM. It is crucial to note that DVM patterns reflect attributes unique to certain species or individuals and are not representative of entire populations (Bollens and Frost, 1991). Therefore, when we are discussing the DVM patterns within groups such as Amphipoda and Cumacea, we mean that specific species or subsets of individuals within the population perform DVM rather than the entire group. In our study, the hyperbenthic taxa were predominantly observed at night in the VPR and WP2 data, indicating that they actively leave the seafloor and enter the pelagic water column at night. They were observed throughout the whole water column, which is particularly useful because being high above the bottom helps their dispersal and habitat selection during settlement (Ullberg and Ólafsson, 2003). Other hyperbenthic organisms migrate to the surface to reproduce (e.g. Annelida; Bartels-Hardege and Zeeck, 1990) or molt (e.g. Cumacea; Gerken *et al.*, 2022; Anger and Valentin, 1976).



Observations over various months within the plankton community hint at the plausible existence of temporal variation in DVM patterns, yet definitive confirmation remains elusive due to the lack of collected data. During the winter months, numerous taxa exhibited low abundances hampering research into their vertical migration patterns. Only Cumacea were sufficiently abundant in November. Their autumn observations seemed to have the greatest abundance during two moments, namely after sunset and before sunrise. Literature however did show that seasonal changes in DVM patterns in hyperbenthic taxa are not uncommon (Brunel, 1979) and can relate to variations in free-swimming behavior between species (Wang and Dauvin, 1994), lifestages, or sexes (Dauvin and Zouhiri, 2009). This phenomenon described in literature implies potential variations in the timing or seasonality of DVM behavior, introducing complexities that warrant further exploration. To gain a deeper understanding of the nuances in DVM patterns, it is imperative to consider the potential influence of varying environmental conditions and temporal dynamics. Our research offers insight into a limited temporal timeframe and observed clear DVM behavior of certain plankton groups, but this might not be representative of the broader migratory behavior within the study system. Additional sampling and research efforts could therefore shed more light on the intricacies of DVM patterns under different contexts and temporal intervals.

Plankton and detritus densities exhibited noteworthy fluctuations within a 24-hour timeframe, as evidenced by both net samples and the VPR. Densities differed for samples of the same location taken just a few hours apart from each other. Initially, we examine whether these results could be attributed to factors influencing the sampling methodology. One consideration is the impact of current speed on VPR image acquisition. If the current speed is too high, this can cause motion blurriness in the pictures. However, in this case the maximum current speed was  $0.6 \text{ m s}^{-1}$  which is lower than the typically  $1.5 - 2 \text{ m s}^{-1}$  (3 – 4 knots) employed during towed deployments of the VPR. Thus, it is unlikely that current speed influenced the results in this way. Current speed can also affect VPR image acquisition by influencing the number of particles passing by the VPR's lens. However, our findings did not consistently reveal lower densities during periods of low current speed (i.e. during slack tide). In addition, the similarity in density patterns observed by both the VPR and WP2 net, with the latter being less influenced by current speed, suggests that additional factors contribute to the observed patterns. Another factor to consider is variations in the water column's depth and the sampled volume of the methods over time. One hypothesis is that during low tide the plankton community condenses to a smaller vertical depth, leading to a higher density per cubic meter compared to high tide. However, the highest densities did not coincide with the lowest maximum sampling depth or sampled volume. Therefore, other environmental or biological patterns must explain these variations in density.

## CHAPTER 4

Our results suggest that the tidal cycle played a role in creating this variety, but peak densities did not necessarily coincide with high or low tide and exhibited a time lag. While previous studies reported on copepods and amphipods being more abundant in the water column during flood than ebb tides (Hough and Naylor 1991, 1992), we found plankton densities to be generally less abundant during flood tides. Due to the observed time lag and difference in the timing of peak densities and tidal cycles in different studies, we infer that a plankton patch with higher densities is oscillating back and forth with the (anticlockwise) tidal gyres, rather than the tides themselves having a direct effect on the plankton community. As the tidal currents change direction within the tidal cycle, they usher in new water masses over the sampling location. Considering the local aggregation and small-scale geographical variations of plankton (Robinson *et al.*, 2021; Benoit-Bird *et al.*, 2013), we can observe a distinct waxing and waning pattern of a high-density plankton and detritus patch passing through the sampling site every 12 hours, which corresponds to the duration of a tidal cycle. This pattern was observed for most plankton taxa, but was the most distinct for passive particles (detritus) and less mobile organisms (*Noctiluca* and *Phaeocystis*). To gain further insight into the potential trajectory and potential distance travelled by the patch, we conducted a simulation at the moment of sampling (from 19-05-2021 19:00 to 20-05-2021 07:00) using the OSERIT model (Legrand *et al.*, 2023). This oil spill model simulates the three-dimensional drift of oil on the sea surface and within the water column. Acknowledging the disparities in characteristics such as buoyancy between plankton and oil, the displacement of both is shaped by environmental factors, leading us to posit that the model's output can provide insights into the potential distance and scale of the distribution of a plankton patch. The model calculates the independent movement of single particles under the combined action of the wind, water current and waves. The simulation depicted that the patch follows an ellipsoid-shaped trajectory over the course of a tidal cycle, with a major axis extending 4.4 km and a total travel distance covering 11.6 km. This suggests that plankton and passive floating marine particles may traverse considerable distances over several kilometres during tidal cycles and that their movements driven by tidal forces may contribute to the spatial heterogeneity of coastal marine communities.

The documented DVM and geographic variation of zooplankton bear implications for both the functioning of the food web and the methodologies employed in plankton sampling. To begin with, zooplankton movements in the water column affect the spatial and temporal overlap of predators and prey resulting in ecosystem-wide implications through changing predator-prey interactions (Reichwaldt and Stibor, 2005; Haupt *et al.*, 2009). Furthermore, the migratory patterns are directly linked with the ocean carbon cycling as organisms engaged in these migrations aid in transporting energy and nutrients across different ocean depths (Steinberg and

Landry, 2017). Regarding sampling methodologies, the timing of plankton sampling emerges as a pivotal consideration that can shape the observed composition and abundance of plankton communities. Focusing solely on samples taken during daylight hours can lead to the oversight of crucial components, particularly the (meroplanktonic larvae of) hyperbenthic organisms, which contribute substantially to the pelagic biomass at night. This discrepancy could lead to underestimations in biomass and the representation of specific marine constituents and is a component that is often overlooked in coastal food web models (Carlotti and Poggiale, 2010). Our results thus further emphasize the significance of including these overlooked entities in the overall ecological picture. Moreover, the impact of tidal cycles on plankton densities adds another layer of complexity to the sampling process. Densities can significantly differ depending on the timing of the tidal cycle (and the location of the plankton patch at that moment), as our findings suggest that tidal currents can significantly alter plankton abundances within hours. These findings bear significant implications for samples collected through stationary observations, as opposed to Lagrangian observations, and introduce a challenge that necessitates careful consideration or appropriate correction methods. However, they also unveil a crucial explanatory factor accounting for a substantial portion of the variance in plankton densities, distinct from the more commonly acknowledged influences like phenological or seasonal shifts.

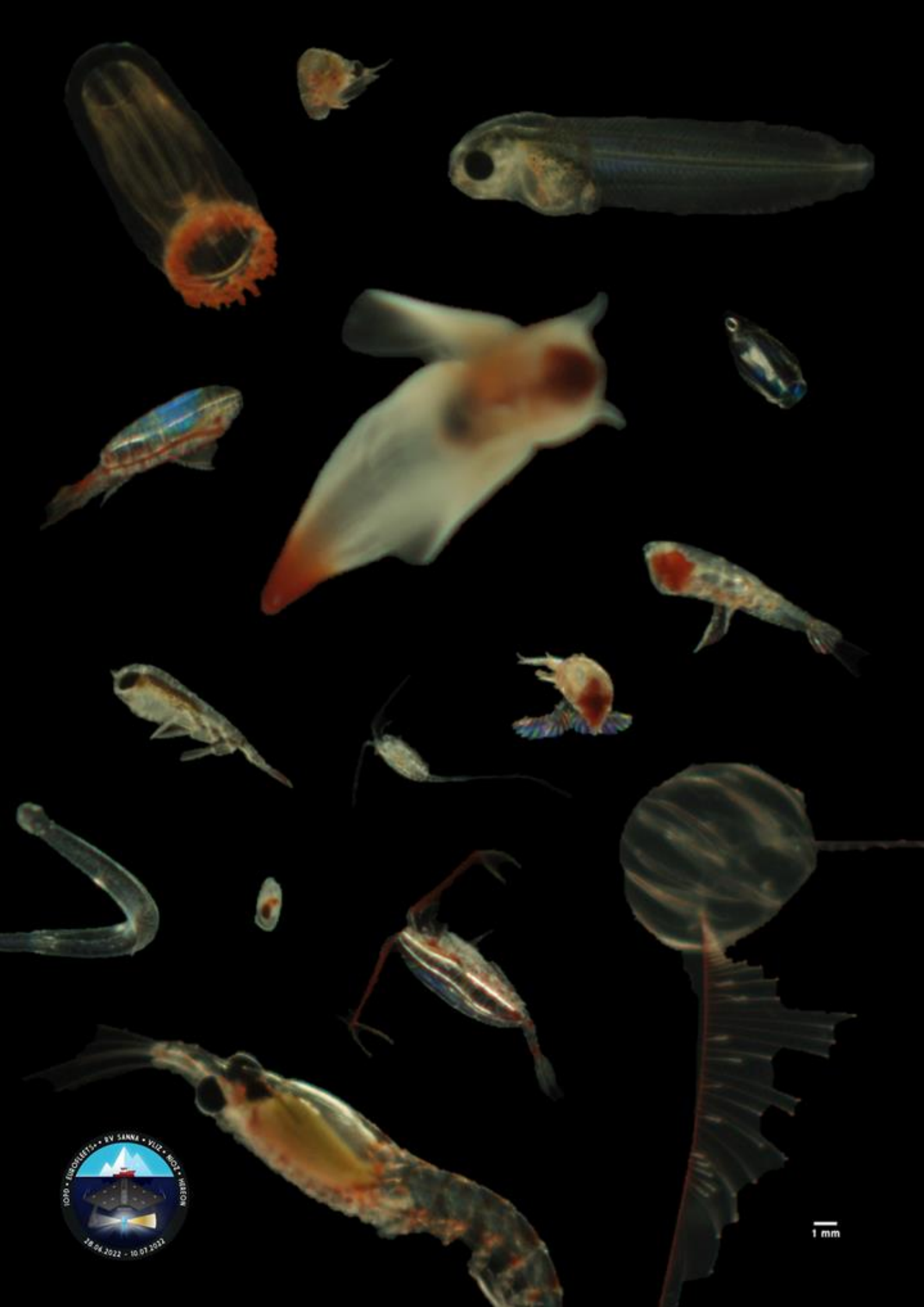
The occurrence of vertical migration and small-scale patchiness among zooplankton is widely acknowledged but rarely quantified, particularly in our study region where little knowledge on the influence of the physical environment on plankton distribution and DVM behavior is available (Fransz *et al.*, 1998; Daro 1985). Our research demonstrates that the VPR is a suitable tool for studying zooplankton DVM and collecting distribution data with high spatiotemporal resolution, a task which is logistically far more difficult with net samples at depth intervals. However, the VPR methodology does come with some inherent limitations, including the exclusion of the top and bottom 3 meters due to safety considerations (Ollevier *et al.*, 2022; chapter 2). To address this limitation, we included complementary data from a vertical WP2 net. While the WP2 net technique might not offer the precise depth-specific plankton data, it does offer valuable insights into plankton densities across a substantial portion of the water column, including the upper layer. The WP2 findings have revealed comparable patterns throughout the entire water column, albeit with a difference in magnitude compared to the VPR. A systematic assessment of this difference is important, which is currently under investigation. In spite of the VPR's missing surface-layer data, its efficacy in capturing similar patterns and providing accurate insights into plankton migration and small-scale patchiness remains evident, corroborated by the observations from the WP2 net. This convergence of findings from both methodologies bolsters the credibility of our research and highlights the VPR's capacity to unveil intricate behaviors like

DVM and patchiness, while also acknowledging the need for continued methodological refinement and careful consideration of complementary data sources.

### 4.5 Conclusion

This study investigated how the abundances and distribution patterns of plankton taxa relate over 24-hour periods, covering tidal and diel cycles, in the southern North Sea. The VPR allowed fine-scale tracking of individual planktonic taxa through a diel cycle, leading to the observation of their daily migration patterns. Next to the migration behavior at night towards the surface layers of pelagic taxa such as Calanoida, this study is the first to describe the migration of Amphipoda and Cumacea from the sea bottom to high up into the water column at night in the southern North Sea. In addition, samples of the same location taken just a few hours apart showed significant differences regarding plankton densities over time. The density peak patterns mirrored a tidal cycle's trend, albeit with some time lag, suggesting planktons' transportation with tidal currents and emphasising its small-scale patchy distribution in the water column. This study documents the wide variability in plankton distribution patterns and highlights that tidal currents can affect plankton densities over time, which has important consequences for samples from stationary observations.





1 mm

# 5

## Plankton fatty acid profiles in West Greenland: Implications for trophic relationships in a changing climate

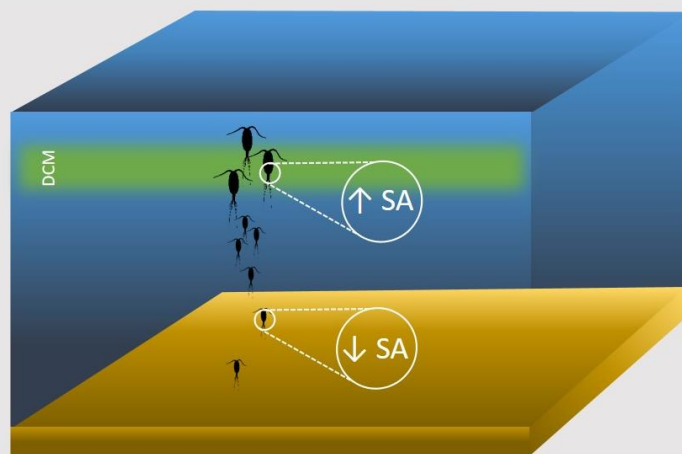
Redrafted after:

Ollevier, A., Ponsini, L., Boone, W., Deneudt, K., Hablützel, P. I., Lagaisse, R., Meire, L., Planken, K., & De Troch, M. (in prep.). Plankton fatty acid profiles in West Greenland: Implications for trophic relationships in a changing climate.

## Abstract

Climate change-induced warming, particularly pronounced in high-latitude regions such as the Arctic, is causing rapid changes in marine ecosystems. To study the potential effects on the food quality of zooplankton, this study analyzed the fatty acid (FA) profiles of micro and mesozooplankton using gas chromatography and focuses on the distribution of copepods along and within fjords by deploying a Video Plankton Recorder (VPR) *in situ* imaging device. Large copepods were often associated with the deep chlorophyll maximum layer and were distributed higher up in the water column compared to their smaller counterparts. Significant differences in FA composition between micro and mesozooplankton indicated potential consequences for the nutritional quality of prey for higher trophic levels, with lower content of polyunsaturated FAs such as stearidonic acid (18:4(n-3)) in microzooplankton. With climate-induced shifts in plankton communities, we hint at a future scenario with a change in quality and distribution of FAs. Alterations in food quality may exert a negative influence on fish and higher trophic levels, yielding repercussions for the overall functioning of the ecosystem. Monitoring and reporting these functional community shifts are essential for understanding and managing the evolving dynamics of marine ecosystems in the face of climate change.

## Graphical abstract



DCM = deep chlorophyll maximum layer; SA = stearidonic acid



## 5.1 Introduction

Climate change and the resulting rise in sea surface temperatures pose a significant threat to marine ecosystems worldwide. This impact is particularly pronounced at higher latitudes, with Arctic warming being reported as up to four times more severe than the global average over the past two decades. Notably, there is an already observable acceleration in mass loss from the Greenland Ice Sheet, a trend projected to intensify in the coming years according to climate models (Stadnyk *et al.*, 2021; Hanna *et al.*, 2008; Velicogna and Wahr, 2006). The anticipated increase in runoff from the Greenland Ice Sheet into fjords, driven by rising temperatures or increased precipitation (Kattsov and Källén, 2005), holds the potential to profoundly alter the water column structure and circulation in these areas (Torsvik *et al.*, 2019) with far-reaching effects on fjord ecosystems. Research indicates that fjords where glaciers have receded onto land experience reduced summer primary productivity (Meire *et al.*, 2017) due to the shift in hydrological patterns.

Tidewater glacier fjords serve as critical feeding grounds for numerous species, including fish, birds, seals, and whales and sustain a diverse food chain because of the nutrients they receive from depth through the nutrient upwelling mechanism of subglacial discharge plumes (Kanna *et al.*, 2018; Meire *et al.*, 2017). A key component of this food chain is the zooplankton community, predominantly composed of copepods, which form the link between primary producers and higher trophic levels. In the Arctic, especially copepods from the *Calanus* complex (*C. hyperboreus*, *C. glacialis* and *C. finmarchicus*) are ecologically important because of their ability to effectively accumulate lipids in their body (Falk-Petersen *et al.*, 2007), making them valuable prey. These large herbivores seasonally accumulate massive amounts of FAs in their lipid sacs during the productive season, before they descend to deeper waters and survive the food-limited winter period. This stored energy supports their metabolism but also aids in buoyancy regulation (Visser and Jónasdóttir, 1999) and facilitates their maturation and egg production (Conover and Siferd, 1993).

Shifts in the plankton community composition have been observed in the past decades. In Disko Bay in West Greenland, the copepod community is taken over by the boreal Atlantic *C. finmarchicus* compared to the Arctic *C. hyperboreus* and *C. glacialis* (Møller and Nielsen, 2020), and also in other regions like the Barents Sea the zooplankton biomass knew an increase in the relative abundance of Atlantic *C. finmarchicus* compared with the Arctic *C. glacialis* (Aarflot *et al.*, 2017). These shifts indicate an ongoing borealization of the zooplankton community, a process describing the altering of the Arctic ecosystems toward a more temperate state (Fossheim *et al.*, 2015). In addition to species shift between organisms with a similar feeding ecology, the study of

Stuart-Lee *et al.* (in prep.) observed different plankton communities between fjords either dominated by land-terminating or tidewater glaciers. Tidewater glaciers were dominated by the herbivorous *Calanus* copepods, whereas land terminating glaciers were characterized by more omnivorous copepod species.

In the context of our rapidly changing world characterized by global warming, a deeper understanding of zooplankton size classes and their food quality becomes imperative. Since earlier studies found that planktivorous fish and specific invertebrates exhibit distinct prey preferences based on size (Kainz *et al.*, 2004), it is essential to comprehend the connection between the FA composition of plankton and their size, as well as how these factors are spatially distributed. Therefore, the primary objective of this paper is to investigate the FA composition of different size classes of plankton and to explore the spatial distribution of copepod size classes in fjord systems.

## 5.2 Methodology

### 5.2.1 Study area

Five fjords and the connecting shelf area were sampled in the Uummannaq region in West Greenland (ca. 70 – 72 °N; ca. 50 – 55 °W; Figure 5.1). The sampled fjords from north to south were the Ukkusissat Fjord, an unnamed fjord, the Kangerlussuup Fjord, another unnamed fjord and the Uummannaq Fjord (Qarajaq Fjord), hereafter referred to as fjord 1 until 5, respectively. Numerous ice caps outboard of the western margin of the GIS into the Uummanaq region and four out of the five sampled fjords (fjord 2 until 5) receive glacial ice and meltwater through marine terminating glaciers. Fjord 2 connects with Ingia Isbrae, a small glacier draining from an ice cap, via a 450 – 500 m deep channel (Rignot *et al.*, 2016). Fjord 3, leading to Kangerlussuup Sermia, is connected to the Uummannaq trough to the south via Inuksat, a 500 – 600 m deep fjord with three sills at 300 m depth and via an unnamed fjord to the west that is uniformly 400 m deep. Fjord 4 is uniformly deep at 500 – 550 m for 80 km until the seafloor quickly rises to 340 m depth about 10 km from the glacier front. The glacier stands in water only 250 m deep (Rignot *et al.*, 2016). A deepening of > 1300 m is found to the north of Uummannaq Island, toward Sermeq Silarleq (and Kangigleq Sermia). The fjord remains 800 m deep until the junction with the terminal valley of Sermeq Silarleq, where both fjords become shallower near the ice fronts (Rignot *et al.*, 2016). At the entrance of fjord 5, east of Uummannaq Island, a deep sector (1480 m) is found. Fjord 5 shoals to 800 m depth to the east and remains relatively flat for another 120 km toward Store Gletscher. The fjord shallows to 550 m towards Store Gletscher (Rignot *et al.*, 2015; 2016). Fjord 1 is a long and narrow fjord of 400 - 500 m deep with a land-terminating glacier at the head of the fjord

(Bendtsen *et al.*, 2021). Satellite imagery reveals that the ice in fjord 1, 2 and, 3 broke up just a few days before the start of the research cruise (Supplementary material 5.1).



Figure 5.1. Field sampling design with indication of the fjords and sampling stations.

## 5.2.2 Sample collection and processing

Samples were taken from 28th of June until 10th of July 2022 aboard the RV Sanna. During the research cruise five fjords and the connecting shelf area were sampled (Figure 5.1). The team of researchers sailed from the shelf edge towards the head of the fjords or until icebergs blocked the way.

### 5.2.2.1 Zooplankton community samples

Physical zooplankton samples were collected with a MultiNet mini (Hydrobios), which was deployed vertically at a speed of  $0.4 \text{ m s}^{-1}$  and was equipped with a flowmeter. The MultiNet consists of five  $50 \text{ }\mu\text{m}$  nets with openings of  $0.125 \text{ m}^2$  that open and close at predefined depth intervals. The topmost net sampled the upper 50 m, the second topmost net the upper 50 - 100 m, and the remaining net intervals varied according to the water column depth. During the cruise one net broke resulting in only four nets and thus only four intervals in the remainder of the cruise. After lifting the net out of the water on the side A-frame of the vessel, the outside of the net is rinsed with a deck wash to concentrate the organisms into the cod-end. The zooplankton collected in the cod-end was transferred to a recipient and was fixated in a 4 % borax-buffered formaldehyde solution. The samples were subsequently sent to the Polar Agency in Poland for microscopic identification, counting and measuring at species or genus, stage and sex level.

### 5.2.2.2 Zooplankton community distribution data

In addition to the net sampling, zooplankton was sampled by means of a Real Time VPR (Seascan, Inc.) that was equipped with a SBE 49 CTD (Sea-Bird Electronics, Inc.) and ECO Puck FLNTU fluorometer and turbidity sensor (WETLabs). The VPR was deployed for approximately 1.5 h at each station, while it was vertically lowered and raised through the water column at a speed of  $0.2 \text{ m s}^{-1}$ . During deployment the VPR stayed 3 m from the surface and sea bottom to avoid hitting the vessel or seafloor, respectively. Maximum depth of the VPR was around 250 m, limited by the length of the winch cable. On station EF01 - EF12, the VPR undulated between surface and as deep as possible whereas on station EF15 - EF47 the VPR made two undulations as deep as possible followed by undulations in the top 50 m layer as most of the zooplankton was observed there.

The image data was manually classified. *Calanus* spp. were classified as Copepoda (large), other copepods as Copepoda (small). Plankton densities were calculated as the number of individuals per sampled volume and then linearly extrapolated to cubic meters of water [ $\text{ind m}^{-3}$ ], in which sampled volume is determined by:

$$\text{Sampled volume [mL]} = \text{Imaged volume [mL frame}^{-1}] * 25 [\text{frames s}^{-1}] * \text{Duration [s]}$$

The imaged volume of every VPR frame was 335.622 mL which was computed as the field of view (magnification setting S3: 46.5 x 34.5 mm) multiplied by focal depth. This latter was determined by the parameters used with the VPR AutoDeck software: a segmentation threshold – low of 0, a segmentation threshold – high of 132, a focus – sobel of 45 and a focus – std dev of 0. The lowest magnification, S3, was chosen due to the large size of the plankton (Supplementary table 5.1; Ollevier *et al.*, 2022; chapter 2).

### 5.2.2.3 Fatty acid samples

Samples for FA analysis were collected by means of a 50  $\mu\text{m}$  MultiNet sample of the entire water column. The cod-ends of the MultiNet were poured together in a recipient and stored for 5 - 6 h in a refrigerator for the plankton to release their gut content, allowing identification of the FA profile of the zooplankton tissue and not their gut content. Subsequently, the microzooplankton fraction (50 - 200  $\mu\text{m}$ ) was separated from the mesozooplankton fraction (> 200  $\mu\text{m}$ ) by sieving, after which both fractions were collected for further analyses separately. At certain stations, one in each fjord, an extra MultiNet was taken to collect 50 specimens of the dominant species for FA analysis to research if the FA composition of these dominant groups elucidates the overall FA profile of the community. With the exception of station EF 18, where a small copepod was selected, the majority of the samples were characterized by the prevalence of larger copepods

(*Calanus*). All samples were stored in a -80 °C freezer until further analysis at the Marine Biology research group of Ghent University (Belgium).

FA methyl esters (FAMES) were prepared from freeze-dried samples using a direct transesterification procedure with 2.5 % (v : v) sulfuric acid in methanol as described by De Troch *et al.* (2012). The FAMES were subsequently extracted with hexane. FA composition analysis was carried out with a gas chromatograph (GC; HP 7890B, Agilent Technologies, Diegem, Belgium) equipped with a flame ionization detector (FID) and connected to an Agilent 5977A Mass Selective Detector (MSD; Agilent Technologies, Diegem, Belgium). The GC was further equipped with a PTV injector (CIS-4, Gerstel, Mülheim an der Ruhr, Germany). An HP88 fused-silica capillary column (60 m × 0.25 mm × 0.20 µm film thickness, Agilent Technologies) was used at a constant helium flow rate (2 ml min<sup>-1</sup>). The injected sample (2 µl, split ratio 1:10) was split equally between the MS and FID at the end of the GC column using an Agilent Capillary Flow Technology Splitter. The oven temperature programme was as follows: at the time of sample injection the column temperature was 50 °C for 2 min, then gradually increased at 30 °C min<sup>-1</sup> to 150 °C, followed by a second increase at 2 °C min<sup>-1</sup> to 230 °C. The injection volume was 2 µL. The injector temperature was held at 250 °C. The transfer line for the column was maintained at 250 °C. The quadrupole and ion source temperatures were 150 and 230 °C, respectively. Mass spectra were recorded at 70 eV ionization voltage over the mass range of 50 - 550 m z<sup>-1</sup> units.

Data analysis was done with MassHunter Quantitative Analysis software (Agilent Technologies). The signal obtained with the FID detector was used to generate relative quantification data of all compounds. Peaks were identified based on their retention times and by the mass spectra obtained with the MS detector. FAME quantification was based on the conversion of peak areas to the weight of the FA by a theoretical response factor for each FA (Ackman and Sipos, 1964; Wolff *et al.*, 1995).

#### 5.2.2.4 Phytoplankton samples

Phytoplankton samples were collected by hauling 50 L of surface water with a bucket from the rear deck of the vessel and pouring it through a 20 µm Apstein net. The samples were fixed with Lugol (5 % final concentration) and stored in cold (4 °C) and dark conditions. In transit, four samples leaked to become unusable (EF1, EF12, EF18 and EF35) and all samples reached room temperature which reduces the preservation quality of the phytoplankton sample. In the lab, samples were processed with a FlowCAM VS-4 (Fluid Imaging Technologies, Yarmouth, Maine, U.S.A.). Each sample was processed twice: once with the 300 µm deep flow cell, the 4X objective and the 5 mL syringe pump, and once with the 100 µm deep flow cell, the 10X objective and the 1 mL syringe pump. All runs were processed using the AutoImage Mode imaging particles in a user -

defined number of frames per second. For all runs the setting of the focus was done directly on the sample, instead of using the focus beads, since this practice is more time effective and allows better focus on real-life cell dimensions instead of manufactured beads. For processing at 4X, frame rate was set to 20 frames per second, flow rate was set to  $1.7 \text{ mL min}^{-1}$  and the basic size acquisition filter was set to 100 - 300  $\mu\text{m}$  ESD. Here, a first pre-run of a 1.5 mL subsample was performed to obtain information on the particle concentration by looking at the Particles Per Used Image (PPUI). If the concentration was too high, the sample was diluted by adding filtered seawater to reach a PPUI below 1.1 to avoid particles overlapping in a single frame. To minimize clogging, each sample was pre-filtered with a 300  $\mu\text{m}$  mesh-size net. To reduce the variability, each sample underwent three technical replicate runs, each of them capturing a maximum of 1,500 particles or covering a maximum Sample Volume Processed of 15 mL. For processing at 10X, frame rate was set to 20 FPS, flow rate was set to  $0.15 \text{ mL min}^{-1}$  and the basic size acquisition filter was set to 20 - 100  $\mu\text{m}$  ESD. Here, a 1mL pre-run was performed to obtain information on the particle concentration by looking at the obtained PPUI. If the concentration was too high, the sample was diluted by adding filtered seawater to reach a PPUI below 1.1 to avoid particles overlapping in a single frame. To minimize clogging, each sample was pre-filtered at 100  $\mu\text{m}$ . To reduce the variability, each sample underwent three technical replicate runs, each of them capturing a maximum of 1,500 particles or covering a maximum Sample Volume Processed of 1.5 mL. In between sample runs, replicate runs and samples, the flow cell is cleaned with three alternating cycles of 5 mL of Milli-Q® water and ethanol (70 %), leaving little air in between fluids, and finishing with Milli-Q® water.

The image data was then predicted by a Convolutional Neural Network trained on phytoplankton data from the Belgian part of the North Sea since only this training set was available. All predicted images were verified by taxonomists through an in-house interface, allowing easy visualization of images and correcting of model predictions where necessary. Because samples reached room temperature conditions during transportation, sample preservation was suboptimal and many cells appeared distorted or were broken, hampering detailed identifications and influencing presence and densities, possibly with an unequal difference between taxa. For further analysis, we therefore used relative instead of absolute taxon abundance data.

## 5.2.3 Data analysis

### 5.2.3.1 Zooplankton biomass

The microscopy data derived from MultiNet samples was split into a micro (50 - 200  $\mu\text{m}$ ) and mesozooplankton (> 200  $\mu\text{m}$ ) fraction based on the length measurements of a maximum of 10 individuals per species per sample (see Supplementary table 5.1 for mean length). Depending on

the proportion that each size fraction contributed to a sample, counts were split between the micro and mesozooplankton fraction. For each size fraction abundance and biomass estimates were made. Biomass estimations follow the methodology used in Planken *et al.* (in prep.) and involve the application of several empirical length-weight relationships. Formula 1 is the predominant power regression for the majority of the taxa, whereas formula 2 was used for *Clione limacina*.

$$DW \text{ or } CW = a * L^b \text{ (1)}$$

$$DW = b^{(a*L)} \text{ (2)}$$

In the equations, DW represents dry weight, CW represents carbon weight, and L signifies body length. The species-specific values for 'a' and 'b' used in the analysis are presented in Supplementary table 5.2. To accurately consider nutritional value, zooplankton biomass was quantified in terms of CW. In cases where length-weight relationships were initially determined for DW, these values were converted to CW by multiplying DW by the average carbon content as reported in the literature.

The top ten copepod species that contribute the most in terms of abundance or biomass to each size fraction within the meso- and microzooplankton categories is represented. Mean abundance, relative abundance, mean depth-integrated biomass and relative biomass estimations are (graphically) represented per taxon for the mesozooplankton and microzooplankton fraction. For better interpretability of the whole community, we opted to group the species to higher taxonomic levels into: Amphipoda, Annelida, Appendicularia, Chaetognatha, Cirripedia, Copepoda, Ctenophora, Euphausiacea, Ostracoda, other crustaceans, Pteropoda, Rotifera, meroplankton and other. 'Meroplankton' consisted of Gastropoda, Bivalvia, Echinodermata, Bryozoa, and Pilidium; 'other crustaceans' of Mysidacea, Decapoda, *Diastylis*, and Isopoda; and 'other' of Foraminifera, Radiolaria, Nematoda, Hydracarina, and fish.

### 5.2.3.2 Statistical analyses

The relative FA contribution in percent of total FAs was converted to a datamatrix (Euclidean distances) and was analyzed using non-parametric multidimensional scaling (nMDS) and a permutational analysis of variance (PERMANOVA). To determine the five FAs that made the most significant contributions to these differences, a similarity percentages test (SIMPER) was conducted. The same analyses were performed on phytoplankton relative abundance data.

To assess the relative influence of phytoplankton abundance and zooplankton biomass simultaneously on zooplankton FA composition a variation partitioning analysis was used. To

capture the inherent structure within each dataset—phytoplankton relative abundance, zooplankton relative biomass, and zooplankton relative FA content—we conducted individual classical multidimensional scaling (MDS) analyses using the Euclidean distance metric. The phytoplankton dataset encompassed various phytoplankton phyla. Subsequently, we performed a redundancy analysis (RDA) on the integrated MDS data. The MDS data was used for variation partitioning analysis using the *vegan* v. 2.6-2 package (Oksanen *et al.*, 2022) in R.

To investigate and elucidate the relationship between FA composition of zooplankton (relative abundance; of micro and meso fraction together) and the composition of phytoplankton (relative abundance; of 4x and 10x magnification together) or zooplankton (relative biomass; of micro and meso fraction together), a correlation analysis using Pearson's correlation coefficient was conducted using R stats's *cor.test* function. It was tested which taxa exhibited statistically significant correlations with specific FAs. Subsequently, the results were visually presented through a heatmap displaying correlation coefficients.

#### 5.2.3.3 Copepod distribution data

Copepod counts of both small and large copepods were aggregated into 1-meter bins, and density estimations were derived from the amount of time the VPR spent within each bin. For consistency across stations and to facilitate meaningful comparisons, we focused on the uppermost 150 m of the water column to allow us to examine the same portion of the water column across all stations.

## 5.3 Results

### 5.3.1 Zooplankton composition and biomass

Copepods dominated the mesozooplankton fraction, constituting 93.52 % of the total counts across all sampling locations (Table 5.1, Figure 5.2). Following this, meroplankton made up a modest 1.67 % and Ostracoda accounted for 1.26 % of the mesozooplankton. In the microzooplankton fraction, copepods also contributed the largest part (88.52 %). Other taxa contributing to this category were meroplankton (1.67 %) and Annelida (1.09 %).

In the mesozooplankton fraction, copepods dominated the total biomass across all stations, accounting for a substantial 85.68 % or 48.19 g C m<sup>-2</sup> when the values were summed over all samples (Table 5.1). The remaining biomass contributors were the taxa Ostracoda (5.78 %) and Pteropoda (4.6 %). In the microzooplankton fraction, copepods also played a major role, representing 92.99 % of the total biomass or 30.17 mg C m<sup>-2</sup>. Additionally, meroplankton contributed 6.97 %, while Annelida made a minor contribution at 0.11 %.



Table 5.1. The mesozooplankton and microzooplankton in terms of mean abundance [ind m<sup>-3</sup>], relative abundance [%], mean depth-integrated biomass [mg C m<sup>-2</sup>], and relative biomass [%] based on MultiNet samples.

Fraction	Taxon	Abundance [ind m <sup>-3</sup> ]	Relative abundance [%]	Depth-integrated biomass [mg C m <sup>-2</sup> ]	Relative biomass [%]
Mesofraction	<b>Amphipoda</b>	0.72	0.17	56.38	1.7
	<b>Annelida</b>	4.52	1.09	5.24	0.16
	<b>Appendicularia</b>	2.47	0.6	1.00	0.03
	<b>Chaetognatha</b>	1.92	0.46	11.66	0.35
	<b>Cirripedia</b>	0.12	0.03	0.16	0
	<b>Cnidaria</b>	3.07	0.74	52.87	1.6
	<b>Copepoda</b>	387.75	93.52	2834.95	85.68
	<b>Ctenophora</b>	0.05	0.01	0.01	0
	<b>Euphausiacea</b>	0.98	0.24	1.46	0.04
	<b>Meroplankton</b>	6.93	1.67	0.44	0.01
	<b>Ostracoda</b>	5.24	1.26	191.15	5.78
	<b>Other</b>	0	0	0.00	0
	<b>Other crustaceans</b>	0.16	0.04	1.30	0.04
	<b>Pteropoda</b>	0.7	0.17	152.26	4.6
	<b>Rotifera</b>	0.02	0	0.00	0
Microfraction	<b>Amphipoda</b>	0	0	0.00	0
	<b>Annelida</b>	0.06	0.06	0.00	0.11
	<b>Appendicularia</b>	0.01	0.01	0.00	0
	<b>Chaetognatha</b>	0	0	0.00	0
	<b>Cirripedia</b>	0	0	0.00	0
	<b>Cnidaria</b>	0	0	0.00	0
	<b>Copepoda</b>	78.8	88.52	1.77	92.88
	<b>Ctenophora</b>	0	0	0.00	0
	<b>Euphausiacea</b>	0	0	0.00	0
	<b>Meroplankton</b>	10.13	11.38	0.13	6.97
	<b>Ostracoda</b>	0	0	0.00	0
	<b>Other</b>	0	0	0.00	0
	<b>Other crustaceans</b>	0	0	0.00	0
	<b>Pteropoda</b>	0	0	0.00	0
	<b>Rotifera</b>	0.02	0.02	0.00	0.04

CHAPTER 5

As copepods dominated the micro and mesofraction of the plankton community in terms of abundance and biomass, the top ten of copepod species contributing to this was represented (Figure 5.3). In the mesofraction *Pseudocalanus* spp., *Oncaea borealis*, *Microsetella norvegica*, *Oithona similis*, and *Calanus* spp. were the most abundant copepod species (between 40 and 97 ind m<sup>-3</sup>), but other species (*C. hyperboreus*, *Metridia longa*, *C. glacialis*, *C. finmarchicus*, and *Paraeuchata norvegica*) made up the majority of the biomass (ranging from 0.16 to 4.48 mg C m<sup>-3</sup>). In the microfraction *O. borealis*, *Microcalanus* spp. and *O. similis* had both the highest abundance (between 5 and 67 ind m<sup>-3</sup>) and biomass (between 0 and 0.003 mg C m<sup>-3</sup>).

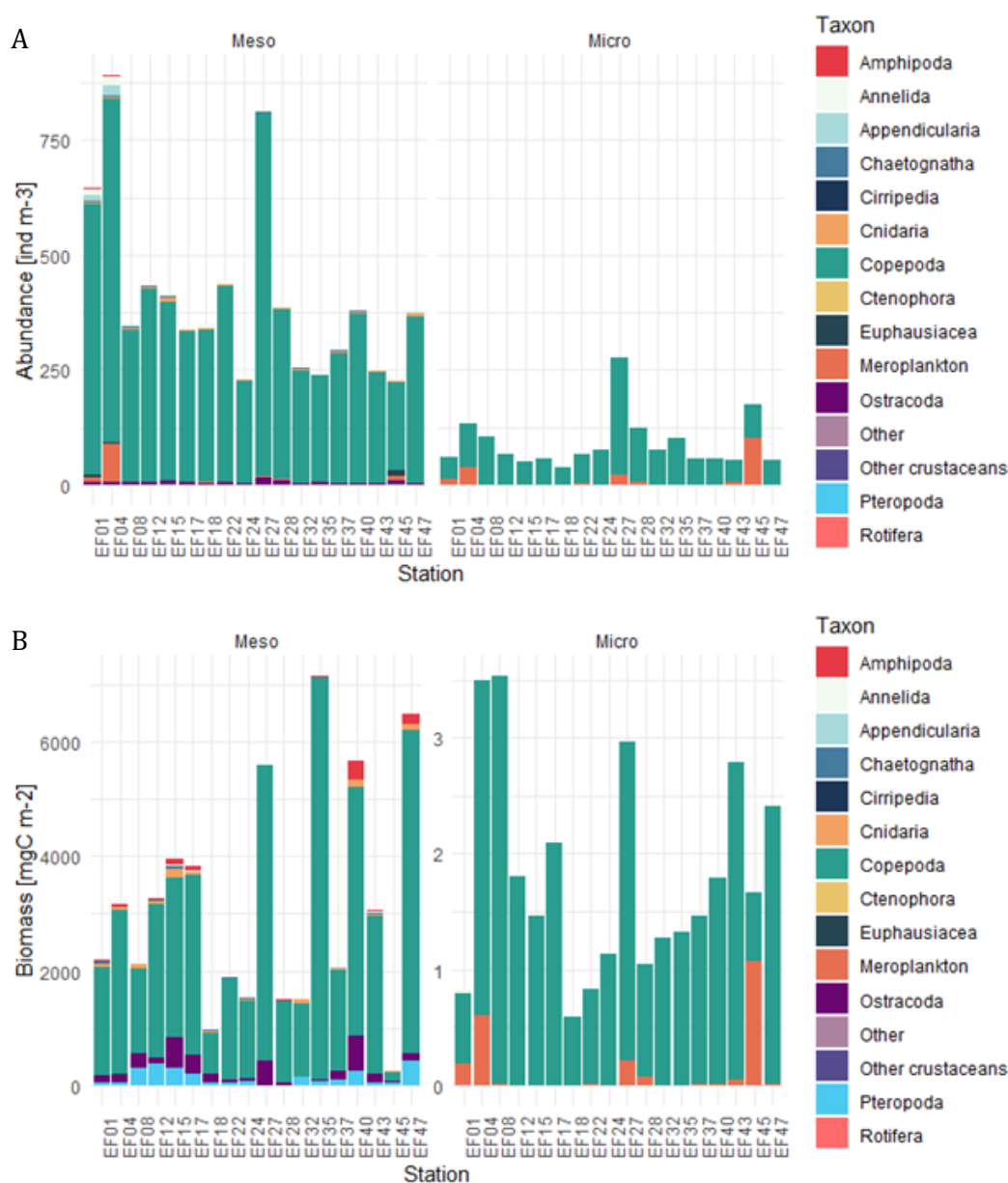


Figure 5.2. (A) Mean abundance [ind m<sup>-3</sup>] and (B) mean depth-integrated biomass [mg C m<sup>-2</sup>] of the zooplankton taxa in the meso and microzooplankton community.

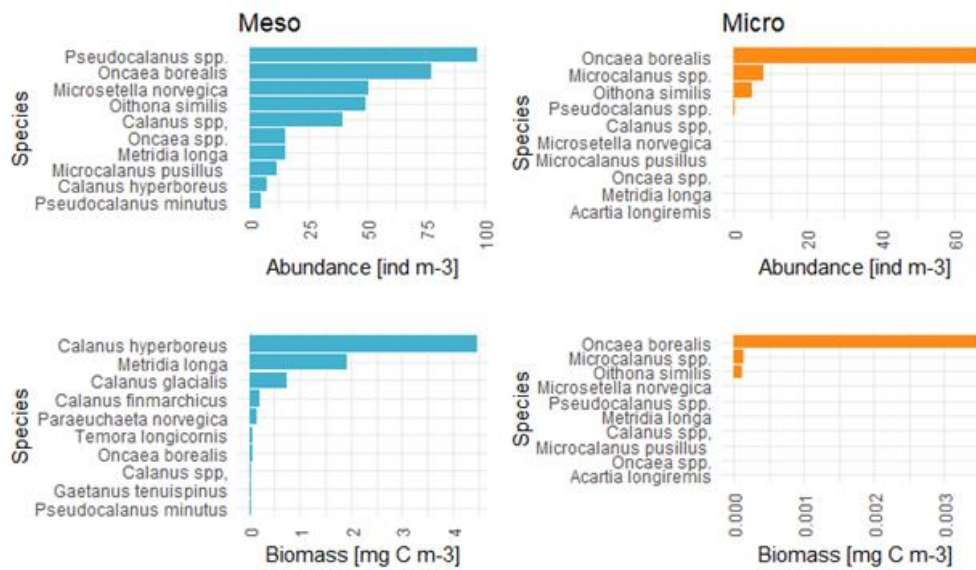


Figure 5.3. Top ten copepod species contributing to the mean density [ind m<sup>-3</sup>] and biomass [mg C m<sup>-3</sup>] of the meso and microzooplankton community.

### 5.3.2 Fatty acid profile of size-fractionated zooplankton

The most abundant FAs in the microzooplankton community (Figure 5.4, Supplementary table 5.3, 5.4) were the saturated FA (SAFA) 16:0, the monounsaturated FAs (MUFAs) 16:1(n-7), 18:1(n-9), the highly unsaturated FAs (HUFAs) 22:6(n-3) and 20:5(n-3) together contributing to almost three quarters of the FA composition. These are further complemented by 14:0 and 18:1(n-7). The most abundant FAs in the mesozooplankton community were the MUFAs 16:1(n-7), 20:1(n-9) and 22:1(n-11) and the HUFAs 22:6(n-3) and 20:5(n-3). The poly unsaturated FA (PUFA) 18:4(n-3) and MUFA 18:1(n-9) further made up the FA profile of the mesozooplankton community.

The relative FA composition significantly differed between the micro and mesozooplankton community (PERMANOVA,  $F = 9.5168$ ,  $p < 0.001$ ; Supplementary material 5.2). The five FAs that contributed most to the difference between size fractions were 16:0, 22:1(n-11), 20:1(n-9), 18:4(n-3) and 14:0 (SIMPER,  $p < 0.05$ ; Supplementary material 5.3). Between sampling stations no significant difference was found (results not shown).

The FA samples grouped per plankton size fraction (MDS, stress: 0.09, Figure 5.5). FA samples with *Calanus* spp. are closely related to the mesozooplankton fraction and suggest that the FA profile of the mesozooplankton community is mainly determined by the FA profile of this dominant *Calanus* spp.. The FA profile of small copepods is more similar to the ones of the microzooplankton fraction.

## CHAPTER 5

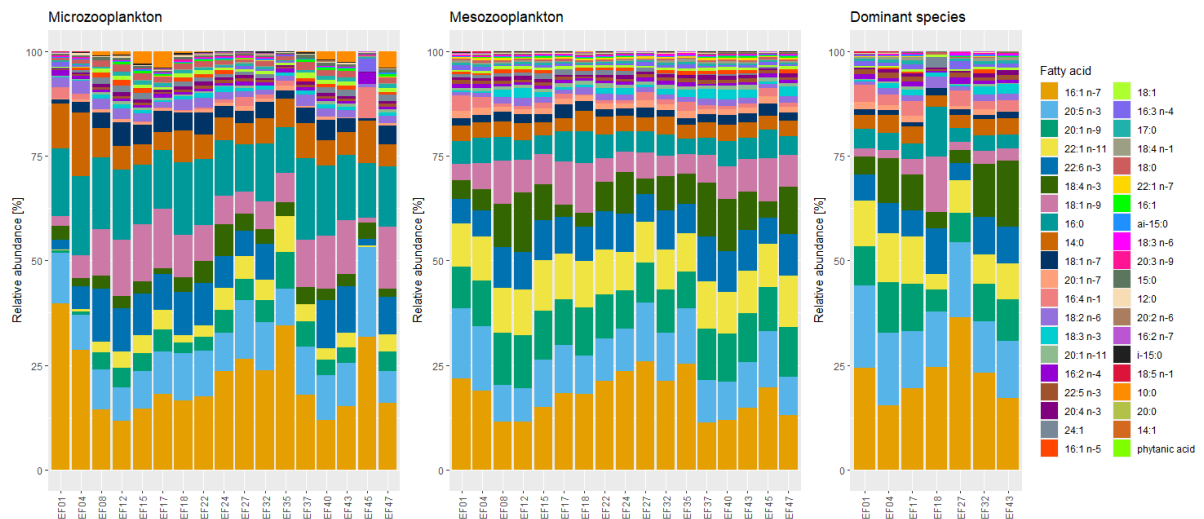


Figure 5.4. FA composition of both the micro and mesofractions within the zooplankton community, along with the dominant species present in the samples. Note: the dominant species varied across stations, featuring a small copepod in EF18 and predominantly large copepods (*Calanus*) in the other represented locations.

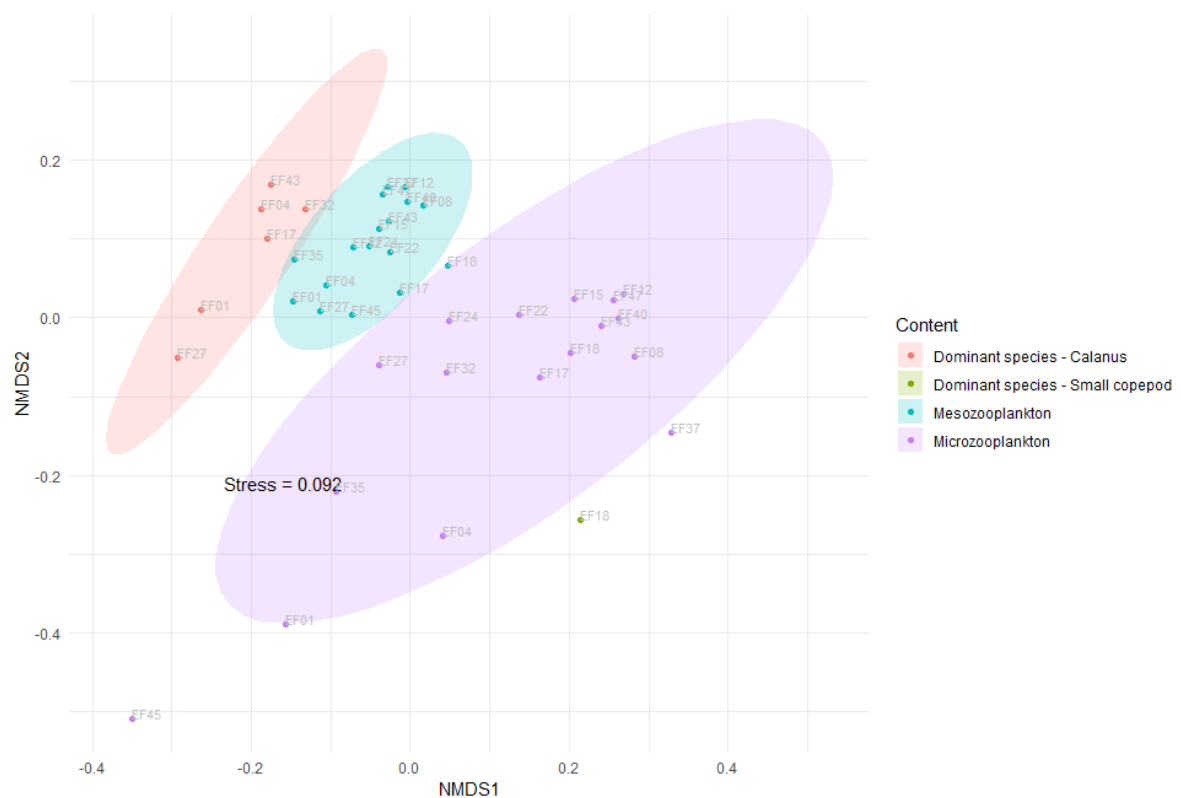


Figure 5.5. NMDS ordination of the FA profiles of samples containing mesozooplankton, microzooplankton, *Calanus* spp., or a small copepod species.

### 5.3.3 Phytoplankton

Within the smaller size fraction (20 - 100  $\mu\text{m}$ ) of the phytoplankton community, more than half of the samples were dominated by two phytoplankton phyla, Bacillariophyta and Myzozoa (Figure 5.6). Notably, centric diatoms made a significant contribution to the composition of this size fraction. In contrast, in the larger size fraction (100 - 300  $\mu\text{m}$ ), the prominent groups were Ciliophora and Bacillariophyta. Among these, *Parafavella*, elongated (chained) diatoms, and *Pseudo-nitzschia* played substantial roles in determining the relative abundance of phytoplankton species in the samples.

The PERMANOVA results indicate a significant difference between the phytoplankton composition of the two phytoplankton size classes ( $F = 30.48$ ,  $p = 0.001$ ; Supplementary material 5.4). The phyla Bacillariophyta, Myzozoa, and Radiozoa significantly (SIMPER,  $p = 0.001$ ) contributed to this difference (Supplementary material 5.5).

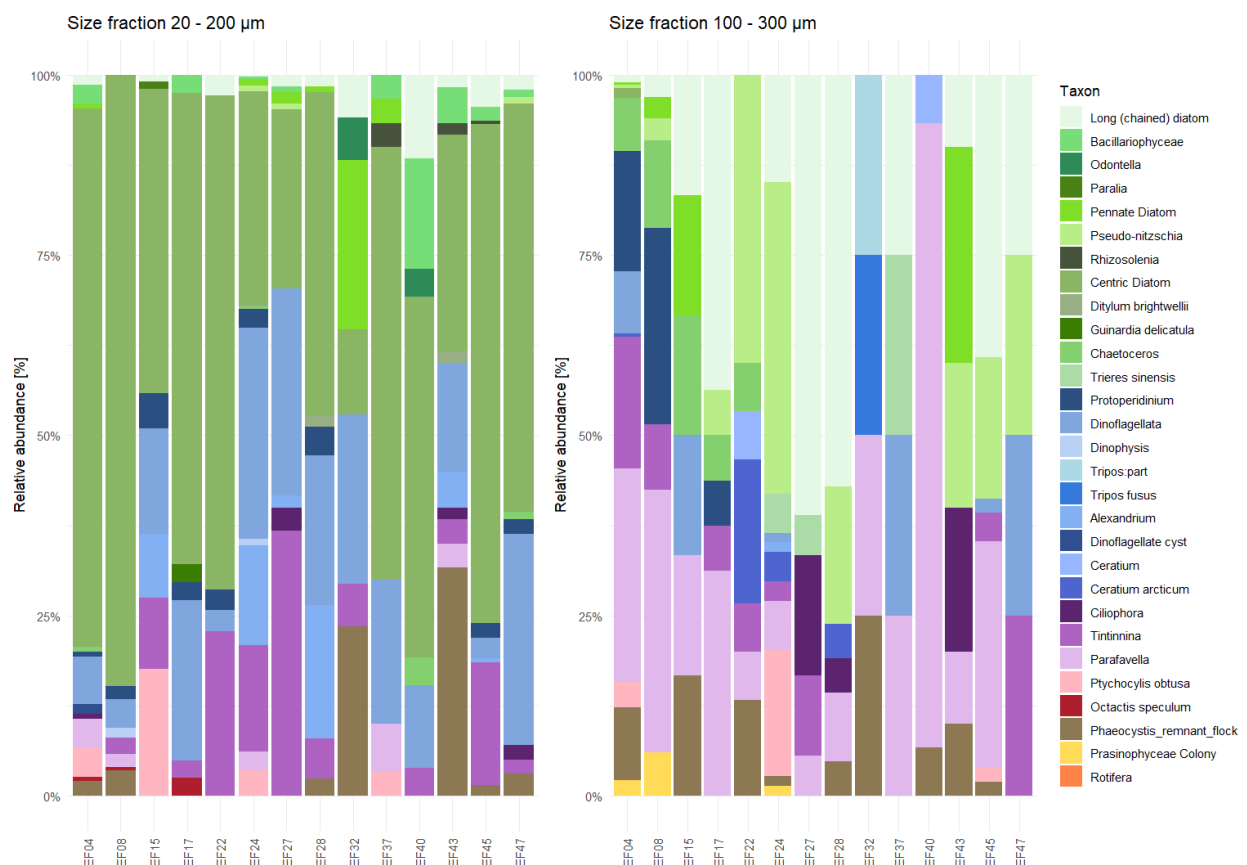


Figure 5.6. Phytoplankton relative abundance of the 20 – 200  $\mu\text{m}$  (10x magnification) and 100 – 300  $\mu\text{m}$  (4x magnification) size fraction of samples processed with a FlowCAM. The taxa have a different color shade per phylum: green = Bacillariophyta; blue = Myzozoa; purple/pink = Ciliophora; red = Radiozoa; brown = Haptophyta; yellow = Chlorophyta; and orange = Rotifera.

### 5.3.4 Covariance of fatty acid profiles with phytoplankton and zooplankton composition

Variation partitioning analysis indicated that phytoplankton abundance and zooplankton biomass together explained 79.8 % of the variation in FA composition of zooplankton (Figure 5.7). The predictors explained an almost equal amount of variation. Phytoplankton abundance purely explained 40.7 % ( $p < 0.05$ ) and zooplankton biomass purely explained 39.1 % ( $p < 0.05$ ). There was no variation shared by both predictors.

A correlation analysis shed light on the correlation of FAs with the phyto- and zooplankton community composition. At the low taxonomic phytoplankton level, only dinoflagellate cysts significantly ( $p < 0.05$ ) correlated with 18:5(n-1) (results not shown). When taxa were grouped to phylum level, no significant correlations were found (results not shown).

Many zooplankton species significantly ( $p < 0.01$ ) correlated with FAs (Figure 5.7, Supplementary material 5.6). We can discern a clear differentiation between two categories: species of the left branch of the correlation plot that have a positive correlation with the FAs 20:1(n-7), 20:1(n-9), 22:1(n-7), and 22:1(n-11) and a negative correlation with the SAFAs 15:0, and 16:0 versus species of the right branch of the correlation plot that have the opposite correlations. The group situated on the right branch of the correlation plot comprises species that were all observed in the microzooplankton fraction. This observation underscores a noticeable distinction in FA content or correlation patterns between mesozooplankton and microzooplankton. Of all taxa *Bivalvia* had the most divergent correlations.

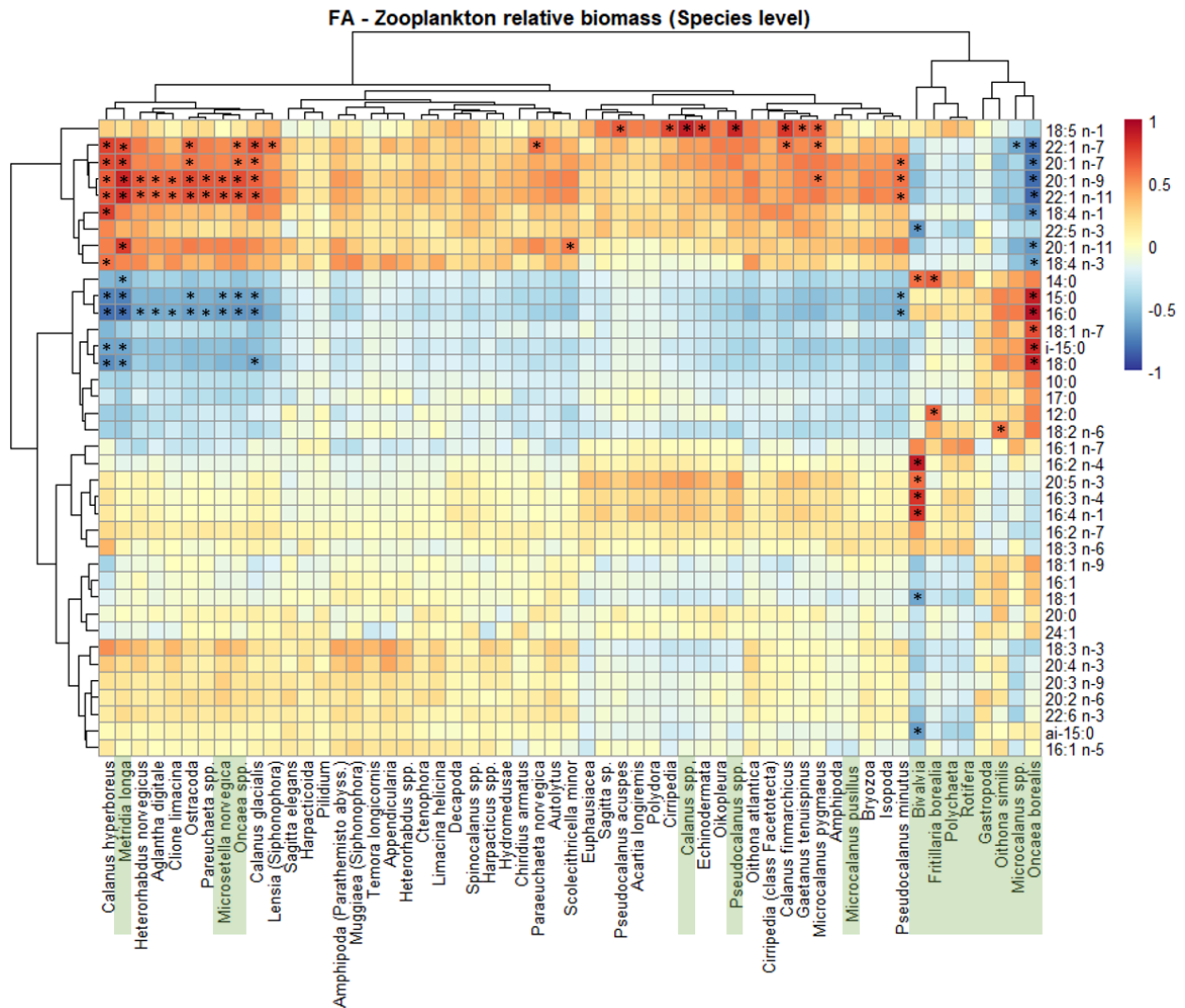


Figure 5.7. Heatmap presenting Pearson correlation coefficients between the FA relative abundance and relative biomass of zooplankton. Significant correlations ( $p < 0.01$ ) are represented with an asterisk. All listed taxa were present in the mesozooplankton fraction and taxa that were additionally present in the microzooplankton fraction are highlighted in green.

### 5.3.5 Copepod distribution

VPR data of multiple stations allows exploration of the copepod distribution inside the water column and along shelf-fjords gradients. Along this gradient fjord 5 exhibited the most pronounced pattern (Figure 5.8, Supplementary figure 5.1, 5.2). Plankton distribution along this fjord-shelf gradient showed large variation and large copepods dominated the offshore areas whereas small copepods were more abundant in the inner fjord. Small copepods showed a preference for deeper waters compared to large copepods and had in-fjord peak abundances around 20 - 30 m depth compared to the in-fjords peaks of large copepods at 5 - 20 m. In addition, small copepods were distributed in low abundances throughout the deeper water. Among the environmental variables —salinity, temperature, turbidity, and chlorophyll a concentrations—

measured by the additional sensors on the VPR, it was observed that peaks in chlorophyll concentrations coincided with the distribution patterns of the large copepods (Figure 5.8, Supplementary figure 5.1, 5.2).

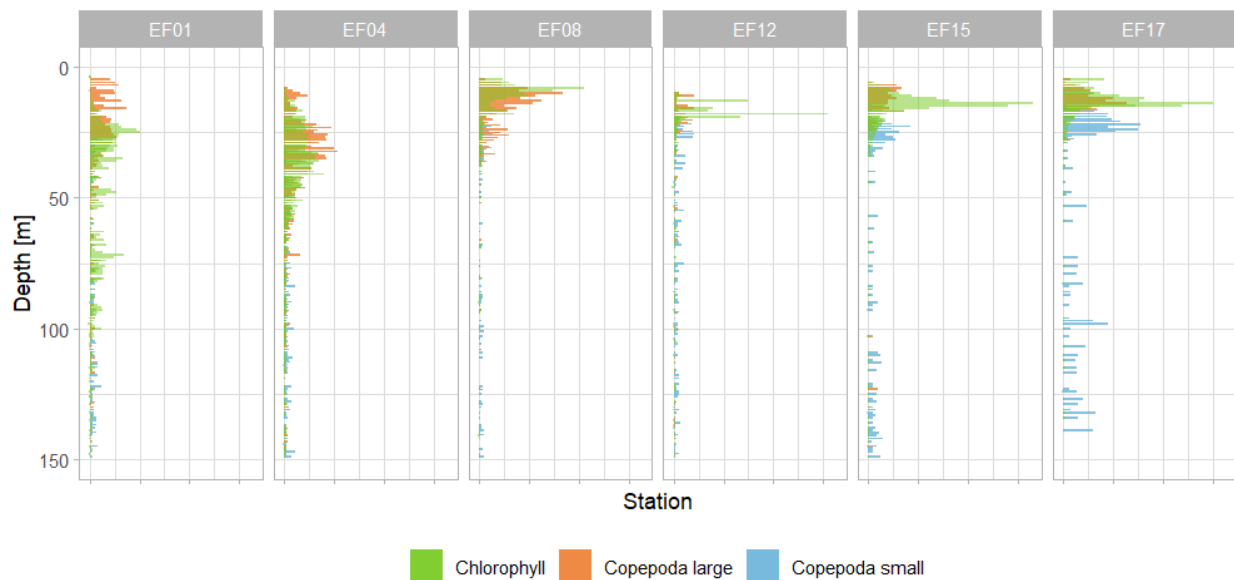


Figure 5.8. Distribution of copepod size fractions (orange for large copepods and blue for small copepods, per 1 m depth bin) in the water column along a shelf - fjord gradient. The leftmost panel is the most offshore sampling station whereas the rightmost panel is located closest to the fjord head. The green bars denote the mean chlorophyll *a* concentration for each 1 m depth bin.

## 5.4 Discussion

### 5.4.1 Plankton in the Uummannaq fjord system

In the Uummannaq fjord system in the early summer of 2022, copepods dominated both abundance and biomass within the plankton community across all size fractions. The biomass of the mesozooplankton fraction was dominated by species of the *Calanus* complex, *Metridia longa*, and *Paraeuchaeta norvegica* and accounted for 0.16 to 4.48 mg C m<sup>-3</sup>. Contributors to small copepod biomass were *Oncaea borealis*, *Microcalanus* spp. and *Oithona similis*, although their biomass remained fairly low (< 0.003 mg C m<sup>-3</sup>). Studies in the same area sampled with a MultiNet in late summer 2017 (i.e., August; Planken *et al.* (in prep.)), reported higher depth-integrated biomass of copepods in the meso fraction (3.8 g C m<sup>-2</sup>) compared to our results (2.8 g C m<sup>-2</sup>). The higher biomass observed in Planken *et al.* (in prep.) may be attributed to the subglacial discharge that enhanced phytoplankton growth and that can sustain increased zooplankton biomass. In contrast, our study took place shortly after ice breakup suggesting that also ice discharge from the glaciers may not have reached comparable levels, potentially explaining the difference in



biomass between the two studies. Within the non-copepod zooplankton, meroplankton (bivalves) occasionally made substantial contributions to the local biomass of the microzooplankton fraction. Pteropoda and Ostracoda emerge as the primary non-copepod contributors to the mesozooplankton biomass, in contrast to Chaetognatha in the study by Planken *et al.* (in prep.).

Copepods exhibited distinct spatial distribution patterns along both the horizontal and vertical axes. There is a clear difference in the distribution of copepods along a fjord-shelf gradient, where small copepods became more dominant in fjords while large *Calanus* species dominated the offshore areas, in correspondence with the results from East Greenland (Beroujon *et al.*, 2022) and the Ummannaq fjord (Planken *et al.*, in prep.). The increased abundance of smaller copepods within fjords may be attributed to the coupling between small copepods grazing on local accumulation of phytoplankton and particulate organic matter brought in by upwelling fronts from tidewater glaciers at the fjord head (Kiørboe, 1993; Le Fèvre, 1987). In addition, the VPR results revealed that within the water column, small and large copepods occupied different depths in the fjord. Large copepods displayed a tendency to inhabit higher positions, aligning notably with the deep chlorophyll maximum, while their smaller counterparts occupied lower depths across all stations. In the 50 m surface layer of the stations towards the head of Ummannaq fjord distinct peaks of large copepods around 15 m and small copepods around 25 m were seen. By occupying different depths, competition for similar food sources is reduced and for small plankton species with sometimes bio-energetic limitations, i.e. species that cannot store large amounts of energy, a continuous supply of food could be guaranteed this way (Dagg, 1977). In addition, in contrast to the herbivorous *Calanus* spp. dominating the large copepod fraction, some small copepods have an omnivorous feeding habit (e.g., *M. longa* and *Oncaea* spp.) and also feed on marine snow and microzooplankton (Koski *et al.*, 2007; Calbet and Saiz, 2005; Svensen and Kiørboe, 2000). This latter feeding mode could explain why some specimens are distributed along the water column to deeper depths and are not closely affiliated with the deep chlorophyll maximum layer in the water column.

## 5.4.2 Plankton fatty acid composition

In addition to the distribution of organisms within and along fjords, also the FA composition of these species is of crucial importance in marine ecosystems, exerting a profound impact on food quality for higher trophic levels. Our findings revealed significant variations in FA profiles between the meso and microzooplankton size fraction. Whereas the microzooplankton fraction contained significantly more 14:0, 16:0, and 22:1(n-11), the mesozooplankton had higher relative abundances of 18:4(n-3) and 20:1(n-9). The saturated FA (SAFA) 16:0 is a common component in marine organisms and predominates in membrane lipids (Lee *et al.*, 2006), as is the case for

14:0. The fatty alcohols 20:1(n-9) and 22:1(n-11) found in the zooplankton samples are not naturally occurring in phytoplankton and are rather exclusively produced *de novo* by herbivorous copepods (Lee *et al.*, 2006). A significant contrast between the zooplankton size fractions lies in the presence of stearidonic acid (18:4(n-3), SA), an essential omega-3 FA. This specific FA primarily incorporates into storage lipids and serves as an indicator of copepod dietary preferences and feeding behavior (Dalsgaard *et al.*, 2003; Graeve *et al.*, 1994). It is considered an essential FA (EFA), along with docosahexaenoic acid (22:6(n-3), DHA) and eicosapentaenoic acid (20:5(n-3), EPA), since animals do not or not sufficiently synthesize them (Kattner and Hagen, 2009) and must mainly rely on dietary sources for them. While there are no significant differences in the EFAs DHA and EPA between the size fractions, they are worth mentioning due to their importance in marine life and human health (Jónasdóttir, 2019). In marine ecosystems the availability of these EFAs results in enhanced somatic growth and reproductive rates. Dietary intake of them is correlated with growth and development in copepods (Lacoste *et al.*, 2001; Tang *et al.*, 2001; Koski *et al.*, 1998), larval fish (Rainuzzo *et al.*, 1997), and invertebrates (Levine and Sulkin, 1984).

FAs of dietary origin can be incorporated unchanged into lipids. These FA trophic markers (FATMs) are useful in the elucidation of dietary relationships between larger groups of phytoplankton. It is assumed that FA 16:1(n-7) and EPA are indicative of diatom consumption, while SA and DHA are associated with dinoflagellate consumption (Reuss and Pulsen, 2002, and references therein; Scott *et al.*, 2002; Kattner *et al.*, 1994). Laboratory studies have highlighted that FA profiles reflect the dietary source and can change with a changing diet. For instance, the FA profile of *C. finmarchicus* can shift from being presumptively dinoflagellate-dominated (as indicated by a high SA content) to diatom-dominated (i.e., high 16:1(n-7) content) when feeding on a diatom monoculture (Graeve *et al.*, 1994). Our results show a 16:1(n-7) dominated FA profile for both size fractions, indicating that diatoms are the primary food source. However, the significantly higher content of SA in the meso fraction also suggests a larger consumption of dinoflagellates. The seasonal succession of phytoplankton in West Greenland fjords follows a well-defined pattern with a spring diatom bloom, followed by a summer flagellate bloom (Bruhn *et al.*, 2021). We did not observe a large predominant bloom, possibly because our study coincided with the early stages of ice melting in the fjords, and blooms were still developing. The magnitude and timing of primary production in fjords are influenced by the release of meltwater, with blooms initially triggered by increasing insolation (sunlight) along with high nutrient concentrations. However, the phytoplankton composition during the campaign primarily consisted of diatoms. Despite the minor quantities of dinoflagellates present, we think that the higher SA ratio in mesozooplankton can be explained by the food preference of nauplii and adult

*Calanus* species for ciliates and dinoflagellates (Turner *et al.*, 2001; Levinsen *et al.*, 2000; Ohman and Runge, 1994; Barthel, 1988).

Furthermore, in our efforts to explain these differences in FA content, we attempted to correlate phytoplankton abundance with the FA profiles of zooplankton. The variation partitioning analysis already revealed that phytoplankton relative abundances, coupled with zooplankton biomass, accounted for 79.8 % of the variation in zooplankton FA composition. However, according to the correlation analysis, individual phytoplankton phyla could not be correlated with species-specific zooplankton FA profiles. This suggests that although the phytoplankton community partly explains the variation in zooplankton FA profiles, the relative abundance of specific phytoplankton phyla do not form a direct and straightforward link with zooplankton FA profiles. The discernible shift in zooplankton FA profile when fed with another phytoplankton monoculture diet in laboratory experiments (Graeve *et al.*, 1994) becomes less apparent when in the field zooplankton have the ability to consume a diverse diet. In addition, various dietary FAs probably incorporate at different rates into the zooplankton body, contributing to this complexity. The use of FAs as trophic biomarkers following the 'You are what you eat' concept does not reveal an unambiguous link between prey abundance of specific phyla and consumer FA profiles when analyzing field samples.

A significant part of the variations in the zooplankton FA profiles finds explanation in the biomass of the zooplankton itself and various zooplankton species show strong correlation with certain FAs, suggesting that some of the variability is inherent to the characteristics of the zooplankton species rather than being solely attributed to the food source. This inherent variability is further emphasized when examining the differences in FAs among size fractions, where a strong correlation with variations in species composition becomes evident. The correlation plot corroborates the findings of the SIMPER analysis, highlighting a distinct separation between species present in the microzooplankton fraction and those exclusive to the mesozooplankton fraction. This correlation analysis underscores a discernible pattern in FA composition, suggesting a link to phylogenetic origin and/or life history characteristics. Similar observations of FA composition variances related to size fractions or taxonomy have been noted in previous studies within aquatic environments (e.g., Hiltunen *et al.*, 2015; Persson and Vrede, 2006; Kainz *et al.*, 2004; Ballantyne *et al.*, 2003) and imply that the size and community composition of zooplankton are important in determining the quality of food available for higher trophic level consumers.

### 5.4.3 Food web implications

Our research has unveiled significant variations in the FA composition across different size fractions of the zooplankton community, with a noteworthy lower content of PUFAs, particularly SA, in the microzooplankton fraction. If glacier retreat of marine-terminating fjords results in plankton community compositions described in Stuart-Lee *et al.* (in prep) for land-terminating fjords, then species with a mainly herbivorous feeding habit will make space for more small and omnivorous species such as *Microstella norvegica* and *Oncaea* spp.. In our micro size fraction, the abundance and biomass of copepods was almost solely attributed to *Oncaea borealis*. This suggests that changes from land to marine-terminating glaciers might go hand in hand with a decrease in 18:4(n-3) and that further changes in FA content and calorific value are expected due to variations in taxonomic composition and feeding habits (Kattner and Hagen, 2009, and references therein). Another potential alteration in plankton communities could arise from an increase of boreal species such as *C. finmarchicus*. The correlation plot findings indicate that *C. finmarchicus* correlates with fewer specific FAs compared to its Arctic counterparts, which might influence the overall quality of bulk FAs as well.

Changes in FA quality can in both scenarios thus be expected, but how FAs quantitatively might vary is less clear. Stuart-Lee *et al.* (in prep.) observed no change in total zooplankton biomass between the two fjord types, but how this exactly translates to total FA content is unknown. On the contrary, in Disko Bay, the shift in *Calanus* composition in the last decades has led to a reduction of the lipid content of the *Calanus* community (Møller and Nielsen, 2020), possibly partly because *C. finmarchicus* is the smallest of the three *Calanus* species and lipid storage is slightly less pronounced compared to the other two *Calanus* species (Kattner and Hagen, 2009). The lipid content in adult *Calanus* females experienced a 34 % reduction from 1992 to 2018, with an estimated 12 % decrease in lipid content for the entire *Calanus* community (Møller and Nielsen, 2020). This however only relates to FAs of *Calanus*, without extending to FAs of other species in the copepod or plankton community which could have increased in abundance leading to a similar total biomass (as observed by Stuart-Lee *et al.* (in prep.)).

Furthermore, a shift in *Calanus* species may impact the timing of FA availability. Owing to differences in phenology, maximum lipid content occurs at varying times among *Calanus* species, resulting in a reduced availability of lipids during spring and early summer (Møller and Nielsen, 2020). *C. hyperboreus* produces eggs during winter at depth (Madsen *et al.*, 2001; Pasternak *et al.*, 2001), depleting lipid stores when females surface in spring. In contrast, females of *C. glacialis* and *C. finmarchicus* migrate to surface waters in spring, utilizing their lipid stores for egg

production and reaching their minimum lipid content during summer (Swailethorp *et al.*, 2011; Plourde and Runge, 1993).

Depending on how plankton community assemblages will evolve, changes in FA timing, quality, and quantity might take place that can impact higher trophic levels. In addition, disparities in spatial distribution in prey, such as those observed between small and large copepods, and FAs could intensify the impact, potentially leading to a mismatch between prey and predator. Changes in plankton community composition could, for example, impact size-selective predators that rely on visual hunting to find food or bulk feeding organisms, such as whales, through changes in food supply and prey biomass. Changes in plankton communities and their impact on higher trophic levels are already evident. For instance, the survival of cod larvae is intricately linked to the synchronization of various factors such as time, space, concentration, size, and energy content of their prey (Beaugrand *et al.*, 2003; Brander *et al.*, 2001; Sundby, 2000; Bainbridge and McKay, 1968). Other studies on the planktivorous capelin (*Mallotus villosus*) in West Greenland revealed a negative correlation between the prevalence of smaller copepods and dietary quality, as evidenced by stomach content (Grønkjær *et al.*, 2018), and observed a smaller growth when *C. finmarchicus* was abundant compared to *C. hyperboreus* (Hedeholm *et al.*, 2010). Ecosystem changes affecting prey and FA content could have detrimental consequences for capelin feeding, impacting the entire ecosystem.

In the face of mounting pressures on Arctic ecosystems driven by climate-induced shifts, sustained research and monitoring efforts focusing on plankton and economically important fish species are imperative. These endeavors not only provide crucial insights but also contribute to predicting the evolving dynamics of marine ecosystems and fishing grounds. This knowledge, in turn, becomes foundational for informed conservation and management strategies in the face of ongoing changes.

## 5.5 Conclusion

This study researched the FA profiles of the micro and mesozooplankton community in the Uummannaq Fjord system and explored the spatial distribution of copepod size classes within fjords. The study unveiled significant differences in FA content between the micro and mesozooplankton, with a reduction in the prevalence of PUFAs, specifically SA, in the microzooplankton fraction. Variations in FA profiles of zooplankton were partly attributed to taxonomy or phylogenetic constraints, in addition to dietary influences. Considering the potential climate change-induced shifts in plankton community, we expect alterations in mainly the quality of FAs, coupled with shifts in their spatial distribution. Notably, large copepods have been

## CHAPTER 5

observed higher up in the water column, often associated with the DCM layer, as opposed to their smaller counterparts. As prey size, energy content and biomass concentration are pivotal elements for fish growth and feeding habit, monitoring the evolving dynamics of these changes becomes paramount because they can have considerable consequences on higher trophic levels in the future.







# 6

General discussion

The research presented in this thesis aims to investigate the applicability and potential contributions of optical imaging approaches to plankton research and monitoring. By employing this methodology, it aimed to attain a more profound understanding of specific aspects of plankton ecology. This chapter contextualizes the findings from the PhD thesis on the VPR and case studies and links up with three main research domains in plankton ecology (Figure 6.1). These three overlapping domains include studies on the diversity of organisms and how they are composed into plankton communities; research regarding their variation across spatiotemporal scales and how they relate to their surroundings; and understanding the complex interactions between them and other trophic levels. This chapter explores the results within a wider scope, discussing the possibilities, advantages, limitations and future prospects of optical imaging devices.

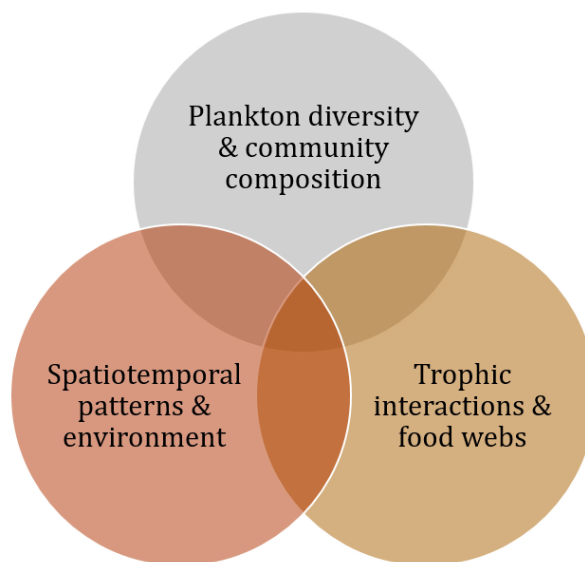


Figure 6.1. Three main aspects of plankton ecology.

## 6.1 Plankton diversity and community composition

Marine zooplankton are extremely abundant, span a broad size range and are very diverse. They consist of approximately 28,000 species distributed among 41 major taxonomic groups spanning 15 phyla (Bucklin *et al.*, 2021) and new species are regularly being discovered (Lawley *et al.*, 2021; Wittmann and Abed-Navandi, 2021). In an ideal world, sampling methods would be able to observe this community that spans various sizes, and to identify large amounts of data with a high taxonomic resolution.

### 6.1.1 Plankton diversity and size

In spite of the high diversity reported, there is no one method that fits all, and each net or optical sampling method has its own advantages and disadvantages for observing plankton. One of the key strengths of the VPR lies in its non-invasive approach, allowing for improved estimates and research on delicate or gelatinous particles (**chapters 2, 3**), such as jellyfish, ctenophores, houses of appendicularians, *Phaeocystis* colonies, and detritus. The destruction of these organisms and particles by plankton nets typically led to underestimations of their biomass and their role in ecosystems (Biard *et al.*, 2016; Lucas *et al.*, 2014). The collection of *in situ* images allows us to capture plankton in their natural environment and in their natural orientation. Moreover, it enables us to observe features of plankton such as the presence of egg sacs, which provides extra information on the sex of certain individuals within the community. Having the images taken with a color camera also allows to see pigmentations which can serve as an indicator of fitness (Vilgrain *et al.*, 2023), that might be lost through preservation methods of net samples. In addition, fixatives used to preserve samples also introduce biases in the biovolume and size estimates due to cell shrinkage (Montagnes *et al.*, 1994).

There are no physical net or optical imaging devices that can sample the whole size range of plankton. Instead, nets with various mesh sizes or optical imaging methods targeting specific size ranges (Figure 6.2) are used. The VPR, equipped with four preset motor positions that determine the field of view and magnification, is ought to capture particles from 100  $\mu\text{m}$  up to a few centimeters, mainly targeting the mesoplankton fraction (0.2 - 20 mm). However, the effective size range of optical methods is often narrower than the theoretical one because small particles can be too small to be imaged or validated efficiently, while larger organisms can be too scarce to be sampled quantitatively due to a too small sampled volume (Lombard *et al.*, 2019). As mentioned in **chapter 3**, a drawback of the VPR is its generally much smaller sampled volume compared to net samples, posing a challenge when sampling the plankton community and estimating its densities. For the VPR, the effective range was missing from technical documentation and therefore needed to be determined experimentally. We found that the highest VPR magnification (field of view: 8.8  $\times$  6.6 mm) was suitable for particles from 0.4 - 0.7 mm and that the lowest magnification (field of view: 46.5  $\times$  34.5 mm) deemed suitable for particles in the 1.0 - 3.8 mm size range (**chapter 2**). However, upon reviewing **chapter 3**, it became apparent that the effective size range per magnification setting was more extensive than initially observed in **chapter 2**. For instance, the lowest magnification in **chapter 3** was found to encompass particles up to 6.2 mm. In **chapter 2**, that aimed to find the best-suited instrument settings for

VPR users, we found that the size range of the plankton community or the targeted species should determine the decision for the most suitable VPR magnification during deployment.

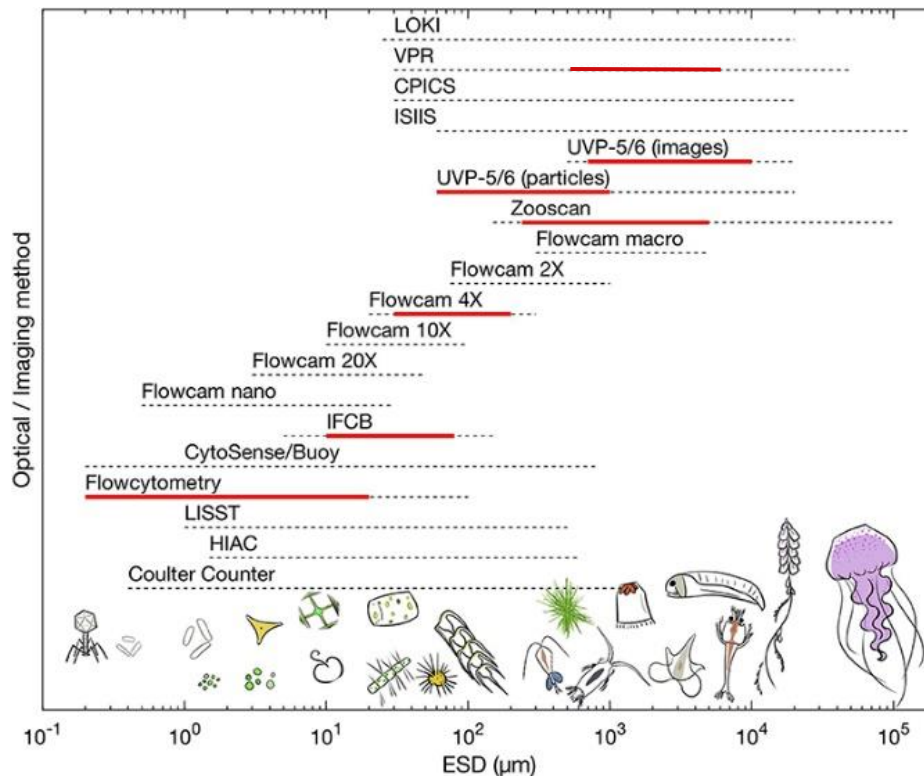


Figure 6.2. Size range of plankton (in equivalent spherical diameter [ $\mu\text{m}$ ]) that available imaging methods can sample. The size range of the VPR was added based on the results of chapters 2 and 3. The dashed lines on the graph depict the overall operational size range derived from commercial data, while the red lines illustrate the practical size range within which acquiring quantitative information is deemed efficient. (Image from Lombard *et al.*, 2019).

## 6.1.2 Taxonomic resolution and processing time

The traditional approach to gather information on plankton composition and abundance has largely relied on the processing of net samples with microscopy. This method can identify organisms to species level or different lifestages within a species, offering excellent taxonomic resolution, but is very labor-intensive and imposes limitations on the number of samples that can be processed. In contrast, faster imaging techniques enable a more rapid analysis of specimens, albeit restricted to broader categorization at the genus or higher taxonomic level, not always being able to differentiate between species or different lifestages within a species (e.g., Broughton and Lough, 2006; Benfield *et al.*, 1996). For instance, echinoderm larvae are clearly distinct from their adult form, but differentiating between stage V and VI copepodites and adult copepods

poses challenges (Broughton and Lough, 2006). Consequently, the VPR primarily is able to differentiate between morphologically very distinct lifestages.

In our VPR studies, taxonomic identification was typically conducted at the phylum, class, or genus level (**chapters 2 - 5**). Notably, VPR studies in Greenland achieved a finer taxonomic resolution, identifying specimens at the class or genus level (Beroujon *et al.*, 2022; Broughton and Lough, 2006). However, such a detailed approach demands substantial expertise of the local plankton community. The choice of taxonomic resolution holds significance, as it can influence the interpretation of results across different levels—be it at the individual, species, or community level. For instance, in **chapter 4**, we observed DVM behavior in specific taxa. However, it is crucial to note that DVM behavior is usually species-specific. Consequently, the observed patterns should not be indiscriminately generalized to the entire copepod or amphipod community. Instead, they suggest that certain species within these groups exhibit migratory behavior.

Although species level is considered as the taxonomic level that provides the most detailed information (Peura *et al.*, 2012) because population dynamics and evolution happen at species level, it is noteworthy that spatiotemporal patterns inherent to species can also manifest at higher taxonomic levels. In some cases, higher-taxon surrogacy allows one to adopt a higher taxonomic level for the identification of phytoplankton and zooplankton without a significant loss of information (Machado *et al.*, 2014; Hirst, 2006). The decision on the appropriate method ultimately depends on the resolution needed to address the research questions effectively, considering that, in some cases, higher taxonomic levels may still capture relevant information and patterns in phytoplankton and zooplankton dynamics. For example, plankton indicators for management, conservation, and policy encompasses multiple scales of plankton organization. It ranges from bulk indicators (such as chlorophyll levels and phytoplankton biomass) to aggregated functional group indicators often supported by taxonomic data (such as the ratio of diatoms to dinoflagellates) to community composition and single species indicators, which are entirely dependent on plankton taxonomic data at species level (McQuatters-Gollop *et al.*, 2017).

### 6.1.3 Automated classifiers and software to advance processing time

*In situ* imaging methods have the potential to significantly reduce the processing time of samples. First, as images are directly collected in a digital format, they do not require handling and processing in the lab (e.g., removing fixative, subsampling, and sorting). Secondly, the major advantage of this digital format lies in the possibility to integrate automated classifiers for an even swifter, less subjective, and potentially real-time identification of plankton data. Throughout this

doctoral thesis, the identification of ROIs has predominantly relied on manual classifications due to the absence of a sufficiently accurate classifier. However, the field of automated classifiers is undergoing significant advancements and shows promising developments. While some algorithms have been adapted from various applications for plankton identification, there has been a distinct emphasis on developing techniques tailored exclusively to this challenge (review in Sosa-Trejo *et al.*, 2023). Among these approaches, advanced deep learning tools such as Convolutional Neural Networks (CNNs) have emerged as promising options for significantly improving the automated identification of plankton images. Differing from traditional machine-learning methods like Artificial Neural Networks, Random Forest, and Support Vector Machines, deep-learning tools eliminate the need for careful feature engineering. Instead, they have the capability to handle raw data directly and autonomously unveil the most suitable representations for classification (Luo *et al.*, 2018).

An essential requirement for these automated classifiers is the need for initial training before they can proficiently execute predictions (Sun *et al.*, 2017). A training set is used to iteratively optimize the network's performance through supervised learning. This process allows the CNN to learn and adjust its parameters based on labeled data to ensure accurate predictions for new, unseen samples. For instance, the VPR data manually validated by myself during this PhD, amounting to 356,660 images, serves as a valuable training set for classifiers. In fact, the validated VPR data from the BPNS was utilized in Hovenkamp *et al.* (submitted) to train a classifier, achieving an accuracy of 92.4 %. This trained classifier can be leveraged in future VPR work, enabling the rapid validation of large volumes of generated images, thus accelerating the validation process.

However, a persistent challenge arises from the scarcity of ample training data. This particularly affects less common taxa and potentially compromises predictions for these groups. Sufficient training data is crucial for the performance of CNNs. Yet, creating a training set is a time-consuming process, with the duration influenced by various factors. The experience of the scientist can expedite the process, while a large number of other particles in the background of the Region of Interest (ROI) can slow it down. Conversely, substantial quantities of similar groups occurring consecutively can accelerate the process. For instance, in the Greenland data, featuring few particles in the background and sporadic occurrences of large quantities of similar images, the average validation reached 7,000 images per day. This is in contrast to the North Sea, where over 95% of the images contain detritus and particles in the background, slowing down the validation process for images.

In addition, employing machine learning approaches allows the characterization of functional traits of plankton from image data (Orenstein *et al.*, 2022). This not only enhances the processing efficiency compared to manual measurements using microscopy or programs like ImageJ, but also unveils a wealth of information within individual images on functional traits. Data on length measurements (e.g., body size; **chapter 2**; Giering *et al.*, 2019) or structure identifications (e.g., lipid sacs in *Calanus* copepods; Schmid *et al.*, 2018) can help to understand plankton's morphological response to variations in ocean hydrography and food quality in the environment.

### 6.1.4 To see is to monitor

Incorporating imaging methods in monitoring programs alongside net samples, provided it is feasible within the cruise planning, can be a valuable asset. The combined use of a VPR with nets promise a more comprehensive understanding of the entire plankton community. Nets have substantial sampling volumes and better ability to capture less prevalent species (**chapters 2, 3**), while optical methods capture gelatinous organisms and *Phaeocystis* colonies (HAB species) very well (e.g., **chapter 3**; Benfield *et al.*, 1996; Gallagher *et al.*, 1996; Davis *et al.*, 1992).

This scenario could also be applicable if, for example, the VPR were incorporated into initiatives such as the monthly LifeWatch monitoring program conducted in the BPNS. Having actively participated in numerous Lifewatch campaigns, I believe that integrating a brief transect or conducting three undulations at some designated sampling stations, all at the lowest magnification, could yield valuable insights into e.g., gelatinous species. Data originating from the VPR are currently not used within the Marine Strategy Framework Directive for the status assessment of pelagic habitats, or for other descriptors such as eutrophication and foodwebs. However, the VPR data could be particularly useful for certain parameters which are not yet available through the techniques currently in use, or for parameters followed by proxies introducing a lot of bias.

Jellyfish and ctenophores typically thrive in areas with high anthropogenic impacts, such as overfishing, eutrophication, and habitat changes (Purcell, 2012; Richardson *et al.*, 2009; Mills, 2001). Their presence significantly influences marine ecosystems (Utne-Palm *et al.*, 2010; Richardson *et al.*, 2009) and has adverse effects on various taxonomic groups (Schneider and Behrend, 1994), fish recruitment (Lynam *et al.*, 2005), fisheries (Kideys *et al.*, 2005), and tourism (De Donno *et al.*, 2014). Despite their ecological and economical significance, long-term data on gelatinous species is often lacking (Brodeur *et al.*, 2016; van Walraven *et al.*, 2015; Boero *et al.*, 2008). The deficiency in comprehensive information on gelatinous organisms was once again highlighted in the latest OSPAR Quality Status Report for the Northeast Atlantic (Holland *et al.*,

2023). Enhancing our understanding of the population dynamics of gelatinous plankton through imaging devices and assessing their socio-economic effects would be instrumental in implementing management measures aimed at preventing or mitigating their impacts (Brodeur *et al.*, 2016).

## 6.2 Spatiotemporal patterns and environmental conditions

The distribution of plankton is intricately linked to the interplay between organisms' behavior and their environment. In dynamic coastal systems, particularly those influenced by strong tidal forces, understanding how plankton is distributed over fine spatial and temporal scales remains a complex challenge (**chapter 4**). Interpreting zooplankton distributional and time-series data is a nuanced task due to the substantial variability in abundance estimates across different spatial and temporal scales caused by patchiness (Haury *et al.*, 1978). To address this, optical imaging methods emerged as powerful tools, surpassing the limitations of net samples that represent isolated points in time and space. Among these optical methods, the VPR stands out for its capability to cover extensive distances during towing, as demonstrated in studies such as the 200 km transects by Ashjian *et al.* (2001). This extended reach allows for the investigation of larger areas. In **chapter 2** various towing procedures were compared and employing a straight trajectory while undulating the VPR through the water proved instrumental in gaining a more comprehensive insight into the distribution of zooplankton over a larger area. This approach had the potential to capture local peaks in plankton abundance and discern their relationship with the spatial variations in environmental conditions.

Furthermore, the VPR enhances spatial and temporal resolution at a small-scale compared to traditional net methods (e.g., Gallager *et al.*, 1996; Davis *et al.*, 1992), a technical advantage necessary to address our research question in **chapter 4**. This improvement resolution is attributed to the possibility to mount additional sensors like CTD, FLNTU, among others, on the VPR frame. The concurrent measurements from these sensors enable a tight coupling between the VPR imagery and environmental data, thus linking biological and physical components. Each captured image from the VPR is accompanied by precise location, depth, and environmental values, facilitating detailed analyses. This feature makes the VPR, and *in situ* imaging instruments in general, invaluable tools for studies e.g., working in stratified environments or studying the vertical distribution, demanding high spatial and temporal resolution.



## 6.2.1 Spatial patterns - Vertical distribution and DVM behavior

**Chapter 4** aimed to unravel plankton distribution over fine spatial and temporal scales within the water column in dynamic coastal systems. Plankton migration is extensively studied in ocean waters where plankton can migrate up to hundreds of meters (Ringelberg, 2010), but less so in shallow coastal areas like the BPNS (maximum depth 40 meters). Deploying the VPR in these shallower systems provided high-resolution data on plankton vertical distribution and DVM behavior. Our study confirmed that in the BPNS copepods perform nocturnal DVM and that their migrations can take place over distances as narrow as  $\pm 3.5$  meters. In addition, for the first time in the study area, DVM patterns for the benthic taxa Amphipoda and Cumacea were observed. The observations shed new light on the dynamics of invertebrate communities in shallow coastal waters. It showed that benthic organisms could reach up high in the water column, a behavior conducive for reproduction, dispersal, and habitat selection during settlement (Ullberg and Ólafsson, 2003).

In **chapter 5**, the VPR demonstrated how large and small copepods differ in distribution throughout the deep fjords in Greenland and the overlying water column, showing that smaller copepods exhibited higher densities under the peaks of *Calanus* species. The variation in copepod distribution was potentially linked to body size and feeding behavior. Occupying different depths minimizes competition for similar food sources, especially benefiting small plankton species with bio-energetic limitations. Unlike the herbivorous *Calanus* spp. that feed on phytoplankton in the surface layers, certain copepods in the small size fraction exhibit an omnivorous feeding habit, consuming marine snow and microzooplankton. This diverse feeding approach may explain why some specimens are distributed throughout the water column at larger depths, not closely tied to and reliant on chlorophyll a in the surface layer. The observed difference in copepod distribution highlights variations in prey fields for predators, which were detected due to the fine-scale spatial resolution of the VPR. In traditional methods using MultiNet systems consisting of nets that can be successively closed, large intervals sample the entire water column, providing a coarse spatial resolution. In deep fjords, the MultiNet typically samples the upper layer with an interval that spans the upper 50 meters, which is too coarse to detect the different peak depths of *Calanus* and other copepods.

## 6.2.2 Spatial patterns - Horizontal distribution and environmental conditions

The distribution of plankton in the water is to a large extent linked to physical processes and environmental conditions, such as oxygenation, temperature, salinity, and stratification (Brandão *et al.*, 2021; Rombouts *et al.*, 2009). To investigate the plankton distribution in dynamic coastal areas, **chapter 4** researched the abundance of plankton taxa and detritus particles in relation to environmental and hydrographic conditions over a 24-hour period. The inclusion of detritus was a deliberate choice, considering its passive floating nature, which allows it to offer insights into distribution patterns unaffected by active biological behaviors. We observed significant variation in plankton and detritus abundance over time where density peak patterns mirrored a tidal cycle's trend, albeit with some time lag compared to high or low tide. Tides emerged as a pivotal factor in elucidating a significant portion of the variability in plankton densities standing apart from the more commonly recognized factors such as phenological or seasonal fluctuations. We suggest that a high-density patch was oscillating back and forth with the tidal gyres. The OSERIT model predicted that this plankton cloud could move in an oval-shaped pattern, with a major axis of 4.4 km and a total travel distance covering 11.6 km. This study emphasizes planktons' small-scale patchy distribution in the water column and how far it can potentially be transported by tidal currents.

The aggregation and distribution of plankton in water observed in **chapter 4** has important implications for accurately estimating plankton densities. Samples from specific stations usually serve as representatives for the plankton community in a larger area. However, due to the presence of short-term spatiotemporal variations, the timing of sampling emerges as a crucial consideration that can influence the observed composition and abundance of plankton communities. For example, daytime samples may overlook hyperbenthic organisms, which substantially contribute to pelagic biomass during the night (**chapter 4**). Additionally, samples taken just a few hours apart at the same location may exhibit densities up to 6 times larger due to the influence of tidal currents (**chapter 4**). Unfortunately, these variations due to tidal influences are often overlooked in coastal food web models (Carlotti and Poggiale, 2010). During research cruises, obtaining multiple replicates at a sampling station can be a practical and easily executable approach to capturing small-scale spatial variation. Nevertheless, addressing short-term temporal fluctuations (such as hourly or diel patterns) is more challenging. Accounting for short-term temporal variation would require the collection of more samples at different time points at a station, but this is often not possible due to limited budgets or time constraints during

scientific cruises. The short-term spatiotemporal variation in plankton densities introduces a challenge that necessitates careful consideration or appropriate correction methods.

### 6.2.3 Constraints on spatial resolution and employability

**Chapter 2** aimed to determine the turbidity limit of the VPR and it turned out that the turbidity of the water column is a major drawback limiting the spatial resolution and general employability of the VPR and other imaging systems. It can hinder the capturing of images and particularly forms a problem in coastal waters. In waters with turbidity values over 6.2 NTU the VPR no longer captures images usable for plankton research. As turbidity increases, captured images progressively lose contrast and become blurred, ultimately reaching a point where no more images are obtained. A VPR uses dark field imaging principles, where light emitted by the stroboscope is diffracted by particles of interest and subsequently captured by the camera lens. However, in high-turbidity conditions, additional particles in the background, including detritus, phytoplankton blooms, or other suspended particulate matter in the water column, can also diffract light, highlighting the background, and diminishing the visibility and contrast of the particle of interest, thereby impeding effective image capture.

Imaging methods employing a configuration where the lens and stroboscope are in closer proximity, as opposed to the VPR, are likely to exhibit a lower turbidity threshold, because the reduced space between the stroboscope and the lens minimize the potential for unwanted particles and materials to scatter light. A collaborative campaign conducted with NIOZ involving a CPICS mounted on the VPR for simultaneous measurements, supported this notion. A CPICS demonstrated an improved functionality compared to a VPR in more turbid waters, albeit to a limited extent. Also Gao *et al.*, (2023) reported that a CPICS operates effectively within a broader turbidity range.

Moreover, in waters with high turbidity and elevated particle levels, the bulk of the captured images consist of detritus (> 95 %). This results in the accumulation of numerous images that may not be pertinent to plankton research and prolong the manual validation time. The presence of detritus particles on the ROIs or the diminished contrast between the background and plankton on the ROIs can also complicate the manual validation process, making it more challenging to identify plankton particles (e.g., Bi *et al.*, 2015).

Another factor that may restrict the spatial range of the Real Time VPR is the length of the optical fiber cable responsible for the data transfer to the deck. The deployment depth of the Real Time VPR is limited to the length of this cable, with a maximum depth of approximately 250 meters in the present study. In deeper regions, such as the fjords in **chapter 5**, this restriction implies that

only the top hundreds of meters can be effectively sampled. Other (optical) devices that do not need an optical fiber cable and an own dedicated winch, can utilize the vessel's winch cables, which often have the capability to reach significant depths (e.g., the cable for the MultiNet in **chapter 5** sampled the whole water column and reached depths of 1500 m).

The future of underwater sampling and monitoring holds great promise with the integration of autonomous underwater vehicles (AUVs) equipped with optical cameras. These unmanned vehicles, capable of autonomously navigating through water, would allow us to deploy a fleet of underwater cameras to collect *in situ* data across broader geographical scales or in challenging places where a Real Time VPR cannot be towed (e.g., depths exceeding 250 m or in ice-covered regions where conventional vessels cannot navigate (Lee *et al.*, 2010). While AUVs have been employed for assessing Antarctic krill using acoustic sensors (Guihen *et al.*, 2014), the prospect of achieving similar outcomes with optical devices necessitates the development of smaller and lighter imaging systems. The demand for compact, lighter tools is not limited to specific research endeavors but extends to broader applications, facilitating a more versatile usage. Notably, the reduced size of a CPICS underwater imaging system enables its deployment on a CTD rosette and on free-drifting or anchored instrument platforms (Lombard *et al.*, 2019), demonstrating its adaptability across a spectrum of platforms. As a result, potential advancements in technology would not only enhance the efficiency of *in situ* sampling but would also facilitate the integration of optical methods on versatile platforms, broadening the scope of underwater exploration.

## 6.2.4 Temporal patterns

Marine ecosystems are dynamic environments where the physical and chemical conditions are continuously changing. Present-day challenges, such as eutrophication, pollution, and climate change put the marine ecosystem under additional pressure. The impact of both natural and anthropogenic changes unfolds across a spectrum of time scales, spanning from daily to decadal (Haury *et al.*, 1978) This dynamic influence manifests in distinct shifts in species composition and abundance within plankton populations, responding to fluctuations in environmental conditions (e.g., Conroy *et al.*, 2023; Mortelmans *et al.*, 2021; Brodeur *et al.*, 2019). To capture these sometimes subtle yet impactful changes, the acquisition of extensive and long-term time series becomes imperative. Collecting reliable data on physical, biological, and chemical variables necessitates replicates over years, forming the foundation for rigorous statistical analyses. The importance of long and repeated time-series of zooplankton cannot be overstated—they substantially enhance the probability of detecting and comprehending environmental changes within the marine ecosystem (Valdés *et al.*, 2007).

Long-term data series or monitoring programs collected with *in situ* imaging devices are not common and most often rely on net samples (e.g., see Ratnarajah *et al.* (2023) for a global overview of long-term monitoring programmes for zooplankton). However, to analyse whether optical imaging methods hold the potential for monitoring approaches and are able to detect temporal patterns as net methods do, we made a comparison between a VPR and net sampling methods in **chapter 3** to research the similarities and discrepancies in the plankton abundance and community composition. The hourly plankton abundance estimates made over a 24-hour period revealed that, despite variations in abundance estimations between the WP2 net and VPR, both methods detected analogous patterns characterized by simultaneous increases and decreases in plankton abundance. This illustrates that optical methods are suitable to detect temporal changes in plankton communities. It offers the possibility to be used for monitoring long-term trends of abundant or gelatinous taxa, as highlighted in section 6.1, but not of less abundant taxa due to the small sampling volume.

Based on the outcome of this PhD, I do not recommend replacing nets with optical devices in ongoing monitoring studies, but to use them complementary. Given the importance of long-term datasets, it is not advisable to change the sampling method and interrupt existing time-series. Instead, it is advised to enable long-term overlap between imaging and traditional techniques to secure continuity and quality control (Giering *et al.*, 2021). Continuing the use of net samples offers the advantage of simplifying global trend comparisons without necessitating the application of conversion factors between sampling methods. This simplicity arises from the widespread utilization of nets across various sampling and research programs. The challenges associated with determining a conversion factor between optical and net sampling methods (**chapter 3**) become apparent when considering the intricate variations between taxa and study regions. The task is further complicated by the potential need to assess the validity of region-specific correlation factors across different seasons.

### 6.2.5 Other applications

There is a growing demand for more data, particularly for monitoring or model development, yet the financial resources to acquire or process such data are not always readily available. Optical imaging, with its capability to generate significant data volumes, presents a valuable method in addressing this demand. Nevertheless, effectively handling this challenge necessitates substantial data storage capacities and the integration of automated classifiers. The continuous improvement in the accuracy and processing speed of these classifiers could potentially pave the way for real-time validation of collected data. This, in turn, opens the possibility of deploying monitoring buoys that can collect and validate data in real-time, with a high temporal resolution. These

## CHAPTER 6

advancements could serve for the detection of harmful or non-indigenous species in the area or contribute to the building of high temporal resolution data series. Data from real-time monitoring stations could contribute to monitoring efforts, model development, or act as input for international projects such as the European Digital Twin of the Ocean (European Commission, n.d.). The latter provides a digital representation of the ocean environment through the integration of real-time sensor data, historical information, and predictive models. Spanning past, present, and future scenarios, with forecasting periods ranging from seasons to multi-decades, this initiative connects data, science, and policymaking by helping them with various applications, including environmental monitoring, resource management, climate research, and decision-making processes related to ocean conservation and sustainability (European Commission, n.d.). In anticipation of future advancements, it is imperative to acknowledge the growing need for harmonizing imaging datasets. This harmonization is essential for enhancing their integration into data systems and use in projects, facilitating seamless comparison or combination of datasets.

As discussed, the VPR offers significant potential for plankton research to gain additional insights into plankton ecology and distribution. While this doctoral thesis primarily focuses on plankton ecology and distribution, numerous other fields of research and interesting areas could benefit from VPR exploration. Apart from plankton organisms themselves, the VPR captures a multitude of other particles, such as the gelatinous houses of appendicularians, fecal pellets, detritus, or marine snow in the water column that can provide insights into research on carbon fluxes, microplastics, or water column turbidity.

Appendicularians can shed multiple gelatinous houses per day (e.g., *Oikopleura dioica*, an abundant appendicularian in the Belgian part of the North Sea (Van Ginderdeuren *et al.*, 2014) sheds 8 - 19 houses per day under experimental conditions (Sato *et al.*, 2001)). This allows appendicularians to maintain optimal feeding efficiency by discarding accumulated debris but also has broader implications for marine ecosystems. Appendicularians occupy an important position in the marine ecosystems and their discarded houses act as both food sources and surface habitats for other organisms (Alldredge, 1976). Consequently, the presence and abundance of appendicularians and their houses contribute to the overall productivity and biodiversity of the surrounding ecosystem. Moreover, their houses have been found to capture microplastics, contributing to the sequestration and transportation of these pollutants in the marine environment (Katija *et al.*, 2017). Additionally, the sinking houses can transport significant amounts of organic carbon to deeper depths, thus enhancing the biological carbon pump and influencing global carbon cycling (Robinson *et al.*, 2005).

Detritus research represents an actively explored field, with a particular emphasis on the role of detritus in the biological carbon pump. The efficiency and speed of the vertical export of detritus from the ocean's surface to the sea bottom is strongly dependent on its morphology and composition (Trudnowska *et al.*, 2021). These characteristics influence aggregation processes, as well as biological interactions, such as colonization and feeding by the plankton community (Stukel *et al.*, 2014). In the past, biogeochemical models (e.g., Omand *et al.*, 2020) and carbon export calculations most often relied on simplifications, assuming fixed mass-to-volume relationships and simple geometries, such as spheres. This simplification was necessitated by the fragile and complex morphological characteristics of marine snow, making it challenging to sample and to study. However, the advent of optical imaging devices improved our ability to study the intricate morphology and features (e.g., size, structure and shape) of these fragile organic particles and enabled a more accurate quantification of their vertical export (Trudnowska *et al.*, 2021; Stukel *et al.*, 2014).

Another valuable application involves investigating water column turbidity and suspended particulate matter. The analysis of image data can provide information on the nature and morphology of suspended particles, distinguishing between living organisms and abiotic entities. In addition, there is the possibility to mount extra sensors on the VPR making it possible to collect *in situ* data simultaneously with other sensors. For example, mounting a LISST-200× (Sequoia Scientific, Inc.) to the VPR provides a more comprehensive understanding of the composition or grain size of the entirety of suspended particles that cause turbidity (Praet *et al.*, 2023). This can be even further complemented with additional sensors beyond the VPR, such as remote sensing satellites or multibeam sonars, to provide a more holistic perspective on water column turbidity and suspended particulate matter.

### 6.3 Trophic interactions and food webs

Plankton are interwoven in the marine food web due to its position at the base of the food web and are linked one to another through different types of interactions. Zooplankton have a position as grazers for algae and bacteria, influencing their community population (Banse, 1994) and in turn act as prey for higher trophic levels. Sampling the plankton community with imaging devices can provide additional image information on its nutritional state or feeding behavior: it's possible to see the stomach content of certain taxa (e.g., of *Noctiluca scintillans* cells) (**chapter 2**), to see the size of the lipid sac (e.g., in *Calanus* copepods), how organisms aggregate around and feed on detritus particles, or the pigmentation of organisms to better estimate the transfer of antioxidants to higher trophic levels (Vilgrain *et al.*, 2023).

However, this provides only limited information for certain organisms where such distinctions can be made. Other methods including stable isotopes analysis, stomach or gut content analysis (Carscallen *et al.*, 2012; Pasquaud *et al.*, 2010), or the use of fatty acid trophic markers (Dalsgaard, 2003), can delve much deeper into food consumption, trophic position or the integration of fatty acids (FAs) across trophic levels. **Chapter 5** aimed to analyse the FA composition of plankton across different zooplankton size fractions in fjord systems and the spatial distribution of copepods. Gas chromatography and mass spectrometry showed significant variations in food quality between the micro and mesozooplankton size fraction. The most notable difference was the reduced concentration of stearidonic acid (18:4(n-3)) in the microzooplankton community, an essential omega-3 FA that animals must obtain from dietary sources. These variations in food quality are important to understand since certain fish species and predators of zooplankton and are known to be size selective and are influenced by the size, quality and distribution of their prey (Beaugrand *et al.*, 2003; Brander *et al.*, 2001; Sundby, 2000; Bainbridge and McKay, 1968). Anticipating climate-driven shifts in plankton communities, we hint at a future scenario with a change in quality and distribution of FAs. Alterations in food quality may exert a negative influence on fish and higher trophic levels, potentially disrupting the overall functioning of ecosystems and carrying implications for economically important fisheries.

## 6.4 General conclusion

For a long time, our knowledge of plankton was captured by plankton nets. Nowadays, optical methods offer an alternative way to sample plankton and form a powerful tool to advance our comprehension of plankton ecology. These optical techniques facilitate the study of (fragile) individual organisms, their interactions, and the environmental factors influencing their distribution and abundance with high spatiotemporal resolution. The VPR emerges as a versatile device for diverse research needs. Its flexibility allows customization based on the specific research question, targeted organisms, and study area which determine the methodological decisions. Yet, it is important to recognize that there is no one-size-fits-all method. Despite the considerable strengths of optical devices, challenges persist, particularly in highly turbid regions like coastal areas, where elevated turbidity levels impede their deployment. Looking ahead, the future holds promise for the integration of more accurate and faster automated classifiers to increase processing efficiency and facilitate real-time classification of image data. By further embracing technological and methodological innovations, we step towards a more comprehensive and dynamic understanding of plankton ecosystems, and reinforce our ability to address the challenges and changes they may face in the evolving marine landscape.



**Box 4. Key findings**

In the general discussion, our findings were framed within the three primary domains of plankton research. In conclusion, the take-home messages representing the key findings from each research chapter are:

**Chapter 2 aimed to answer which towing procedures and instrument settings are best suited for VPR users, in particular in the southern North Sea, and examine the turbidity limit of the VPR.**

- The straight tow type is preferable for plankton studies over larger areas, capturing local abundance peaks and relating them to environmental conditions.
- Optimal magnification settings vary based on plankton size, with a high magnification suitable for organisms ranging from 0.3 to 0.7 mm and a low magnification for those between 1.0 to 3.8 mm.
- Turbidity values exceeding 6.2 NTU hinder VPR's data collection for plankton research, posing challenges in coastal and transitional waters.

**Chapter 3 researched the similarities and discrepancies in the plankton abundance and community composition obtained from VPR and net sampling methods.**

- The VPR's non-invasive nature improved density estimates for fragile and gelatinous taxa, emphasizing the substantial contribution of gelatinous species to the zooplankton community.
- Hydrographic conditions led to varied results; in eutrophic sites, WP2 net densities surpassed VPR densities, while in clear water sites, VPR and MultiNet densities were more similar. Factors such as water turbidity, plankton size, community density, and net mesh size contributed to observed inconsistencies between sampling sites.
- The VPR proved particularly effective in clear waters with low plankton densities.
- Over a 24-hour period, both VPR and net sampling methods revealed similar plankton dynamics, highlighting the temporal consistency between the two techniques.

**Chapter 4 questioned how plankton is distributed over fine spatial and temporal scales within the water column in dynamic coastal systems under strong tidal forces.**

- Fine-scale VPR tracking reveals copepods' diel vertical migration and the nocturnal migration of hyperbenthic taxa from the sea bottom.

- Tidal currents significantly impact plankton distribution and densities, causing substantial variation within a 24-hour period at a single sample location.

**Chapter 5 analyzed how the fatty acid composition of plankton varies across different zooplankton size classes within fjords, and how copepods are spatially distributed in fjords.**

- Fatty acid composition significantly differs between micro and mesozooplankton, with lower polyunsaturated FAs, such as 18:4(n-3), in microzooplankton.
- Along a fjord-shelf gradient, large copepods dominate the offshore areas, whereas small copepods are more abundant in the inner fjord.
- Large copepods were often associated with the deep chlorophyll maximum layer and were distributed higher up in the water column compared to small copepods.





## Cited literature

- Aarflot, J. M., Skjoldal, H. R., Dalpadado, P., & Skern-Mauritzen, M. (2017). Contribution of Calanus species to the mesozooplankton biomass in the Barents Sea. *ICES Journal of Marine Science*, 75(7), 2342–2354. <https://doi.org/10.1093/icesjms/fsx221>
- Ackman, R. G., & Sipos, J. C. (1964). Application of specific response factors in the gas chromatographic analysis of methyl esters of fatty acids with flame ionization detectors. *Journal of the American Oil Chemists' Society*, 41(5), 377–378. Portico. <https://doi.org/10.1007/bf02654818>
- Allredge, A. L. (1976). Discarded appendicularian houses as sources of food, surface habitats, and particulate organic matter in planktonic environments. *Limnology and Oceanography*, 21(1), 14–24. Portico. <https://doi.org/10.4319/lo.1976.21.1.0014>
- Anger, K., & Valentin, C. (1976). In-situ-Untersuchungen zum täglichen Aktivitätsrhythmus von *Diastylis rathkei* (Cumacea, Crustacea) und ihre Bedeutung für das „Hyperbenthos“. *Helgoländer Wissenschaftliche Meeresuntersuchungen*, 28(2), 138–144. <https://doi.org/10.1007/bf01610349>
- Appeltans, W., Ahyong, S. T., Anderson, G., Angel, M. V., Artois, T., Bailly, N., ... & Costello, M. J. (2012). The magnitude of global marine species diversity. *Current biology*, 22(23), 2189–2202. <https://doi.org/10.1016/j.cub.2012.09.036>
- Ashjian, C. J., Davis, C. S., Gallager, S. M., & Alatalo, P. (2001). Distribution of plankton, particles, and hydrographic features across Georges Bank described using the Video Plankton Recorder. *Deep Sea Research Part II: Topical Studies in Oceanography*, 48(1–3), 245–282. [https://doi.org/10.1016/s0967-0645\(00\)00121-1](https://doi.org/10.1016/s0967-0645(00)00121-1)
- Aurelia, Jessica Luo, Josette\_BoozAllen, Josh Sullivan, Steve Mills, Will Cukierski. (2014). National Data Science Bowl. Kaggle. <https://kaggle.com/competitions/datasciencebowl>
- Baeye, M., Fettweis, M., Voulgaris, G., & Van Lancker, V. (2011). Sediment mobility in response to tidal and wind-driven flows along the Belgian inner shelf, southern North Sea. *Ocean Dynamics*, 61(5), 611–622. doi:10.1007/s10236-010-0370-7
- Bainbridge, V., & McKay, B. J. (1968). The feeding of cod and redfish larvae. *ICNAF Spec. Publ*, 7, 187–217.

## CITED LITERATURE

- Ballantyne, A. P., Brett, M. T., & Schindler, D. E. (2003). The importance of dietary phosphorus and highly unsaturated fatty acids for sockeye (*Oncorhynchus nerka*) growth in Lake Washington — a bioenergetics approach. *Canadian Journal of Fisheries and Aquatic Sciences*, 60(1), 12–22. <https://doi.org/10.1139/f02-166>
- Bandara, K., Varpe, Ø., Wijewardene, L., Tverberg, V., & Eiane, K. (2021). Two hundred years of zooplankton vertical migration research. *Biological Reviews*, 96(4), 1547–1589. <https://doi.org/10.1111/brv.12715>
- Banase, K. (1994). Grazing and Zooplankton Production as Key Controls of Phytoplankton Production in the Open Ocean. *Oceanography*, 7(1), 13–20. <https://doi.org/10.5670/oceanog.1994.10>
- Bar-On, Y. M., & Milo, R. (2019). The Biomass Composition of the Oceans: A Blueprint of Our Blue Planet. *Cell*, 179(7), 1451–1454. <https://doi.org/10.1016/j.cell.2019.11.018>
- Bar-On, Y. M., Phillips, R., & Milo, R. (2018). The biomass distribution on Earth. *Proceedings of the National Academy of Sciences*, 115(25), 6506–6511. <https://doi.org/10.1073/pnas.1711842115>
- Bartels-Hardege, H. D., & Zeeck, E. (1990). Reproductive behavior of *Nereis diversicolor* (Annelida: Polychaeta). *Marine Biology*, 106(3), 409–412. <https://doi.org/10.1007/bf01344320>
- Barthel, K. G. (1988). Feeding of three *Calanus* species on different phytoplankton assemblages in the Greenland Sea. *Meeresforschung (Hamburg)*, 32(2), 92–106.
- Basedow, S. L., Tande, K. S., Norrbin, M. F., & Kristiansen, S. A. (2013). Capturing quantitative zooplankton information in the sea: Performance test of laser optical plankton counter and video plankton recorder in a *Calanus finmarchicus* dominated summer situation. *Progress in Oceanography*, 108, 72–80. <https://doi.org/10.1016/j.pocean.2012.10.005>
- Beaugrand, G., Brander, K. M., Alistair Lindley, J., Souissi, S., & Reid, P. C. (2003). Plankton effect on cod recruitment in the North Sea. *Nature*, 426(6967), 661–664. <https://doi.org/10.1038/nature02164>
- Beaugrand, G., Reid, P. C., Ibañez, F., Lindley, J. A., & Edwards, M. (2002). Reorganization of North Atlantic Marine Copepod Biodiversity and Climate. *Science*, 296(5573), 1692–1694. <https://doi.org/10.1126/science.1071329>
- Bedford, J., Johns, D., Greenstreet, S., & McQuatters-Gollop, A. (2018). Plankton as prevailing conditions: A surveillance role for plankton indicators within the Marine Strategy Framework Directive. *Marine Policy*, 89, 109–115. <https://doi.org/10.1016/j.marpol.2017.12.021>
- Behrenfeld, M. J., Gaube, P., Della Penna, A., O'Malley, R. T., Burt, W. J., Hu, Y., Bontempi, P. S., Steinberg, D. K., Boss, E. S., Siegel, D. A., Hostetler, C. A., Tortell, P. D., & Doney, S. C. (2019). Global satellite-observed daily vertical migrations of ocean animals. *Nature*, 576(7786), 257–261. <https://doi.org/10.1038/s41586-019-1796-9>
- Bender, S. J., Moran, D. M., McIlvin, M. R., Zheng, H., McCrow, J. P., Badger, J., DiTullio, G. R., Allen, A. E., & Saito, M. A. (2018). Colony formation in *Phaeocystis antarctica* connecting molecular mechanisms with iron biogeochemistry. *Biogeosciences*, 15(16), 4923–4942. <https://doi.org/10.5194/bg-15-4923-2018>

- Bendtsen, J., Rysgaard, S., Carlson, D. F., Meire, L., & Sejr, M. K. (2021). Vertical Mixing in Stratified Fjords Near Tidewater Outlet Glaciers Along Northwest Greenland. *Journal of Geophysical Research: Oceans*, 126(8). Portico. <https://doi.org/10.1029/2020jc016898>
- Benfield, M. C., Davis, C. S., Wiebe, P. H., Gallagher, S. M., Gregory Lough, R., & Copley, N. J. (1996). Video Plankton Recorder estimates of copepod, pteropod and larvacean distributions from a stratified region of Georges Bank with comparative measurements from a MOCNESS sampler. *Deep Sea Research Part II: Topical Studies in Oceanography*, 43(7–8), 1925–1945. [https://doi.org/10.1016/s0967-0645\(96\)00044-6](https://doi.org/10.1016/s0967-0645(96)00044-6)
- Benoit-Bird, K. J., Battaile, B. C., Heppell, S. A., Hoover, B., Irons, D., Jones, N., Kuletz, K. J., Nordstrom, C. A., Paredes, R., Suryan, R. M., Waluk, C. M., & Trites, A. W. (2013). Prey Patch Patterns Predict Habitat Use by Top Marine Predators with Diverse Foraging Strategies. *PLoS ONE*, 8(1), e53348. <https://doi.org/10.1371/journal.pone.0053348>
- Bernard, K. S., Cimino, M., Fraser, W., Kohut, J., Oliver, M. J., Patterson-Fraser, D., Schofield, O. M. E., Statscewich, H., Steinberg, D. K., & Winsor, P. (2017). Factors that affect the nearshore aggregations of Antarctic krill in a biological hotspot. *Deep Sea Research Part I: Oceanographic Research Papers*, 126, 139–147. <https://doi.org/10.1016/j.dsr.2017.05.008>
- Beroujon, T., Christiansen, J. S., & Norrbin, F. (2022). Spatial occurrence and abundance of marine zooplankton in Northeast Greenland. *Marine Biodiversity*, 52(5). <https://doi.org/10.1007/s12526-022-01280-6>
- Bi, H., Guo, Z., Benfield, M. C., Fan, C., Ford, M., Shahrestani, S., & Sieracki, J. M. (2015). A Semi-Automated Image Analysis Procedure for In Situ Plankton Imaging Systems. *PLOS ONE*, 10(5), e0127121. <https://doi.org/10.1371/journal.pone.0127121>
- Biard, T., & Ohman, M. D. (2019). Vertical niche definition of test-bearing protists (Rhizaria) into the twilight zone revealed by in situ imaging. <https://doi.org/10.1101/573410>
- Boero, F., Bouillon, J., Gravili, C., Miglietta, M., Parsons, T., & Piraino, S. (2008). Gelatinous plankton: irregularities rule the world (sometimes). *Marine Ecology Progress Series*, 356, 299–310. <https://doi.org/10.3354/meps07368>
- Boersma, M., Malzahn, A. M., Greve, W., & Javidpour, J. (2007). The first occurrence of the ctenophore *Mnemiopsis leidyi* in the North Sea. *Helgoland Marine Research*, 61(2), 153–155. <https://doi.org/10.1007/s10152-006-0055-2>
- Bollens, S. M., & Frost, B. W. (1991). Diel vertical migration in zooplankton: rapid individual response to predators. *Journal of Plankton Research*, 13(6), 1359–1365. <https://doi.org/10.1093/plankt/13.6.1359>
- Boon, A. R., & Kromkamp, J. C. (2022). Climate change and intensifying human use call for a monitoring upgrade of the Dutch North Sea. *Journal of Sea Research*, 182, 102185. <https://doi.org/10.1016/j.seares.2022.102185>
- Borcard, D., Gillet, F., & Legendre, P. (2011). *Numerical Ecology with R*. <https://doi.org/10.1007/978-1-4419-7976-6>
- Bowman, J. S., & Ducklow, H. W. (2019). Bacterioplankton. *Encyclopedia of Ocean Sciences*, 500–507. <https://doi.org/10.1016/b978-0-12-409548-9.11404-6>

## CITED LITERATURE

- Boyd, P. W., Claustre, H., Levy, M., Siegel, D. A., & Weber, T. (2019). Multi-faceted particle pumps drive carbon sequestration in the ocean. *Nature*, 568(7752), 327–335. <https://doi.org/10.1038/s41586-019-1098-2>
- Brandão, M.C., Benedetti, F., Martini, S. et al. Macroscale patterns of oceanic zooplankton composition and size structure. *Sci Rep* 11, 15714 (2021). <https://doi.org/10.1038/s41598-021-94615-5>
- Brander, K. (2001). Modelling the timing of plankton production and its effect on recruitment of cod (*Gadus morhua*). *ICES Journal of Marine Science*, 58(5), 962–966. <https://doi.org/10.1006/jmsc.2001.1086>
- Brodeur, R. D., Auth, T. D., & Phillips, A. J. (2019). Major Shifts in Pelagic Micronekton and Macrozooplankton Community Structure in an Upwelling Ecosystem Related to an Unprecedented Marine Heatwave. *Frontiers in Marine Science*, 6. <https://doi.org/10.3389/fmars.2019.00212>
- Brodeur, R. D., Link, J. S., Smith, B. E., Ford, M. D., Kobayashi, D. R., & Jones, T. T. (2016). Ecological and Economic Consequences of Ignoring Jellyfish: A Plea for Increased Monitoring of Ecosystems. *Fisheries*, 41(11), 630–637. Portico. <https://doi.org/10.1080/03632415.2016.1232964>
- Broughton, E. A., & Lough, R. G. (2006). A direct comparison of MOCNESS and Video Plankton Recorder zooplankton abundance estimates: Possible applications for augmenting net sampling with video systems. *Deep Sea Research Part II: Topical Studies in Oceanography*, 53(23–24), 2789–2807. <https://doi.org/10.1016/j.dsr2.2006.08.013>
- Bruhn, C. S., Wohlrab, S., Krock, B., Lundholm, N., & John, U. (2021). Seasonal plankton succession is in accordance with phycotoxin occurrence in Disko Bay, West Greenland. *Harmful Algae*, 103, 101978. <https://doi.org/10.1016/j.hal.2021.101978>
- Brunel, P. (1979). Seasonal Changes of Daily Vertical Migrations in a Suprabenthic Coldlayer Shelf Community Over Mud in the Gulf of St. Lawrence. *Cyclic Phenomena in Marine Plants and Animals*, 383–390. <https://doi.org/10.1016/b978-0-08-023217-1.50056-4>
- Bucklin, A., Peijnenburg, K. T. C. A., Kosobokova, K. N., O'Brien, T. D., Blanco-Bercial, L., Cornils, A., Falkenhaus, T., Hopcroft, R. R., Hosia, A., Laakmann, S., Li, C., Martell, L., Questel, J. M., Wall-Palmer, D., Wang, M., Wiebe, P. H., & Weydmann-Zwolicka, A. (2021). Toward a global reference database of COI barcodes for marine zooplankton. *Marine Biology*, 168(6). <https://doi.org/10.1007/s00227-021-03887-y>
- Calbet, A., & Saiz, E. (2005). The ciliate-copepod link in marine ecosystems. *Aquatic Microbial Ecology*, 38, 157–167. <https://doi.org/10.3354/ame038157>
- Campbell, M. D., Schoeman, D. S., Venables, W., Abu-Alhaija, R., Batten, S. D., Chiba, S., ... & Richardson, A. J. (2021). Testing Bergmann's rule in marine copepods. *Ecography*, 44(9), 1283–1295. <https://doi.org/10.1111/ecog.05545>
- Carlotti, F., & Poggiale, J. C. (2010). Towards methodological approaches to implement the zooplankton component in “end to end” food-web models. *Progress in Oceanography*, 84(1–2), 20–38. <https://doi.org/10.1016/j.pocean.2009.09.003>
- Carroll, D., Sutherland, D. A., Curry, B., Nash, J. D., Shroyer, E. L., Catania, G. A., Stearns, L. A., Grist, J. P., Lee, C. M., & de Steur, L. (2018). Subannual and Seasonal Variability of Atlantic-Origin



- Waters in Two Adjacent West Greenland Fjords. *Journal of Geophysical Research: Oceans*, 123(9), 6670–6687. Portico. <https://doi.org/10.1029/2018jc014278>
- Carscallen, W. M. A., Vandenberg, K., Lawson, J. M., Martinez, N. D., & Romanuk, T. N. (2012). Estimating trophic position in marine and estuarine food webs. *Ecosphere*, 3(3), 1–20. Portico. <https://doi.org/10.1890/es11-00224.1>
- Castellani, C., & Edwards, M. (Eds.). (2017). *Marine Plankton: A practical guide to ecology, methodology, and taxonomy*. Oxford University Press. doi:10.1093/oso/9780199233267.001.0001
- Chappell, M. A., Shoemaker, V. H., Janes, D. N., Bucher, T. L., & Maloney, S. K. (1993). Diving Behavior During Foraging in Breeding Adelie Penguins. *Ecology*, 74(4), 1204–1215. Portico. <https://doi.org/10.2307/1940491>
- Chivers, W. J., Walne, A. W., & Hays, G. C. (2017). Mismatch between marine plankton range movements and the velocity of climate change. *Nature Communications*, 8(1). <https://doi.org/10.1038/ncomms14434>
- Cohen, J. H., & Forward Jr, R. B. (2016). Zooplankton Diel Vertical Migration — A Review of Proximate Control. *Oceanography and Marine Biology*, 89–122. <https://doi.org/10.1201/9781420094220-5>
- Conover, R. J., & Siferd, T. D. (1993). Dark-Season Survival Strategies of Coastal Zone Zooplankton in the Canadian Arctic. *ARCTIC*, 46(4). <https://doi.org/10.14430/arctic1357>
- Conroy, J., Steinberg, D., Thomas, M., & West, L. (2023). Seasonal and interannual changes in a coastal Antarctic zooplankton community. *Marine Ecology Progress Series*, 706, 17–32. <https://doi.org/10.3354/meps14256>
- Conway, D. V. P., & Minton, R. C. (1976). Vertical distribution of zooplankton and larval gadoids in the northern North Sea. Department of Agriculture and Fisheries for Scotland, Marine Laboratory (Aberdeen), New Series, 13.
- Dagg, M. (1977). Some effects of patchy food environments on copepods. *Limnology and Oceanography*, 22(1), 99–107. Portico. <https://doi.org/10.4319/lo.1977.22.1.0099>
- Dalsgaard, J., St. John, M., Kattner, G., Müller-Navarra, D., & Hagen, W. (2003). Fatty acid trophic markers in the pelagic marine environment. *Advances in Marine Biology*, 225–340. [https://doi.org/10.1016/s0065-2881\(03\)46005-7](https://doi.org/10.1016/s0065-2881(03)46005-7)
- Daro, M. H. (1974). Etude des migrations nycthemerales du zooplancton dans un milieu marin peu profond. *Hydrobiologia*, 44, 149-160.
- Daro, M. H. (1985). Feeding rhythms and vertical distribution of marine copepods. *Bulletin of Marine Science*, 37(2), 487-497.
- Dauvin, J.-C., & Zouhiri, S. (1996). Suprabenthic crustacean fauna of a dense Ampeliscacommunity from the English Channel. *Journal of the Marine Biological Association of the United Kingdom*, 76(4), 909–929. <https://doi.org/10.1017/s0025315400040881>
- Davis, C. S., Gallagher, S. M., & Solow, A. R. (1992). Microaggregations of Oceanic Plankton Observed by Towed Video Microscopy. *Science*, 257(5067), 230–232. <https://doi.org/10.1126/science.257.5067.230>

## CITED LITERATURE

- Davis, C. S., Gallagher, S. M., Berman, M. S., Haury, L. R., & Strickler, J. R. (1992). The video plankton recorder (VPR): design and initial results. *Arch. Hydrobiol. Beih*, 36, 67-81.
- Davis, C., Hu, Q., Gallagher, S., Tang, X., & Ashjian, C. (2004). Real-time observation of taxa-specific plankton distributions: an optical sampling method. *Marine Ecology Progress Series*, 284, 77-96. doi:10.3354/meps284077
- De Donno, A., Idolo, A., Bagordo, F., Grassi, T., Leomanni, A., Serio, F., Guido, M., Canitano, M., Zampardi, S., Boero, F., & Piraino, S. (2014). Impact of Stinging Jellyfish Proliferations along South Italian Coasts: Human Health Hazards, Treatment and Social Costs. *International Journal of Environmental Research and Public Health*, 11(3), 2488-2503. <https://doi.org/10.3390/ijerph110302488>
- De Galan, S., Elskens, M., Goeyens, L., Pollentier, A., Brion, N., & Baeyens, W. (2004). Spatial and temporal trends in nutrient concentrations in the Belgian Continental area of the North Sea during the period 1993-2000. *Estuarine, Coastal and Shelf Science*, 61(3), 517-528. doi:10.1016/j.ecss.2004.06.015
- de Graaf, M., Jager, Z., Vreugdenhil, C. B., & Elorche, M. (2004). Numerical simulations of tidally cued vertical migrations of flatfish larvae in the North Sea. *Estuarine, Coastal and Shelf Science*, 59(2), 295-305. <https://doi.org/10.1016/j.ecss.2003.09.010>
- De Lafontaine, Y., & Leggett, W. C. (1989). Changes in size and weight of hydromedusae during formalin preservation. *Bulletin of marine science*, 44(3), 1129-1137.
- De Troch, M., Boeckx, P., Cnudde, C., Van Gansbeke, D., Vanreusel, A., Vincx, M., & Caramujo, M. (2012). Bioconversion of fatty acids at the basis of marine food webs: insights from a compound-specific stable isotope analysis. *Marine Ecology Progress Series*, 465, 53-67. <https://doi.org/10.3354/meps09920>
- Dennett, M. R., Caron, D. A., Michaels, A. F., Gallagher, S. M., & Davis, C. S. (2002). Video plankton recorder reveals high abundances of colonial Radiolaria in surface waters of the central North Pacific. *Journal of Plankton Research*, 24(8), 797-805. doi:10.1093/plankt/24.8.797
- Dolan, J. R. (2019). Ernst Haeckel's Radiolarians and Medusa: The influence of his visits to Villefranche on his science and his art. *Arts et Sciences*, 3(2). <https://doi.org/10.21494/iste.op.2019.0420>
- Dolan, J. R. (2023). Beauty of the plankton: from the first issue of Haeckel's Art Forms of Nature. *Journal of Plankton Research*, 45(2), 235-238. <https://doi.org/10.1093/plankt/fbac076>
- Ducklow, H., Steinberg, D., & Buesseler, K. (2001). Upper Ocean Carbon Export and the Biological Pump. *Oceanography*, 14(4), 50-58. <https://doi.org/10.5670/oceanog.2001.06>
- Easter, S. S. (1980). *Visual Adaptations: The Ecology of Vision*. J. N. Lythgoe. Clarendon (Oxford University Press), New York, 1979. xii, 244 pp., Science, 209(4464), 1508-1509. <https://doi.org/10.1126/science.209.4464.1508.b>
- European Commission. (n.d.). European Digital Twin Ocean (DTO). Horizon Europe - EU Missions. [https://research-and-innovation.ec.europa.eu/funding/funding-opportunities/funding-programmes-and-open-calls/horizon-europe/eu-missions-horizon-europe/restore-our-ocean-and-waters/european-digital-twin-ocean-european-dto\\_en](https://research-and-innovation.ec.europa.eu/funding/funding-opportunities/funding-programmes-and-open-calls/horizon-europe/eu-missions-horizon-europe/restore-our-ocean-and-waters/european-digital-twin-ocean-european-dto_en)

- Falk-Petersen, S., Pavlov, V., Timofeev, S., & Sargent, J. R. (2007). Climate variability and possible effects on arctic food chains: The role of Calanus. *Arctic Alpine Ecosystems and People in a Changing Environment*, 147–166. [https://doi.org/10.1007/978-3-540-48514-8\\_9](https://doi.org/10.1007/978-3-540-48514-8_9)
- Falk-Petersen, S., Sargent, J. R., & Tande, K. S. (1987). Lipid composition of zooplankton in relation to the sub-arctic food web. *Polar Biology*, 8(2), 115–120. <https://doi.org/10.1007/bf00297065>
- Fettweis, M., Nechad, B., & Van den Eynde, D. (2007). An estimate of the suspended particulate matter (SPM) transport in the southern North Sea using SeaWiFS images, in situ measurements and numerical model results. *Continental Shelf Research*, 27(10-11), 1568–1583. doi:10.1016/j.csr.2007.01.017
- Fettweis, M., & Nechad, B. (2011). Evaluation of in situ and remote sensing sampling methods for SPM concentrations, Belgian continental shelf (southern North Sea). *Ocean Dynamics*, 61(2-3), 157–171. <https://doi.org/10.1007/s10236-010-0310-6>
- Field, C. B., Behrenfeld, M. J., Randerson, J. T., & Falkowski, P. (1998). Primary Production of the Biosphere: Integrating Terrestrial and Oceanic Components. *Science*, 281(5374), 237–240. <https://doi.org/10.1126/science.281.5374.237>
- Flanders Marine Institute (VLIZ) (2019). LifeWatch Observatory Data: Nutrient, Pigment, Suspended Matter and Secchi Measurements in the Belgian Part of the North Sea. (Oostende: Flanders Marine Institute (VLIZ)).
- Flanders Marine Institute (VLIZ), Belgium (2020): LifeWatch observatory data: monthly CTD temperature and salinity measurements in the Belgian Part of the North Sea <https://doi.org/10.14284/537>. Accessed through the LifeWatch Data Explorer / lwdataexplorer R package [Accessed 8 November 2023].
- Fossheim, M., Primicerio, R., Johannesen, E., Ingvaldsen, R. B., Aschan, M. M., & Dolgov, A. V. (2015). Recent warming leads to a rapid borealization of fish communities in the Arctic. *Nature Climate Change*, 5(7), 673–677. <https://doi.org/10.1038/nclimate2647>
- Franz, H., Gonzalez, S., & Steeneken, S. (1998). Metazoan plankton and the structure of the plankton community in the stratified North Sea. *Marine Ecology Progress Series*, 175, 191–200. <https://doi.org/10.3354/meps175191>
- Gallager, S. M., Davis, C. S., Epstein, A. W., Solow, A., & Beardsley, R. C. (1996). High-resolution observations of plankton spatial distributions correlated with hydrography in the Great South Channel, Georges Bank. *Deep Sea Research Part II: Topical Studies in Oceanography*, 43(7-8), 1627–1663. [https://doi.org/10.1016/s0967-0645\(96\)00058-6](https://doi.org/10.1016/s0967-0645(96)00058-6)
- Gallager, S.M. (2016). The Continuous Plankton Imaging and Classification Sensor (CPICS): a sensor for quantifying Mesoplankton Biodiversity and Community Structure. *Am. Geophys. Union* 2016, 52A–57A.
- Gallienne, C. ., Robins, D. ., & Woodd-Walker, R. . (2001). Abundance, distribution and size structure of zooplankton along a 20° west meridional transect of the northeast Atlantic Ocean in July. *Deep Sea Research Part II: Topical Studies in Oceanography*, 48(4-5), 925–949. doi:10.1016/s0967-0645(00)00114-4
- Gao, H., Liu, B., Liu, C., & Wang, R. (2023). A case study of in situ observation on particles and plankton in East China Sea by using of the Continuous Particle Imaging and Classification

## CITED LITERATURE

- System (CPICS), in: The Sixth Xiamen Symposium on Marine Environmental Sciences (XMAS-VI), January 9th-12th, 2023, Xiamen, China.
- Gasparini, S., & Antajan, E. (2018) Plankton Identifier: a software for automatic recognition of planktonic organisms. Available at: [http://www.obs-  
vlfr.fr/~gaspari/Plankton\\_Identifier/index.php](http://www.obs-vlfr.fr/~gaspari/Plankton_Identifier/index.php). [Accessed 2 November 2023].
- Gerbersdorf, S. U., & Schubert, H. (2011). Vertical migration of phytoplankton in coastal waters with different UVR transparency. *Environmental Sciences Europe*, 23(1). <https://doi.org/10.1186/2190-4715-23-36>
- Gerken, S., Meland, K., & Glenner, H. (2022). First multigene phylogeny of Cumacea (crustacea: Peracarida). *Zoologica Scripta*, 51(4), 460–477. Portico. <https://doi.org/10.1111/zsc.12542>
- Giering, S. L. C., Culverhouse, P. F., Johns, D. G., McQuatters-Gollop, A., & Pitois, S. G. (2022). Are plankton nets a thing of the past? An assessment of in situ imaging of zooplankton for large-scale ecosystem assessment and policy decision-making. *Frontiers in Marine Science*, 9. <https://doi.org/10.3389/fmars.2022.986206>
- Giering, S. L. C., Wells, S. R., Mayers, K. M. J., Schuster, H., Cornwell, L., Fileman, E. S., Atkinson, A., Cook, K. B., Preece, C., & Mayor, D. J. (2019). Seasonal variation of zooplankton community structure and trophic position in the Celtic Sea: A stable isotope and biovolume spectrum approach. *Progress in Oceanography*, 177, 101943. <https://doi.org/10.1016/j.pocean.2018.03.012>
- Giron-Nava, A., James, C., Johnson, A., Dannecker, D., Kolody, B., Lee, A., Nagarkar, M., Pao, G., Ye, H., Johns, D., & Sugihara, G. (2017). Quantitative argument for long-term ecological monitoring. *Marine Ecology Progress Series*, 572, 269–274. <https://doi.org/10.3354/meps12149>
- Gislason, A., Logemann, K., & Marteinsdottir, G. (2016). The cross-shore distribution of plankton and particles southwest of Iceland observed with a Video Plankton Recorder. *Continental Shelf Research*, 123, 50–60. doi:10.1016/j.csr.2016.04.004
- Gorsky, G., Ohman, M. D., Picheral, M., Gasparini, S., Stemmann, L., Romagnan, J.-B., ... Prejger, F. (2010). Digital zooplankton image analysis using the ZooScan integrated system. *Journal of Plankton Research*, 32(3), 285–303. doi:10.1093/plankt/fbp124
- Graeve, M., Kattner, G., & Hagen, W. (1994). Diet-induced changes in the fatty acid composition of Arctic herbivorous copepods: Experimental evidence of trophic markers. *Journal of Experimental Marine Biology and Ecology*, 182(1), 97–110. [https://doi.org/10.1016/0022-0981\(94\)90213-5](https://doi.org/10.1016/0022-0981(94)90213-5)
- Grønkjær, P., Nielsen, K. V., Zoccarato, G., Meire, L., Rysgaard, S., & Hedeholm, R. B. (2018). Feeding ecology of capelin (*Mallotus villosus*) in a fjord impacted by glacial meltwater (Godthåbsfjord, Greenland). *Polar Biology*, 42(1), 81–98. <https://doi.org/10.1007/s00300-018-2400-8>
- Grosjean, P., Picheral, M., Warembourg, C., & Gorsky, G. (2004). Enumeration, measurement, and identification of net zooplankton samples using the ZOOSCAN digital imaging system. *ICES Journal of Marine Science*, 61(4), 518–525. doi:10.1016/j.icesjms.2004.03.012

- Grünbaum, D., & Veit, R. R. (2003). Black-browed albatrosses foraging on Antarctic krill: density-dependence through local enhancement?. *Ecology*, 84(12), 3265-3275. <https://doi.org/10.1890/01-4098>
- Guihen, D., Fielding, S., Murphy, E. J., Heywood, K. J., & Griffiths, G. (2014). An assessment of the use of ocean gliders to undertake acoustic measurements of zooplankton: the distribution and density of Antarctic krill (*Euphausia superba*) in the Weddell Sea. *Limnology and Oceanography: Methods*, 12(6), 373-389. Portico. <https://doi.org/10.4319/lom.2014.12.373>
- Guthrie, D. M. (1986). Role of Vision in Fish Behavior. *The Behavior of Teleost Fishes*, 75-113. [https://doi.org/10.1007/978-1-4684-8261-4\\_4](https://doi.org/10.1007/978-1-4684-8261-4_4)
- Gutkowska, A., Paturej, E., & Kowalska, E. (2012). Qualitative and quantitative methods for sampling zooplankton in shallow coastal estuaries. *Ecohydrology & Hydrobiology*, 12(3), 253-263. [https://doi.org/10.1016/s1642-3593\(12\)70208-2](https://doi.org/10.1016/s1642-3593(12)70208-2)
- Hablützel, P., Rombouts, I., Dillen, N., Lagaisse, R., Mortelmans, J., Ollevier, A., Perneel, M., & Deneudt, K. (2021). Exploring New Technologies for Plankton Observations and Monitoring of Ocean Health. *Oceanography*, 20-25. <https://doi.org/10.5670/oceanog.2021.supplement.02-09>
- Haeckel, E. (1900). *Kunstformen der Natur*. Zweite Sammlung. Fünfzig Illustrationstafeln mit beschreibendem Text. Verlag des Bibliographischen Instituts: Leipzig und Wien. [50], plates 51-100 pp
- Hanna, E., Huybrechts, P., Steffen, K., Cappelen, J., Huff, R., Shuman, C., Irvine-Fynn, T., Wise, S., & Griffiths, M. (2008). Increased Runoff from Melt from the Greenland Ice Sheet: A Response to Global Warming. *Journal of Climate*, 21(2), 331-341. <https://doi.org/10.1175/2007jcli1964.1>
- Haupt, F., Stockenreiter, M., Baumgartner, M., Boersma, M., & Stibor, H. (2009). *Daphnia* diel vertical migration: implications beyond zooplankton. *Journal of Plankton Research*, 31(5), 515-524. <https://doi.org/10.1093/plankt/fbp003>
- Haury, L. R., McGowan, J. A., & Wiebe, P. H. (1978). Patterns and Processes in the Time-Space Scales of Plankton Distributions. *Spatial Pattern in Plankton Communities*, 277-327. [https://doi.org/10.1007/978-1-4899-2195-6\\_12](https://doi.org/10.1007/978-1-4899-2195-6_12)
- Hays, G., Richardson, A., & Robinson, C. (2005). Climate change and marine plankton. *Trends in Ecology & Evolution*, 20(6), 337-344. <https://doi.org/10.1016/j.tree.2005.03.004>
- Hedgpeth, J. W., & Ladd, H. S. (1957). *Treatise on Marine Ecology and Paleoecology*. Geological Society of America Memoirs. <https://doi.org/10.1130/mem67v2>
- Hiltunen, M., Strandberg, U., Taipale, S. J., & Kankaala, P. (2015). Taxonomic identity and phytoplankton diet affect fatty acid composition of zooplankton in large lakes with differing dissolved organic carbon concentration. *Limnology and Oceanography*, 60(1), 303-317. Portico. <https://doi.org/10.1002/lno.10028>
- Hirst, A. (2006). Influence of taxonomic resolution on multivariate analyses of arthropod and macroalgal reef assemblages. *Marine Ecology Progress Series*, 324, 83-93. <https://doi.org/10.3354/meps324083>

## CITED LITERATURE

- Holinde, L., & Zielinski, O. (2016). Bio-optical characterization and light availability parameterization in Uumannaq Fjord and Vaigat–Disko Bay (West Greenland). *Ocean Science*, 12(1), 117–128. <https://doi.org/10.5194/os-12-117-2016>
- Holland, M., Louchart, A., Artigas, L. F. and McQuatters-Gollop, A. 2023. Changes in Phytoplankton and Zooplankton Communities. In: OSPAR, 2023: The 2023 Quality Status Report for the Northeast Atlantic. OSPAR Commission, London.
- Hough, A. R., & Naylor, E. (1992). Endogenous rhythms of circatidal swimming activity in the estuarine copepod *Eurytemora affinis* (Poppe). *Journal of Experimental Marine Biology and Ecology*, 161(1), 27–32. [https://doi.org/10.1016/0022-0981\(92\)90187-f](https://doi.org/10.1016/0022-0981(92)90187-f)
- Hough, A., & Naylor, E. (1991). Field studies on retention of the planktonic copepod *Eurytemora affinis* in a mixed estuary. *Marine Ecology Progress Series*, 76, 115–122. <https://doi.org/10.3354/meps076115>
- Hovenkamp, P.; van Walraven, L.; Ollevier, A.; van Oevelen, D.; van der Stappen, F. (submitted). Optimising automated classification of colour images from zooplankton in coastal conditions. Submitted to *Limnology and Oceanography: Methods*
- Huntley, M. E. (1992). Temperature-Dependent Production of Marine Copepods: A Global Synthesis. *The American Naturalist*, 140(2), 201–242. <https://doi.org/10.1086/285410>
- Hutchinson, G. E. (1957). A treatise on limnology. *Geography, physics and chemistry*, 1015.
- IPCC. (2021). *Climate Change 2021: The Physical Science Basis. Contribution of Working Group I to the Sixth Assessment Report* (V. Masson-Delmotte, P. Zhai, A. Pirani, S. L. Connors, C. Péan, S. Berger, N. Caud, Y. Chen, L. Goldfarb, M. I. Gomis, M. Huang, K. Leitzell, E. Lonnoy, J. B. R. Matthews, T. K. Maycock, T. Waterfield, O. Yelekçi, R. Yu, & B. Zhou, Eds.). Cambridge University Press. <https://doi.org/10.1017/9781009157896>
- Jacobsen, H., & Norrbin, M. (2009). Fine-scale layer of hydromedusae is revealed by video plankton recorder (VPR) in a semi-enclosed bay in northern Norway. *Marine Ecology Progress Series*, 380, 129–135. doi:10.3354/meps07954
- Jónasdóttir, S. (2019). Fatty Acid Profiles and Production in Marine Phytoplankton. *Marine Drugs*, 17(3), 151. <https://doi.org/10.3390/md17030151>
- Jónasdóttir, S. H., & Koski, M. (2011). Biological processes in the North Sea: comparison of *Calanus helgolandicus* and *Calanus finmarchicus* vertical distribution and production. *Journal of Plankton Research*, 33(1), 85–103. <https://doi.org/10.1093/plankt/fbq085>
- Jonasdottir, S. H., Visser, A. W., Richardson, K., & Heath, M. R. (2015). A seasonal copepod ‘lipid pump’ promotes carbon sequestration in the deep North Atlantic. <https://doi.org/10.1101/021279>
- Kainz, M., Arts, M. T., & Mazumder, A. (2004). Essential fatty acids in the planktonic food web and their ecological role for higher trophic levels. *Limnology and Oceanography*, 49(5), 1784–1793. Portico. <https://doi.org/10.4319/lo.2004.49.5.1784>
- Kanna, N., Sugiyama, S., Ohashi, Y., Sakakibara, D., Fukamachi, Y., & Nomura, D. (2018). Upwelling of Macronutrients and Dissolved Inorganic Carbon by a Subglacial Freshwater Driven Plume in Bowdoin Fjord, Northwestern Greenland. *Journal of Geophysical Research: Biogeosciences*, 123(5), 1666–1682. Portico. <https://doi.org/10.1029/2017jg004248>

- Katija, K., Choy, C. A., Sherlock, R. E., Sherman, A. D., & Robison, B. H. (2017). From the surface to the seafloor: How giant larvaceans transport microplastics into the deep sea. *Science Advances*, 3(8). <https://doi.org/10.1126/sciadv.1700715>
- Kattner, G., & Hagen, W. (2009). Lipids in marine copepods: latitudinal characteristics and perspective to global warming. *Lipids in Aquatic Ecosystems*, 257–280. [https://doi.org/10.1007/978-0-387-89366-2\\_11](https://doi.org/10.1007/978-0-387-89366-2_11)
- Kattner, G., Graeve, M., & Hagen, W. (1994). Ontogenetic and seasonal changes in lipid and fatty acid/alcohol compositions of the dominant Antarctic copepods *Calanus propinquus*, *Calanoides acutus* and *Rhincalanus gigas*. *Marine Biology*, 118(4), 637–644. <https://doi.org/10.1007/bf00347511>
- Kattsov, V. M., Källén, E., Cattle, H. P., Christensen, J., Drange, H., Hanssen-Bauer, I., ... & Vavulin, S. (2005). Future climate change: modeling and scenarios for the Arctic.
- Kelley, D., & Richards, C., (2022). oce: Analysis of Oceanographic Data. R package version 1.7-2. <https://CRAN.R-project.org/package=oce>
- Keskinen, E., Leu, E., Nygård, H., Røstad, A., & Thormar, J. (2004). New findings of diel vertical migration in high Arctic ecosystems. Svalbard, Norway: University Centre Publication Series (UNIS), Report AB320.
- Kideys, A., Roohi, A., Bagheri, S., Finenko, G., & Kamburska, L. (2005). Impacts of Invasive Ctenophores on the Fisheries of the Black Sea and Caspian Sea. *Oceanography*, 18(2), 76–85. <https://doi.org/10.5670/oceanog.2005.43>
- Kjørboe, T. (1993). Turbulence, Phytoplankton Cell Size, and the Structure of Pelagic Food Webs. *Advances in Marine Biology Volume 29*, 1–72. [https://doi.org/10.1016/s0065-2881\(08\)60129-7](https://doi.org/10.1016/s0065-2881(08)60129-7)
- Koski, M., Klein Breteler, W., & Schøgt, N. (1998). Effect of food quality on rate of growth and development of the pelagic copepod *Pseudocalanus elongatus* (Copepoda, Calanoida). *Marine Ecology Progress Series*, 170, 169–187. <https://doi.org/10.3354/meps170169>
- Koski, M., Møller, E. F., Maar, M., & Visser, A. W. (2007). The fate of discarded appendicularian houses: degradation by the copepod, *Microsetella norvegica*, and other agents. *Journal of Plankton Research*, 29(7), 641–654. <https://doi.org/10.1093/plankt/fbm046>
- Lacoste, A., Poulet, S. A., Cueff, A., Kattner, G., Ianora, A., & Laabir, M. (2001). New evidence of the copepod maternal food effects on reproduction. *Journal of Experimental Marine Biology and Ecology*, 259(1), 85–107. [https://doi.org/10.1016/s0022-0981\(01\)00224-6](https://doi.org/10.1016/s0022-0981(01)00224-6)
- Lawley, J. W., Gamero-Mora, E., Maronna, M. M., Chiaverano, L. M., Stampar, S. N., Hopcroft, R. R., Collins, A. G., & Morandini, A. C. (2021). The importance of molecular characters when morphological variability hinders diagnosability: systematics of the moon jellyfish genus *Aurelia* (Cnidaria: Scyphozoa). *PeerJ*, 9, e11954. <https://doi.org/10.7717/peerj.11954>
- Le Fèvre, J. (1987). Aspects of the Biology of Frontal Systems. *Advances in Marine Biology Volume 23*, 163–299. [https://doi.org/10.1016/s0065-2881\(08\)60109-1](https://doi.org/10.1016/s0065-2881(08)60109-1)
- Lee, C., Melling, H., Eicken, H., Schlosser, P., Gascard, J. C., Proshutinsky, A., ... & Polykov, I. (2010). Autonomous platforms in the arctic observing network. *Proceedings of Ocean Obs09*:

## CITED LITERATURE

- Sustained Ocean Observations and Information for Society, 2, 306.  
<https://doi.org/10.5270/oceanobs09.cwp.54>
- Lee, R. F. (1975). Lipids of Arctic zooplankton. *Comparative Biochemistry and Physiology Part B: Comparative Biochemistry*, 51(3), 263–266. [https://doi.org/10.1016/0305-0491\(75\)90003-6](https://doi.org/10.1016/0305-0491(75)90003-6)
- Lee, R., Hagen, W., & Kattner, G. (2006). Lipid storage in marine zooplankton. *Marine Ecology Progress Series*, 307, 273–306. <https://doi.org/10.3354/meps307273>
- Legrand S., Allen-Perkins S., Ayensa G., Lepers L., Montero P. & Orsi S., 2023. D5.3 - MANIFESTS DSS - User guides Royal Belgian Institute of Natural Sciences, MANIFESTS project report(D5.3).
- Leinaas, H. P., Jalal, M., Gabrielsen, T. M., & Hessen, D. O. (2016). Inter- and intraspecific variation in body- and genome size in calanoid copepods from temperate and arctic waters. *Ecology and Evolution*, 6(16), 5585–5595. Portico. <https://doi.org/10.1002/ece3.2302>
- Letcher, B. H., & Rice, J. A. (1997). Prey patchiness and larval fish growth and survival: inferences from an individual-based model. *Ecological Modelling*, 95(1), 29–43. [https://doi.org/10.1016/s0304-3800\(96\)00015-4](https://doi.org/10.1016/s0304-3800(96)00015-4)
- Levine, D. M., & Sulkin, S. D. (1984). Nutritional significance of long-chain polyunsaturated fatty acids to the zoeal development of the brachyuran crab, *Eurypanopeus depressus* (Smith). *Journal of Experimental Marine Biology and Ecology*, 81(3), 211–223. [https://doi.org/10.1016/0022-0981\(84\)90141-2](https://doi.org/10.1016/0022-0981(84)90141-2)
- Levinsen, H., Turner, J., Nielsen, T., & Hansen, B. (2000). On the trophic coupling between protists and copepods in arctic marine ecosystems. *Marine Ecology Progress Series*, 204, 65–77. <https://doi.org/10.3354/meps204065>
- Liboschik, T., Fokianos, K., & Fried, R. (2017). tscount: An R package for analysis of count time series following generalized linear models. *Journal of Statistical Software*, 82, 1-51.
- Lindenmayer, D. B., Likens, G. E., Andersen, A., Bowman, D., Bull, C. M., Burns, E., ... & Wardle, G. M. (2012). Value of long-term ecological studies. *Austral Ecology*, 37(7), 745–757. <https://doi.org/10.1111/j.1442-9993.2011.02351.x>
- Lombard, F., Boss, E., Waite, A. M., Vogt, M., Uitz, J., Stemmann, L., Sosik, H. M., Schulz, J., Romagnan, J.-B., Picheral, M., Pearlman, J., Ohman, M. D., Niehoff, B., Möller, K. O., Miloslavich, P., Lara-Lpez, A., Kudela, R., Lopes, R. M., Kiko, R., ... Appeltans, W. (2019). Globally Consistent Quantitative Observations of Planktonic Ecosystems. *Frontiers in Marine Science*, 6. <https://doi.org/10.3389/fmars.2019.00196>
- Loose, C. J., & Dawidowicz, P. (1994). Trade-Offs in Diel Vertical Migration by Zooplankton: The Costs of Predator Avoidance. *Ecology*, 75(8), 2255. <https://doi.org/10.2307/1940881>
- Lucas, C. H., Jones, D. O. B., Hollyhead, C. J., Condon, R. H., Duarte, C. M., Graham, W. M., Robinson, K. L., Pitt, K. A., Schildhauer, M., & Regetz, J. (2014). Gelatinous zooplankton biomass in the global oceans: geographic variation and environmental drivers. *Global Ecology and Biogeography*, 23(7), 701–714. Portico. <https://doi.org/10.1111/geb.12169>
- Luo, J. Y., Irisson, J., Graham, B., Guigand, C., Sarafraz, A., Mader, C., & Cowen, R. K. (2018). Automated plankton image analysis using convolutional neural networks. *Limnology and*



- Oceanography: Methods, 16(12), 814–827. Portico.  
<https://doi.org/10.1002/lom3.10285>
- Luo, J., Ortner, P. B., Forcucci, D., & Cummings, S. R. (2000). Diel vertical migration of zooplankton and mesopelagic fish in the Arabian Sea. *Deep Sea Research Part II: Topical Studies in Oceanography*, 47(7–8), 1451–1473. [https://doi.org/10.1016/s0967-0645\(99\)00150-2](https://doi.org/10.1016/s0967-0645(99)00150-2)
- Lynam, C., Heath, M., Hay, S., & Brierley, A. (2005). Evidence for impacts by jellyfish on North Sea herring recruitment. *Marine Ecology Progress Series*, 298, 157–167. <https://doi.org/10.3354/meps298157>
- Machado, K. B., Borges, P. P., Carneiro, F. M., de Santana, J. F., Vieira, L. C. G., de Moraes Huszar, V. L., & Nabout, J. C. (2014). Using lower taxonomic resolution and ecological approaches as a surrogate for plankton species. *Hydrobiologia*, 743(1), 255–267. <https://doi.org/10.1007/s10750-014-2042-y>
- Mackas, D. L., Goldblatt, R., & Lewis, A. G. (1998). Interdecadal variation in developmental timing of *Neocalanus plumchrus* populations at Ocean Station P in the subarctic North Pacific. *Canadian Journal of Fisheries and Aquatic Sciences*, 55(8), 1878–1893. <https://doi.org/10.1139/f98-080>
- Mackas, D. L., Greve, W., Edwards, M., Chiba, S., Tadokoro, K., Eloire, D., Mazzocchi, M. G., Batten, S., Richardson, A. J., Johnson, C., Head, E., Conversi, A., & Peluso, T. (2012). Changing zooplankton seasonality in a changing ocean: Comparing time series of zooplankton phenology. *Progress in Oceanography*, 97–100, 31–62. <https://doi.org/10.1016/j.pocean.2011.11.005>
- Madsen, S. D., Nielsen, T. G., & Hansen, B. W. (2001). Annual population development and production by *Calanus finmarchicus*, *C. glacialis* and *C. hyperboreus* in Disko Bay, western Greenland. *Mar Biol*, 139(1), 75–83. <https://doi.org/10.1007/s002270100552>
- McQuatters-Gollop, A., Johns, D. G., Bresnan, E., Skinner, J., Rombouts, I., Stern, R., Aubert, A., Johansen, M., Bedford, J., & Knights, A. (2017). From microscope to management: The critical value of plankton taxonomy to marine policy and biodiversity conservation. *Marine Policy*, 83, 1–10. <https://doi.org/10.1016/j.marpol.2017.05.022>
- Meire, L., Mortensen, J., Meire, P., Juul-Pedersen, T., Sejr, M. K., Rysgaard, S., Nygaard, R., Huybrechts, P., & Meysman, F. J. R. (2017). Marine-terminating glaciers sustain high productivity in Greenland fjords. *Global Change Biology*, 23(12), 5344–5357. Portico. <https://doi.org/10.1111/gcb.13801>
- MicrobiologyUSP. (n.d.). Dark-field Microscopy. Microbiology USP Wiki. [https://microbiologyusp.fandom.com/wiki/Dark-field\\_Microscopy](https://microbiologyusp.fandom.com/wiki/Dark-field_Microscopy)
- Miller, C. B., Crain, J. A., & Morgan, C. A. (2000). Oil storage variability in *Calanus finmarchicus*. *ICES Journal of Marine Science*, 57(6), 1786–1799. <https://doi.org/10.1006/jmsc.2000.0975>
- Mills, C. E. (2001). Jellyfish blooms: are populations increasing globally in response to changing ocean conditions? *Jellyfish Blooms: Ecological and Societal Importance*, 55–68. [https://doi.org/10.1007/978-94-010-0722-1\\_6](https://doi.org/10.1007/978-94-010-0722-1_6)

## CITED LITERATURE

- Miner, J. G., & Stein, R. A. (1993). Interactive Influence of Turbidity and Light on Larval Bluegill (*Lepomis macrochirus*) Foraging. *Canadian Journal of Fisheries and Aquatic Sciences*, 50(4), 781–788. <https://doi.org/10.1139/f93-090>
- Møller, E. F., & Nielsen, T. G. (2019). Borealization of Arctic zooplankton—smaller and less fat zooplankton species in Disko Bay, Western Greenland. *Limnology and Oceanography*, 65(6), 1175–1188. Portico. <https://doi.org/10.1002/lno.11380>
- Möller, K., St John, M., Temming, A., Floeter, J., Sell, A., Herrmann, J., & Möllmann, C. (2012). Marine snow, zooplankton and thin layers: indications of a trophic link from small-scale sampling with the Video Plankton Recorder. *Marine Ecology Progress Series*, 468, 57–69. doi:10.3354/meps09984
- Montagnes, D. J. S., Berges, J. A., Harrison, P. J., & Taylor, F. J. R. (1994). Estimating carbon, nitrogen, protein, and chlorophyll a from volume in marine phytoplankton. *Limnology and Oceanography*, 39(5), 1044–1060. Portico. <https://doi.org/10.4319/lo.1994.39.5.1044>
- Mortelmans, J., Aubert, A., Reubens, J., Otero, V., Deneudt, K., & Mees, J. (2021). Copepods (Crustacea: Copepoda) in the Belgian part of the North Sea: Trends, dynamics and anomalies. *Journal of Marine Systems*, 220, 103558. <https://doi.org/10.1016/j.jmarsys.2021.103558>
- Mortelmans, J., Deneudt, K., Cattrijsse, A., Beauchard, O., Daveloose, I., Vyverman, W., ... Mees, J. (2019). Nutrient, pigment, suspended matter and turbidity measurements in the Belgian part of the North Sea. *Scientific Data*, 6(1). doi:10.1038/s41597-019-0032-7
- Mortelmans, J., Goossens, J., Amadei Martínez, L., Deneudt, K., Cattrijsse, A., & Hernandez, F. (2019). LifeWatch observatory data: Zooplankton observations in the Belgian part of the North Sea. *Geoscience Data Journal*, 6(2), 76–84. Portico. <https://doi.org/10.1002/gdj3.68>
- Motoda, S. (1959). Devices of simple plankton apparatus. *Memoirs of the faculty of fisheries Hokkaido University*, 7(1-2), 73-94.
- Murison, L. D., & Gaskin, D. E. (1989). The distribution of right whales and Zooplankton in the Bay of Fundy, Canada. *Canadian Journal of Zoology*, 67(6), 1411–1420. <https://doi.org/10.1139/z89-200>
- Nicol, S., & Foster, J. (2003). Recent trends in the fishery for Antarctic krill. *Aquatic Living Resources*, 16(1), 42–45. [https://doi.org/10.1016/s0990-7440\(03\)00004-4](https://doi.org/10.1016/s0990-7440(03)00004-4)
- Nielsen, T., Løkkegaard, B., Richardson, K., Bo Pedersen, R., & Hansen, L. (1993). Structure of plankton communities in the Dogger Bank area (North Sea) during a stratified situation. *Marine Ecology Progress Series*, 95, 115–131. doi:10.3354/meps095115
- Nihoul, J. C. J., Ronday, F. C., Peters, J. J., & Sterling, A. (1978). Hydrodynamics of the Scheldt Estuary. *Elsevier Oceanography Series*, 27–53. doi:10.1016/s0422-9894(08)71270-4
- Nishikawa, J., & Terazaki, M. (1996). Tissue shrinkage of two gelatinous zooplankton, *Thalia democratica* and *Dolioletta gegenbauri* (Tunicata: Thaliacea) in preservative. *Bulletin of Plankton Society of Japan*, 43(1), 1-7.
- Ogle, D. H., Doll, J. C., Wheeler, A. P., & Dinno, A. (2023). FSA: Simple Fisheries Stock Assessment Methods. R package version 0.9.4. <https://CRAN.R-project.org/package=FSA>

- Ohman, M. D., & Lavaniegos, B. E. (2002). Comparative zooplankton sampling efficiency of a ring net and bongo net with comments on pooling of subsamples.
- Ohman, M. D., & Runge, J. A. (1994). Sustained fecundity when phytoplankton resources are in short supply: Omnivory by *Calanus finmarchicus* in the Gulf of St. Lawrence. *Limnology and Oceanography*, 39(1), 21–36. Portico. <https://doi.org/10.4319/lo.1994.39.1.0021>
- Oksanen, J., Simpson, G. L., Blanchet, F. G., Kindt, R., Legendre, P., Minchin, P. R., ... & Weedon, J. (2022). *vegan: Community Ecology Package*. R package version 2.6-2. <https://CRAN.R-project.org/package=vegan>
- Ollevier, A., Mortelmans, J., Aubert, A., Deneudt, K., & Vandegheuchte, M. B. (2021). Noctiluca scintillans: Dynamics, Size Measurements and Relationships With Small Soft-Bodied Plankton in the Belgian Part of the North Sea. *Frontiers in Marine Science*, 8. <https://doi.org/10.3389/fmars.2021.777999>
- Ollevier, A., Mortelmans, J., Deneudt, K., Hablützel, P. & De Troch, M. (Submitted.). Diel Vertical Migration and Tidal Influences on Plankton Densities in Dynamic Coastal Systems. Submitted to *Estuarine, Coastal and Shelf Science*.
- Ollevier, A., Mortelmans, J., Vandegheuchte, M. B., Develter, R., De Troch, M., & Deneudt, K. (2022). A Video Plankton Recorder user guide: Lessons learned from in situ plankton imaging in shallow and turbid coastal waters in the Belgian part of the North Sea. *Journal of Sea Research*, 188, 102257. <https://doi.org/10.1016/j.seares.2022.102257>
- Omand, M. M., Govindarajan, R., He, J., & Mahadevan, A. (2020). Sinking flux of particulate organic matter in the oceans: Sensitivity to particle characteristics. *Scientific Reports*, 10(1). <https://doi.org/10.1038/s41598-020-60424-5>
- Omori, M. (1978). Zooplankton fisheries of the world: a review. *Marine Biology*, 48(3), 199–205. <https://doi.org/10.1007/BF00397145>.
- Omori, M., Ikeda, T. (1992). *Methods in Marine Zooplankton Ecology*. Malabar, USA: Krieger Publishing Company. ISBN 0-89464-653-2.
- Omori, M., & Nakano, E. (2001). Jellyfish fisheries in southeast Asia. *Jellyfish Blooms: Ecological and Societal Importance*, 19–26. [https://doi.org/10.1007/978-94-010-0722-1\\_3](https://doi.org/10.1007/978-94-010-0722-1_3)
- Orenstein, E. C., Ayata, S., Maps, F., Becker, É. C., Benedetti, F., Biard, T., de Garidel-Thoron, T., Ellen, J. S., Ferrario, F., Giering, S. L. C., Guy-Haim, T., Hoebeke, L., Iversen, M. H., Kiørboe, T., Lalonde, J., Lana, A., Laviale, M., Lombard, F., Lorimer, T., ... Irisson, J. (2022). Machine learning techniques to characterize functional traits of plankton from image data. *Limnology and Oceanography*, 67(8), 1647–1669. Portico. <https://doi.org/10.1002/lno.12101>
- Otto, L., Zimmerman, J. T. F., Furnes, G. K., Mork, M., Saetre, R., & Becker, G. (1990). Review of the physical oceanography of the North Sea. *Netherlands Journal of Sea Research*, 26(2–4), 161–238. [https://doi.org/10.1016/0077-7579\(90\)90091-t](https://doi.org/10.1016/0077-7579(90)90091-t)
- Pan, J., Cheng, F., & Yu, F. (2018). The diel vertical migration of zooplankton in the hypoxia area observed by video plankton recorder.

## CITED LITERATURE

- Pasquaud, S., Pillet, M., David, V., Sautour, B., & Elie, P. (2010). Determination of fish trophic levels in an estuarine system. *Estuarine, Coastal and Shelf Science*, 86(2), 237–246. <https://doi.org/10.1016/j.ecss.2009.11.019>
- Pasternak, A., Arashkevich, E., Tande, K., & Falkenhaus, T. (2001). Seasonal changes in feeding, gonad development and lipid stores in *Calanus finmarchicus* and *C. hyperboreus* from Malangen, northern Norway. *Marine Biology*, 138(6), 1141–1152. <https://doi.org/10.1007/s002270100553>
- Pauly, D., Christensen, V., Dalsgaard, J., Froese, R., & Torres, F. (1998). Fishing Down Marine Food Webs. *Science*, 279(5352), 860–863. <https://doi.org/10.1126/science.279.5352.860>
- Pearre, S. (2003). Eat and run? The hunger/satiation hypothesis in vertical migration: history, evidence and consequences. *Biological Reviews of the Cambridge Philosophical Society*, 78(1), 1–79. <https://doi.org/10.1017/s146479310200595x>
- Persson, J., & Vrede, T. (2006). Polyunsaturated fatty acids in zooplankton: variation due to taxonomy and trophic position. *Freshwater Biology*, 51(5), 887–900. <https://doi.org/10.1111/j.1365-2427.2006.01540.x>
- Peura, S., Eiler, A., Hiltunen, M., Nykänen, H., Tiirola, M., & Jones, R. I. (2012). Bacterial and Phytoplankton Responses to Nutrient Amendments in a Boreal Lake Differ According to Season and to Taxonomic Resolution. *PLoS ONE*, 7(6), e38552. <https://doi.org/10.1371/journal.pone.0038552>
- Pinel-Alloul, P. (1995). Spatial heterogeneity as a multiscale characteristic of zooplankton community. *Hydrobiologia*, 300–301(1), 17–42. <https://doi.org/10.1007/bf00024445>
- Planken, K.J.T., Stuart-Lee, A., Meire, P., & Meire, L. (in prep.): Impact of subglacial discharge on the biogeochemistry and zooplankton of Uummannaq Fjord, west Greenland.
- Plourde, S., & Runge, J. (1993). Reproduction of the planktonic copepod *Calanus finmarchicus* in the Lower St. Lawrence Estuary: relation to the cycle of phytoplankton production and evidence for a *Calanus* pump. *Marine Ecology Progress Series*, 95, 217–227. <https://doi.org/10.3354/meps095217>
- Prado-Cabrero, A., & Nolan, J. M. (2021). Omega-3 nutraceuticals, climate change and threats to the environment: The cases of Antarctic krill and *Calanus finmarchicus*. *Ambio*, 50(6), 1184–1199. <https://doi.org/10.1007/s13280-020-01472-z>
- Praet, N., Collart, T., Ollevier, A., Roche, M., Degrendele, K., De Rijcke, M., Urban, P., & Vandorpe, T. (2023). The Potential of Multibeam Sonars as 3D Turbidity and SPM Monitoring Tool in the North Sea. *Remote Sensing*, 15(20), 4918. <https://doi.org/10.3390/rs15204918>
- Purcell, J. E. (2012). Jellyfish and Ctenophore Blooms Coincide with Human Proliferations and Environmental Perturbations. *Annual Review of Marine Science*, 4(1), 209–235. <https://doi.org/10.1146/annurev-marine-120709-142751>
- R Core Team (2020). R: A language and environment for statistical computing. R Foundation for Statistical Computing, Vienna, Austria. URL <https://www.R-project.org/>.
- Rainuzzo, J. R., Reitan, K. I., & Olsen, Y. (1997). The significance of lipids at early stages of marine fish: a review. *Aquaculture*, 155(1–4), 103–115. [https://doi.org/10.1016/s0044-8486\(97\)00121-x](https://doi.org/10.1016/s0044-8486(97)00121-x)

- Raskoff, K. A., Sommer, F. A., Hamner, W. M., & Cross, K. M. (2003). Collection and Culture Techniques for Gelatinous Zooplankton. *The Biological Bulletin*, 204(1), 68–80. <https://doi.org/10.2307/1543497>
- Ratnarajah, L., Abu-Alhaija, R., Atkinson, A., Batten, S., Bax, N. J., Bernard, K. S., Canonico, G., Cornils, A., Everett, J. D., Grigoratou, M., Ishak, N. H. A., Johns, D., Lombard, F., Muxagata, E., Ostle, C., Pitois, S., Richardson, A. J., Schmidt, K., Stemmann, L., ... Yebra, L. (2023). Monitoring and modelling marine zooplankton in a changing climate. *Nature Communications*, 14(1). <https://doi.org/10.1038/s41467-023-36241-5>
- Reichwaldt, E.S., Stibor, H. The impact of diel vertical migration of *Daphnia* on phytoplankton dynamics. *Oecologia* 146, 50–56 (2005). <https://doi.org/10.1007/s00442-005-0176-3>
- Reid, P. C., Fischer, A. C., Lewis-Brown, E., Meredith, M. P., Sparrow, M., Andersson, A. J., Antia, A., Bates, N. R., Bathmann, U., Beaugrand, G., Brix, H., Dye, S., Edwards, M., Furevik, T., Gangstø, R., Hátún, H., Hopcroft, R. R., Kendall, M., Kasten, S., ... Washington, R. (2009). Chapter 1 Impacts of the Oceans on Climate Change. *Advances in Marine Biology*, 1–150. [https://doi.org/10.1016/s0065-2881\(09\)56001-4](https://doi.org/10.1016/s0065-2881(09)56001-4)
- Remsen, A., Hopkins, T. L., & Samson, S. (2004). What you see is not what you catch: a comparison of concurrently collected net, Optical Plankton Counter, and Shadowed Image Particle Profiling Evaluation Recorder data from the northeast Gulf of Mexico. *Deep Sea Research Part I: Oceanographic Research Papers*, 51(1), 129–151. <https://doi.org/10.1016/j.dsr.2003.09.008>
- Reuss, N., & Poulsen, L. (2002). Evaluation of fatty acids as biomarkers for a natural plankton community. A field study of a spring bloom and a post-bloom period off West Greenland. *Marine Biology*, 141, 423–434. <https://doi.org/10.1007/s00227-002-0841-6>
- Richardson, A. J. (2008). In hot water: zooplankton and climate change. *ICES Journal of Marine Science*, 65(3), 279–295. <https://doi.org/10.1093/icesjms/fsn028>
- Richardson, A. J., Bakun, A., Hays, G. C., & Gibbons, M. J. (2009). The jellyfish joyride: causes, consequences and management responses to a more gelatinous future. *Trends in Ecology & Evolution*, 24(6), 312–322. <https://doi.org/10.1016/j.tree.2009.01.010>
- Rignot, E., Fenty, I., Xu, Y., Cai, C., & Kemp, C. (2015). Undercutting of marine-terminating glaciers in West Greenland. *Geophysical Research Letters*, 42(14), 5909–5917. Portico. <https://doi.org/10.1002/2015gl064236>
- Rignot, E., Fenty, I., Xu, Y., Cai, C., Velicogna, I., Cofaigh, C. Ó., Dowdeswell, J. A., Weinrebe, W., Catania, G., & Duncan, D. (2016). Bathymetry data reveal glaciers vulnerable to ice-ocean interaction in Uummannaq and Vaigat glacial fjords, west Greenland. *Geophysical Research Letters*, 43(6), 2667–2674. Portico. <https://doi.org/10.1002/2016gl067832>
- Ringelberg, J. (2010). Diel Vertical Migration of Zooplankton in Lakes and Oceans. <https://doi.org/10.1007/978-90-481-3093-1>
- Robinson, K. L., Sponaugle, S., Luo, J. Y., Gleiber, M. R., & Cowen, R. K. (2021). Big or small, patchy all: Resolution of marine plankton patch structure at micro- to submesoscales for 36 taxa. *Science Advances*, 7(47). <https://doi.org/10.1126/sciadv.abk2904>

## CITED LITERATURE

- Robinson, K., Ruzicka, J., Decker, M. B., Brodeur, R., Hernandez, F., Quiñones, J., Acha, M., Uye, S., Mianzan, H., & Graham, W. (2014). Jellyfish, Forage Fish, and the World's Major Fisheries. *Oceanography*, 27(4), 104–115. <https://doi.org/10.5670/oceanog.2014.90>
- Robison, B. H., Reisenbichler, K. R., & Sherlock, R. E. (2005). Giant Larvacean Houses: Rapid Carbon Transport to the Deep Sea Floor. *Science*, 308(5728), 1609–1611. <https://doi.org/10.1126/science.1109104>
- Rombouts, I., Beaugrand, G., Ibañez, F., Gasparini, S., Chiba, S., & Legendre, L. (2009). Global latitudinal variations in marine copepod diversity and environmental factors. *Proceedings of the Royal Society B: Biological Sciences*, 276(1670), 3053–3062. <https://doi.org/10.1098/rspb.2009.0742>
- Rothschild, B. J., & Osborn, T. R. (1988). Small-scale turbulence and plankton contact rates. *Journal of Plankton Research*, 10(3), 465–474. <https://doi.org/10.1093/plankt/10.3.465>
- Royal Belgian Institute of Natural Sciences. (n.d.). ERDDAP - Data Access Protocol. ERDDAP. <https://erddap.naturalsciences.be/erddap/index.html>
- RStudio Team (2020). RStudio: Integrated Development for R. RStudio, PBC, Boston, MA URL <http://www.rstudio.com/>.
- Sainmont, J., Gislason, A., Heuschele, J., Webster, C. N., Sylvander, P., Wang, M., & Varpe, Ø. (2014). Inter- and intra-specific diurnal habitat selection of zooplankton during the spring bloom observed by Video Plankton Recorder. *Marine Biology*, 161(8), 1931–1941. doi:10.1007/s00227-014-2475-x
- Sato, R., Tanaka, Y., & Ishimaru, T. (2001). House Production by *Oikopleura dioica* (Tunicata, Appendicularia) Under Laboratory Conditions. *Journal of Plankton Research*, 23(4), 415–423. <https://doi.org/10.1093/plankt/23.4.415>
- Schmid, M. S., Maps, F., & Fortier, L. (2018). Lipid load triggers migration to diapause in Arctic *Calanus* copepods—insights from underwater imaging. *Journal of Plankton Research*, 40(3), 311–325. <https://doi.org/10.1093/plankt/fby012>
- Schneider, C. A., Rasband, W. S., & Eliceiri, K. W. (2012). NIH Image to ImageJ: 25 years of image analysis. *Nature Methods*, 9(7), 671–675. <https://doi.org/10.1038/nmeth.2089>
- Schneider, G. and Behrends, G. (1994). Population dynamics and the trophic role of *Aurelia aurita* medusae in the Kiel Bight and western Baltic. *ICES Journal of Marine Science*, 51(4), 359–367. <https://doi.org/10.1006/jmsc.1994.1038>
- Scott, C., Kwasniewski, S., Falk-Petersen, S., & Sargent, J. (2002). Species differences, origins and functions of fatty alcohols and fatty acids in the wax esters and phospholipids of *Calanus hyperboreus*, *C. glacialis* and *C. finmarchicus* from Arctic waters. *Marine Ecology Progress Series*, 235, 127–134. <https://doi.org/10.3354/meps235127>
- Seascan, Inc. (2014). Real Time Video Plankton Recorder Owner's Manual. Falmouth, WA: Author.
- Semmouri, I., De Schampelaere, K. A. C., Mortelmans, J., Mees, J., Asselman, J., & Janssen, C. R. (2023). Decadal decline of dominant copepod species in the North Sea is associated with ocean warming: Importance of marine heatwaves. *Marine Pollution Bulletin*, 193, 115159. <https://doi.org/10.1016/j.marpolbul.2023.115159>

- Sidabutar, T., Srimariana, E. S., & Wouthuyzen, S. (2020). The potential role of eutrophication, tidal and climatic on the rise of algal bloom phenomenon in Jakarta Bay. *IOP Conference Series: Earth and Environmental Science*, 429(1), 012021. <https://doi.org/10.1088/1755-1315/429/1/012021>
- Siegel, D. A., DeVries, T., Cetinić, I., & Bisson, K. M. (2023). Quantifying the Ocean's Biological Pump and Its Carbon Cycle Impacts on Global Scales. *Annual Review of Marine Science*, 15(1), 329–356. <https://doi.org/10.1146/annurev-marine-040722-115226>
- Skjoldal, H. R., Prokopchuk, I., Bagøien, E., Dalpadado, P., Nesterova, V., Rønning, J., & Knutsen, T. (2019). Comparison of Juday and WP2 nets used in joint Norwegian–Russian monitoring of zooplankton in the Barents Sea. *Journal of Plankton Research*, 41(5), 759–769. <https://doi.org/10.1093/plankt/fbz054>
- Skjoldal, H. R., Wiebe, P. H., Postel, L., Knutsen, T., Kaartvedt, S., & Sameoto, D. D. (2013). Intercomparison of zooplankton (net) sampling systems: Results from the ICES/GLOBEC sea-going workshop. *Progress in Oceanography*, 108, 1–42. <https://doi.org/10.1016/j.pocean.2012.10.006>
- Sosa-Trejo, D., Bandera, A., González, M., & Hernández-León, S. (2023). Vision-based techniques for automatic marine plankton classification. *Artificial Intelligence Review*, 56(11), 12853–12884. <https://doi.org/10.1007/s10462-023-10456-w>
- Stadnyk, T. A., Tefs, A., Broesky, M., Déry, S. J., Myers, P. G., Ridenour, N. A., Koenig, K., Vonderbank, L., & Gustafsson, D. (2021). Changing freshwater contributions to the Arctic. *Elementa: Science of the Anthropocene*, 9(1). <https://doi.org/10.1525/elementa.2020.00098>
- Steinberg, D. K., & Landry, M. R. (2017). Zooplankton and the ocean carbon cycle. *Annual review of marine science*, 9, 413-444. <https://doi.org/10.1146/annurev-marine-010814-015924>
- Strand, E., Klevjer, T., Knutsen, T., & Melle, W. (2020). Ecology of mesozooplankton across four North Atlantic basins. *Deep Sea Research Part II: Topical Studies in Oceanography*, 180, 104844. <https://doi.org/10.1016/j.dsr2.2020.104844>
- Stuart-Lee, A. E., Møller, E. F., Winding, M., van Oevelen, D., Hendry, K., & Meire, L. (in prep.) Glacier type drives copepod community composition but not biomass in two Greenland fjords.
- Studio 3T Team (2022). Studio 3T: The Professional Client, IDE & GUI for MongoDB, <https://studio3t.com>.
- Stukel, M. R., Mislán, K. A. S., Décima, M., & Hmelo, L. (2014). Detritus in the pelagic ocean. In *Eco-DAS IX Symposium Proceedings* (pp. 49-76). Waco, TX: Association for the Sciences of Limnology and Oceanography.
- Sun, C., Shrivastava, A., Singh, S., & Gupta, A. (2017). Revisiting Unreasonable Effectiveness of Data in Deep Learning Era. 2017 IEEE International Conference on Computer Vision (ICCV). <https://doi.org/10.1109/iccv.2017.97>
- Sundby, S. (2000). Recruitment of Atlantic cod stocks in relation to temperature and advection of copepod populations. *Sarsia*, 85(4), 277–298. <https://doi.org/10.1080/00364827.2000.10414580>

## CITED LITERATURE

- Svensen, C. (2000). Remote prey detection in *Oithona similis*: hydromechanical versus chemical cues. *Journal of Plankton Research*, 22(6), 1155–1166. <https://doi.org/10.1093/plankt/22.6.1155>
- Swalethorp, R., Kjellerup, S., Dünweber, M., Nielsen, T., Møller, E., Rysgaard, S., & Hansen, B. (2011). Grazing, egg production, and biochemical evidence of differences in the life strategies of *Calanus finmarchicus*, *C. glacialis* and *C. hyperboreus* in Disko Bay, western Greenland. *Marine Ecology Progress Series*, 429, 125–144. <https://doi.org/10.3354/meps09065>
- Takahashi, K., Ichikawa, T., Fukugama, C., Yamane, M., Kakehi, S., Okazaki, Y., ... Furuya, K. (2015). In situ observations of a doliolid bloom in a warm water filament using a video plankton recorder: Bloom development, fate, and effect on biogeochemical cycles and planktonic food webs. *Limnology and Oceanography*, 60(5), 1763–1780. doi:10.1002/lno.10133
- Tang, K. W., Jakobsen, H. H., & Visser, A. W. (2001). *Phaeocystis globosa* (Prymnesiophyceae) and the planktonic food web: Feeding, growth, and trophic interactions among grazers. *Limnology and Oceanography*, 46(8), 1860–1870. Portico. <https://doi.org/10.4319/lo.2001.46.8.1860>
- Taylor, A., Allen, J., & Clark, P. (2002). Extraction of a weak climatic signal by an ecosystem. *Nature*, 416(6881), 629–632. doi: 10.1038/416629a
- Thibault-Botha, D., & Bowen, T. (2004). Impact of formalin preservation on *Pleurobrachia bachei* (Ctenophora). *Journal of Experimental Marine Biology and Ecology*, 303(1), 11–17. <https://doi.org/10.1016/j.jembe.2003.10.017>
- Tiselius, P. (1998). An in situ video camera for plankton studies: design and preliminary observations. *Marine Ecology Progress Series*, 164, 293–299. <https://doi.org/10.3354/meps164293>
- Torsvik, T., Albretsen, J., Sundfjord, A., Kohler, J., Sandvik, A. D., Skarðhamar, J., Lindbäck, K., & Everett, A. (2019). Impact of tidewater glacier retreat on the fjord system: Modeling present and future circulation in Kongsfjorden, Svalbard. *Estuarine, Coastal and Shelf Science*, 220, 152–165. <https://doi.org/10.1016/j.ecss.2019.02.005>
- Trudnowska, E., Lacour, L., Ardyna, M., Rogge, A., Irisson, J. O., Waite, A. M., Babin, M., & Stemmann, L. (2021). Marine snow morphology illuminates the evolution of phytoplankton blooms and determines their subsequent vertical export. *Nature Communications*, 12(1). <https://doi.org/10.1038/s41467-021-22994-4>
- Turner, J., Levinsen, H., Nielsen, T., & Hansen, B. (2001). Zooplankton feeding ecology: grazing on phytoplankton and predation on protozoans by copepod and barnacle nauplii in Disko Bay, West Greenland. *Marine Ecology Progress Series*, 221, 209–219. <https://doi.org/10.3354/meps221209>
- Ullberg, J., & Ólafsson, E. (2003). Free-living marine nematodes actively choose habitat when descending from the water column. *Marine Ecology Progress Series*, 260, 141–149. <https://doi.org/10.3354/meps260141>
- Utne-Palm, A. C., Salvanes, A. G. V., Currie, B., Kaartvedt, S., Nilsson, G. E., Braithwaite, V. A., Stecyk, J. A. W., Hundt, M., van der Bank, M., Flynn, B., Sandvik, G. K., Klevjer, T. A., Sweetman, A. K., Brüchert, V., Pittman, K., Peard, K. R., Lunde, I. G., Strandabø, R. A. U., & Gibbons, M. J.



- (2010). Trophic Structure and Community Stability in an Overfished Ecosystem. *Science*, 329(5989), 333–336. <https://doi.org/10.1126/science.1190708>
- Valdés, L., López-Urrutia, A., Cabal, J., Alvarez-Ossorio, M., Bode, A., Miranda, A., Cabanas, M., Huskin, I., Anadón, R., Alvarez-Marqués, F., Llope, M., & Rodríguez, N. (2007). A decade of sampling in the Bay of Biscay: What are the zooplankton time series telling us? *Progress in Oceanography*, 74(2–3), 98–114. <https://doi.org/10.1016/j.pocean.2007.04.016>
- van Genuchten, C. M., Hopwood, M. J., Liu, T., Krause, J., Achterberg, E. P., Rosing, M. T., & Meire, L. (2022). Solid-phase Mn speciation in suspended particles along meltwater-influenced fjords of West Greenland. *Geochimica et Cosmochimica Acta*, 326, 180–198. <https://doi.org/10.1016/j.gca.2022.04.003>
- Van Ginderdeuren, K. (2013). Zooplankton and its role in North Sea food webs: community structure and selective feeding by Pelagic fish in Belgian marine waters (Doctoral dissertation, Ghent University).
- Van Ginderdeuren, K., Van Hoey, G., Vincx, M., & Hostens, K. (2014). The mesozooplankton community of the Belgian shelf (North Sea). *Journal of Sea Research*, 85, 48–58. <https://doi.org/10.1016/j.seares.2013.10.003>
- Van Lancker, V., Moerkerke, G., Du Four, I., Verfaillie, E., Rabaut, M., & Degraer, S. (2012). Fine-Scale Geomorphological Mapping of Sandbank Environments for the Prediction of Macrobenthic Occurrences, Belgian Part of the North Sea. *Seafloor Geomorphology as Benthic Habitat*, 251–260. <https://doi.org/10.1016/b978-0-12-385140-6.00014-1>
- van Leeuwen, S., Tett, P., Mills, D., & van der Molen, J. (2015). Stratified and nonstratified areas in the North Sea: Long-term variability and biological and policy implications. *Journal of Geophysical Research: Oceans*, 120(7), 4670–4686. <https://doi.org/10.1002/2014jc010485>
- Van Walraven, L., Langenberg, V. T., Dapper, R., Witte, J. IJ., Zuur, A. F., & van der Veer, H. W. (2014). Long-term patterns in 50 years of scyphomedusae catches in the western Dutch Wadden Sea in relation to climate change and eutrophication. *Journal of Plankton Research*, 37(1), 151–167. <https://doi.org/10.1093/plankt/fbu088>
- Vanaverbeke, J., Gheschiere, T., & Vincx, M. (2000). The Meiobenthos of Subtidal Sandbanks on the Belgian Continental Shelf (Southern Bight of the North Sea). *Estuarine, Coastal and Shelf Science*, 51(5), 637–649. [doi:10.1006/ecss.2000.0703](https://doi.org/10.1006/ecss.2000.0703)
- Velicogna, I., & Wahr, J. (2006). Acceleration of Greenland ice mass loss in spring 2004. *Nature*, 443(7109), 329–331. <https://doi.org/10.1038/nature05168>
- Verfaillie, E., 2008. PhD Thesis. Ontwikkeling en validering van een ruimtelijke verspreidingsmodellen van mariene habitats, ter ondersteuning van het ecologisch waarden van de zeebodem = Development and validation of spatial distribution models of marine habitats, in support of the ecological valuation of the seabed. Instituut voor de Aanmoediging van Innovatie door Wetenschap en Technologie in Vlaanderen/RCMG/Universiteit Gent: Brussel, p. 207 pp.
- Vernet, M. (2000). Effects of UV radiation on the physiology and ecology of marine phytoplankton. *The Effects of UV Radiation in the Marine Environment*, 237–278. <https://doi.org/10.1017/cbo9780511535444.010>

## CITED LITERATURE

- Vilgrain, L., Maps, F., Basedow, S., Trudnowska, E., Madoui, M., Niehoff, B., & Ayata, S. (2023). Copepods' true colors: astaxanthin pigmentation as an indicator of fitness. *Ecosphere*, 14(6). Portico. <https://doi.org/10.1002/ecs2.4489>
- Vinyard, G. L., & O'Brien, W. J. (1976). Effects of Light and Turbidity on the Reactive Distance of Bluegill (*Lepomis macrochirus*). *Journal of the Fisheries Research Board of Canada*, 33(12), 2845–2849. <https://doi.org/10.1139/f76-342>
- Visser, A. W., & Jónasdóttir, S. H. (1999). Lipids, buoyancy and the seasonal vertical migration of *Calanus finmarchicus*. *Fisheries Oceanography*, 8(s1), 100–106. Portico. <https://doi.org/10.1046/j.1365-2419.1999.00001.x>
- Wang, Z., & Dauvin, J. C. (1994). The suprabenthic crustacean fauna of the infralittoral fine sand community from the Bay of Seine (Eastern English Channel): composition, swimming activity and diurnal variation. *Cahiers de Biologie Marine*, 35(2), 135-156.
- Wickham, H. (2016). *ggplot2: Elegant Graphics for Data Analysis*. Springer-Verlag New York. ISBN 978-3-319-24277-4, <https://ggplot2.tidyverse.org>.
- Wiltshire, K. H., Kraberg, A., Bartsch, I., Boersma, M., Franke, H.-D., Freund, J., Gebühr, C., Gerdt, G., Stockmann, K., & Wichels, A. (2009). Helgoland Roads, North Sea: 45 Years of Change. *Estuaries and Coasts*, 33(2), 295–310. <https://doi.org/10.1007/s12237-009-9228-y>
- Wirtz, K., & Smith, S. L. (2020). Vertical migration by bulk phytoplankton sustains biodiversity and nutrient input to the surface ocean. *Scientific Reports*, 10(1). <https://doi.org/10.1038/s41598-020-57890-2>
- Wittmann, K. J., & Abed-Navandi, D. (2021). Four new species of *Heteromysis* (Crustacea: Mysida) from public aquaria in Hawaii, Florida, and Western to Central Europe. *European Journal of Taxonomy*, 735, 133–175. <https://doi.org/10.5852/ejt.2021.735.1247>
- Wolff, R. L., Bayard, C. C., & Fabien, R. J. (1995). Evaluation of sequential methods for the determination of butterfat fatty acid composition with emphasis on trans -18:1 acids. Application to the study of seasonal variations in french butters. *Journal of the American Oil Chemists' Society*, 72(12), 1471–1483. Portico. <https://doi.org/10.1007/bf02577840>
- Wood, S.N. (2011) Fast stable restricted maximum likelihood and marginal likelihood estimation of semiparametric generalized linear models. *Journal of the Royal Statistical Society (B)* 73(1):3-36
- Woods Hole Oceanographic Institution. (n.d.). CFIN\_GOM: Coastal Fisheries in the Gulf of Maine. [https://www2.whoi.edu/staff/rji/cfin\\_gom/](https://www2.whoi.edu/staff/rji/cfin_gom/)
- Zuur, A. F., Ieno, E. N., Walker, N., Saveliev, A. A., & Smith, G. M. (2009). Mixed effects models and extensions in ecology with R. In *Statistics for Biology and Health*. Springer New York. <https://doi.org/10.1007/978-0-387-87458-6>





# Supplementary material

## Supplementary material chapter 2

*Supplementary table 2.1. Vertical distribution of Noctiluca and Phaeocystis in the Z-pattern. The surface layer included specimens from 4 to 6m, the middle layer from 11 to 13m and the deep layer from 23 to 24m.*

<b>Taxon</b>	<b>Bin</b>	<b>Mean depth [m]</b>	<b>Count [ind]</b>	<b>Deployment time [s]</b>	<b>Density [ind m<sup>-3</sup>]</b>
<b>Noctiluca</b>	Surface	4.99	373	1200	17441.97
	Middle	11.57	157	1200	7341.53
	Deep	24.17	81	1200	3787.67
<b>Phaeocystis</b>	Surface	4.99	29	1200	1356.08
	Middle	11.58	61	1200	2852.44
	Deep	24.17	123	1200	5751.64

*Supplementary table 2.2. Horizontal distribution of the most abundant taxa in the straight pattern.*

<b>Taxon</b>	<b>Bin</b>	<b>Mean depth [m]</b>	<b>Count [ind]</b>	<b>Deployment time [s]</b>	<b>Density [ind m<sup>-3</sup>]</b>
<b>Calanoida</b>	North of sand bank	14.02	140	3642	2157.03
	South of sand bank	9.22	11	2259	273.24
<b>Cnidaria</b>	North of sand bank	13.89	31	3642	477.63
	South of sand bank	11.23	15	2259	372.60
<b>Noctiluca</b>	North of sand bank	12.02	493	3642	7595.82
	South of sand bank	9.50	463	2259	11500.92
<b>Phaeocystis</b>	North of sand bank	13.72	266	3642	4098.36
	South of sand bank	11.69	40	2259	993.60

SUPPLEMENTARY MATERIAL

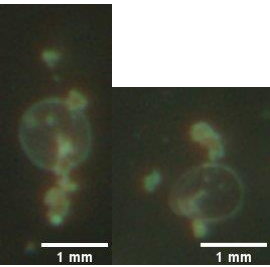
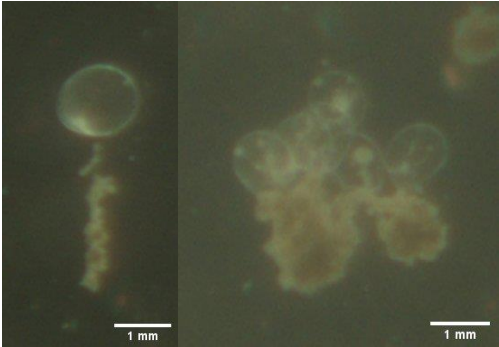
Supplementary table 2.3. Counts [ind], densities [ind m<sup>-3</sup>] and size [mm] with standard deviation per magnification setting. Note that S0-S2 was deployed for approximately 1h and S3 for ½ hour. Size was determined by ImageJ length measurements of the particles [mm], with a maximum of 10 measured particles per taxa per magnification. Note that size does not reflect the head-tail length of the organisms, but are the longest or widest part of an organism.

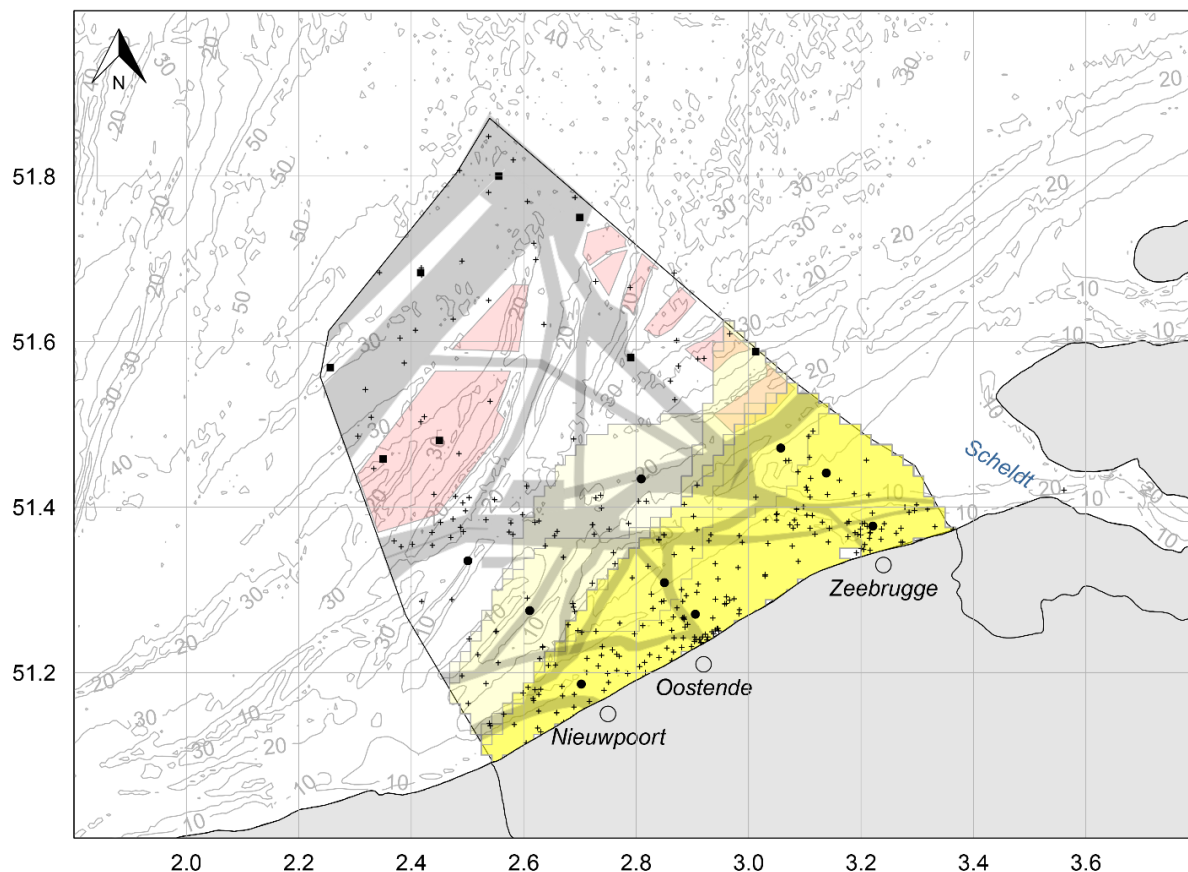
	Count [ind]				Density [ind/m <sup>3</sup> ]				Size [mm] with standard deviation			
	S0	S1	S2	S3	S0	S1	S2	S3	S0	S1	S2	S3
<b>Annelida</b>	0	0	7	8	0.00	0.00	8.49	7.96			3.069 ± 1.235	3.292 ± 1.633
<b>Appendicularia</b>	0	7	46	159	0.00	78.48	55.79	158.25		2.064 ± 0.444	2.276 ± 0.260	2.563 ± 0.317
<b>Appendicularia house</b>	0	1	7	867	0.00	11.21	8.49	862.92		2.191 ± 0	2.563 ± 0.483	3.766 ± 0.856
<b>Calanoida</b>	3	0	7	22	422.19	0.00	8.49	21.90	0.706 ± 0.087		1.026 ± 0.360	1.145 ± 0.221
<b>Caridea</b>	0	0	0	3	0.00	0.00	0.00	2.99				2.794 ± 0.261
<b>Chaetognatha</b>	0	0	0	1	0.00	0.00	0.00	1.00				
<b>Cnidaria</b>	1	11	75	80	140.73	123.33	90.96	79.62	0.379 ± 0	1.478 ± 0.327	1.593 ± 0.294	2.205 ± 1.076
<b>Ctenophora</b>	0	1	0	0	0.00	11.21	0.00	0.00		2.059 ± 0		
<b>Cumacea</b>	0	0	9	0	0.00	0.00	10.91	0.00			2.526 ± 0.135	
<b>Echinodermata</b>	0	2	11	36	0.00	22.42	13.34	35.83		1.443 ± 0.087	1.683 ± 0.594	1.540 ± 0.499
<b>Noctiluca</b>	38 6	827	503 3	227 08	54321.5 5	9272.35	6103.77	22601.2 1	0.715 ± 0.066	0.683 ± 0.078	0.694 ± 0.076	0.965 ± 0.207
<b>Phaeocystis</b>	0	0	0	128 0	0.00	0.00	0.00	1273.98				2.768 ± 0.763
<b>Fish larvae</b>	0	0	1	1	0.00	0.00	1.21	1.00			2.667 ± 0	3.441 ± 0
<b>Σ</b>	39 0	849	519 6	251 65	54884.4 6	9519.02	6301.45	25046.6 5				

Supplementary table 2.4. Mean ZooScan length measurements with standard deviation [mm] of a WP2 sample that was diluted 7 times.

<b>Taxon</b>	<b>Count</b>	<b>Mean size ± standard deviation [mm]</b>
<b>Appendicularia</b>	21	0.803 ± 0.306
<b>Brachyura zoe</b>	1	0.806 ± 0
<b>Calanoida</b>	187	0.631 ± 0.159
<b>Cirripeda nauplius</b>	3	0.424 ± 0.067
<b>Cnidaria</b>	79	0.859 ± 0.219
<b>Cumacea</b>	2	0.847 ± 0.14
<b>Echinodermata</b>	13	0.47 ± 0.174
<b>Noctiluca</b>	572	0.51 ± 0.108
<b>Podon</b>	11	0.425 ± 0.04

Supplementary table 2.5. Overview of the turbidity values in [NTU] and their impact on the VPR images.

<b>Turbidity [NTU]</b>	<b>Quality of the image</b>	<b>Example of an image</b>
< 3.2	Good images	
6.2	Blurry images with less contrast	
> 10.2	No images captured	/



Supplementary figure 2.1. The Belgian part of the North Sea (outlined by the solid line) with ship wrecks (plus sign), shipping routes (dark grey areas), concession zones of windmill parks (red areas) and coastal areas with a turbidity > 6.2 NTU (yellow areas). The yellow areas were based on monthly interpolated SPM values (dataset from Flanders Marine Institute, 2019). The more intense the yellow color, the more often per year the water column is inaccessible for image collection by the VPR. On the map the monthly (black dot) and seasonal (black square) visited monitoring stations of the LifeWatch project are given. The gray lines represent the depth of the water column [m].



## Supplementary material chapter 3

Supplementary table 3.1. Overview of the AutoDeck settings used during VPR deployment for the three cruises.

	Methodological cruise				24-hour cruise		Greenland cruise
	High (S1) downcasts	High (S1) transect	Low (S3) downcasts	Low (S3) transect	High (S1) downcasts		Low (S3) transects
Segmentation threshold - low	0	0	0	0	0	0	0
Segmentation threshold - high	132	132	132	132	131	132	132
Focus - sobel	18	18	18	18	23	25	45
Focus - stdv	1	1	1	1	2	2	0

Supplementary table 3.2. Outcomes of the autoregression coefficients for each taxa in the WP2 and VPR dataset. Coefficients close to 1 indicate a strong positive temporal autocorrelation.

Taxon	Autoregression coefficient	
	WP2	VPR
Amphipoda	0.7064	0.9562163
Annelida	0.1982735	0.5112977
Anomura	0.09939388	-
Appendicularia	1.713648E-11	4.82E-11
Brachyura	0.035898	-
Branchiopoda	8.013722E-12	-
Calanoida	0.4091464	0.3662576
Caridae	1.008482E-06	2.698766e-11
Chaetognatha	9.055013E-11	4.82E-11
Cirripedia cyprus	0.1155572	8.89E-11
Cirripedia nauplius	0.6246556	-
Cnidaria	6.484222E-12	1.98E-12
Ctenophora	6.484222E-12	-
Cumacea	0.5835156	0.8722871
Echinodermata	0.3737251	0.3732714
Fish eggs	6.083999E-12	4.82E-11
Fish larvae	1.01E-06	-
Harpacticoida	0.54127	3.458631e-12
Mollusca	2.022521E-11	-
Mysida	3.458631E-12	-
Noctiluca	1.922259E-09	0.5614057
Phaeocystis	-	0.8368964

## Supplementary material chapter 4

Supplementary table 4.1. The GAM model output of the distribution of Amphipoda, Annelida, Calanoida, Cumacea, detritus, Noctiluca and Phaeocystis.

<b>Taxon</b>	<b>Model</b>	<b>Deviance explained</b>
<b>Amphipoda</b>	Amphipoda ~ s(Depth) + s(Diel) + ti(Depth, Diel) + s(Tides) + s(Detritus)	26.4%
<b>Annelida</b>	Annelida ~ s(Depth) + s(Diel) + ti(Depth, Diel) + s(Tides) + s(Detritus)	22.1%
<b>Calanoida</b>	Calanoida ~ s(Depth) + s(Diel) + ti(Depth, Diel) + s(Tides) + s(Detritus)	6.17%
<b>Cumacea</b>	Cumacea ~ s(Depth) + s(Diel) + ti(Depth, Diel) + s(Tides) + s(Detritus)	21.1%
<b>Detritus</b>	Detritus ~ s(Depth) + s(Diel) + ti(Depth, Diel) + s(Tides)	44.9%
<b>Noctiluca</b>	Noctiluca ~ s(Depth) + s(Diel) + ti(Depth, Diel) + s(Tides) + s(Detritus)	17.2%
<b>Phaeocystis</b>	Phaeocystis ~ s(Depth) + s(Diel) + ti(Depth, Diel) + s(Tides) + s(Detritus)	28.7%

Supplementary table 4.2. Densities [ind m<sup>-3</sup>] per deployment [h] for all detected classes as registered by the VPR averaged over the whole water column.

Hour	Amphipoda	Annelida	Appendicularia	Calanoida	Caridae	Chaetognatha	Cirripedia cypris	Cirripedia nauplius	Cnidaria	Cumacea	Echinodermata	Fish egg	Harpacticoida	Noctiluca	Phaeocystis
15	0	0	0	11.97	0	0	0	0	0	0	1.50	0	0	205.04	70.34
16	0	0	0	46.36	0	0	0	0	0	0	7.24	0	0	169.49	43.46
18	0	0	0	59.21	1.48	0	1.48	0	0	0	7.40	0	0	387.84	199.84
19	0	0	0	30.83	0	0	0	0	0	0	2.28	0	0	282.02	202.09
20	0	0	0	8.74	0	0	0	0	0	0	1.46	0	0	214.09	148.55
21	0	0	0	7.26	1.45	0	0	0	0	0	4.36	1.45	0	499.39	139.36
22	1.37	0	0	27.36	0	0	0	1.37	0	1.37	10.94	0	0	807.15	455.56
23	14.28	4.76	0	34.90	0	0	0	0	0	14.28	14.28	0	0	1129.35	810.53
0	4.64	17.03	0	44.89	0	0	1.55	0	0	1.55	10.84	0	0	1320.49	687.33
1	0	4.56	0	57.70	0	0	0	0	0	0	19.74	0	0	1193.55	560.33
2	2.90	1.45	0	53.66	0	0	0	0	0	2.90	14.50	0	0	1129.67	262.48
3	0	1.25	0	10	0	0	0	0	0	3.75	8.75	0	0	284.92	112.47
4	0	0	0	14.01	0	0	0	0	0	0	1.75	0	0	269.69	43.78
5	0	0	0	29.42	0	0	0	0	0	0	6.54	0	0	169.97	45.76
6	0	0	0	5.34	0	0	0	0	5.34	0	0	0	0	202.92	28.48
7	0	0	0	17.45	0	0	0	0	0	0	3.49	0	10.47	171.03	205.93
8	0	0	0	12.72	0	0	0	0	1.41	1.41	7.07	0	0	200.75	385.94
9	0	0	0	5.37	0	0	0	0	0	0	1.79	0	1.79	541.87	416.69
10	0	0	1.59	12.73	0	1.59	0	0	0	0	15.92	0	0	697.09	631.84
11	0	0	0	40.44	1.69	0	0	0	0	0	13.48	0	0	1024.57	1002.66
12	0	0	0	21.56	0	0	0	0	0	0	24.64	0	0	1137.97	1818.59
13	0	0	0	41.50	0	0	0	0	0	0	6.92	0	0	1250.28	1172.46
14	0	5.95	0	25.77	0	0	0	0	0	0	7.93	0	0	961.34	445.98

SUPPLEMENTARY MATERIAL

Supplementary table 4.3. Densities [ind m<sup>-3</sup>] per deployment [h] for all detected classes collected by the WP2 net over the whole water column.

Hour	Amphipoda	Annelida	Anomura	Appendicularia	Brachyura	Branchiopoda	Calanoida	Caridae	Chaetognatha	Cirripedia cypris
15	0	0	0	0	45.57	0	1811.29	0	0	11.39
16	0	0	0	22.19	0	0	10527.69	0	177.5	55.47
18	0	5.67	0	0	0	0	4709.26	0	0	68
19	0	0	0	0	0	0	2499.59	0	0	27.17
20	0	0	0	0	10.98	0	7820.87	0	0	16.48
21	0	0	0	0	0	0	1309.08	0	0	0
22	0	2.76	0	0	0	5.53	268.05	0	0	0
23	57.01	22.8	0	11.4	0	0	6396.71	0	0	11.4
0	94.37	70.78	0	0	0	0	23427.76	0	47.19	70.78
1	49.27	197.07	0	24.63	24.63	0	46409.7	0	24.63	24.63
2	74.12	172.96	24.71	24.71	24.71	0	34393.41	0	24.71	49.42
3	24.55	24.55	12.27	0	12.27	0	9610.33	0	36.82	0
4	0	47.44	0	47.44	47.44	0	22816.87	0	71.15	142.31
5	0	0	0	0	11.6	0	10424.84	0	5.8	57.98
6	0	0	0	0	11.26	0	6562.29	0	16.88	39.4
7	0	2.7	1.35	0	5.39	0	1421.87	0	0	4.04
8	2.65	0	0	0	1.32	0	689.17	0	0	0
9	0	0	0	0	42.77	0	491.87	0	0	0
10	0	0	0	0	11.08	0	2935.79	0	0	0
12	0	0	0	11.4	0	0	4262.49	0	0	22.79
13	0	317.29	0	0	0	0	35371.48	0	23.5	11.75
14	0	0	23.86	0	23.86	0	29605.7	0	0	0

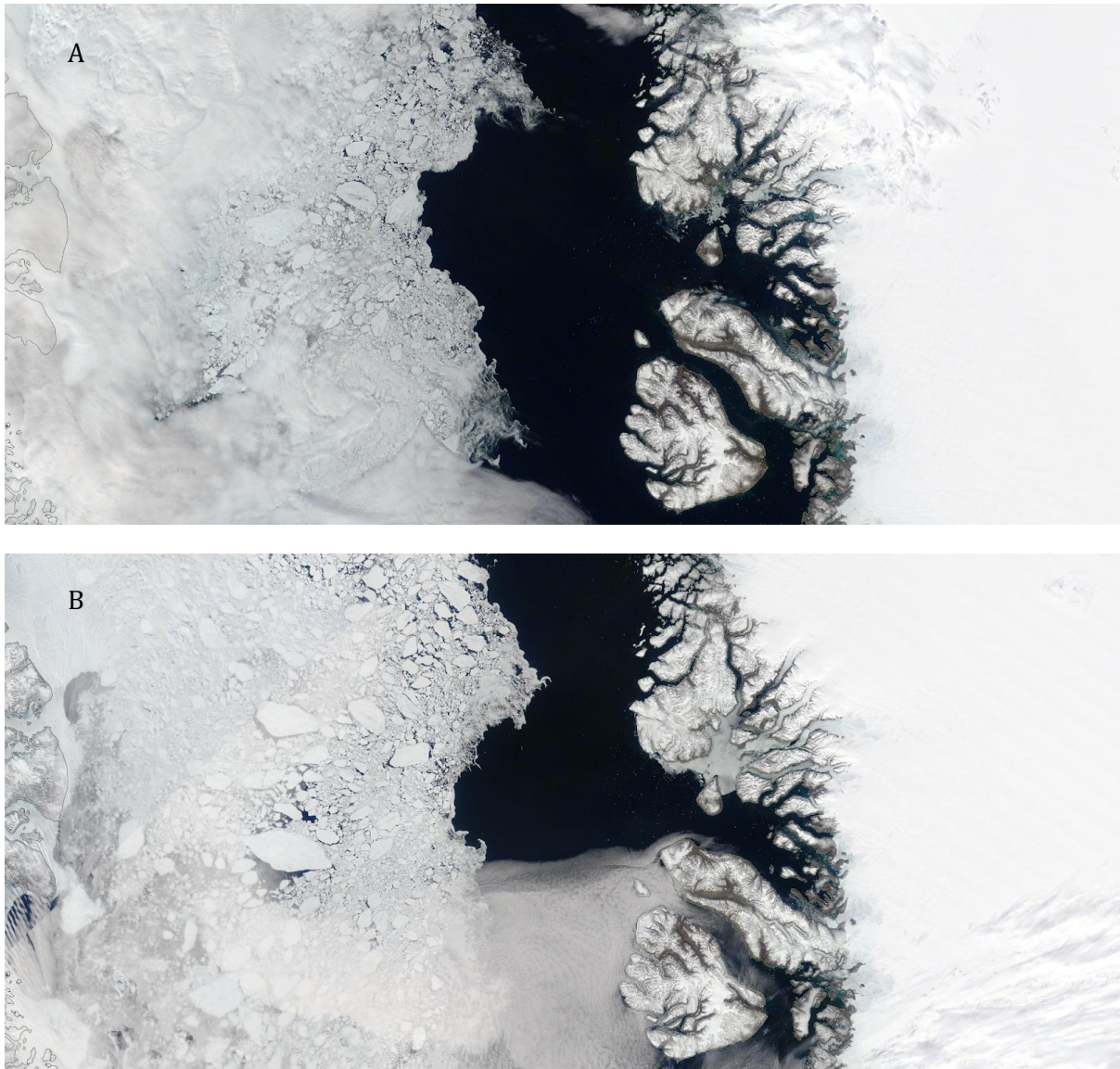
Hour	Cirripedia nauplius	Cnidaria	Ctenophora	Cumacea	Echinodermata	Fish egg	Harpacticoida	Mollusca	Mysida	Noctiluca
15	45.57	0	0	0	68.35	56.96	11.39	0	0	3246.65
16	122.03	0	0	0	133.12	0	0	0	0	1508.71
18	73.67	0	0	0	181.34	11.33	90.67	0	0	6001.33
19	78.79	0	0	0	78.79	13.58	54.34	2.72	0	777.05
20	318.55	0	0	5.49	274.61	10.98	93.37	10.98	0	1049.01
21	0	0	0	0	160.95	10.73	10.73	0	0	40763.8
22	8.29	0	0	0	66.32	0	2.76	0	0	3631.09
23	57.01	0	0	22.8	182.44	0	34.21	0	0	6510.73
0	94.37	0	0	0	188.74	23.59	94.37	70.78	0	10923.52
1	24.63	0	0	49.27	443.4	0	295.6	0	0	17120.35
2	74.12	0	0	74.12	420.03	24.71	222.37	24.71	0	14182.34
3	171.83	0	0	36.82	306.84	0	98.19	0	12.27	11365.48
4	260.9	0	0	94.87	806.42	94.87	308.34	0	0	22437.38
5	179.74	0	0	11.6	179.74	5.8	17.39	0	0	1652.44
6	56.28	0	0	28.14	230.75	28.14	5.63	0	0	2594.53
7	29.65	0	0	0	107.82	5.39	17.52	0	0	1261.49
8	1.32	0	0	0	55.56	0	2.65	2.65	0	353.18
9	21.39	0	0	0	0	42.77	0	0	0	33575.34
10	0	0	0	0	398.82	22.16	22.16	55.39	0	14235.82
12	0	0	0	0	182.35	0	68.38	11.4	0	10804.39
13	23.5	0	0	0	470.05	35.25	23.5	35.25	0	18543.59
14	0	23.86	23.86	0	954.25	0	310.13	0	0	16174.59

SUPPLEMENTARY MATERIAL

*Supplementary table 4.4. The interquartile range during daytime and nighttime of Amphipoda, Annelida, Calanoida, Cumacea, detritus, Noctiluca and Phaeocystis.*

<b>Taxon</b>	<b>Daytime Q1 - Q3</b>	<b>Nighttime Q1 - Q3</b>
<b>Amphipoda</b>	NA	6.6 - 11
<b>Annelida</b>	9.65 - 9.8	4.05 - 11.9
<b>Calanoida</b>	9.2 - 15.7	5.7 - 11.6
<b>Cumacea</b>	6.5 - 6.5	6.6 - 13
<b>Detritus</b>	10.9 - 16.9	11.1 - 16.2
<b>Noctiluca</b>	6.6 - 14.1	7.1 - 14
<b>Phaeocystis</b>	9.4 - 16.3	9.6 - 15.5

## Supplementary material chapter 5



*Supplementary material 5.1. Satellite data of the study area on (A) the 28th of June 2022, at the start of the research cruise, and (B) the 20th on June 2022, a week before the start of the cruise, where ice is still blocking the entrance of the most northern sampled fjords. Images from NASA Earthdata Worldview tool.*

SUPPLEMENTARY MATERIAL

Supplementary table 5.1. Mean length [ $\mu\text{m}$ ] and standard deviation of plankton as measured with microscopy.

<b>Taxon</b>	<b>Mean length <math>\pm</math> SD [<math>\mu\text{m}</math>]</b>
<i>Acartia longiremis</i>	1000
<i>Aglantha digitale</i>	5544 $\pm$ 1638
Amphipoda	2440 $\pm$ 559
Amphipoda (Parathemisto abyss.)	6498 $\pm$ 897
Appendicularia	1900
<i>Autolytus</i>	4698 $\pm$ 2197
Bivalvia	157 $\pm$ 24
Bryozoa	311 $\pm$ 23
<i>Calanus finmarchicus</i>	2709 $\pm$ 188
<i>Calanus glacialis</i>	3717 $\pm$ 206
<i>Calanus hyperboreus</i>	5017 $\pm$ 350
<i>Calanus</i> spp.	720 $\pm$ 58
Chaetognatha	3509 $\pm$ 404
<i>Chiridius armatus</i>	2708 $\pm$ 192
Cirripedia	861 $\pm$ 51
Cirripedia (class Facetotecta)	473 $\pm$ 14
<i>Clione limacina</i>	466 $\pm$ 88
Copepoda	312 $\pm$ 17
Ctenophora	1347 $\pm$ 85
Ctenophora ( <i>Beroe</i> )	1600 $\pm$ 453
Decapoda	28720
<i>Diastylis</i> (Compylaspis)	1920
<i>Dimophyes</i> spp.	4251 $\pm$ 1069
Echinodermata	1180 $\pm$ 189
<i>Eukhronia</i> spp.	15389 $\pm$ 6683
Euphausiacea	534 $\pm$ 59
Fish	3080
Foraminifera	230 $\pm$ 37
<i>Fritillaria borealis</i>	259 $\pm$ 37
<i>Gaetanus tenuispinus</i>	1952 $\pm$ 292
Gastropoda	267 $\pm$ 52
<i>Haloptilus aculifrons</i>	2800
Harpacticoida	669
<i>Harpacticus</i> spp.	1230
<i>Heterorhabdus norvegicus</i>	2927 $\pm$ 28
<i>Heterorhabdus robustus</i>	3960 $\pm$ 0
<i>Heterorhabdus</i> spp.	1887 $\pm$ 368
Hydromedusae	1415
Isopoda	778 $\pm$ 231
<i>Lensia</i> (Siphonophora)	4386 $\pm$ 841
<i>Limacina helicina</i>	1649 $\pm$ 64
<i>Lubbockia</i>	880



<i>Metridia longa</i>	1901 ± 104
<i>Microcalanus pusillus</i>	603 ± 46
<i>Microcalanus pygmaeus</i>	415 ± 31
<i>Microcalanus</i> spp.	150 ± 32
<i>Microsetella norvegica</i>	476 ± 55
<i>Mormonilla</i> spp.	800
<i>Muggiaea</i> (Siphonophora)	4544 ± 1439
Mysidacea	24389 ± 10017
<i>Oikopleura</i>	659 ± 273
<i>Oithona</i>	322 ± 33
<i>Oithona atlantica</i>	747 ± 18
<i>Oithona similis</i>	401 ± 32
<i>Oncaea borealis</i>	328 ± 31
<i>Oncaea</i> spp.	288 ± 17
Ostracoda	1739 ± 708
<i>Paraeuchaeta norvegica</i>	3926 ± 82
<i>Pareuchaeta</i> spp.	1400 ± 99
<i>Pilidium</i>	600
Polychaeta	470 ± 163
<i>Polydora</i>	6720 ± 2376
<i>Pseudocalanus acuspes</i>	1053 ± 61
<i>Pseudocalanus minutus</i>	1193 ± 76
<i>Pseudocalanus</i> spp.	592 ± 37
<i>Pseudocyclopia stephoides</i>	1030 ± 14
Radiolaria	293 ± 38
Rotifera	205
<i>Sagitta elegans</i>	28333
<i>Sagitta</i> spp.	7151 ± 1052
<i>Scolecithricella minor</i>	1081 ± 71
<i>Spinocalanus</i> spp.	1072 ± 248
<i>Temora longicornis</i>	1090 ± 28
<i>Thysanoessa inermis</i>	27000
<i>Thysanoessa longicaudata</i>	21333
<i>Tomopteris helgolandica</i>	3973 ± 1273

---

SUPPLEMENTARY MATERIAL

Supplementary table 5.2. The zooplankton conversion values 'a' and 'b' used for biomass calculations. Values were based on Planken et al., (in prep.) and modified or supplemented for some taxa.

Taxon	a	b	Units	Based on	Reference	Carbon content
<b>Copepoda large</b>						
<i>Calanus finmarchicus</i>	4.80E-03	3.569	mm	<i>Calanus finmarchicus</i> & <i>Calanus glacialis</i>	Madsen et al. (2001)	NA
<i>Calanus glacialis</i>	4.80E-03	3.569	mm	<i>Calanus finmarchicus</i> & <i>Calanus glacialis</i>	Madsen et al. (2001)	NA
<i>Calanus hyperboreus</i>	2.80E-03	3.39	mm	<i>Calanus hyperboreus</i>	Hirche & Mumm (1992)	0.502
<i>Calanus</i> spp.	9.50E-03	3.384	mm	<i>Calanus finmarchicus</i> & <i>Calanus glacialis</i>	Hirche & Mumm (1992)	0.502
<i>Chiridius armatus</i>	9.50E-03	3.384	mm	<i>Calanus finmarchicus</i> & <i>Calanus glacialis</i>	Hirche & Mumm (1992)	0.5
<i>Gaetanus tenuispinus</i>	1.55E-02	3.169	mm	<i>Gaidius variabilis</i>	Yamaguchi & Ikeda (2000b)	0.5
<i>Heterorhabdus</i> spp.	8.76E-03	3.463	mm	<i>Heterorhabdus tanneri</i>	Yamaguchi & Ikeda (2000a)	0.5
<i>Heterorhabdus norvegicus</i>	8.76E-03	3.463	mm	<i>Heterorhabdus tanneri</i>	Yamaguchi & Ikeda (2000a)	0.5
<i>Heterorhabdus robustus</i>	8.76E-03	3.463	mm	<i>Heterorhabdus tanneri</i>	Yamaguchi & Ikeda (2000a)	0.5
<i>Metridia longa</i>	1.21E-02	3.017	mm	<i>Metridia longa</i>	Hirche & Mumm (1992)	0.51
<i>Paraeuchaeta norvegica</i>	6.61E-06	6.82	mm	<i>Paraeuchaeta norvegica</i>	Tønnesson et al. (2006)	NA
<i>Paraeuchaeta</i> spp.	4.27E-03	3.01	mm	<i>Paraeuchaeta norvegica</i>	Tønnesson et al. (2006)	NA
<b>Copepoda small</b>						
<i>Acartia longiremis</i>	1.11E-11	2.92	µm	<i>Acartia tonsa</i>	Berggreen et al. (1988)	NA
Harpacticoida	2.40E-11	2.85	µm	<i>Pseudocalanus</i> spp.	Liu & Hopcroft (2008)	0.5
<i>Harpacticus</i> spp.	2.40E-11	2.85	µm	<i>Pseudocalanus</i> spp.	Liu & Hopcroft (2008)	0.5
<i>Microcalanus pusillus</i>	2.40E-11	2.85	µm	<i>Pseudocalanus</i> spp.	Liu & Hopcroft (2008)	0.5
<i>Microcalanus pygmaeus</i>	2.40E-11	2.85	µm	<i>Pseudocalanus</i> spp.	Liu & Hopcroft (2008)	0.5
<i>Microcalanus</i> spp.	2.40E-11	2.85	µm	<i>Pseudocalanus</i> spp.	Liu & Hopcroft (2008)	0.5
<i>Microsetella norvegica</i>	2.6500E-09	1.95	µm	<i>Microsetella norvegica</i>	Uye et al. (2002)	NA
<i>Oithona atlantica</i>	3.41E-13	3.643	µm	<i>Oithona hebes</i>	Ara (2001)	0.465
<i>Oithona similis</i>	3.41E-13	3.643	µm	<i>Oithona hebes</i>	Ara (2001)	0.465
<i>Oithona</i> spp.	3.41E-13	3.643	µm	<i>Oithona hebes</i>	Ara (2001)	0.465
Cyclopoida spp.	3.41E-13	3.643	µm	<i>Oithona hebes</i>	Ara (2001)	0.465
<i>Oncaea borealis</i>	2.51E-11	2.9	µm	<i>Oncaea</i> spp.	Satapoomin (1999)	NA
<i>Oncaea</i> spp.	2.51E-11	2.9	µm	<i>Oncaea</i> spp.	Satapoomin (1999)	NA
<i>Pseudocalanus acuspes</i>	2.40E-11	2.85	µm	<i>Pseudocalanus</i> spp.	Liu & Hopcroft (2008)	0.497
<i>Pseudocalanus minutus</i>	2.40E-11	2.85	µm	<i>Pseudocalanus</i> spp.	Liu & Hopcroft (2008)	0.497
<i>Pseudocalanus</i> spp.	2.40E-11	2.85	µm	<i>Pseudocalanus</i> spp.	Liu & Hopcroft (2008)	0.497
<i>Scolecithricella minor</i>	1.82E-13	3.669	µm	<i>Scolecithricella minor</i>	Yamaguchi (1999)	0.5
<i>Spinocalanus</i> spp.	2.40E-11	2.85	µm	<i>Pseudocalanus</i> spp.	Liu & Hopcroft (2008)	0.5
<i>Temora longicornis</i>	27.05	2.62	mm	<i>Temora longicornis</i>	Dam & Peterson (1991)	0.433

**Amphipoda**

Amphipoda spp.	4.85E-03	2.957	mm	<i>Themisto japonica</i>	Ikeda (1990)	0.4
Amphipoda (Gammaridae)	4.85E-03	2.957	mm	<i>Themisto japonica</i>	Ikeda (1990)	0.4
Amphipoda (Parathemisto abyss.)	4.85E-03	2.957	mm	<i>Themisto japonica</i>	Ikeda (1990)	0.4
<i>Hyperia galba</i>	4.85E-03	2.957	mm	<i>Themisto japonica</i>	Ikeda (1990)	0.4

**Other crustacean**

Decapoda	1.19		NA	Decapoda	Hop <i>et al.</i> (2019)	0.36
Isopoda	1.90E-02	NA	NA	Isopoda	Hop <i>et al.</i> (2019)	0.4

**Chaetognatha**

Chaetognatha	6.40E-05	3.3	mm	<i>Parasagitta elegans</i>	Matthews & Hestad (1977)	0.399
<i>Eukrohnia</i> spp.	1.70E-05	3.748	mm	<i>Eukrohnia hamata</i>	Kosobokova & Hopcroft (2021)	0.399
<i>Sagitta</i> spp.	6.40E-05	3.3	mm	<i>Parasagitta elegans</i>	Matthews & Hestad (1977)	0.399
<i>Sagitta elegans</i>	6.40E-05	3.3	mm	<i>Parasagitta elegans</i>	Matthews & Hestad (1977)	0.399

**Rotifera**

Rotifera	1.90E-04	NA	NA	<i>Brachionus plicatilis</i>	Øie <i>et al.</i> (1997)	NA
----------	----------	----	----	------------------------------	--------------------------	----

**Pteropoda**

<i>Limacina helicina</i>	1.37E-01	1.501	mm	<i>Limacina helicina antarctica</i>	Bednaršek <i>et al.</i> (2012)	0.333
<i>Clione limacina</i>	2.39E-01	1.615	mm	<i>Clione limacina</i>	Böer <i>et al.</i> (2005)	0.3

**Annelida**

Polychaeta	1.58E-07	1.38	µm	<i>Polydora</i> spp.	Hansen (1999)	NA
<i>Autolytus</i>	1.58E-07	1.38	µm	<i>Polydora</i> spp.	Hansen (1999)	NA
<i>Polydora</i>	1.58E-07	1.38	µm	<i>Polydora</i> spp.	Hansen (1999)	NA

**Appendicularia**

Appendicularia	1.18E-12	3.2	µm	<i>Oikopleura vanhoeffeni</i>	Deibel (1986)	NA
<i>Fritillaria borealis</i>	7.76E-13	3.21	µm	<i>Fritillaria pellucida</i>	Fenaux (1976)	0.545
<i>Oikopleura</i>	1.18E-12	3.2	µm	<i>Oikopleura vanhoeffeni</i>	Deibel (1986)	NA

**Cnidaria**

<i>Aglantha digitale</i>	1.94E-03	3.15	mm	<i>Aglantha digitale</i>	Matthews & Hestad (1977)	0.101
Cnidaria	1.90E-03	NA	NA	Hydrozoa larvae	Hop <i>et al.</i> (2019)	0.1
<i>Dimophyes</i> spp.	1.00E-03	3.61	mm	<i>Dimophyes arctica</i>	Mumm <i>et al.</i> (1991)	0.1
Hydromedusae	1.94E-03	3.15	mm	<i>Aglantha digitale</i>	Matthews & Hestad (1977)	0.101
Siphonophora ( <i>Lensia</i> )	1.00E-03	3.61	mm	<i>Dimophyes arctica</i>	Mumm <i>et al.</i> (1991)	0.1
Siphonophora ( <i>Muggiaea</i> )	1.00E-03	3.61	mm	<i>Dimophyes arctica</i>	Mumm <i>et al.</i> (1991)	0.1

**Ctenophora**

Ctenophora	1.90E-03	NA	NA	Ctenophora larvae	Hop <i>et al.</i> (2019)	0.1
Ctenophora ( <i>Beroe</i> )	1.90E-03	NA	NA	Ctenophora larvae	Hop <i>et al.</i> (2019)	0.1

**Meroplankton**

Bivalvia	3.06E-11	2.88	µm	<i>Mytilus edulis</i>	Fotel <i>et al.</i> (1999)	NA
Bryozoa	1.00E-03	NA	NA	Bryozoa larvae	Hop <i>et al.</i> (2019)	0.402
Echinodermata	1.00E-03	NA	NA	Echinodermata larvae	Hop <i>et al.</i> (2019)	0.142

SUPPLEMENTARY MATERIAL

Gastropoda	4.06E-10	2.76	µm	<i>Philine aperta</i>	Hansen & Ockelmann (1991)	NA
Pilidium	1.00E-03	NA	NA	Nemertea pilidium	Hop <i>et al.</i> (2019)	0.4
<b>Cirripedia</b>						
Cirripedia	1.20E-02	NA	NA	Cirripedia cypris/nauplii	Hop <i>et al.</i> (2019)	0.437
Facetotecta	1.20E-02	NA	NA	Facetotecta nauplii	Hop <i>et al.</i> (2019)	0.437
<b>Euphausiacea</b>						
Euphausiacea (nauplii)	4.00E-03	NA	NA	Euphausiacea	Hop <i>et al.</i> (2019)	0.395
Euphausiacea (calyptopis)	9.84E-02	NA	NA	Euphausiacea	Hop <i>et al.</i> (2019)	0.395
Euphausiacea (furcilia)	3.14E-01	NA	NA	Euphausiacea	Hop <i>et al.</i> (2019)	0.395
<b>Ostracoda</b>						
Ostracoda (<1 mm)	1.36E-02	NA	NA	Ostracoda	Hop <i>et al.</i> (2019)	0.4
Ostracoda (1 - 2 mm)	4.38E-02	NA	NA	Ostracoda	Hop <i>et al.</i> (2019)	0.4
Ostracoda (2 - 3 mm)	2.67E-01	NA	NA	Ostracoda	Hop <i>et al.</i> (2019)	0.4

SUPPLEMENTARY MATERIAL

Supplementary table 5.3. Fatty acid composition of the microzooplankton fraction per station.

Relative abundance per fatty acid.

	EF01	EF04	EF08	EF12	EF15	EF17	EF18	EF22	EF24	EF27	EF32	EF35	EF37	EF40	EF43	EF45	EF47
<b>10:0</b>	0.03	0.09	1.04	0.72	2.97	3.86	0.44	0.15	0.10	0.03	0.10	0.16	0.35	1.96	2.57	0.03	3.82
<b>12:0</b>	0.15	0.48	0.17	0.20	0.19	0.20	0.40	0.23	0.20	0.12	0.27	0.21	0.24	0.24	0.22	0.10	0.22
<b>14:0</b>	10.7 4	15.1 5	6.86	5.66	4.80	4.32	7.55	5.86	5.43	4.92	6.10	6.71	8.26	6.03	5.47	10.1 5	5.25
<b>15:0</b>	0.51	0.43	0.65	0.61	0.58	0.45	0.50	0.40	0.35	0.32	0.48	0.34	0.86	0.73	0.62	0.36	0.64
<b>i-15:0</b>	0.07	0.15	0.29	0.35	0.32	0.31	0.30	0.21	0.18	0.20	0.26	0.15	0.32	0.37	0.34	0	0.32
<b>ai-15:0</b>	0.08	0.14	0.12	0.25	0.25	0.26	0.19	0.18	0.20	0.15	0.26	0.26	0.29	0.23	0.24	0.07	0.28
<b>16:0</b>	16.1 4	18.8 2	17.1 7	16.7 2	14.2 1	14.0 2	17.1 9	15.8 1	13.2 5	11.3 7	13.7 2	10.9 8	19.5 8	16.7 7	15.5 5	12.9 9	14.4 7
<b>16:1</b>	0	0	0	0.53	0.57	0.46	0.23	0.30	0.25	0.15	0.17	0	0.53	0.51	0.60	0	0.67
<b>16:1 n-7</b>	39.6 9	28.6 2	14.3 5	11.7 2	14.6 1	18.1 4	16.4 6	17.6 0	23.5 4	26.4 1	23.7 9	34.5 1	17.8 6	11.8 6	15.2 1	31.7 7	16.0 0
<b>16:1 n-5</b>	0	0.56	1.07	1.28	1.01	0	0.98	0.87	0.89	0	0	0	0.81	0.74	1.02	0	0.62
<b>16:2 n-7</b>	0.14	0.10	0	0	0	0.09	0	0.16	0.15	0.14	0.22	0	0	0	0	0.23	0
<b>16:2 n-4</b>	1.39	0.78	0.55	0.55	0.57	0.92	0.66	0.62	0.62	1.10	0.77	1.06	0.67	0.68	0.67	2.74	0.65
<b>16:3 n-4</b>	1.27	0.36	0	0	0.09	0.16	0.13	0.14	0.25	0.89	0.44	0.48	0	0.07	0.17	2.99	0
<b>16:4 n-1</b>	2.78	1.45	0	0	0.31	0.29	0.22	0.52	0.86	2.03	1.06	1.19	0	0	0	7.54	0
<b>17:0</b>	0.31	0.33	0.52	0.90	0.89	0.77	0.66	0.53	0.38	0.49	0.54	0.22	0.74	0.86	0.88	0.55	1.00
<b>18:0</b>	0.57	0.95	1.49	1.79	1.46	1.41	1.41	1.30	0.82	0.67	1.09	0.86	1.93	1.53	1.51	0.19	1.47
<b>18:1 n-9</b>	2.43	5.39	11.2 0	13.6 0	13.7 6	14.1 8	10.1 4	8.61	6.91	5.34	6.64	6.86	11.2 9	12.5 9	12.8 6	1.16	14.8 6
<b>18:1 n-7</b>	0.97	2.67	3.85	5.64	4.79	5.09	4.28	5.29	2.73	2.95	3.80	1.97	3.78	4.88	3.26	0.49	4.46
<b>18:1</b>	0.11	0.30	0.89	1.11	0.86	0.69	0.95	0.92	0.55	0.47	0.79	0.51	1.23	0.94	0.81	0	0.87
<b>18:2 n-6</b>	2.36	3.06	2.61	2.56	1.82	1.45	2.49	2.24	1.70	1.47	1.18	1.15	2.65	2.02	1.72	0.60	1.80
<b>18:3 n-6</b>	0.32	0.27	0	0.12	0.12	0.11	0.10	0.15	0.20	0.32	0.17	0.23	0	0.13	0.15	0.25	0.07
<b>18:3 n-3</b>	0.13	0.29	0.91	1.04	0.81	0.34	0.85	1.13	1.34	0.72	0.83	0.70	1.12	0.93	0.84	0.07	0.77
<b>18:4 n-3</b>	3.33	2.01	3.06	2.93	2.90	1.46	3.54	5.28	7.53	4.03	3.52	3.37	4.04	2.84	2.90	4.03	1.98
<b>18:4 n-1</b>	0.15	0.12	0	0	0.22	0.13	0.23	0.19	0.31	0.35	0.20	0	0	0	0	0.07	0.09
<b>18:5 n-1</b>	0.19	0.12	0	0	0	0	0	0	0	0.02	0	0	0	0	0	0.05	0
<b>20:0</b>	0.01	0.03	0	0.10	0.06	0.10	0.07	0.10	0.06	0.05	0.06	0	0	0	0	0	0.08
<b>20:1 n-11</b>	0.11	0.18	0.57	0.67	0.59	0.52	0.30	0.36	0.28	0.52	0	0	0	0.73	0.63	0	0.70
<b>20:1 n-9</b>	0.46	0.93	3.96	4.68	4.27	5.26	2.59	3.27	5.36	5.24	5.34	8.92	6.02	3.73	3.86	0	4.52
<b>20:1 n-7</b>	0.13	0.44	0.70	0.71	0.47	0.46	0.47	0.66	0.69	1.25	0.84	1.23	0.35	0.67	0.34	0	0.54
<b>20:2 n-6</b>	0.02	0.06	0	0.19	0.15	0.12	0.25	0.19	0.14	0.19	0.15	0	0	0.23	0	0	0
<b>20:3 n-9</b>	0.05	0.11	0	0.13	0.06	0.05	0.53	0.30	0.37	0.17	0.17	0	0	0.09	0.10	0	0.07
<b>20:4 n-3</b>	0.30	0.40	0.77	0.86	0.65	0.44	0.88	0.98	0.67	0.62	0.45	0.39	0.85	0.78	0.59	0.24	0.65
<b>20:5 n-3</b>	12.1 4	8.28	9.63	8.03	9.00	10.0 4	11.3 2	10.8 7	9.23	14.0 0	11.3 8	8.64	11.6 3	10.7 1	10.2 4	21.3 8	7.62
<b>22:1 n-11</b>	0.31	0.61	2.55	3.73	4.33	4.76	1.74	2.77	5.33	5.27	4.93	8.50	4.06	2.68	3.49	0.35	4.16
<b>22:1 n-7</b>	0	0	0	0	0.15	0.14	0	0.11	0.10	0.16	0.16	0	0	0	0	0	0.14
<b>22:5 n-3</b>	0.14	0.34	0.62	0.70	0.65	0.55	0.52	0.74	0.67	0.83	0.68	0.38	0.57	0.61	0.63	0.03	0.64
<b>22:6 n-3</b>	2.27	5.38	12.7 1	10.3 2	9.78	8.46	10.3 9	10	7.55	6.10	8.52	0	0	11.4 6	11.0 1	1.57	8.91
<b>24:1</b>	0.19	0.58	1.65	1.61	1.71	0	1.07	0.97	0.80	0.93	0.92	0	0	1.36	1.51	0	1.62

SUPPLEMENTARY MATERIAL

Supplementary table 5.4. Fatty acid compoition of the macrozooplankton fraction per station.

Relative abundance per fatty acid.

	EF01	EF04	EF08	EF12	EF15	EF17	EF18	EF22	EF24	EF27	EF32	EF35	EF37	EF40	EF43	EF45	EF47
<b>10:0</b>	0.04	0.03	0.07	0.05	0.05	0.06	0.13	0.05	0.03	0.03	0.03	0.01	0.04	0.03	0.03	0.05	0.05
<b>12:0</b>	0.16	0.18	0.18	0.15	0.12	0.11	0.27	0.20	0.14	0.13	0.14	0.10	0.13	0.13	0.12	0.09	0.13
<b>14:0</b>	3.84	3.56	3.65	4.07	3.16	3.05	4.90	4.22	3.63	3.28	4.38	3.24	3.59	3.99	3.60	3.40	3.57
<b>15:0</b>	0.14	0.16	0.18	0.17	0.15	0.18	0.24	0.16	0.15	0.12	0.16	0.09	0.17	0.18	0.18	0.13	0.16
<b>i-15:0</b>	0.08	0.08	0.08	0.09	0.06	0.11	0.13	0.12	0.08	0.07	0.11	0.05	0.10	0.11	0.11	0.06	0.10
<b>ai-15:0</b>	0.16	0.16	0.22	0.22	0.22	0.20	0.24	0.22	0.22	0.17	0.22	0.21	0.23	0.23	0.23	0.17	0.23
<b>16:0</b>	5.30	6.05	5.55	4.67	4.49	7.24	7.58	5.74	4.87	5.19	4.95	3.83	4.17	6.06	5.04	6.82	4.55
<b>16:1</b>	0.14	0.18	0.31	0.23	0.30	0.33	0.26	0.15	0.14	0.12	0.15	0.10	0.25	0.28	0.38	0.20	0.28
<b>16:1 n-7</b>	21.7 6	18.9 1	11.5 4	11.4 7	14.9 7	18.3 6	18.1 7	21.2 1	23.5 4	25.8 7	21.1 5	25.2 7	11.2 9	11.9 0	14.8 4	19.7 3	12.9 9
<b>16:1 n-5</b>	0.54	0.50	0.91	0.92	0.72	0	0.78	0.67	0.78	0	0.67	0.92	0.85	1.09	0.71	0	0.95
<b>16:2 n-7</b>	0.12	0.13	0.08	0.07	0.12	0.09	0.09	0.11	0.10	0.11	0.10	0.15	0.08	0.08	0.10	0.12	0.09
<b>16:2 n-4</b>	1.06	0.95	0.57	0.59	0.80	0.81	0.68	0.73	0.68	0.98	0.89	1.03	0.55	0.56	0.68	1.00	0.62
<b>16:3 n-4</b>	1.23	1.09	0.17	0.30	0.56	0.52	0.22	0.35	0.39	0.94	0.53	1.06	0.33	0.27	0.42	0.75	0.38
<b>16:4 n-1</b>	3.65	2.45	0.63	0.80	1.46	1.16	0.29	0.66	0.92	1.95	1.29	2.33	0.92	0.77	1.01	1.88	1.03
<b>17:0</b>	0.55	0.49	0.41	0.53	0.55	0.35	0.27	0.34	0.45	0.35	0.50	0.60	0.55	0.53	0.44	0.44	0.50
<b>18:0</b>	0.35	0.43	0.50	0.40	0.41	0.62	0.42	0.31	0.25	0.26	0.32	0.12	0.38	0.46	0.45	0.54	0.38
<b>18:1 n-9</b>	4.05	6.21	10.4 5	7.69	7.19	10.4 4	11.8 3	5.53	4.87	6.18	4.99	4.72	6.71	7.79	7.78	10.3 2	7.54
<b>18:1 n-7</b>	1.69	1.88	2.38	2.10	1.91	3.23	2.32	1.78	1.71	2.21	1.42	1.57	1.98	2.35	2.16	2.95	1.95
<b>18:1</b>	0.42	0.47	0.82	0.74	0.67	0.79	0.66	0.61	0.62	0.42	0.65	0.50	0.77	0.77	0.71	0.40	0.68
<b>18:2 n-6</b>	0.95	1.04	1.71	1.99	1.31	0.97	1.64	1.64	1.32	1.04	1.11	1.10	1.63	1.59	1.35	1.10	1.59
<b>18:3 n-6</b>	0.18	0.17	0.11	0.12	0.19	0.17	0.09	0.17	0.25	0.34	0.23	0.37	0.15	0.12	0.17	0.24	0.15
<b>18:3 n-3</b>	0.28	0.39	1.72	2.33	1.12	0.50	0.64	1.45	1.46	0.73	1.43	1.67	2.23	2.27	1.82	0.61	2.24
<b>18:4 n-3</b>	4.33	5.15	10.2 1	14.2 3	8.51	2.87	3.33	7.18	10.0 7	3.61	8.11	7.21	12.7 0	12.4 4	9.21	3.84	11.3 8
<b>18:4 n-1</b>	0.52	0.49	0.29	0.52	0.46	0.27	0.18	0.24	0.37	0.31	0.66	0.74	0.41	0.43	0.44	0.19	0.43
<b>18:5 n-1</b>	0.31	0.36	0.05	0.04	0.09	0.07	0	0	0.03	0.04	0.04	0.06	0.05	0.04	0.04	0.06	0.02
<b>20:0</b>	0.04	0.06	0.06	0.04	0.03	0.04	0.08	0.06	0.02	0.04	0.05	0.02	0.06	0.02	0.04	0.02	0.04
<b>20:1 n-11</b>	0.55	0.73	0.81	0.71	0.81	1.05	0.90	1.00	0.84	0.68	0.93	0.81	0.72	1.05	1.25	0.86	0.93
<b>20:1 n-9</b>	10.0 4	10.9 1	12.4 4	12.5 9	11.7 3	10.9 2	11.3 9	10.5 6	9.13	9.66	10.1 4	8.68	12.3 8	11.6 3	11.7 9	10.5 5	11.9 2
<b>20:1 n-7</b>	1.75	1.74	1.28	1.22	1.30	1.51	1.30	1.39	1.16	1.88	1.38	1.64	1.20	1.31	1.44	1.65	1.39
<b>20:2 n-6</b>	0.05	0.09	0.18	0.20	0.12	0.12	0.18	0.16	0.13	0.07	0.11	0.08	0.18	0.15	0.12	0.06	0.13
<b>20:3 n-9</b>	0.09	0.11	0.22	0.29	0.16	0.05	0.17	0.28	0.20	0.10	0.19	0.11	0.25	0.28	0.18	0.09	0.25
<b>20:4 n-3</b>	0.47	0.51	0.92	1.07	0.78	0.45	0.43	0.70	0.86	0.48	0.79	0.73	1.14	1.00	0.84	0.49	0.94
<b>20:5 n-3</b>	16.7 6	15.2 8	8.65	7.98	11.3 2	11.3 9	9.11	10.1 8	10.1 3	13.9 7	11.6 4	13.2 9	10.0 5	9.07	10.8 4	13.4 3	9.17
<b>22:1 n-11</b>	10.2 0	10.6 1	10.8 9	10.9 7	12.0 2	10.9 8	11.1 1	10.6 4	9.10	9.78	9.73	9.25	11.1 8	9.82	10.0 9	10.2 3	12.2 3
<b>22:1 n-7</b>	0.43	0.61	0.40	0.16	0.37	0.31	0.38	0.40	0.36	0.42	0.39	0.38	0.59	0.39	0.45	0.13	0.34
<b>24:1</b>	0.86	0.81	0.87	0.66	1.29	1.35	0.99	1.12	1.07	1.00	0.27	0.11	0.24	0.37	0.45	0.39	0

*Supplementary material 5.2. PERMANOVA on FA data with respect to the zooplankton size fractions.*

Permutation test for adonis under reduced model  
 Terms added sequentially (first to last)  
 Permutation: free  
 Number of permutations: 999  
 adonis2(formula = fa.dist ~ Content, data = data\_sim\_env, permutations = 999, method = "eucl")

	Df	SumOfSqs	R2	F	Pr(>F)
Content	3	2951.2	0.43555	9.5168	0.001 ***
Residual	37	3824.7	0.56445		
Total	40	6775.9	1.00000		

---  
 Signif. codes: 0 '\*\*\*' 0.001 '\*\*' 0.01 '\*' 0.05 '.' 0.1 ' ' 1

*Supplementary material 5.3. SIMPER analysis representing the five significant FA's most contributing to the difference between the meso and micro fraction.*

Contrast: Microzooplankton\_Mesozooplankton

	average	sd	ratio	ava	avb	cumsum	p
16:0	0.049020	0.012764	3.841000	15.222000	5.417000	0.155	0.001 ***
22:1 n-11	0.035070	0.011033	3.179000	3.505000	10.519000	0.389	0.001 ***
20:1 n-9	0.034730	0.012010	2.891000	4.024000	10.968000	0.499	0.001 ***
18:4 n-3	0.023680	0.016996	1.393000	3.458000	7.905000	0.574	0.016 *
14:0	0.016540	0.013553	1.220000	7.016000	3.713000	0.747	0.001 ***

---  
 Signif. codes: 0 '\*\*\*' 0.001 '\*\*' 0.01 '\*' 0.05 '.' 0.1 ' ' 1  
 Permutation: free  
 Number of permutations: 999

*Supplementary material 5.4. PERMANOVA on phytoplankton abundance with respect to the FlowCAM magnifications.*

Permutation test for adonis under reduced model  
 Terms added sequentially (first to last)  
 Permutation: free  
 Number of permutations: 999  
 adonis2(formula = fyto.dist ~ Magnification, data = test\_wide[, 1:2], permutations = 999, method = "eucl")

	Df	SumOfSqs	R2	F	Pr(>F)
Magnification	1	12234	0.53966	30.48	0.001 ***
Residual	26	10435	0.46034		
Total	27	22669	1.00000		

---  
 Signif. codes: 0 '\*\*\*' 0.001 '\*\*' 0.01 '\*' 0.05 '.' 0.1 ' ' 1

SUPPLEMENTARY MATERIAL

Supplementary material 5.5. SIMPER analysis representing the five significant phytoplankton phyla most contributing to the difference between the 10x and 4x magnification of the FlowCAM.

Contrast: 10X\_4X

	average	sd	ratio	ava	avb	cumsum	p
Bacillariophyta	0.39960	0.16939	2.35880	45.90000	6.85400	0.568	0.001 ***
Myzozoa	0.15760	0.11194	1.40750	18.35000	3.72800	0.791	0.001 ***
Ciliophora	0.09970	0.09878	1.00980	10.49000	8.65900	0.933	1.000
Haptophyta	0.04500	0.07351	0.61260	3.99000	1.64100	0.997	0.893
Radiozoa	0.00200	0.00528	0.37230	0.18000	0.00000	1.000	0.001 ***

---

Signif. codes: 0 '\*\*\*' 0.001 '\*\*' 0.01 '\*' 0.05 '.' 0.1 ' ' 1

Permutation: free

Number of permutations: 999

Supplementary material 5.6. Test results of correlation analysis between the fatty acid composition of zooplankton and the biomass of zooplankton. Only significant results ( $p < 0.01$ ) are shown.

*Aglantha digitale*: 16:0, 20:1(n-9), 22:1(n-11)

*Bivalvia*: 14:0, ai-15:0, 16:2(n-4), 16:3(n-4), 18:1, 16:4(n-1), 20:5(n-3), 22:5(n-3)

*Calanus finmarchicus*: 18:5(n-1), 22:1(n-7)

*Calanus glacialis*: 15:0, 16:0, 18:0, 20:1(n-9), 20:1(n-7), 22:1(n-11), 22:1(n-7)

*Calanus hyperboreus*: i-15:0, 15:0, 16:0, 18:0, 20:1(n-9), 20:1(n-7), 18:4(n-3), 18:4(n-1), 22:1(n-11), 22:1(n-7)

*Calanus spp.*: 18:5(n-1)

*Cirripedia*: 18:5(n-1)

*Clione limacina*: 16:0, 20:1(n-9), 22:1(n-11)

*Echinodermata*: 18:5(n-1)

*Fritillaria borealia*: 12:0, 14:0

*Gaetanus tenuispinus*: 18:5(n-1)

*Heterorhabdus norvegicus*: 16:0, 20:1(n-9), 22:1(n-11)

*Lensia* (Siphonophora): 22:1(n-7)

*Metridia longa*: 14:0, i-15:0, 15:0, 16:0, 18:0, 20:1(n-11), 20:1(n-9), 20:1(n-7), 22:1(n-11), 22:1(n-7)

*Microcalanus pygmaeus*: 20:1(n-9), 18:5(n-1), 22:1(n-7)

*Microcalanus spp.*: 22:1(n-7)

*Microsetella norvegica*: 15:0, 16:0, 20:1(n-9), 22:1(n-11)

*Oithona similis*: 18:2(n-6)

*Oncaea borealis*: i-15:0, 15:0, 16:0, 18:0, 18:1(n-7), 20:1(n-11), 20:1(n-9), 20:1(n-7), 18:4(n-3), 18:4(n-1), 22:1(n-11), 22:1(n-7)

*Oncaea spp.*: 15:0, 16:0, 20:1(n-9), 20:1(n-7), 22:1(n-11), 22:1(n-7)

*Ostracoda*: 15:0, 16:0, 20:1(n-9), 20:1(n-7), 22:1(n-11), 22:1(n-7)

*Paraeuchaeta norvegica*: 22:1(n-7)

*Pareuchaeta spp.*: 16:0, 20:1(n-9), 22:1(n-11)

*Pseudocalanus acuspes*: 18:5(n-1)

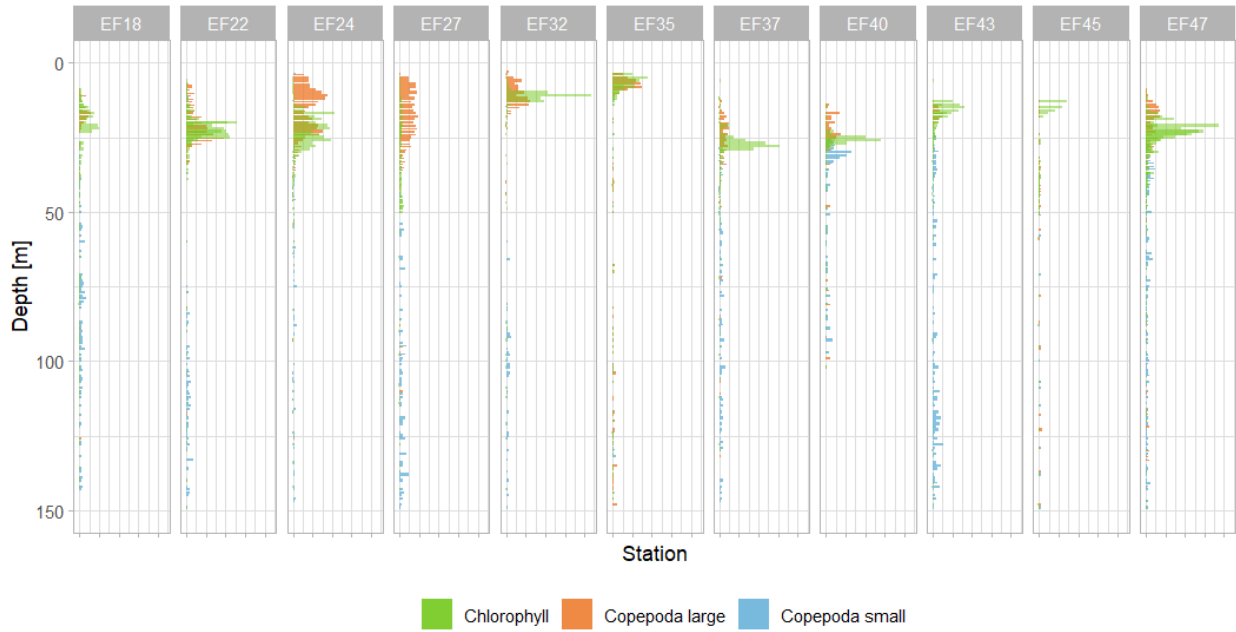
*Pseudocalanus minutus*: 15:0, 16:0, 20:1(n-9), 20:1(n-7), 22:1(n-11)

*Pseudocalanus spp.*: 18:5(n-1)

*Scolecithricella minor*: 20:1(n-11)

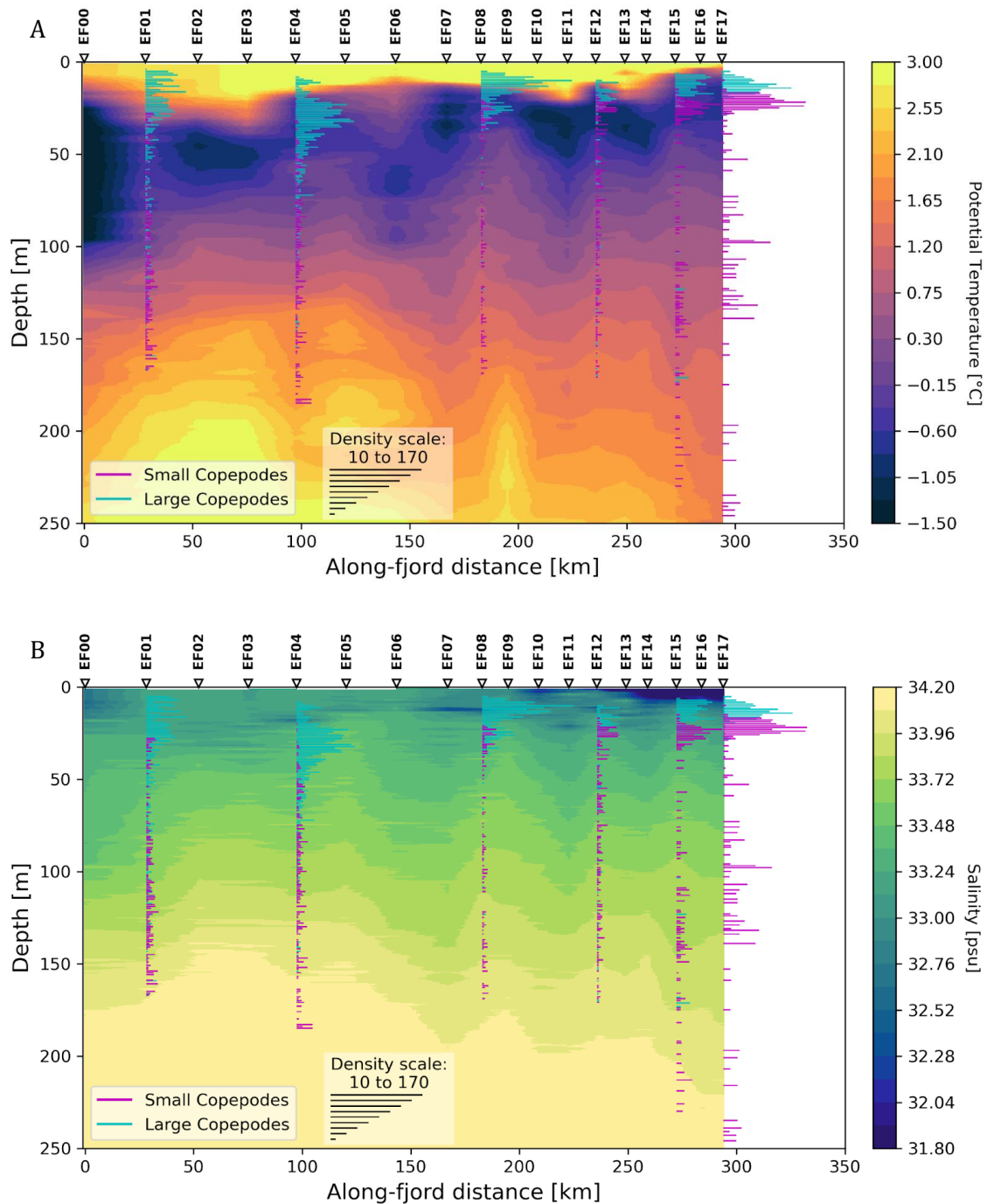


Supplementary figure 5.1. Distribution of copepod size fractions (orange for large copepods and blue for small copepods, per 1 m depth bin) in the water column for the stations of fjord 1 – 4. The green bars denote the mean chlorophyll a concentration for each 1 m depth bin.



SUPPLEMENTARY MATERIAL

Supplementary figure 5.2. Vertical distribution of small (purple) and large (blue) copepods from the shelf area (EF00) to fjord 5 (EF17). Density scale represented in counts of individuals [ind]. The distribution is plotted on interpolations of (A) the potential temperature [°C] and (B) salinity [psu] from CTD profiles of multiple stations.







# Publication list

## A1 publications

Praet, N.; Collart, T.; **Ollevier, A.**; Roche, M.; Degrendele, K.; De Rijcke, M.; Urban, P.; Vandorpe, T. (2023). The potential of multibeam sonars as 3D turbidity and SPM monitoring tool in the North Sea. *Remote Sens.* 15(20): 4918. <https://dx.doi.org/10.3390/rs15204918>

**Ollevier, A.**; Mortelmans, J.; Vandegehuchte, M.; Develter, R.; De Troch, M.; Deneudt, K. (2022). A Video Plankton Recorder user guide: Lessons learned from in situ plankton imaging in shallow and turbid coastal waters in the Belgian part of the North Sea. *J. Sea Res.* 188: 102257. <https://dx.doi.org/10.1016/j.seares.2022.102257>

Hablützel, P.I.; Rombouts, I.; Dillen, N.; Lagaisse, R.; Mortelmans, J.; **Ollevier, A.**; Perneel, M.; Deneudt, K. (2021). Exploring new technologies for plankton observations and monitoring of ocean health, in: Kappel, E.S. *et al.* *Frontiers in ocean observing: Documenting ecosystems, understanding environmental changes, forecasting hazards.* Oceanography, Suppl. 34(4): pp. 20-25. <https://dx.doi.org/10.5670/oceanog.2021.supplement.02-09>

**Ollevier, A.**; Mortelmans, J.; Aubert, A.; Deneudt, K.; Vandegehuchte, M. (2021). *Noctiluca scintillans*: Dynamics, size measurements and relationships with small soft-bodied plankton in the Belgian Part of the North Sea. *Front. Mar. Sci.* 8: 777999. <https://dx.doi.org/10.3389/fmars.2021.777999>

Luger, A.M.; **Ollevier, A.**; De Kegel, B.; Herrel, A.; Adriaens, D. (2019). Is variation in tail vertebral morphology linked to habitat use in chameleons? *J. Morphol.* 281(2): 229-239. <https://dx.doi.org/10.1002/jmor.21093>

## In the pipeline

**Ollevier, A.**; Mortelmans, J.; Deneudt, K.; Hablützel, P. I.; De Troch, M. (submitted). Diel Vertical Migration and Tidal Influences on Plankton Densities in Dynamic Coastal Systems. Submitted to *Estuarine, Coastal and Shelf Science*.

**Ollevier, A.**; Mortelmans, J.; Boone, W.; Deneudt, K.; De Troch, M.; Develter, R.; Goossens, C.; Meire, L.; Möller, K. O.; Ponsoni, L.; Hablützel, P. I. (in prep.). Picturing plankton: How optical imaging can improve assessing plankton community dynamics.

## PUBLICATION LIST

Hovenkamp, P.; van Walraven, L.; **Ollevier, A.**; van Oevelen, D.; van der Stappen, F. (submitted). Optimising automated classification of colour images from zooplankton in coastal conditions. Submitted to *Limnology and Oceanography: Methods*.

Ponsoni, L., **Ollevier, A.**, *et al.* (in prep.). Long-term evolution of the water masses properties in the Uummannaq fjord system.

## Datasets

**Ollevier, A.**; Meire, L.; Bladfort, D.; Develter, R.; Möller, K.O.; Planken, K.; Ponsoni, L.; Schulz, K.; van Oevelen, D.; Boone, W.; (2023): Data from IOPD cruise Part 1 Physical and imaging data. Marine Data Archive. <https://marineinfo.org/id/dataset/8430>

**Ollevier, A.**, Meire, L., Bladfort, D., Develter, R., Möller, K. O., Planken, K., Ponsoni, L., Schulz, K., Van Oevelen, D., & Boone, W. (2022). Data from IOPD cruise Part 2 Water sample analysis and plankton identifications. SEANOE. <https://doi.org/10.17882/96813>

**Ollevier, A.**, Meire, L., Bladfort, D., Develter, R., Möller, K. O., Planken, K., Ponsoni, L., Schulz, K., Van Oevelen, D., & Boone, W. (2022). Data from IOPD cruise Part 3 Water sample analysis. SEANOE. <https://doi.org/10.17882/97076>

Mortelmans, J; **Ollevier, A.**; Dillen, N; Flanders Marine Institute: Belgium; (2023): LifeWatch Cruise 21-870: Trip 4079. Marine Data Archive. <https://doi.org/10.14284/616>

Praet, N.; Vandorpe T.; **Ollevier, A.**; Dierssen, H.; Flanders Marine Institute (VLIZ): Belgium; University of Connecticut: USA; (2022): TIMBERS in-situ sensor dataset. Marine Data Archive. <https://doi.org/10.14284/572>

## Posters and oral presentations at conferences

**Ollevier, A.**; Ponsoni, L.; Develter, R.; Mortelmans, J.; Lagaisse, R.; De Troch, M.; Hablützel, P.; Boone, W. (2023). Oceanic drivers, nutrient dynamics and plankton communities in West-Greenland's fjord system: A multidisciplinary study, *in: Mees, J. et al. Book of abstracts – VLIZ Marine Science Day, 1 March 2023, Bruges. VLIZ Special Publication*, 90: pp. 79

**Ollevier, A.**; Mortelmans, J.; Vandegheuchte, M.; Develter, R.; De Troch, M.; Deneudt, K. (2023). Lessons learned from in situ plankton imaging in shallow and turbid coastal waters in the Belgian part of the North Sea: a Video Plankton Recorder study, *in: The Sixth Xiamen Symposium on Marine Environmental Sciences (XMAS-VI), January 9th-12th, 2023, Xiamen, China*.

Ponsoni, L.; **Ollevier, A.**; Develter, R.; Boone, W. (2023). Freshwater input and water mass interactions in the Uummannaq fjord system, *in: EGU General Assembly 2023. Vienna, Austria & Online, 23–28 April 2023*. pp. EGU23-11323. <https://dx.doi.org/10.5194/egusphere-egu23-11323>

Ponsoni, L.; **Ollevier, A.**; Develter, R.; Boone, W. (2023). A multidisciplinary data analysis approach for understanding the water masses distribution in the Uumannaq area fjords, *in: 54th International Liège Colloquium on Ocean Dynamics: machine learning and data analysis in oceanography*. pp. 1

- Ponsoni, L.; **Ollevier, A.**; Develter, R.; Boone, W. (2023). Freshwater input variability and water mass distribution in the system of fjords in the Ummannaq area, Western Greenland, *in*: Mees, J. *et al. Book of abstracts – VLIZ Marine Science Day, 1 March 2023, Bruges. VLIZ Special Publication*, 90: pp. 91
- Praet, N.; Collart, T.; **Ollevier, A.**; Roche, M.; Degrendele, K.; De Rijcke, M.; Vandorpe, T. (2023). The potential of multibeam sonars as 3D turbidity and SPM monitoring tool in the North Sea, *in*: Mees, J. *et al. Book of abstracts – VLIZ Marine Science Day, 1 March 2023, Bruges. VLIZ Special Publication*, 90: pp. 92-93
- Ollevier, A.**; Mortelmans, J.; Aubert, A.; Deneudt, K.; Vandegheuchte, M.B. (2022). The life of sea sparkle: dynamics, drivers and interactions of *Noctiluca scintillans* in the Belgian part of the North Sea, *in*: Mees, J. *et al. Book of abstracts – VLIZ Marine Science Day, Online event 2 March 2022. VLIZ Special Publication*, 88: pp. 22-23
- Ollevier, A.**; Mortelmans, J.; Deneudt, K.; De Troch, M.; Vandegheuchte, M. (2021). Assessing feasibility and best practices of zooplankton observations with the Video Plankton Recorder in coastal turbid waters, *in*: Mees, J. *et al. Book of abstracts – VLIZ Marine Science Day, Online event 3 March 2021. VLIZ Special Publication*, 85: pp. 18
- Mortelmans, J.; **Ollevier, A.**; Hernandez, C.; Deneudt, K. (2020). LifeWatch biodiversity data: trends and dynamics of Copepods in the Belgian Part of the North Sea, *in*: Mees, J. *et al. Book of abstracts – VLIZ Marine Science Day. Oostende, Belgium, 18 March 2020. VLIZ Special Publication*, 84: pp. 67
- Ollevier, A.**; Mortelmans, J.; Deneudt, K.; Vandegheuchte, M. (2020). Population dynamics of *Noctiluca scintillans* in the Belgian part of the North Sea and its effect on small gelatinous plankton, *in*: Mees, J. *et al. Book of abstracts – VLIZ Marine Science Day. Oostende, Belgium, 18 March 2020. VLIZ Special Publication*, 84: